Molecular determinants of human oocyte quality in assisted reproduction

David Cornet Bartolomé

Molecular determinants of human oocyte quality in assisted reproduction

David Cornet Bartolomé

PhD Thesis

2019

PROGRAMA DE DOCTORAT EN GENÈTICA

Departament de Genètica, Microbiologia i Estadística

Facultat de Biologia

Molecular determinants of human oocyte quality in assisted reproduction

Memòria presentada per en **David Cornet Bartolomé** per optar al grau de Doctor per la Universitat de Barcelona

Daniel Grinberg Vaisman

Director i tutor

Rita Vassena

Directora

David Cornet Bartolomé

Doctorand

With the support of the Secretary for Universities and Research of the Ministry of Economy and Knowledge of the Government of Catalonia

En primer lugar, me gustaría agradecer a Rita y Daniel la oportunidad que me habéis dado para poder empezar este proyecto, por haber confiado en mí y por haberme prestado toda vuestra sabiduría. Es un honor tener una tesis dirigida por vosotros.

También me gustaría agradecer a Montse toda la ayuda y conocimientos que me has aportado cada día y por enseñarme la importancia de los controles.

Gracias también a Gustavo, Filippo, Anna y Susana por vuestro rigor científico y vuestros consejos que han ayudado a mejorar esta tesis.

Muchas gracias a Marc, Paula, Evi y Farners por todo vuestro apoyo moral, tan necesario en algunas ocasiones. No podría pedir unos compañeros de laboratorio mejores.

Me gustaría hacer especial mención a Agus. La persona más fuerte y valiente que conozco, con un optimismo desbordante que contagia a toda la gente que le rodea. No cambies nunca.

Gracias a toda la gente del laboratorio clínico de Eugin por su dedicación y paciencia a la hora de recoger las muestras que necesitaba para mi tesis. Gracias también a Désirée por aportar tus conocimientos sobre estadística.

Me gustaría agradecer también a la gente del departamento de genética de la UB, en especial a Noelia, por hacerme sentir como en casa y ayudarme con todos los experimentos.

Finalmente, me gustaría agradecer este trabajo especialmente a mi familia: Claudia (para mí ya formas parte de ella), Carles y mis padres Josep y Luisa. Gracias por vuestra paciencia en los momentos difíciles, por todo vuestro apoyo y comprensión incondicional y por estar siempre ahí.

TABLE OF CONTENTS

ABBREVIATIONS LIST

AFC: Antral Follicular Count

ART: Assisted Reproductive Technologies

AS: Alternative Splicing

ATP: Adenosine Triphosphate

BMI: Body Mass Index

Ca^{2+}: Calcium ion

cAMP: Cyclic Adenosine Monophosphate

CBP: Cap Binding Protein

CCs: Cumulus Cells

cDNA: complementary DNA

ChIRP: Chromatin Isolation by RNA Purification

CI: Confidence Interval

CMV: Citomegalovirus

COCs: Cumulus-Oocyte Complexes

CV: Coefficient of Variation

DIG: Digoxigenin

DMEM: Dulbecco′s Modified Eagle′s Medium

DMSO: Dimethyl Sulfoxide

DNA: Desoxiribonucleic Acid

DOR: Diminished ovarian reserve

DTT: Dithiothreitol

EDTA: Ethylenediaminetetraacetic acid

EGA: Embryonic Genomic Activation

ER: Endoplasmic Reticulum

ET: Embryo Transfer

FDR: False Discovery Rate

FSH: Follicle Stimulating Hormone

GFP: Green Fluorescent Protein

GnRH: Gonadotropin-Releasing Hormone

GO: Gene Ontology

GSP: Gene Specific Primer

GV oocyte: Germinal Vesicle oocyte

GVBD: Germinal Vesicle Breakdown

HB: Hypotonic Buffer

HEK293-T: Human embryonic kidney 293 easy to transfect cells

HIV: Human Immunodeficiency Viruses

H-MII group: women up to 30 years old with high AFC

HRG: Homogeneous Reference Genes

ICSI: Intracytoplasmic Sperm Injection

IVF: In Vitro Fertilization

LBR: Live Birth Rate

LH: Luteinizing Hormone

lincRNA: long intergenic non-coding RNA

L-MII group: women with low AFC

LMP: Last Menstrual Period

LNA: Locked Nucleic Acid

lncRNA: long non-coding RNA

LOF: Loss of Function

MII oocyte: Metaphase II oocyte

miRNA: micro RNA

mRNA: messenger RNA

mtDNA: mitochondrial DNA

ncRNA: non-coding RNA

NGS: Next Generation Sequencing

O/N: Overnight

OH group: Old women with high AFC

OL group: Old women with low AFC

O-MII group: women above 31 years old with high AFC

OPU: Oocyte Pick-Up

OR: Odd Ratio

PB: Polar Body

PBS: Phosphate Buffered Saline buffer

PCA: Principal Component Analysis

PCR: Polymerase Chain Reaction

PGCs: Primordial Germ Cells

PIP_2: Phosphatidylinositol 4,5-bisphosphate

piRNA: piwi-interacting RNA

PN: Pronucleus

QC: Quality Control

qPCR: quantitative PCR

RACE: Rapid amplification of cDNA ends

RCT: Randomized Controlled Trial

RISC: RNA-Induced Silencing Complex

RLE: Relative Log Expression

RMA: Robust Multiarray Average

RNA: Ribonucleic Acid

RT: Room Temperature

rTDT: recombinant Terminal Deoxynucleotidyl Transferase

RU: Relative units

SD: Standard Deviation

SDS: Sodium Dodecyl Sulphate

shRNA: short hairpin RNA

siRNA: small interfering RNA

TAC: Transcriptome Analysis Console

tRNA: transfer RNA

TZPs: Transzonal Projections

UTRs: Untranslated Regions

VIT: Vitrification

WHO: World Health Organization

YH group: Young women with High AFC

YL group: Young women with Low AFC

ZP: Zona Pellucida

1. INTRODUCTION

1.1. ASSISTED REPRODUCTION

Infertility, as described by the World Health Organization (WHO) is "a disease of the reproductive system defined by the failure to achieve a clinical pregnancy after 12 months or more of regular unprotected sexual intercourse" (WHO-ICMART glossary). Infertility affects both social and financial aspects on a global scale, affecting 1 in 9 couples in reproductive age worldwide (Mascarenhas et al., 2012). Most of these couples will only achieve pregnancy through assisted reproductive techniques (ART), where the gametes are manipulated outside the human body to increase the chances of a pregnancy.

In vitro fertilization (IVF) is a common ART which consist on the suppression of the natural menstrual cycle followed by the controlled ovarian stimulation with the follicle stimulating hormone (FSH), which increases the number of oocytes that will mature in order to obtain more oocytes to fertilize (see penultimate paragraph of folliculogenesis section). After 10-12 days, the controlled ovarian stimulation is suppressed and the oocytes are collected. Then, a sperm sample is collected and the spermatozoa with the better motility are incubated with the oocyte. As an alternative approach, intracytoplasmic sperm injection (ICSI) can be conducted, which consists of injecting a single spermatozoon directly into the oocyte's ooplasm. Finally, the oocytes that are successfully fertilized are then transferred into the uterine cavity (2-5 days after the oocyte fertilization).

While many improvements have been made in the last few decades in the field of assisted reproduction, no method has been able to achieve 100% success. There are many variables that could affect the outcome of assisted reproductive cycles, and one of the most important is undoubtedly the quality of the embryo transferred to the woman's uterus. In order to have a fully functional and properly developing embryo, both sperm and oocyte must be of adequate quality (Krisher, 2004). Specifically, the oocyte must be

able to resume meiosis after being meiotically quiescent for an extended period of time, cleave after fertilization and form a good quality embryo that can induce a pregnancy and develop to term (Sirard et al., 2006).

1.2. MATERNAL DETERMINANTS OF OOCYTE QUALITY

Maternal age is the most important factor affecting women's ability to conceive and give birth. Over the past few decades, the average age of first-time mothers has increased world-wide due to educational, social, and economic factors (te Velde and Pearson, 2002). This is not different in Spain, since as it can be observed in Figure 1, is the European country with the latest maternity (measured up to 2015).

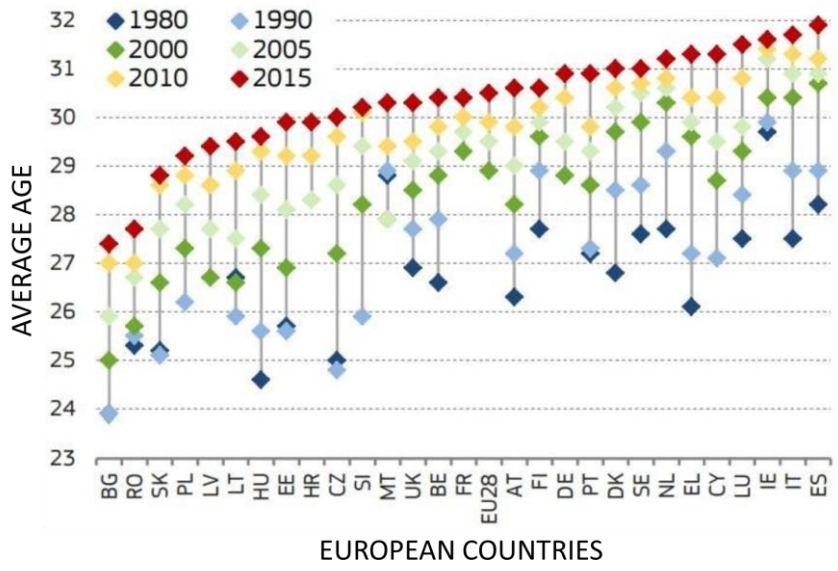

Figure 1: Mean age of first childbirth, 1980-2015, in Europe. Spain (ES). From http://www.attittud.com.

Female reproductive aging is associated with reduced oocyte quality (Miao et al., 2009; Broekmans, 2009; Qiao et al., 2014) (Figure 2), however the underlying molecular mechanisms remain poorly understood (Keefe et al., 2015). Although most of the declining quality associated with age can be assigned to increased meiotic errors, such as

aneuploidy (Armstrong, 2001), other correlated factors like cellular energy production and balance, metabolism, epigenetic regulation, and cell cycle check-points are also likely to play important roles. Gene expression studies in oocytes from several species showed differences in expression levels of genes involved in cell-cycle regulation, spindle formation and organelle integrity, suggesting that these mechanisms could be altered in oocytes from older individuals (Patel et al., 2007, Santonocito et al., 2013). Aging also originates an aberrant degradation of maternal transcripts during maturation. Thus, insufficient storage of transcripts during maturation of aged oocytes might also intervene in the reduction of oocyte quality (Jiao et al., 2012).

It is also well stablished that as woman age increases, her ovarian reserve diminishes. The term ovarian reserve determines the capacity of the ovary to supply high quality oocytes to provide a healthy and successful pregnancy and can be defined as the number of the remaining follicles in both ovaries at a given age (Broekmans, 2009). Women are born with a finite number of follicles (1-2 millions), and this number diminish with age (Faddy et al., 1992; Wallace and Kelsey, 2010). Decline in follicle numbers dictates the occurrence of irregular cycles and menopause (Figure 2; Broekmans et al., 2009). Although ovarian reserve declines with age, young women can be affected with diminished ovarian reserve as well; nevertheless, it is unknown whether this represents an acceleration of physiologic ovarian aging, or a distinct pathology (Skiadas et al., 2012). Published reports have shown convincing evidence that females with reduced ovarian reserve have aberrant gene expression in follicular fluid, granulosa and cumulus cells regardless of age. Nevertheless, it is not clear whether these molecular changes affect the quality of the oocyte (Ireland et al., 2007; 2011; Krisher, 2013).

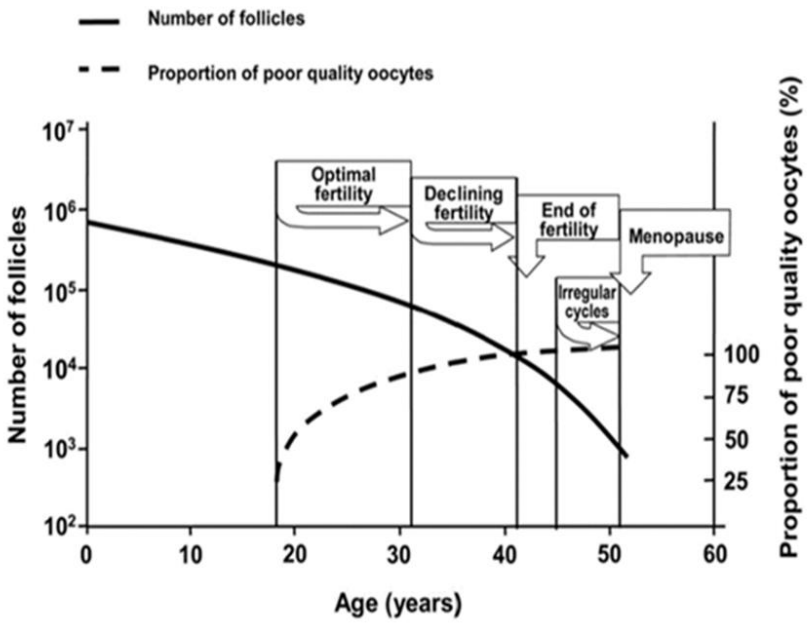

Figure 2: Schematic representation of the number of primordial follicles present in the ovaries and the quality of oocytes in relation to female age and corresponding reproductive events (from Broekmans et al., 2009).

In assisted reproduction, it is generally accepted that reduced antral follicle count (AFC), an indirect measure of ovarian reserve, indicates low ovarian reserve and is associated with poor response to ovarian stimulation (Broer et al., 2009; 2013; Grande et al., 2014), but it does not reliably predict failure to conceive (Committee on Gynecologic Practice, 2015). Moreover, oocyte quality is not only related to follicle number but also to follicle size. Oocyte growth coincides with the growth of the follicle. Oocytes recovered from small follicles have lower maturation and fertilization rates and are less able to develop into a good quality embryo (Marchal et al., 2002; Rosen et al., 2008). This is explained because, oocytes from small follicles have not been able to complete the cytoplasmic maturation and, therefore, they have not accumulated all the transcripts and proteins necessary for the development. This deficiency would lead to a decreased oocyte quality (Liu et al., 2002).

Over the last decade, our understanding of the molecular determinants of oocyte quality has increased considerably. Despite continuous research, routine evaluation of oocyte quality in IVF clinics is still performed at the morphological level which, apart from a few obvious examples (giant oocytes and polar bodies and smooth endoplasmic reticulum aggregates), is unreliable for judging the competence of living oocytes. In fact, currently there is no means to evaluate oocyte quality that is not invasive and/or requires the destruction of the oocyte. An increased understanding of oocyte quality determinants will help to identify key regulators that might be used as oocyte quality biomarkers that ultimately will give researchers and clinicians the ability to improve fertility and pregnancy outcomes for many women.

In order to deeply understand oocyte quality acquisition, we need to take into account several biological processes such as folliculogenesis and oogenesis and understand how the hormones regulating these two processes change their levels throughout the menstrual cycle.

1.3. MENSTRUAL CYCLE

The first half of the menstrual cycle is called follicular phase. At the beginning of such phase, estrogen levels are low. Gonadotrophin-releasing hormone (GnRH) start stimulating the pituitary gland to secrete follicle stimulating hormone (FSH) and low levels of luteinizing hormone (LH). These hormones, stimulate the growth of several follicles, each one containing one oocyte. Around the seventh day of the menstrual cycle, estrogen levels in blood rise significantly and begin to inhibit the secretion of FSH. When FSH levels decrease, smaller follicles stop growing and undergo atresia. At the end of the follicular phase, midway of the menstrual cycle (day 14), the estrogen levels are

sufficiently high to stimulate the production of GnRH, which in turn stimulates the pituitary gland to secrete LH. The sudden release of LH triggers the final maturation and extrusion of the mature oocyte from the follicle. After ovulation, the cells in the ovarian follicle undergo a transformation and become the corpus luteum.

The second half of the menstrual cycle is called luteal phase. Luteal phase begins with ovulation and lasts approximately 14 days. During this period, the corpus luteum produce, in addition to estrogen, high amounts of progesterone to prepare the lining of the uterus (endometrium) for implantation. Under the influence of progesterone, the uterus begins to create a highly vascularized tissue for the fertilized oocyte. If oocyte fertilization and implantation occur, the corpus luteum continues to produce progesterone until about 10 weeks of gestation, preventing the endometrium from being shed. Otherwise, if fertilization has not occurred, no embryo implants in the endometrium, therefore, the circulating levels of progesterone decline with the degeneration of the corpus luteum and the endometrium is shed, leading to bleeding (Figure 3).

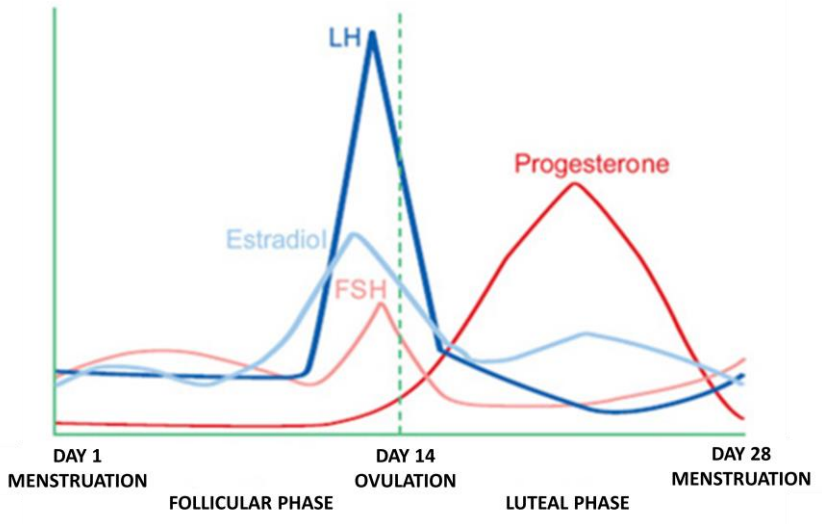

Figure 3: Hormonal profiles during the menstrual cycle. Illustration adapted from Anatomy & Physiology, Connexions Web site. http://cnx.org/content/col11496/1.6/.

1.4. FOLLICULOGENESIS

As mentioned before, each oocyte is embedded inside a follicle and as it grows and matures, the whole follicle itself goes through a series of changes in preparation for ovulation. The quality of the oocyte is determined during folliculogenesis (Krisher, 2004). Folliculogenesis occurs within the cortex of the ovary, where follicles with different sizes representing various stages of folliculogenesis are present (Figure 4). The principal objective of folliculogenesis is to produce a single dominant follicle from a pool of follicles in different growing stages.

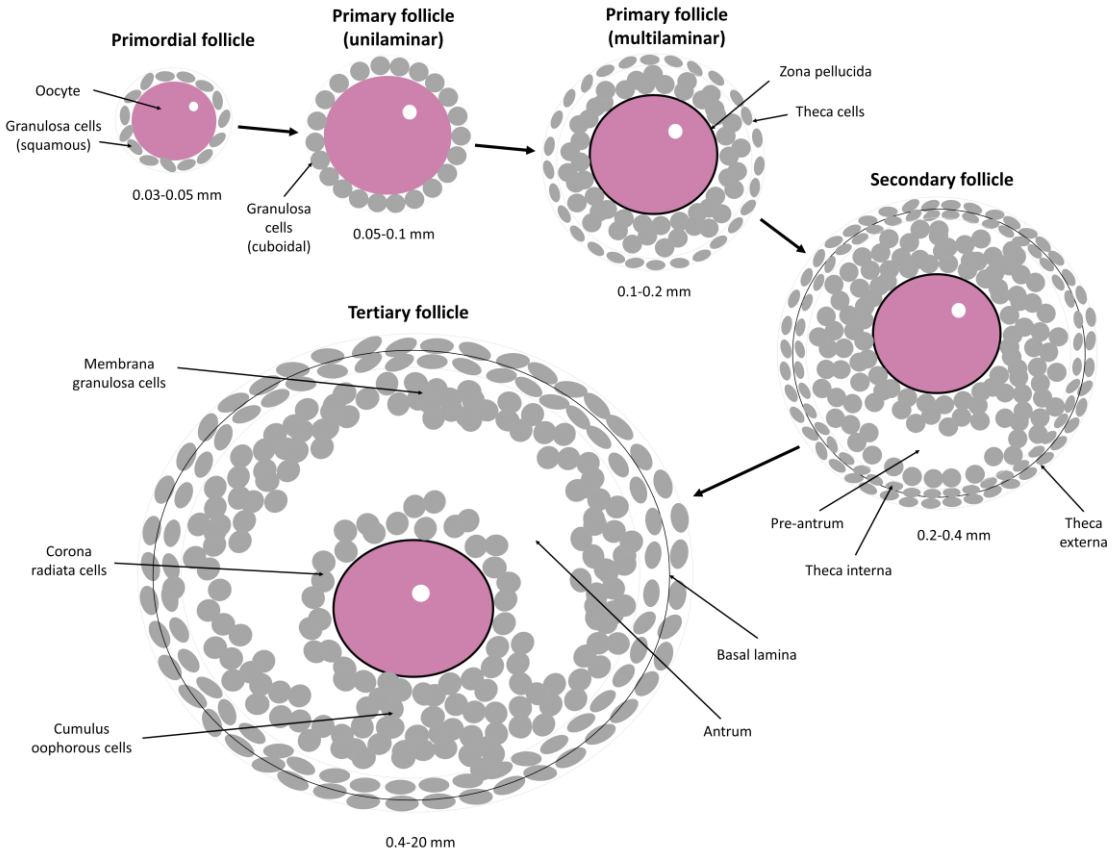

Figure 4: Illustration of follicular development.

All primordial follicles present in the human ovaries are formed in the fetus reaching its maximum number (4 to 5 million on average) at 18-22 weeks post-conception (Wallace

and Kelsey, 2010). The total number of primordial follicles (ovarian reserve) decreases throughout the reproductive life of the women until the pool of primordial follicles is exhausted at the menopause.

In the human fetus, follicular development begins with a primordial follicle, a small dormant follicle about 0.03-0.05 mm in diameter that contains a flattened layer of squamous granulosa cells that surround the oocyte. As primordial follicle grows, increasing to almost 0.1 mm in diameter, granulosa cells change from a squamous to a cuboidal structure, making the beginning of the primary follicle or preantral follicle. The change in the shape of the granulosa cells is followed by the expression of FSH receptors and the start of the RNA synthesis and mitosis, a process controlled by autocrine/paracrine mechanisms (Yamoto et al., 1992; Oktay et al., 1997).

The transition from the primary to the secondary follicle is characterized by an increase in the diameter of the follicle (from 0.1 mm to 0.2-0.4 mm) (Johnson and Everitt, 2003). This is explained by the continuous mitotic divisions of the granulosa cells which end up forming six to nine layers. One of the most important events in the secondary follicle development is the condensation of the stromal cells surrounding the primary follicle to form the theca layer (Johnson and Everitt, 2003). The theca layer is formed around the basal lamina, the follicle's outermost layer, and undergo cytodifferentiation to become the theca interna and theca externa. Parallelly, an extensive network of capillary vessels is formed through angiogenesis between these two theca layers and blood begins to circulate around the follicle, bringing hormones and nutrients.

The transition from the secondary follicle to a tertiary follicle, also known as antral follicle or Graafian follicle, is only possible when women enter puberty. This transition begins with the appearance of a fluid-filled cavity in the granulosa cells known as antrum. This process is called cavitation and is controlled by autocrine/paracrine mechanisms,

such as growth factors like activin and Kit ligand (Li et al., 1995; Yoshida et al., 1997). The basic structure of the mature follicle is now established and it will not change its appearance and complexity during growth. Nevertheless, there are dramatic changes in the size of the tertiary follicles, explained in part by the high rate of mitotic divisions undergone by theca and granulosa cells, only hampered by the availability of FSH and LH. These hormones are also crucial in the follicular fluid formation which leads to an increase in the antrum volume and therefore the follicle size (Palermo, 2007). All these events lead to the formation of tertiary follicles with very different sizes, from 0.4 to 20 mm, but with a similar structure, characterized by the presence of an antrum containing the follicular fluid, the theca interna and externa, the basal lamina, granulosa cells and the oocyte (Sorensen and Wassarman, 1976). The granulosa cells of the tertiary follicle are divided into four different regions depending to its position within the follicle: the corona radiata, surrounding the zona pellucida, membrana granulosa and periantral, the outermost and innermost domains, respectively and the cumulus oophorous, a cluster of cells (called cumulus cells, CCs) which connects the membrana granulosa and corona radiata together and are crucial for oocyte maturation as will be explained in the oogenesis section.

Tertiary follicles have only two possible fates: continue the development or suffer atresia. The tertiary follicles that continue the development, become progressively more differentiated with time until they reach the preovulatory stage. In contrast, atretic follicles are normally smaller than 10 mm in diameter since their granulosa cells stop dividing and start to express genes related to apoptosis (Johnson and Everitt, 2003). The fate that the tertiary follicles will follow is determined by the increase in the FSH levels. Follicles that have fewer FSH-receptors in the cumulus cells or that are in areas with lower concentrations of FSH, will not be able to develop further and will become atretic.

The follicles that continue the development compete with each other for the growth-inducing FSH and secrete estrogen and inhibin to reduce FSH levels until only one follicle is viable, the dominant follicle (Palermo, 2007). The granulosa cells of this dominant follicle begin to divide very rapidly, leading to a rapid growth of the follicle up to 20 mm in diameter that will eventually be the preovulatory follicle. At this step is when ART acts, since in the controlled ovarian stimulation of the IVF cycles, the supplementary hormones administered (FSH), prevent the selection of a single dominant follicle and allow the concomitant maturation of multiple follicles. This is performed in order to collect the maximum number of oocytes to ensure the success of fertilization.

Finally, at the end of the follicular phase, following a LH surge, an opening is formed in the cumulus oophorous layer of the preovulatory follicle and the oocyte is released to the oviduct with a complement of cumulus cells, a process called ovulation that marks the end of folliculogenesis.

1.5. OOGENESIS

Oogenesis is the process by which an oocyte develops from its primordial state (primordial germ cell, PGC) to a fully-grown and matured oocyte that is able of being fertilized (Edson et al., 2009). Oocyte development consists of three phases: proliferation of PGCs, oocyte growth, and oocyte maturation (Figure 5). In most mammals, oogenesis occurs over the span of many years and these three phases take place at different time points throughout a female's life.

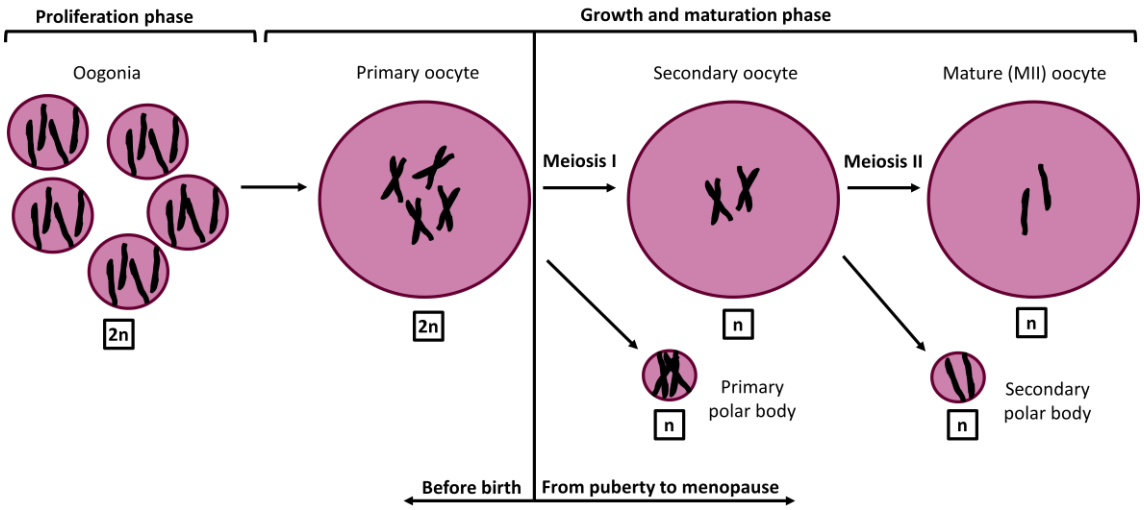

Figure 5: Oogenesis process.

1.5.1. Proliferation phase

Early in embryogenesis, primordial germ cells (PGCs) migrate from the yolk sac endoderm to the genital ridge (developing fetal ovary). The generation of PGCs takes place in the fetal ovary at approximately 3 weeks after fertilization and begins with a series of mitotic divisions that increase the number of PGCs within the fetal ovary to up to 1-2 million cells and form the oogonia (Edson et al., 2009; Senger, 2012). After several rounds of mitotic germ cell division, at approximately the 11th or 12th week of gestation, oogonia condense to form individual primordial follicles (Guraya, 2008). Then, oogonia interrupt mitotic activity and enter meiosis, becoming primary oocytes (Gondos et al., 1986; Goto et al., 1999; Martins da Silva et al., 2004). At this point, oocytes are within primordial follicles and continue through meiosis until they enter prophase 1, where development is arrested at the diplotene stage (Mandelbaum, 2000). The arrest is maintained mainly by high levels of intracellular cyclic adenosine monophosphate (cAMP) secreted by the surrounding granulosa cells that are transported into the oocyte (Zhang and Xia, 2012). The cAMP synthesis is controlled by the FSH (Sanchez and

Smith, 2012) which is responsible to maintain the oocyte in this arrested state from birth until the time it is recruited for ovulation (Desai et al., 2013). Morphologically, oocytes arrested in prophase of meiosis 1 are at the germinal vesicle (GV) stage, which is characterized by an enlarged nucleus.

1.5.2. Oocyte growth

The process of oocyte growth begins when the primordial follicle is formed and continues until the development of the tertiary or Graafian follicle (Johnson and Everitt, 2003). Oocyte growth is tightly controlled by the activity of the CCs of the follicle, which surround the oocyte during follicular development and ovulation and helps the oocyte to acquire its quality (Eppig, 2001; Guraya, 2008). On the other hand, oocytes also control cumulus and granulosa cell function since they determine the rate of follicle growth and maturation and regulate CCs metabolic activity and gene expression (Gilchrist et al., 2006; Diaz et al., 2007). Oocytes and CCs also have metabolic cooperativity. For instance, oocytes are unable to metabolize glucose and cannot conduct the biosynthesis of cholesterol. Besides, they seem to have poor capacity to uptake amino acid, compared to CCs. Thus, oocytes need the CCs to do all these metabolic processes for them in order to support their growth and maturation (Eppig and Steckman, 1976). CCs are bidirectionally communicated with the oocyte by paracrine signals and/or through gap junctions (intercellular channels composed by connexins) which allow the exchange of small molecules (< 1kDa) such as transcripts, amino acids and metabolites (Beyer, 1993; Kumar et al., 1996; Hussein et al., 2006; Gilchrist et al., 2008). Oocytes are surrounded by a glycoprotein layer called zona pellucida. For this reason, gap junctions between CCs and oocytes have specialized projections (transzonal projections [TZPs]) that penetrate the zona pellucida and reach the oocyte membrane (Macaulay et al., 2015).

During oocyte growth, the oocyte increases its size (almost 100-fold increase in volume) and accumulates new RNAs, ions and metabolic substrates such as sugars and lipids, required for its growth and maturation and for early embryonic development (Marteil et al., 2009; Gosden and Lee., 2010; Do et al., 2018). The number of transcripts synthetized and accumulated during the growth phase of the oocyte is relevant, since transcription all but stops in fully-grown oocytes. This means that the accumulated transcripts will support the final steps of oocyte maturation as well as the initial divisions of the embryo, until the activation of the embryonic genome (Do et al., 2018). The oocyte also produces, reorganizes and replicates new cytoplasmic organelles such as mitochondria and secretes the glycoproteins that will form the zona pellucida and the cortical granules, necessary for fertilization (Picton et al., 1998).

When a woman enters puberty, follicles will be exposed to higher levels of gonadotropins (LH and FSH). Thanks to this rise in gonadal hormones, the oocyte can complete the growth phase (reaching a final size of 60-120 µm), undergo germinal vesicle breakdown (GVBD) and resume meiosis (Zhang and Xia, 2012). After the LH surge, oocytes regulate the expression of the CCs genes responsible for the CCs expansion, which is produced by the secretion of a mucinous matrix that contains hyaluronic acid. When the CCs expand, gap junctions dissociate from the oocyte allowing the resumption of meiosis and ultimately, ovulation (Combelles et al., 2004; Motola et al., 2007).

After resuming meiosis, the oocyte will start the final maturation phase, a precisely regulated process essential for ovulation and subsequent fertilization, in which the oocytes complete the first meiotic division and proceeds from prophase I to metaphase II of meiosis (Mehlmann, 2005; Jamnongjit and Hammes, 2005).

1.5.3. Oocyte maturation

Oocyte maturation is one of the most important processes of oogenesis, since it will determine the quality of the ovulated oocyte, better defined as "developmental competence". Oocyte developmental competence is the ability to sustain embryonic development at least until the developing embryo is able to activate its own genome (in human this happens in a stepwise manner and it is not complete until approximately day 4 of in vitro culture (Braude et al., 1988; Vassena et al., 2011). Developmental competence is determined by two aspects:

- Nuclear maturation: Refers to the ability of the oocyte to undergo complete meiosis. Nuclear competence can be influenced by the number and location of the crossovers during meiosis I. Crossovers too close to the telomeres (end of the chromosomes) or centromeres (DNA sequence that links the sister chromatids) can have deleterious effects on subsequent oocyte and embryo development (Hassold et al., 2007).
- Cytoplasmic maturation: Refers to the acquisition of a global population of transcripts, proteins and organelles that will provide the required substrate for early preimplantation development (Gosden and Lee, 2010). Cytoplasmic competence depends on a large number of factors, many of which can only be assessed at the cellular and molecular level (Coticchio et al., 2004).

Nuclear maturation

Nuclear maturation begins with the LH surge which causes the breakdown of the germinal vesicle of the oocyte and its meiotic resumption. The oocyte progresses from prophase I to metaphase I and the homologous chromosomes align in the metaphase plate,

assembling the first meiotic spindle. Then, the sister chromatids of the homologous chromosomes separate at anaphase I. The oocyte now undergoes an asymmetric cytokinesis and almost all of the cytoplasm remains with the oocyte which becomes the secondary oocyte. At this moment, at telophase I, the sister chromatids of the homologous chromosomes migrate to opposite poles. In parallel, the first polar body (PB) is formed and its extruded from the oocyte. This PB contains a very small proportion of the cytoplasm and half of the genetic material. The oocyte arrests again at metaphase II after ovulation and wait for fertilization (Chaube, 2001). At this point the oocyte is considered meiotically mature and it is called MII oocyte.

At fertilization, the sperm binds to a receptor on the surface of the oocyte and triggers a signal that stimulates the hydrolysis of phosphatidylinositol 4,5-bisphosphate (PIP_2) which results in an increase in the level of Ca^{2+} in the oocyte. This increase in the cytosolic Ca^{2+} following fertilization triggers the metaphase to anaphase transition by activating the anaphase promoting complex, which leads to the completion of the second meiotic division, with asymmetric cytokinesis (as in meiosis I) giving rise to the extrusion of a second PB (reviewed by Yeste et al., 2016).

Cytoplasmic maturation

Cytoplasmic maturation can be divided in 3 interrelated events: organelle distribution, cytoskeleton reorganization and molecular maturation. These processes are regulated by differences in the hormonal concentration secreted by the cumulus cells (Ferreira et al., 2009). Although in this section the three processes are summarized, the present work will focus mainly in the study of the molecular factors that influence cytoplasmic maturation,

since is thought to be the process with the highest impact in determining oocyte quality and its ability to acquire developmental competence (Sirard et al., 2006).

a. Organelle distribution

Organelle distribution begins at the time of the LH surge and is characterized by an extensive redistribution of intracellular organelles as oocyte progresses to metaphase II. Among all cellular organelles, the mitochondrial status become one of the most relevant to evaluate the quality of the oocyte. This implies the analysis of the number, activity, mtDNA content and organization of the mitochondria present in the cytoplasm of the oocytes. Mitochondria are responsible for producing the energy supply (adenosine triphosphate, ATP) required for oocyte maturation. Variations in ATP content in human oocytes and embryos affect oocyte quality and embryo development (Slotte et al., 1990). Higher ATP levels have been correlated with better reproductive results, whereas mitochondrial dysfunction decreases the quality of the oocyte (Zhao and Li, 2012). Moreover, during bovine oocyte development, mitochondria are reorganized to areas of high energy consumption to provide local energy supply (Stojkovic et al., 2001). In GV oocytes from mice and pigs, mitochondria are aggregated in large clusters around the germinal vesicles whereas after the GVBD, the mitochondria clusters become more numerous and disperse throughout the cytoplasm in MII oocytes (Motta et al., 2000; Sathananthan and Trounson, 2000; Familiari et al., 2006). Numerous studies have demonstrated that an aberrant mitochondrial distribution leads to oocyte with less developmental competence (Bavister and Squirrell, 2000; Sun et al., 2001; Au et al., 2005; Brevini et al., 2005). Endoplasmic reticulum (ER), the major store of calcium ions (Ca^{2+}), is also rearranged in anticipation of the phasic release of Ca^{2+} from ER stores after fertilization. At the GV stage of human oocytes, the ER forms a fine network uniformly

distributed throughout the cortex and the cytoplasm, whereas, in MII oocytes, the ER is accumulated in large clusters (Mann et al., 2010). This is different from what it is observed in the mouse, since in MII oocytes the ER is located mainly in the cortex (FitzHarris et al., 2007). Golgi apparatus in human GV oocytes is present in the whole ooplasm in the form of a membranous system; however, upon GVBD, it is no longer essential for maturation and it is fragmented and dispersed throughout the oocyte (Sathananthan et al., 2002). Nevertheless, the significance of the dynamics of the Golgi apparatus during oocyte maturation is no yet clear. Finally, the cortical granules originated from Golgi membranes during oocyte growth migrate towards the cortex to prepare for blocking polyspermy (Sathananthan, 1994).

b. Cytoskeleton reorganization

The cytoskeleton is a dynamic structure that extend from the nucleus to the cell membrane of all the cells and contains cytoskeletal filaments (microtubules, microfilaments and intermediate filaments) that perform a wide variety of functions (Theurkauf, et al., 1992). In the oocyte as in other eukaryotic cells, cytoskeleton ensures structural support, provides a scaffold to organize organelles in the cytoplasm and it is required for intracellular transport (Alberts et al., 2008). Oocyte growth, maturation and fertilization relies on the correct distribution of the cellular organelles and this is accomplished through the reorganization of microtubules and microfilaments (Sun and Schatten, 2006). Microtubules are dynamic filaments of the cytoskeleton and consist of globular and compacted polymers of α- and β-tubulin subunits. Microtubules are responsible for the distribution of organelles throughout the cytoplasm and the segregation of the chromosomes in meiosis (Sun and Schatten, 2006). Microfilaments consist of similarly

globular and compacted actin subunits engaged in the regulation of chromatin movement and cortical granules migration and also participates in the arrangement of the meiotic spindle and the extrusion of the first polar body (Tremoleda et al., 2001). In GV oocytes, microtubules and microfilaments are distributed throughout the ooplasm, however, their dynamics differ after GVBD. In MII oocytes microtubules are located around the condensed chromatin and begin to migrate to the cortical region, while microfilaments are accumulated in the subcortical region of oocytes and close to the spindle (Sathananthan, 1994). Intermediate filaments are formed by tetramers of fibrous polypeptides subunits that provide mechanical integrity to the oocyte. Nevertheless, the role of intermediate filaments in oocyte maturation is still poorly understood (Mao et al., 2014).

c. Molecular maturation

Molecular maturation occurs by the end of GV oocyte growth, when transcription is silenced, and includes all the events related to the processing and storage of transcripts and molecules that will be used for fertilization and early embryonic development (Humblot et al., 2005). Global transcriptional silencing in the oocyte is needed for developmental competence and has been associated to chromatin condensation surrounding the nucleolus configuration (Mattson and Albertini 1990, Inoue et al., 2008). The number and profile of the accumulated transcripts prior the onset of transcriptional silencing can determine the oocyte developmental competence and its ability to sustain early embryonic development (De la Fuente and Eppig, 2001). Alterations in the abundance of maternal transcripts can affect the health of the embryo and therefore, its ability to activate the embryonic genome. Regulation of transcript abundance in the oocyte is a tightly controlled process that depends on different factors that ultimately will

dictate the fate of the transcript, to be either used, degraded or stored. Most of these regulatory factors interact with specific sequences at the 3′ and 5′ untranslated regions (UTRs) of RNA and regulates its stability through processes such as:

- Polyadenylation, where a poly(A) tail (>150 residues) is added to the 3'end of some transcripts and confers stability and protection from degradation by exonucleases.
- Deadenylation, which shortens the poly(A) tail of the transcript affecting its stability.
- Association with cap binding complexes (CBP20/CBP80) and initiation factors which aid in the export of the mRNA, confers protection from degradation and are crucial for the initiation of translation.
- Association with lncRNAs and proteins that mask the RNA to avoid translation.
- Association with small non-coding RNAs such as small-interfering RNAS (siRNAs) and micro RNAs (miRNAs) that silence target RNAs through the RNA-induced silencing complex (RISC) (Chu and Rana 2008).
- Alternative splicing (AS), which generates several transcript isoforms from a given gene increasing transcriptome and proteome complexity.

During human and mouse oocyte maturation there is a selective degradation of maternal transcripts, which causes that around 30% of the genes decrease their abundance in mice (Jones et al., 2008; Paynton et al., 1988). Degradation of maternal transcripts is crucial in order to lose oocyte identity after fertilization and successfully complete the transition to an embryo (Su et al., 2007; Medvedev et al., 2008). Alterations in these regulating mechanisms, such as in the degradation machinery or in the maintenance of some transcripts during oocyte maturation could compromise oocyte developmental competence and embryo quality (Alizadeh et al., 2005).

1.6. ASSESSING OOCYTE QUALITY

Currently there is no accurate means for evaluating oocyte quality that is not invasive and/or requires the destruction of the oocyte. Nevertheless, oocyte examination at different levels can provide information to identify oocyte quality biomarkers allowing to select the "most competent" within a cohort.

1.6.1. Morphological criteria of oocyte quality

Morphological evaluation was the first parameter to be ever used for oocyte selection (De Vos et al., 1999; Balakier et al., 2002; Rosenbusch et al., 2002), and it involves the evaluation of the morphology of cumulus-oocyte complexes (COCs), oocyte cytoplasm, polar body, zona pellucida, perivitelline space and meiotic spindle. In general, the use of these morphological criteria to predict oocyte quality is still controversial because of its subjectivity. However, they can provide valuable information in order to pre-select oocytes with the highest quality that will generate embryos with increased developmental potential (Wang et al., 2007). In fact, routine evaluation of oocyte quality in IVF clinics is performed at the morphological level.

- Polar body: PB extrusion is the most common criteria to evaluate nuclear competence since it is quick and non-invasive. The assessment is based on the visualization of the extruded first polar body, which is an indication of a mature (MII) oocyte (Sirard et al., 2006). However, the extrusion of the first polar body alone does not give any information regarding oocyte's cytoplasmic competence. Some authors have reported that human oocytes with smooth, well-shaped, normal size and intact (not fragmented) first polar body have higher frequencies of ongoing pregnancies and implantations (Figure 6B) (Ebner et al., 2002; Rienzi

et al., 2008; Navarro et al., 2009). Nevertheless, these findings have not been confirmed by other authors (Verlinksy et al., 2003; Ciotti et al., 2004; De Santis et al., 2005; Ten et al., 2007).

Figure 6: Different sizes of the polar body. (A) big; (B) normal; (C) small (from clinical embryology notebook, ASEBIR).

- Cumulus-oocyte complex (COC): The evaluation of the oocyte quality is performed according to the compactness of the cumulus cells (Figure 7). It is believed that good quality human oocytes are normally embedded in a well-expanded cumulus cells of at least five layers surrounded by a radiant array of corona cell layers (Coticchio et al., 2004).

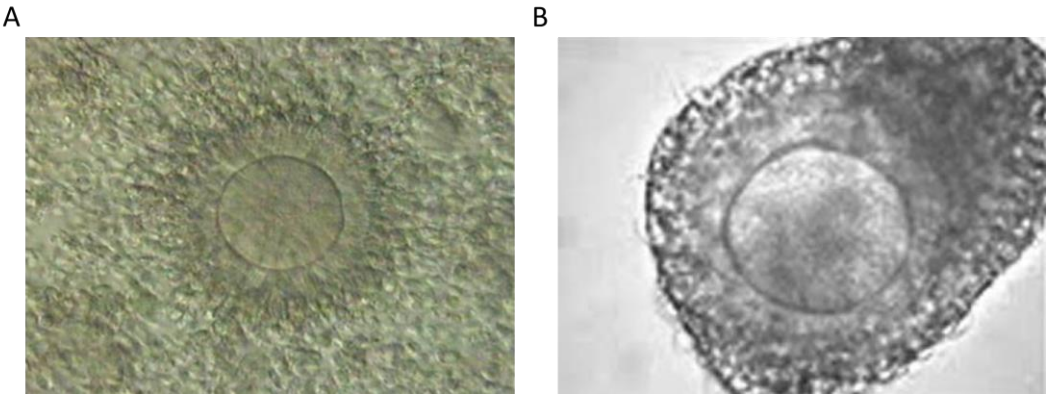

Figure 7: Cumulus-oocyte complex (COC). (A) COC obtained following ovarian stimulation showing an oocyte surrounded by expanded CCs (from Albertini et al., 2001). (B) COC recovered from an IVM cycle showing an oocyte surrounded by unexpanded, compact CCs (from the atlas of human embryology, ESHRE).

- Oocyte cytoplasm: Oocytes are classified according to the color of the cytoplasm and the size and distribution of the vacuoles and granules present in it. Best quality human oocytes are thought to be the ones with no shape abnormalities, with an almost transparent, turgid and homogeneous cytoplasm without any granules and few to no vacuoles (Balaban and Urman, 2006; Ebner et al., 2006; Rienzi et al., 2008; Figueira et al., 2010).

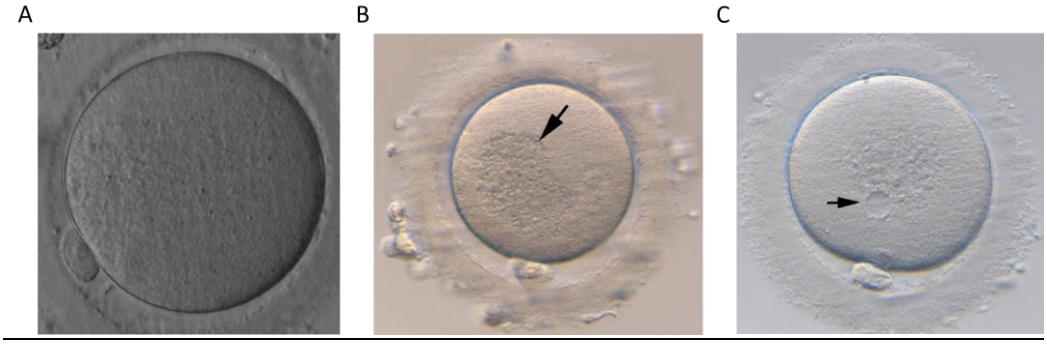

Figure 8: Denuded MII oocytes. (A) Good quality MII oocyte. (B) MII oocyte with granules located in the center (arrow). (C) MII oocyte with a vacuole (arrow). Obtained from the atlas of human embryology, ESHRE.

- Zona pellucida: Oocytes are classified based on the thickness and the colour of the zona pellucida (Figure 9). Best quality human oocytes are the ones that have a birefringent zona pellucida of about 20 µm (Rama Raju et al., 2007).

Figure 9: Oocyte with a dark zona pellucida (from clinical embryology notebook, ASEBIR).

- Perivitelline space: The evaluation is performed according to the size and content of the perivitelline space (Figure 10). It is estimated that human oocytes with large perivitelline space and with grains have lower developmental competence than those with normal perivitelline space and no grains (Xia et al., 1997; Hassan-Ali et al., 1998).

Figure 10: Detritus in the perivitelline space (arrows). From clinical embryology notebook, ASEBIR.

- Meiotic spindle: The correct alignment of chromosomes at the meiotic spindle is fundamental for their proper segregation during meiosis and later for fertilization. The parameters of meiotic spindle used to determine the quality of oocytes are: location and refraction (Figure 11). Nevertheless, some studies have reported no relationship between spindle location with oocyte developmental competence (Wang et al., 2001; Moon et al., 2003; Rienzi et al., 2003). Conversely, oocytes with birefringent spindles have been associated with higher developmental potential after fertilization (Wang et al., 2001; Moon et al., 2003; Shen et al., 2006; Fang et al., 2007).

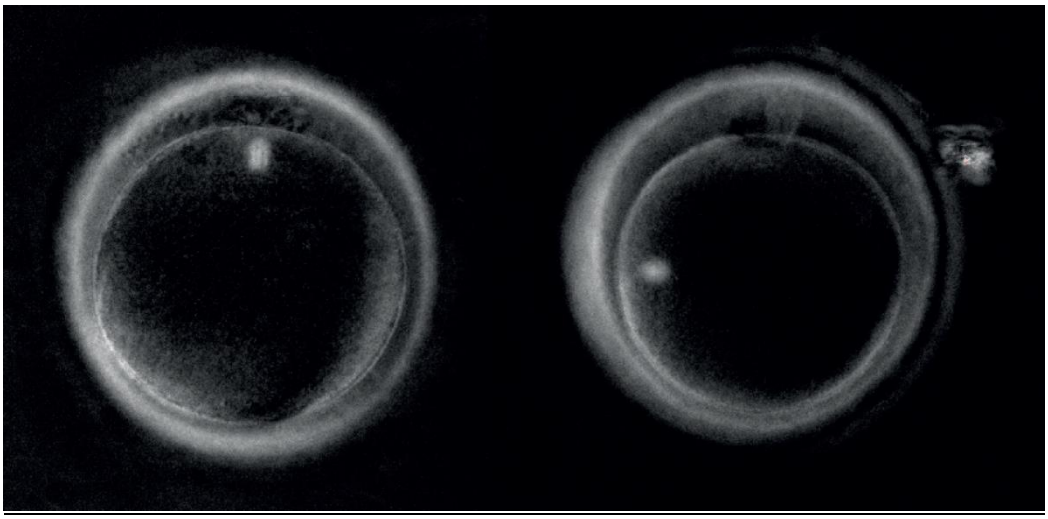

Figure 11: Polscope imaging of two human oocytes. The meiotic spindle is observed in both oocytes. On the left, the spindle is in the correct position, relative to the 1st polar body. In the image on the right, the spindle is offset 90º. Obtained from clinical embryology notebook, ASEBIR.

In conclusion, many of the morphological criteria used in IVF clinics to predict oocyte quality are good starting points for assessing the general developmental competence of an oocyte but there are many underlying issues that cannot be measured through these methods. Therefore, molecular assays need to be conducted in the oocyte itself or in the follicular cells and fluid, in order to find an accurate mean of assessing oocyte quality.

1.6.2. Gene expression analysis

The most important factor to asses oocyte quality is the analysis of its transcriptome. As already mentioned, oocyte growth and maturation are associated with dynamic transcriptional changes, featured by high transcriptional activity of growing oocytes and transcriptional silencing of mature oocytes. Understanding the differences in transcript profiles abundance in individual oocytes might provide knowledge of how to predict their competence and potential to produce viable embryos. With this aim, multiple microarray and next-generation sequencing (NGS) studies have been performed in several mammal

models: mouse, rabbit, rat, bovine and monkey (Su et al., 2007; Kues et al., 2008; Marjani et al., 2009; Vigneault et al., 2009; Ruebel et al., 2018). Nevertheless, little information regarding the transcriptome of human oocytes is available, due to the scarcity of the material available for research (Steuerwald et al., 2007; Fragouli et al., 2010; Grondahl et al., 2010). Moreover, O'Shea and colleagues conducted a meta-analysis on previously published microarray data on various models of oocyte and embryo quality candidate genes (O'Shea et al., 2012). They were able to identify 63 candidate genes suggested to be associated with oocyte quality across several mammalian species (mouse, bovine, monkey and human). Other studies have also found genes differentially expressed between high and low quality oocytes based on their morphology and its ability to develop to the blastocyst stage. As an example, the expression profiles of MII oocytes collected from young mice (5-6 weeks-old) were compared with those collected from old mice (42-45 weeks-old). It was found 530 genes differentially expressed among these two groups, including the ones involved in mitochondrial function and oxidative stress (Hamatani et al., 2004). Another study performed in mice, found that mRNAs for structural genes of zona pellucida (Zp1, Zp2 and Zp3) were highly abundant in fully-grown GV oocytes but become virtually undetectable in mature (MII) oocytes (Evsikov et al., 2006). Finally, in bovines, Biase and colleagues found 29 genes differentially expressed between good and bad oocytes. However, there was no enrichment of functional categories in this list of differentially expressed genes (Biase et al., 2014). All these studies provided a wealth of information and confirmed that oocytes at different stages have distinct molecular profiles, and that an aberrant gene expression can lead to lower oocyte quality. Nevertheless, more transcriptomic studies need to be conducted in order to understand the biological role of transcribed genes in the processes involved in human oocyte

maturation and to find robust and reliable biomarkers of oocyte quality and embryo development that are consistent across studies.

1.6.3. Analysis of the non-coding RNA → Long non-coding RNAs (lncRNAs)

One approach to investigate the molecular mechanism that take part in oocyte maturation and early embryo development can be the analysis of the non-coding transcriptome. Traditionally, transcriptome analysis of cells and tissues, including oocytes and embryos, has focused on protein-coding mRNA transcripts and its role in cellular processes (Vassena et al., 2007; Vassena et al., 2011). However, non-coding RNAs have long been known to play vital roles in eukaryotic gene regulation: mRNA polyadenylation occurs by events regulated by small nuclear and nucleolar RNAs; mRNA translation is mediated by ribosomal RNAs and transfer RNAs and is negatively regulated by micro RNAs. Finally, small-interfering RNAs and piwi-interacting RNAs (piRNAs) regulate mRNA abundance (Siomi et al., 2011; Wang et al., 2012). More recently, a new class of non-coding RNA longer than the ones previously mentioned, has been identified (Mercer et al., 2009; Hangauer et al., 2013). This new class of non-coding RNAs is known as long non-coding RNAs (lncRNAs), and have been detected at different stages of human preimplantation development, indicating that they could represent a new level of relative importance in the regulation of oocyte maturation and embryo early development (P. Caley et al., 2010; Fatica et al., 2014; Xu et al., 2014; Taylor et al., 2015).

Information on the general coding transcriptome and lncRNAs is remarkably scarce in human oocytes. There are very few reports on the transcriptome of human oocytes in general and almost no information is found about lncRNAs in oocytes in the literature.

LncRNAs were discovered with the advent of microarrays and next generation sequencing techniques, that were developed with the aim to characterize the mammalian transcriptome (Rinn et al., 2003; Shiraki et al., 2003; Bertone et al., 2004; Carninci et al., 2005). With these new tools, in fact, there is no need of an *a priori* knowledge of the targets to study gene expression, and different transcriptome wide studies revealed a high number of RNAs that do not code for proteins in different systems and species (Kampa et al., 2004; Carnici et al., 2005; Kapranov et al., 2005). Despite at the beginning most of the non-coding genome was considered transcriptional noise, their important regulatory function became rapidly clear (Wang et al., 2009; Bartel, 2009; Rinn and Chang, 2012).

To date, the specific sequence or structural and biochemical characteristics that define a lncRNA is still unclear. Nevertheless, the definition of transcripts that do not code for a protein and are longer than 200 nucleotides is generally accepted. This is an arbitrary size cut-off that was put to differentiate lncRNAs from smaller non-coding RNAs like miRNAs, siRNAs, piRNAs and transfer RNAs (tRNAs) (Mattick and Rinn, 2015; Bouckenheimer et al., 2016). Despite not being responsible for encoding a protein, lncRNA are mostly present in intronic regions of protein coding transcripts. Recently, it has been reported that approximately 81% (humans) and the 70% (mouse) of the protein coding genes have transcriptionally active introns after the splicing process (Louro et al., 2008; 2009). LncRNA are classified into two main subclasses, according to their genome location: intragenic lncRNAs and intergenic lncRNAs (Figure 12) (Kim et al., 2009).

- Intragenic lncRNAs: lncRNAs located within a protein-coding gene. Can be divided into four sub-groups depending on their position relative to the associated protein-coding gene. Sense lncRNAs overlap with a protein-coding gene on the same DNA strand while antisense lncRNAs overlap on the opposite strand. Intronic RNAs are located within an intron of a protein-coding gene and

bidirectional lncRNAs are transcripts in which the transcription start site is located less than 1kb away from its neighboring protein-coding gene.

- Intergenic lncRNAs: lncRNAs located more than 5 kb away from the starting transcription site of a protein-coding gene (Bouckenheimer et al., 2016).

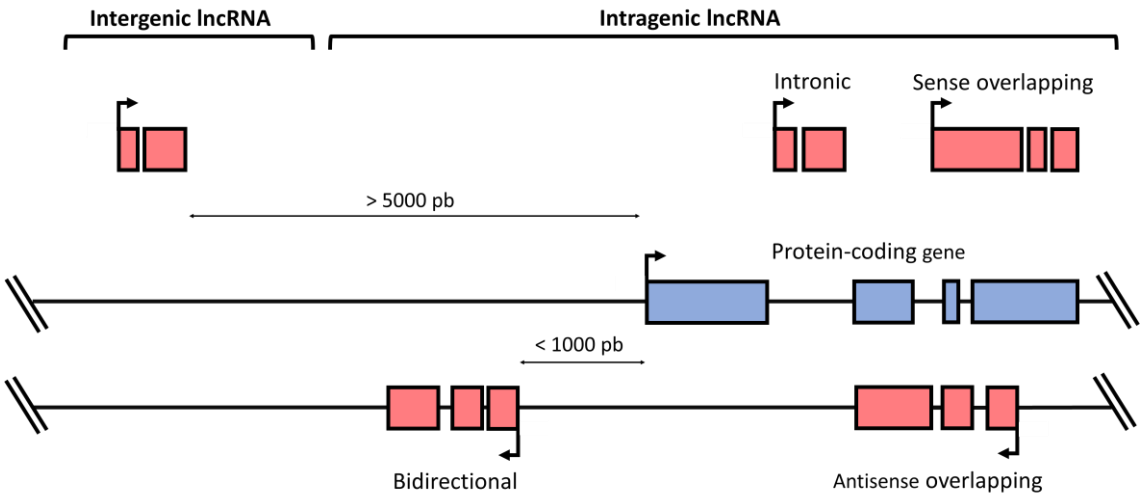

Figure 12: General classification of lncRNAs based on their location. Red: lncRNA and blue: protein-coding gene.

Research methods and strategies to study lncRNA are still in its infancy. Moreover, the analysis of the functional roles of the lncRNAs is a complex process and normally involve 5 strategies (Baker, 2011; Wu and Du, 2017):

1- LncRNA new species identification: LncRNA discovery is difficult because of tissue specificity and low expression levels. Nevertheless, many kinds of methods still exist for identifying new lncRNAs, such as microarray, RNA-seq, Smart-Seq, etc.

2- Bioinformatic analysis: Using lncRNA databases such as (lncRNAdb, NONCODE, FANTOM, LNCipedia, etc.) in order to gain knowledge about the interested lncRNAs.

3- Subcellular localization: using subcellular fractionation protocols or fluorescence in situ hybridization (FISH) to visualize the subcellular localization of a certain lncRNA.
4- Gain or loss of function: Over-expression or knock down of the lncRNA by lentivirus, GAPMERS, shRNA or siRNA, to gain insights into the functions of the lncRNA.
5- Molecular interaction: Using methods such as RNA immunoprecipitation, chromatin isolation by RNA purification (ChIRP), Splikerette-PCR among others, to analyze the interactions of the interested lncRNA among other RNAs, and also DNAs and proteins.

Only a small fraction of lncRNAs has known functional activity (Volders et al., 2015). Moreover, recent evidence links the lncRNAs with cellular functions including interactions with promoters and transcription factors, the alternative regulation of the splicing process of RNA transcripts encoding proteins, or epigenetic control of gene expression, stabilizing transcripts encoding proteins and finally, global gene expression regulation by trans-acting control mechanisms (Guil et al., 2012; Taylor et al., 2015). LncRNAs have different mechanisms of action: they can act as scaffold, guide, molecular decoy, miRNA sponge and enhancer RNAs among others (Figure 13) (Bouckenheimer et al., 2016).

Several lncRNAs have been recently associated with important developmental processes such as apoptosis, proliferation, and lineage commitment, making them interesting to study in order to investigate development (Yan et al., 2013; Yerushalmi et al., 2014; Xu et al., 2014). Further comprehension of the biological role of the lncRNAs may increase the knowledge on the vast majority of the procedures associated with human oocyte development and can be a source to find new biomarkers of oocyte quality.

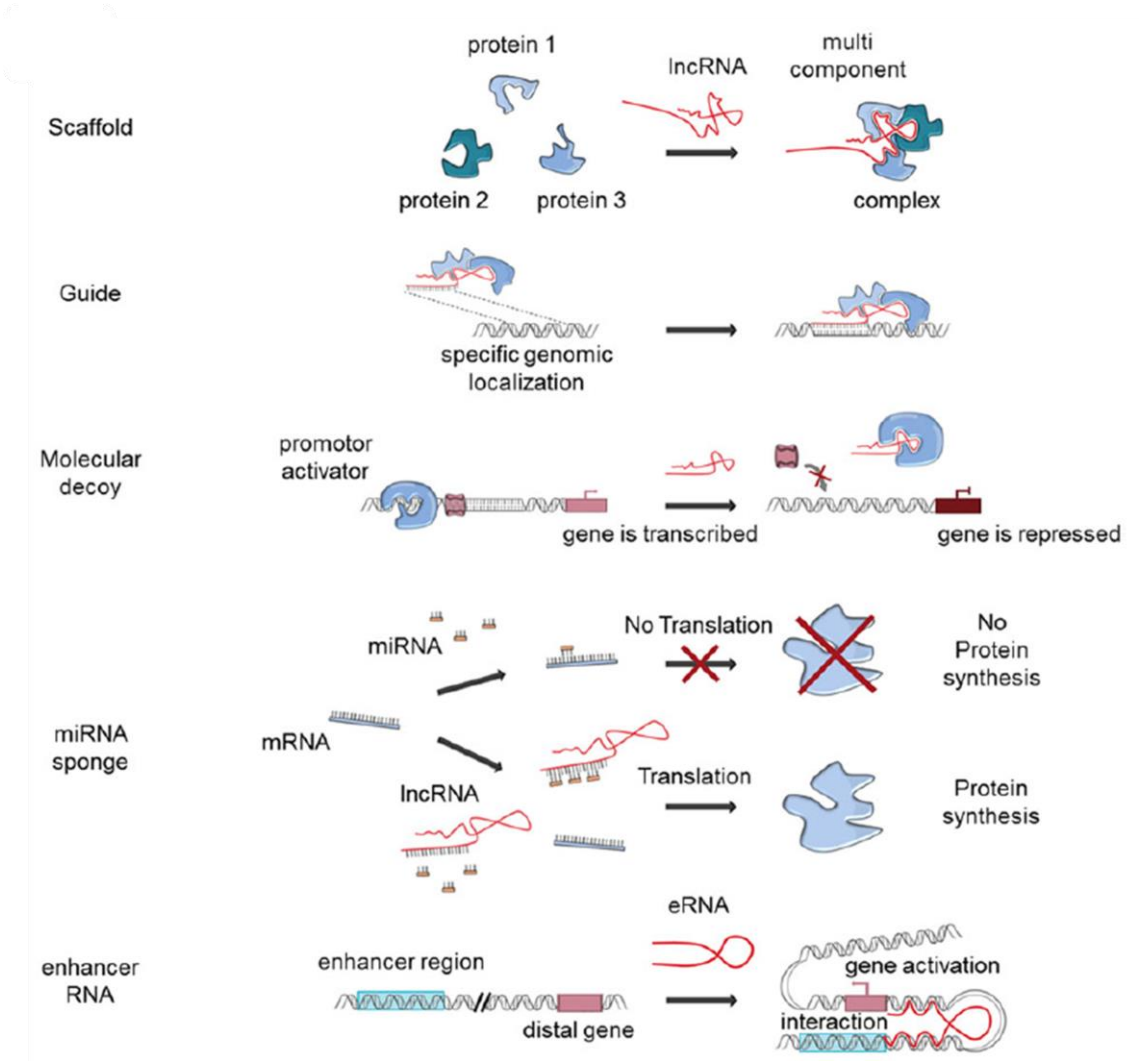

Figure 13: Mechanisms of action of the lncRNAs. Scaffold: lncRNA can serve as adaptors of multiple components. Guide: lncRNA can guide molecules to a specific genomic location via standard base pairing. Molecular decoy: lncRNA can bind to protein complexes and prevent their interaction with their natural targets. miRNA sponge: lncRNA can bind to numerous miRNAs, leading to the active transcription os their mRNA targets. Enhancer RNAs: lncRNA can regulate neighboring gene expression. Obtained from Bouckenheimer et al., 2016.

1.6.4. Alternative splicing (AS)

Another approach that might provide novel information on the molecular mechanisms driving early development, as well as new potential biomarkers of oocyte quality can be the analysis of alternative pre-mRNA splicing (AS).

Classically, transcriptomic analysis of oocytes has focused on gene expression analysis to identify genes involved in the control of oocyte maturation and embryo development (reviewed in Evsikov et al., 2009). As already mentioned, the coding RNA transcripts of the oocyte are accumulated at the Germinal Vesicle (GV) stage. The accumulated transcripts support the final steps of oocyte maturation, where transcription is undetectable, as well as the initial cell divisions of the embryo, until embryonic genome activation at the 4-cell stage (Gosden and Lee, 2010; Vassena et al., 2011). The lack of transcription during final oocyte maturation suggests that gamete fertilization and zygote development depend on a very finely tuned regulation of protein expression, driven by mechanisms that are unrelated to the modulation of transcription rate (Bachvarova et al., 1985; Do et al., 2018). However, the mechanisms involved in human oocytes are poorly known. Among the possible mechanisms, selective degradation of mRNA transcripts is the best understood (Lequarre et al., 2004; Bettegowda et al., 2006; Su et al., 2007). In addition, AS might be also involved in human oocyte transcript regulation (Salisbury et al., 2009; Tang et al., 2011).

AS is a tightly regulated mechanism mediated by the spliceosome, a molecular machine assembled from small nuclear RNAs and approximately 80 proteins that removes introns from a transcribed pre-mRNA, affecting up to 94% of human genes (Modrek and Lee, 2002; Wang et al., 2008). AS may generate several transcript isoforms from a given gene, increasing both transcriptome and proteome complexity. The major mechanisms by which AS generate different isoforms include:

- Cassette-exon or exon skipping, when an exon is retained or skipped from the transcript. This is the most common splicing event in mammals.
- Mutually exclusive exons, when two or more regions are spliced or retained in a coordinated manner.

- Alternative 5' donor site, where the 3' boundary of the upstream exon is changed.
- Alternative 3' acceptor site, where the 5' boundary of the downstream exon is changed.
- Intron retention, when a sequence is not spliced out and is retained in the transcript. This splicing event can change the reading frame, altering the function and localization of the resulting protein isoforms. This is the rarest splicing event in mammals (Figure 14).

These differences might affect the stability of the transcript, its localization or translation. It is now established that a fine control of the isoform balance is required for proper development and adult tissue homeostasis (Yan et al., 2013; Baralle and Giudice, 2017). Moreover, imbalances in the production of specific protein isoforms have been associated with a decreased developmental competence in Xenopus oocytes, where AS defects in certain genes (such as *MCAK* and *NDC80*) result in faulty meiotic spindle assembly, and increased rates of aneuploidy in embryos (Grenfell et al., 2016). In mouse, the deletion of the Serine and Arginine Rich Splicing Factor 3 (*SRSF3*), which has critical roles in the regulation of pre-mRNA splicing, compromises the oocyte capacity to conduct germinal vesicle breakdown (GVBD) and consequently entry into meiosis (Do et al, 2018). This suggest that AS is also needed for GVDB in mouse. Besides, these studies in animal models indicate that the oocyte requires a controlled AS mechanism to acquire not only the correct transcript abundance but also the correct isoforms. Nevertheless, information on the spliced mRNA isoforms in human oocytes is very scarce. The study of the different AS in human oocytes could identify novel biomarkers of oocyte quality and could aid in the understanding of the processes involved in oocyte maturation.

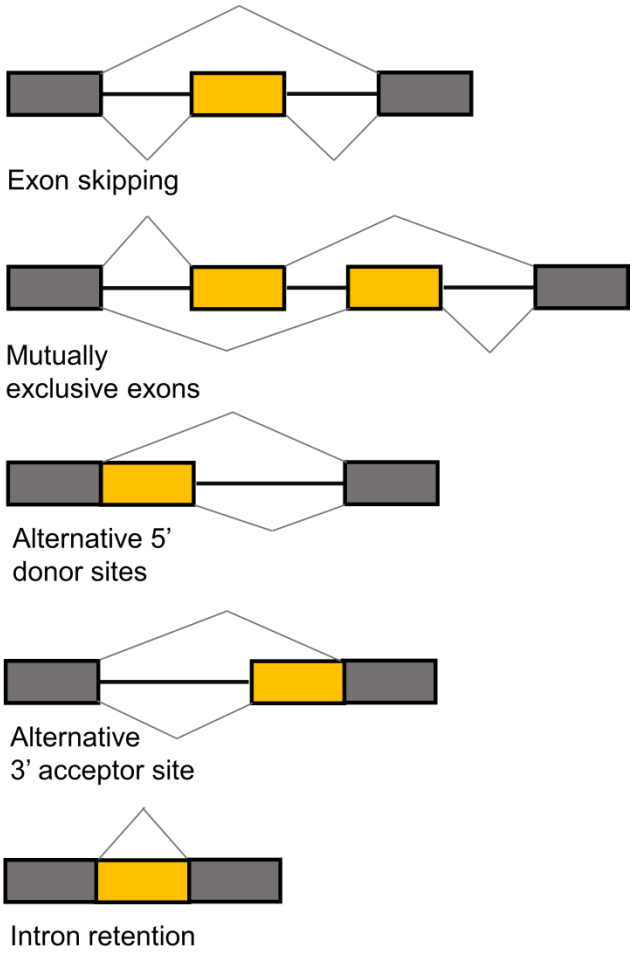

Figure 14: Traditional classification of basic types of alternative RNA splicing events. Exons are represented as grey and yellow blocks, introns as lines in between.

1.6.5. Non-invasive methods for oocyte quality biomarkers identification

The procedures used to evaluate most of the oocyte intrinsic predictors, although providing fundamental knowledge for establishing objective criteria of oocyte quality, fail to preserve oocyte viability and, thereby, are unpractical for clinical practice. Therefore, the identification of factors related to developmental capacity outside the oocyte itself could provide extra information on the status of the oocyte. With this aim, numerous transcriptomic, and more recently, proteomic and metabolomic studies have been conducted in the follicular fluid and follicular cells (granulosa and cumulus cells) in order to find non-invasive biomarkers of oocyte quality (Xia and Younglai, 2010; Piñero-

Sagredo et al., 2010; Ambekar et al., 2013; Fragouli et al., 2014; Zamah et al., 2015; Shen et al., 2017; Karaer et al., 2019; Montani et al., 2019).

Follicular fluid

Human follicular fluid is a complex body fluid that constitutes the microenvironment of developing follicles in the ovary. Transcriptomic studies identified some possible biomarkers that could predict oocyte quality. For instance, the expression of insulin-like factors was positively correlated by many authors with oocyte quality (Oosterhuis et al., 1998; Fried et al., 2003; Nicholas et al., 2005). Proteomic studies have identified novel proteins that have not been described previously, mainly belonging to categories related to growth factors, signaling molecules, hormones and immune defense, such as ODF3L2, MYOZ2, PLAC4, SPOCK3, TKTL-2, etc. (Ambekar et al., 2013; Shen et al., 2017). Results from metabolomic studies indicate that carbohydrate, amino acid and lipid metabolism have a high influence in the oocyte developmental competence acquisition (Collado-Fernandez et al., 2012). Nevertheless, it is not the analysis of the follicular fluid but the analysis of the follicular cells (granulosa and cumulus cells) what is considered the best non-invasive strategy available today for the identification of surrogate markers of oocyte competence, since follicular cells are in close contact with the oocyte and have bidirectional communication.

Analysis of cumulus granulosa cells (CCs)

As it has been explained in previous sections, the oocyte-CCs interaction is crucial before and after the LH surge. Before the LH surge, the follicular cells are differentiated into CCs that surround the oocyte and mural cells, which are located in the outer part of the

follicle. In the recent years, remarkable progress has been made in the investigation of oocyte–granulosa cell interaction and of oocyte control of CCs function (Sugiura et al., 2005; Gilchrist et al., 2006; Diaz et al., 2007). This regulated interaction seems to be mediated by GDF9, BMP15 and FGF8 signaling pathways, together with the effects of the FSH which determines CCs phenotype and functionality (Diaz et al., 2007). Moreover, numerous studies have been conducted in humans with the objective of identifying cumulus biomarker genes as prognosis tools for oocyte quality. As an example, *PTX3* expression was positively correlated with oocyte competence in pooled CCs (Zhang et al., 2005). Another study performed with pooled CCs also found 5 genes (*CYPI9AI, SERPINE2, CDC42, FDXI* and *HSD3BI*) positively correlated with pregnancy (Hamel et al., 2008). Studies performed with CCs from individual oocytes have also found various genes positively associated with oocyte and embryo competence (Cillo et al., 2007; Hamel et al., 2010; Huang and Wells, 2010; Parks et al., 2016). Some groups also reported genes associated with negative oocyte competence (van Monfoort et al., 2008; Anderson et al., 2009). Moreover, Assou and colleagues identified 45 possible biomarker genes related to global processes such as ion binding, transcription, cell communication and adhesion and regulation of cellular processes (Assou et al., 2008). Remarkably, no common biomarkers stand out among all these studies. Undoubtedly, further investigation of the expression profile of CCs will enhance the comprehension of the mechanism of oocyte maturation and reveal reliable predictors of oocyte quality. One approach can be the study of the transcriptional profile of the CCs of an aging ovarian tissue and its association with ovarian reserve and oocyte maturation rates, since they can provide a better understanding of how transcriptional changes related to aging in human ovarian tissues, could be used as a non-invasive marker for developmental competence of the oocyte quality.

As it has been described in this introduction, an extraordinary effort has been made in order to increase the comprehensive understanding of the molecular determinants of oocyte quality. Nevertheless, despite that continuous research, oocyte quality evaluation in IVF clinics is mainly conducted at the morphological level due to the lack of unreliable biomarkers of oocyte quality. Therefore, there is an unmet need for robust and reliable biomarkers of oocyte quality and embryo development in order to expand the knowledge of the processes involved in human oocyte maturation and improve fertility and pregnancy outcomes in ART cycles.

2. OBJECTIVES

The main objective of this thesis is to explore new possibilities for the identification of oocyte quality biomarkers at the molecular level in order to better understand the oocyte and how its developmental competence can be improved. To achieve this main aim, three specific objectives are considered:

- Objective 1: Identify important genes for oocyte quality by the analysis of the transcriptional profiles and post-transcriptional mechanisms (alternative splicing) present in *in vivo* matured MII oocytes and evaluate their regulation by the comparison with GV stage oocytes.
- Objective 2: Identify non-invasive biomarkers for oocyte developmental competence by the evaluation of the association between the expression analysis of different aging markers in human cumulus cells, the ovarian reserve and the oocyte maturation rates.
- Objective 3: Analyze whether oocyte vitrification affects oocyte developmental competence by comparing the reproductive outcomes of fresh and vitrified donor oocytes from the same stimulation cycle.

3. MATERIALS AND METHODS

3.1. ETHICS

Approval to conduct these studies was obtained from the Ethical Committee for Clinical Research of Clínica Eugin. All procedures performed were in accordance with the ethical standards of the institutional research committees and with the 1964 Helsinki declaration of the Ethical principles for medical research involving human subjects, as revised in 2013 in Fortaleza (World Medical, 2013). Written informed consents to participate were obtained from all participants prior to their inclusions in the prospective studies (objectives 1 and 2).

3.2. ASSISTED REPRODUCTION TECHNIQUES

The following techniques were performed by the clinical staff from Clínica Eugin, not by me, but are helpful in order to understand all the aspects of this work.

Study population – Oocyte donors

All oocyte donors were between 18 and 35 years old (maximum age for oocyte donation in Spain), had a body mass index (BMI) between 18 and 30 kg/m^2, normal karyotype and no evidence of systemic or reproductive conditions. They were all non-carrier of clinically relevant alleles for cystic fibrosis and fragile X. All oocyte donors tested negative for human immunodeficiency viruses (HIV), sexually transmitted diseases and both hepatitis B and C.

Donor ovarian Stimulation

Controlled ovarian stimulation was induced with either recombinant FSH (GONAL-f®) (Merck Serono Europe Limited) or highly purified hMG (Menopur®, Ferring S.A.U., Spain), and pituitary suppression achieved with GnRH antagonist (Cetrotide®, 0.25 mg) (Merck-Serono Europe Limited, UK). Trigger criterion was 3 or more follicles ≥18 mm, ovulation was triggered with 0.3 mg of GnRH agonist (Decapeptyl®, Ipsen Pharma S.A., Spain).

Cumulus cells manipulation and processing

Cumulus oocyte complexes (COCs) were collected by transvaginal ovum pick up (OPU) 36 hours after trigger. COCs were then released from the follicle aspirate and were placed in bicarbonate-buffered medium containing human serum albumin (IVF®, Vitrolife, Göteborg, Sweden). COCs were incubated at 37ºC, 95% relative humidity and 6% CO_2 for thirty minutes before cumulus cell removal (denudation). Denudation was achieved by exposure to 80 IU/ml of hyaluronidase (Hyase-10X®) (Vitrolife, Goteborg, Sweden) in buffer medium (G-MOPS® PLUS, Vitrolife), followed by gentle pipetting. Once the CCs were mechanically separated from the oocytes, were pooled, resuspended in RNA lysis buffer (Cryoprotect II, Nidacon International Göteborg, Sweden), and immediately processed for total RNA extraction.

Oocyte manipulation

Donor oocytes were used either fresh or vitrified. Vitrification was performed using Kuwayama's method 2 hours after ovum pick up (Kuwayama, 2007). Briefly, oocytes

were placed in 'equilibrium solution' (7.5% (v/v) ethylene glycol, 7.5% DMSO and 20% synthetic substitutive serum in TCM 199) for 12–15 minutes. Oocytes were then moved for 1 minute in the 'vitrification solution' (15% of ethylene glycol, 15% DMSO and 0.5 M sucrose). Cryopreservation of oocytes was conducted in liquid nitrogen using a Cryotop vitrification open system (KITAZATO BIOPharma Co., Ltd, Fuji, Japan).

For warming, the straw was rapidly placed in warming solution containing 1 M sucrose at 37ºC for 1 minute. The oocytes were then moved for 3 minutes in a solution with 0.5 M sucrose and rinsed for 6 minutes in TCM 199 medium with serum. Finally, oocytes were cultured in buffered medium containing hyaluronan (G-1®, Vitrolife) at 37ºC, 95% relative humidity and 6% CO_2 until insemination.

After warming, oocytes used for research, were left for 2 hours at 37ºC and 6% CO_2, to allow for reassembly of the metaphase plate (Bromfield et al., 2009). The zona pellucida was removed using Pronase (Roche Diagnostics, Spain) and oocytes were immediately and individually placed in 45 µl of a Proteinase K-based lysis buffer (20 mM DTT, 0.5% SDS, 1 µg/µl proteinase K, 10 mM Tris.HCl, pH 7.4), incubated at 65ºC for 15 minutes, and stored at -80ºC until use (Gonzalez-Roca et al., 2010).

Sperm manipulation

Semen samples were either from donors (frozen) or normozoospermic partners (frozen or fresh). Semen freezing was performed in 1:1 (v/v) with cryoprotectant (Sperm CryoProtect II®, Nidacon, Sweden) and thawed on the day of ICSI. All semen samples underwent capacitation by swim-up (Wong et al., 1986) prior to ICSI.

Insemination

All oocytes were inseminated by intracytoplasmic sperm injection (ICSI). Fertilization was assessed 16-19 hours post ICSI by visualization of two pronuclei and two polar bodies. The best quality embryos (Coroleu et al., 2006) were transferred to the uterus of the recipient on days 2 to 5 of embryo culture, depending on medical indication and patient preference.

Endometrial preparation

The recipient endometrium was prepared with either 6 mg/day of oral estradiol valerate, (Progynova, Bayer Hispania S.L., Spain), or 150 µg/day transdermal estradiol hemihydrate (Estradot Novartis Pharma GmbH, Germany). The day after OPU in donors, recipients were administered with 400 mg/12 hours of micronized vaginal progesterone (Utrogestan®, SEID SA, Spain or Progeffik®, Effik, Spain). This treatment continued until the first assay of ßhCG in blood 14 days after embryo transfer. In case of a positive pregnancy test, the treatment was prolonged until week 12 of pregnancy.

Pregnancy

A biochemical pregnancy was defined when ßhCG levels were higher than 5 IU in serum 15 days after the ET. Clinical pregnancy was defined when a sac with a visible embryo with beating heart 7 weeks after last menstrual period (LMP) was observed. Ongoing pregnancy was a normally progressing pregnancy by ultrasound 12 weeks after LMP.

3.3. SEARCH FOR NEW TRANSCRIPTOMIC MARKERS OF HUMAN OOCYTE QUALITY

RNA extraction and cDNA synthesis

Total RNA extraction and amplification from human oocytes were based on the Pico-Profiling protocol and successive improvements for single oocyte use (Gonzalez-Roca et al., 2010; Vassena et al., 2011). Pico-profiling faithfully amplifies the total RNA from as little as 10 somatic cells, or 1 MII oocyte, with a level of false positive signal in downstream analysis that is equivalent to that obtained without an amplification step. Briefly, RNA was purified from individual oocytes using RNA Clean XP bead suspension (Agencourt Bioscience, La Jolla, CA, USA) and eluted in 20 µl water. The RNA preparation was used for library preparation and amplification by Whole Transcriptome Amplification (WTA2, Sigma-Aldrich, Spain). SYBRGreen (Sigma-Aldrich, Spain) was added to the amplification reaction, which was performed in a CFX Real-time instrument (Bio-Rad, CA, USA) to monitor amplification yield. The amplification reaction was stopped when the SYBRGreen signal reached a plateau, and cDNA was purified and quantified on a Nanodrop ND-1000 spectrophotometer (Thermo-Fischer, MA, USA). A second round of amplification was performed from 10 ng of cDNA; 8 µg cDNA (3.2 µg from the first round and 4.8 µg from the second) were subsequently fragmented by DNAseI and biotinylated by terminal transferase (GeneChip Mapping 250K Nsp assay kit; Affymetrix, CA, USA). Biotin-labeled cDNA was hybridized on an Affymetrix GeneChip Human Transcriptome Array 2.0 (HTA 2.0). This GeneChip allows for analysis of more than 245,000 transcripts, covering 44,699 protein coding gene models and more than 40,000 transcripts covering 22,829 non-coding gene models. Moreover, to ensure uniform coverage of the transcriptome, HTA 2.0 was designed with approximately ten probes per exon and four probes per exon-exon splice junction.

Total RNA isolation from Human embryonic kidney 293 easy to transfect cells (HEK293-T) and cumulus cells (CCs) was conducted with the RNeasy Mini Kit (Qiagen, Germany) according to the manufacturer's protocol. Total RNA was quantified using Quawell by measurement of absorbance at λ=260 nm and was stored individually at -80ºC until all samples included in the study were collected. Once all the samples were obtained, equal amounts of total RNA of each sample were retro-transcribed to cDNA with the SuperScriptTM IV First-Strand Synthesis Kit (Invitrogen, ThermoFisher, USA) using random hexamers following the manufacturer's protocol. The reverse transcription reaction was performed in a CFX96 Real-Time PCR system (Bio-Rad).

Microarray hybridization and raw data processing

Each array was hybridized, washed and scanned according to the manufacturer's instructions. The washing and staining were performed in a GeneChip® Fluidics Station 450, and the scanning was performed in a GeneChip® Scanner 3000, according to Affymetrix specifications. The scanned images were transformed into intensities by GeneChip® Command Console® Software (AGCC, Affymetrix). RMA normalization and probeset signal summarization was applied using Expression Console software (Affymetrix) version 1.4.1.

Microarray data for mature MII oocytes and non-matured GV oocytes were deposited at GEO under GSE87201.

Alternative splicing analysis (AS)

Human exon array CEL files for 4 non-matured oocytes (GV) and 12 in vivo matured MII oocytes were analyzed for gene expression (fold change >|2| and raw p-value <0.05)

and AS using AltAnalyze software version 2.1.0 (Emig et al., 2010). Probe-level signals were summarized to estimate both exon and gene expression levels in the samples. Briefly, raw CEL microarray data were normalized using the FIRMA method implemented in AltAnalyze, followed by the identification of AS isoforms evaluated in non-differentially expressed genes using ASPIRE and FIRMA algorithms with all of the default parameters of AltAnalyze. Differentially expressed exons (AS events) were determined by a bioinformatic calculation based on the relative intensity of each exon in reference to the exons that surround it and to the probes that identify junctions of non-consecutive exons.

Quantitative PCR (qPCR)

Array validation (gene expression and AS) was performed by qPCR analysis using 5 ng (in triplicates) of the oocyte cDNA libraries previously constructed and hybridized. For the lncRNA knock-down experiments 10 ng of HEK293-T in triplicates were used. For the aging markers expression analysis in CCs, 4 ng of CCs cDNA (also in triplicates) were used. Selected transcripts were quantified by SYBRgreen fluorescence (Bio-Rad) using a CFX Real-Time PCR system (Bio-Rad). The program used in each qPCR run consisted of an initial denaturalization step of 30 seconds at 95ºC, and 40 cycles of 95ºC for 5 seconds and 60ºC for 30 seconds. Intra- and Inter-assay reproducibility and error measurement was assessed by adding a common reference sample in each qPCR plate. Baseline correction, threshold setting and relative expression were performed using the automatic calculation of the CFX Manager Software (Bio-Rad). The software includes algorithms generated to analyze gene expression results using multiple reference genes (Vandesompele et al., 2002). To determine the best normalization set of genes four different algorithms (geNorm, BestKeeper, NormFinder and the comparative Ct method)

were applied to qPCR data over 11 putative reference genes (e.g. *ACTB, GAPDH, GUSB, PGK1, RPLP0, SDHA, TBP, UBC, YWHAZ, 18S* and *DNMT1*). The corresponding normalization factor (Ref) was then used to correct the relative gene expression values: (ΔCq = [Cq (gene A) - Cq (Ref)]). The following formula was applied to do ΔCq analysis: normalized target gene expression level = $2^{-(\Delta Cq)}$. All primer sequences are specified in Table 1.

3.4. SPECIFIC TECHNIQUES USED FOR THE FUNCTIONAL CHARACTERIZATION OF LNCRNA CANDIDATES

HEK293-T cell culture

Human embryonic kidney 293 easy to transfect cells (HEK293-T) were purchased from the American Type Culture Collection (ATCC, Manassas, VA, USA). HEK293-T cells were grown in Dulbecco′s Modified Eagle′s Medium (DMEM) with GlutaMAX™ (Gibco, ThermoFisher, USA). Media was supplemented with 10% fetal bovine serum (FBS), 1 mM sodium pyruvate, penicillin (100 IU/ml) and streptomycin (50 mg/ml). Cells were kept at 37ºC and media was changed every other day.

LncRNA primers design

Almost all lncRNAs analyzed were not previously described in literature and were not previously annotated in the common reference databases (Ensembl, FANTOM, NONCODE, NCBI, LNCipedia, lncRNAdb, etc). Therefore, to design the lncRNA primers, the genomic sequence of each lncRNA was linked to an Affymetrix 2.0 Array cluster of probes, based on its exons and introns profile. Then, primers were designed

within the zones mapped by the cDNA (when it was possible) or within the zones mapped by the array probes.

Polymerase chain reaction (PCR)

All PCR were conducted according to the Phusion HF DNA Polymerase reaction protocol (New England Biolabs, Ipswich, USA). The amplification reaction was performed in a CFX96 Real-Time PCR system (Bio-Rad).

Electrophoresis

In 50 ml Tris-acetate-EDTA buffer (TAE) 1X agarose gel (1% w/v gel) were charged 5-25 µl of the DNA samples and run in a voltage of 80 V for 1 hour. The markers used (100 pb and 1 Kb) were from Thermo Scientific (Waltham, USA).

Gel Extraction and purification

For gel extraction and prurification, the QIAquick gel extraction kit from (Qiagen, Germany) was used. DNA fragments were excised from the agarose gel with a scalpel and were weighted. 3 volumes of Buffer QG were added to 1 volume gel and the mix was incubated 10 minutes at 50ºC on the heated shaker. 1 volume isopropanol was added and the samples were mixed gently. QIAquick spin columns were placed in 2 ml collection tubes. Samples were applied to the column and centrifuged for 1 minute. Flow-through was discarded and the QIAquick columns were placed back into the same tube. 500 µl Buffer QG were added to the QIAquick columns and centrifuged for 1 minute. Flow-through was discarded and the QIAquick columns were placed back into the same tubes.

Then, samples were washed with 750 µl buffer PE for 5 minutes at room-temperature (RT). A centrifugation of 1 minute was conducted and the flow-through was discarded. This centrifugation was repeated again to remove residual wash buffer PE. Finally, the spin columns were placed in a 1.5 ml micro-centrifuge tube and the DNA was eluted in 30-50 µl water, depending on the amount of pellet observed.

Restriction enzyme digestion

All restriction enzyme digestions were performed as follows: in a total volume of 50 µl, 10 units of the specific restriction enzyme were mix with 5 µl 10x Buffer and 1 µg of DNA. The mix was then incubated 1 hour at 37ºC.

Ligation

The ligation reaction was conducted with the T4 DNA Ligase protocol from New England Biolabs (Ipswich, USA). Briefly, in a 20 µl total reaction volume, 2 µl of 10x T4 DNA Ligase was mixed with 0.06 pmols insert DNA, 0.02 pmols vector DNA and 1 ul T4 DNA ligase. The reaction was then incubated at 16ºC overnight (O/N).

Transformation

For transformation, 5 µl of ligation reaction were mixed with 50 µl One Shot TOP10 chemically competent *E. Coli* competent cells (Invitrogen, ThermoFisher, USA). The mix was placed on ice for 30 minutes followed by a 45 seconds heat-shock step at 42ºC on a water bath. After these 45 seconds, the samples were again placed on ice for 5 minutes. Then, 500 µl of recovery medium (LB) was added to each tube and the mix was left at

37ºC, 225 rpm on the shaker for 1 hour. After 1 hour, the solution was rubbed in 2x100 µl and 300 µl in 3 different petri-dishes with LB and Amp. Finally, the petri-dishes were incubated O/N at 37ºC.

Miniprep

Despite trying first with a "homemade" kit, the plasmid Mini kit from QIAGEN was finally used, since a better plasmid purification was obtained (no RNA contamination was observed).

The plasmid Mini kit from QIAGEN protocol was as follows: 1.5 ml of bacterial culture were centrifuged at 16,000 x g for 5 minutes at 4ºC to pellet cells. Flow-through was discarded and cells were re-suspended in 0.3 ml of buffer P1. Then, 0.3 ml of buffer P2 was added. The solution was mixed gently and incubated at RT for 5 minutes. After the incubation, 0.3 ml of buffer P3 was immediately added and the solution was vigorously mixed by inverting the tubes 4-6 times. Samples were incubated 5 minutes on ice and centrifuged at 16,000 x g for 10 minutes at 4ºC. Supernatant was applied to a QIAGEN-tip previously equilibrated with 1 ml buffer QBT. QIAGEN-tip was washed with 2 x 2 ml Buffer QC. DNA was eluted with 0.8 ml buffer QF into a clean 1.5 ml vessel. Then, DNA was precipitated by the addition of 0.56 ml RT isopropanol. Solution was mixed gently and centrifuged at 16,000 x g for 30 minutes at 4ºC. Flow-through was discarded and pellets were washed with 1 ml 70% ethanol. A final centrifuge was conducted at 16,000 x g for 10 minutes. Flow-through was discarded and pellets were finally re-suspended in 30-50 µl miliQ water, depending of the amount of pellet seen.

Midiprep

Plasmid Midi kit from QIAGEN was used. 50 ml of bacterial culture were centrifuged at 6,000 x g for 15 minutes at 4ºC to pellet cells. Flow-through was discarded and cells were re-suspended in 4 ml of buffer P1. Then, 4 ml of buffer P2 was added. The solution was mixed gently and incubated at RT for 5 minutes. After the incubation, 4 ml of buffer P3 was immediately added and the solution was vigorously mixed by inverting the tubes 4-6 times. Samples were incubated 15 minutes on ice and centrifuged at 5,500 x g for 30 minutes at 4ºC. This centrifugation step was conducted twice. Supernatant was applied to a QIAGEN-tip 100 previously equilibrated with 4 ml buffer QBT. QIAGEN-tip was washed with 2 x 10 ml Buffer QC. DNA was eluted with 5 ml buffer QF into a clean 15 ml vessel. Then, DNA was precipitated by the addition of 3.5 ml isopropanol. Solution was mixed gently and centrifuged at 5,500 x g for 30 minutes at 4ºC. Flow-through was discarded and pellets were transferred into a 1.5 ml micro-centrifuge tube with 1 ml 70% ethanol. A final centrifuge was conducted at 15,000 x g for 10 minutes. 1 ml 70% ethanol was added again and the previous centrifuge was repeated. Flow-through was discarded and pellets were finally re-suspended in 200 µl miliQ water.

Poly(A) tailing reaction

To perform the poly(A) tailing reaction, the Terminal Deoxynucleotidyl Transferase, recombinant enzyme (rTDT) was used (Invitrogen, ThermoFisher, USA). In a 25 µl total reaction volume, 1 µg of purified DNA was mixed with 10 ul 5x Tailing Buffer, 1 µl dATP (Thermo scientific, Waltham, USA) and 1 µl (15 units) of rTDT. The mix was incubated 5 minutes at 37ºC and then 5 minutes at 65ºC to inactivate the rTDT.

Plasmid transfection

For HEK293-T transfection, Fugene HD transfection reagent (Promega, Madison, USA) was used. The day before transfection, HEK293-T cells were plated at 30-40% confluency. The day of transfection, Fugene HD transfection reagent was mixed with the DNA at a ratio 3:1. Transfection efficiency was analyzed with a fluorescence microscope 48 hours after transfection.

lncRNA subcellular fractionation

For the subcellular localization of the selected lncRNA candidates (*lncANXA5* and *RP11-809N8.2-001*) in HEK293-T cells, several variations of the protocol were tested in order to optimize the technique and obtain clean cytoplasm and nuclear fractions. Various concentrations of HEK293-T cells were used as starting material. Moreover, different lysis buffers, with or without a non-ionic detergent (10% NP-40), and various incubation and centrifugation times were tested. The efficiency of the subcellular fractionation was assessed by western blot and qPCR. Subcellular fractionation was optimized at the protein level using the mouse monoclonal anti-Histone H3 tri methyl K27 antibody (H3K27) (Abcam, Cambridge, UK) as a nuclear marker and the mouse monoclonal anti α-Tubulin antibody (Sigma-Aldrich, Spain) as a cytoplasm marker. At the transcript level the lncRNAs *MALAT1* and *NEAT1* were used as nuclear markers and *GAPDH* and *DANCR* were used as cytoplasm markers (primers detailed in Table 1).

The protocol that showed the best results was the one where $2x10^6$ HEK293-T cells were used as starting material and were lysed after 20 minutes incubation with hypotonic buffer (20 mM Tris-HCl [pH 7.4], 10 mM NaCl and 3 mM $MgCl_2$) without detergent (NP-40).

Briefly, $2x10^6$ HEK293-T cells were plated in a 6 well plate in 3 ml of complete growth medium (DMEM) and incubated O/N at 37ºC. The day after, DMEM medium was removed and cells were washed with 2 ml cold PBS 1x. Then, cells were lysed with 500 µl Hypotonic Buffer and were incubated on ice for 20 minutes. Cells were de-attached from the plate by pipetting up and down and were transferred into a 1.5 ml Eppendorf. The homogenate was centrifuge 5 minutes at 700 x g and 4ºC for DNA precipitation. After the centrifugation, the supernatant, containing the cytoplasmic fraction was separated from the nuclear pellet and was stored at -80ºC. The remaining pellet was washed twice with 500 µl Hypotonic Buffer and was centrifuged 5 minutes at 700 x g and 4ºC discarding the supernatant each time.

Total protein extraction from cell culture

HEK293-T cells were washed twice with ice-cold phosphate buffered saline buffer (PBS) and incubated for 30 minutes on ice with RIPA buffer containing 50 mM Tris (pH 8.0), 150 mM sodium chloride, 1% Triton X-100, 0.5% sodium deoxycholate, 0.1% sodium dodecyl sulphate (SDS), 1% protease inhibitor cocktail (Thermo Fisher, USA) and 1% phosphatase inhibitor cocktail (Thermo Fisher, USA). Cells were vortexed every 5 minutes and centrifuged at 13000 x g for 5 minutes at 4ºC. Supernatants were recovered and the protein content was quantified by the BCA kit (Pierce Biotechnology, Waltham, USA).

Western Blot

Western blot analysis was carried out size-separating equal amounts of protein by electrophoresis on SDS polyacrylamide gels and electroblotting them onto Immobilon-P

transfer membranes (Millipore, Burlington, USA). The membranes were blocked with 5% of non-fat dry milk in PBS with 0.1% Tween 1 hour at RT and then incubated with specific primary antibodies O/N at 4ºC. Next, membranes were treated with the appropriate secondary antibody for 1 hour at RT. All blots were visualized on Super RX-N Fuji medical X-Ray films (Fujifilm, Spain) with chemiluminescence detection using Westar ECL-SUN (Cyanagen, Bologna, Italy).

siRNA and GAPMERS transfection

In vitro transfection conditions for gene knockdown by gapmers and siRNAs were optimized using *GAPDH* siRNA (Silencer™ Select; Ambion Applied Biosystems, Austin, TX) and *MALAT1* gapmer (Exiqon, Qiagen, Germany) as positive controls and scrambled RNAs as negative controls (Silencer™ Select Negative Control No. 1 siRNA, Ambion Applied Biosystems, Austin, TX) and (LNA™ longRNA Gapmer, Negative control A, Exiqon, Qiagen, Germany). Transfections were conducted via Lipofectamine™ RNAiMAX Transfection reagent (Invitrogen, ThermoFisher, USA) at different molarities (1 nM, 5 nM, 10 nM and 50 nM).

A total of 7 gapmers (3 for *lncANXA5* and 4 for *RP11-809N8.2-00*1) and 12 silencer select siRNAs (5 for *RELT*, 3 for *ANXA5*, 2 for lncANXA5 and 2 for RP11-809N8.2-001) were tested (Table 2).

The final protocol used was as follows: one day before transfection, 120.000 HEK293-T cells were plated in 1 ml of complete growth medium (DMEM) without antibiotics in a 12-well plate in order to reach 30-50% confluency at the time of transfection. The following day, for each well to be transfected, RNAi duplex-Lipofectamine™ RNAiMAX complexes were prepared. For that, Lipofectamine™ RNAiMAX was diluted

3/50 in Opti-MEM medium (ThermoFisher, Waltham, MA, USA) for a total volume of 100 µl. The siRNA/gapmer was also diluted to the required molarity in OptiMEM medium (100 µl total volume). Then, the diluted siRNA/gapmer was combined with the diluted Lipofectamine™ RNAiMAX (1:1 ratio) and was incubated 15 minutes at RT. Finally, siRNA/Gapmer-Lipofectamine™ RNAiMAX complexes were added to the wells containing cells and incubated at 37ºC in a CO_2 incubator for 48 hours. Transfection efficiencies were evaluated by qPCR 48 hours post-transfection.

Northern Blot

To visualize the selected *lncANXA5*, the DIG Northern Starter Kit (Roche, Switzerland) was used. To prepare the DNA template, the lncRNA was amplified from HEK293-T cDNA by using the primers described in Table 1. PCR conditions were as follows: denaturation at 98ºC for 30 seconds, followed by 35 cycles of amplification (98ºC for 5 seconds, 57ºC for 30 seconds and 72ºC for 30 seconds) and an elongation step at 72ºC for 10 minutes. The amplified DNA fragment from the lncRNA was independently ligated to the PT7 vector and mixed with *E. Coli* competent cells for transformation. Then, the ligated vector (PT7 vector + lncRNA fragment) was purified and linearized with the SpeI restriction enzyme. The antisense transcript covering the respective full-length of the lncRNA and internally labeled with digoxigenin-UTP was synthesized from the linearized vector containing the lncRNA sequence (1 µg) according to the DIG-RNA labelling protocol provided by Roche Diagnostics, Mannheim, Germany.

The formaldehyde gel preparation, RNA transfer and fixation and the hybridization and detection sections of the northern blot were conducted according to the Northern Starter Kit protocol. Briefly, 1 µg of denatured total RNA was loaded on a formaldehyde gel

(2%) and was ran at 4 v/cm during 4.30 hours. RNA samples were then transferred by capillary from the gel to a nylon membrane positively charged O/N. The day after, UV-crosslinking was conducted to fix the RNA samples to the nylon membrane. For hybridization, 15 ml of pre-heated hybridization solution (termed 'DIG Easy Hyb Granules', Roche Diagnostics) were added to the membrane with the DIG-RNA labelled probe (100 ng/ml) and were placed in a hybridization tube. Hybridization was conducted O/N at 68ºC under slow rotation in a hybridization oven. Finally, immunological detection was performed according to the instructions of the DIG Northern Starter Kit (Roche Diagnostics). Super RX-N Fuji medical X-Ray films (Fujifilm, Spain) were exposed to the membrane for chemiluminescence detection (usually 20–45 minutes).

Rapid amplification of 5' complementary DNA ends (5'RACE)

Total RNA from HEK293-T (5 µg) was mixed with 1 µl reverse gene-specific primer (10 µM) and 2 µl of 10 mM dNTPs in a 12 µl total reaction volume. The RNA and the primer were denatured by incubating 5 minutes at 65ºC and the first strand cDNA synthesis was performed following the Cloned AMV first strand synthesis kit protocol (Invitrogen, ThermoFisher, USA). A poly(A) tail was then appended to first-strand cDNA products. Two rounds of amplification using <250 ng of DNA were then conducted. The first round was conducted with a universal hybrid primer that contains an adaptor sequence and an oligo(dT) that binds to the poly(A) tail of our transcripts, one forward primer (Q_0) that binds to the adaptor sequence and a gene-specific primer (GSP) that binds to the transcript of interest. The second round was conducted to reduce the yield of non-specifically amplified products obtained after only 1 round of amplification. For that, a second primer that binds to a 3' region of the adaptor (Q_1) and the same gene-specific primer were used. Primer sequences are specified in Table 1. In both rounds, PCR conditions were as

follows: denaturation at 98ºC for 30 seconds, followed by 35 cycles of amplification (98ºC for 5 seconds, 60ºC for 30 seconds and 72ºC for 2 minutes) and an elongation step at 72ºC for 10 minutes (Figure 15).

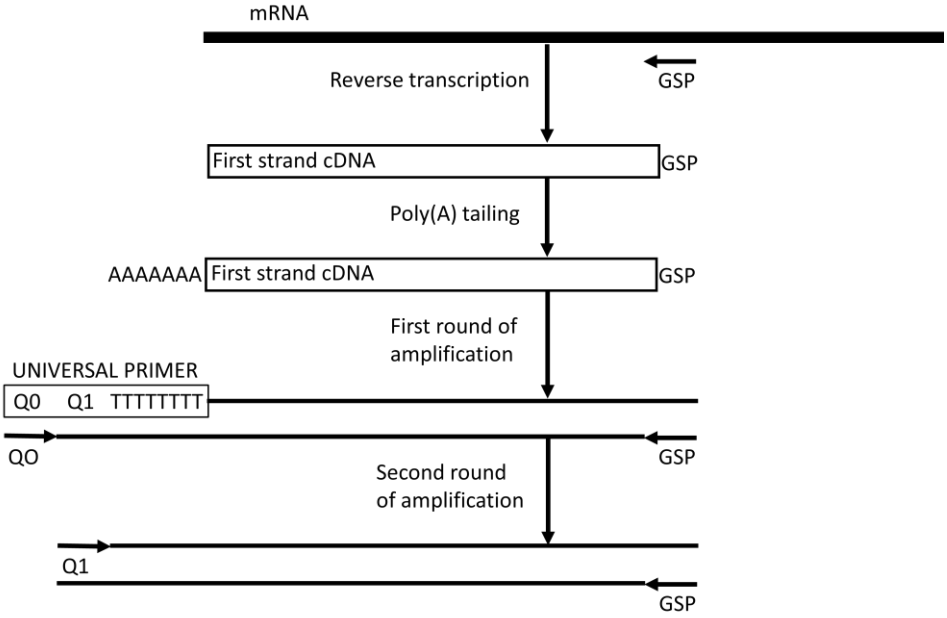

Figure 15: A schematic representation of classic 5'RACE. GSP: Gene-specific primer. Q0: Forward primer that binds to the adaptor sequence of the universal hybrid primer. Q1: Second forward primer complementary to the adaptor sequence of the universal primer. GSP: Reverse gene-specific primer.

3.5. STATISTICAL ANALYSIS

For the microarray data based on gene expression, statistical analysis was performed using the Transcriptome Analysis Console (TAC, v3.0.0.466) (Affymetrix) applying One-Way Between-Subject ANOVA (unpaired) and False Discovery Rate (FDR) based on Benjamini-Hochberg Step-Up (Benjamini and Hocheberg, 1995). The FDR was fixed as FDR <0.05 to retrieve results. Both linear regression and a pairwise comparison (P<0.05, with 2-fold changes) were used to analyze expression differences among groups.

For the AS analysis, AltAnalyze software with default parameters was used.

The relative expression levels of aging markers were plotted against age, ovarian reserve and oocyte maturation rates and non-parametric analysis (Spearman's rho) was conducted to evaluate their correlation ($P<0.05$).

Principal Component Analysis (PCA) was performed with Affymetrix Transcriptome Analysis Console (TAC) version 4.0.1 to determine the success of hybridizations.

To generate Venn diagrams, Venny's on-line software was used (http://bioinfogp.cnb.csic.es/tools/venny/index.html).

Hierarchical clusters were constructed with the ClustVis tool (Metsalu and Vilo, 2015). For GO enrichment analysis, biological functions of the differentially expressed genes and AS events were assessed with the PANTHER tool (Ashburner et al., 2000; Mi et al., 2017).

One-Way Between-Subject ANOVA was performed for qPCR validations.

All the comparisons performed in order to analyze whether vitrification affects oocyte quality (third objective) were made using fresh and frozen oocytes from the same stimulation cycle. Differences on laboratory outcomes (fertilization rate and embryo quality) between fresh and frozen oocytes were evaluated with a univariate analysis using a Student T-test. Differences on reproductive outcomes (biochemical, clinical and ongoing pregnancies and LBR) between these two study groups were also evaluated with a univariate analysis using a Pearson's Chi^2 test. To validate the results observed in the univariate analysis, a multivariate analysis using a linear regression model was conducted to analyze the effect of oocyte vitrification on laboratory outcomes. The effect of oocyte vitrification on pregnancy outcomes and live-birth was also evaluated by a logistic multilevel regression. The potential confounding factors included in the multivariable analysis were: recipient's age (years) and BMI (kg/m^2), sperm status (fresh or frozen) and

origin (partner or donor), number of embryos transferred (1, 2 or 3) and embryo quality measured by the embryo morphological score system described by Coroleu and colleagues (Coroleu et al. 2006), which considers the number, symmetry and the percentage of fragmentation of the cells.

All analyses conducted to compare reproductive results of fresh vs vitrified oocytes were performed using SPSS version 22.0. A p-value <0.05 was set as statistically significant.

Table 1: List of primers used. The primers used in more than one section are only indicated once. All lncRNAs not previously described are named as "lnc" and the name of the closest protein-coding gene at 3'. Primers highlighted in yellow did not have good efficiencies (between 80-110%) or did not amplifiy the desired nucleotide sequence (analyzed by sanger sequence) and, therefore, were excluded from the analysis.

HOUSEKEEPING GENES		
Gene Symbol	**Primer name**	**Primer sequence (5'→3')**
ACTß	ACTB F ACTB R	GGACTTCGAGCAAGAGATGG AGCACTGTGTTGGCGTACAG
UBC	UBC F UBC R	ATTTGGGTCGCGGTTCTTG TGCCTTGACATTCTCGATGGT
RPLP0	RPLP0 F RPLP0 R	GGCGACCTGGAAGTCCAACT CCATCAGCACCACAGCCTTC
YWHAZ	YWHAZ F YWHAZ R	ACTTTTGGTACATTGTGGCTTCAA CCGCCAGGACAAACCAGTAT
SDHA	SDHA F SDHA R	TGGGAACAAGAGGGCATCTG CCACCACTGCATCAAATTCATG
PGK1	PGK1 F PGK1 R	CTGTGGGGGTATTTGAATGG CTTCCAGGAGCTCCAAACTG
GAPDH	GAPDH F GAPDH R	GAGTCAACGGATTTGGTCGT TTGATTTTGGAGGGATCTCG
GUSB	GUSB F GUSB R	AAACGATTGCAGGGTTTCAC CTCTCGTCGGTGACTGTTCA
RPLP0	RPLP0 F RPLP0 R	GGCGACCTGGAAGTCCAACT CCATCAGCACCACAGCCTTC
TBP	TBP F TBP R	TATAATCCCAAGCGGTTTGC GCTGGAAAACCCAACTTCTG
18S	18S F 18S R	TCTGTCGAGATCACAAGTTGC AGCATAGAAGATGATACCCGTGT
SEARCH FOR NEW TRANSCRIPTOMIC MARKERS OF HUMAN OOCYTE QUALITY		
Microarray validation - Gene expression		
Stable lncRNAs used as putative reference genes		
Gene Symbol	**Primer name**	**Primer sequence (5'→3')**

RP11-473E2.2	RP11-473E2.2 F RP11-473E2.2 R	CATGAGCGTCTCGAGGATTT ACTTGGCCTCTGAGCACATT
RP5-1024G6.2	RP5-1024G6.2 F RP5-1024G6.2 R	CTCGTGGACAGGACATTGTG GGAAATCCAGGCACATCTGA
RP11-260E18.1	RP11-260E18.1 F RP11-260E18.1 R	GCGAAGTTTTCAAGCACGAT GCTCCTTCTCCTCCCTCATT
RP11-434D9.2	RP11-434D9.2 F RP11-434D9.2 R	GCTGGGAGCTGTAGACCTGA ACCAAGTGCTTGATGTGTGG
RP11-399K21.11	RP11-399K21.11 F RP11-399K21.11 R	CTCCAACTCCAGACCACCAC CACAAGGGATCTCTCCGATG
RP11-284G10.1	RP11-284G10.1 F RP11-284G10.1 R	TTGCTTCCCAAAGCTAAGGA TGATGACATGGTCCTGTTCTG
RP11-506M13.3	RP11-506M13.3 F RP11-506M13.3 R	GCATTCTTCTACCACCACAGG ATTTGTGGCTTTTGGCTAGA
DHPS-002	DHPS-002 F DHPS-002 R	TAGTCCCGCACTTACAGACG CACCTGAGTCAGAGCCATCA
RP11-129M6.1	RP11-129M6.1 F RP11-129M6.1 R	CCCTCACATGCTTCAGCAAC CCTTTTTATGTATTCCTCTCCCACA
RP11-314013.1	RP11-314013.1 F RP11-314013.1 R	GCTGCCTTCCGTAGAAGATG CGAGTTCCAGTGGACAAGGT
Differentially expressed genes analysed		
Gene Symbol	**Primer name**	**Primer sequence (5'→3')**
ANXA5	ANXA5 F ANXA5 R	GACCCTCTATTATGCTATGAAG TCCTAAACTCCTTCCTGATG
CDK4	CDK4 F CDK4 R	GAACATTCTGGTGACAAGTG CAAAGATACAGCCAACACTC
DNMT1	DNMT1 F DNMT1 R	TGGACGACCCTGACCTCAAAT GCTTACAGTACACACTGAAGCA
FIGN	FIGN F FIGN R	CCTTCTTTTTGACTCCACTC GGTAGAAATAAAGCAGGAGC
GEM	GEM F GEM R	GAAGATACATATGAACGAACCC CCCTTATTTTCCCACATATCC
GPR119	GPR119 F GPR119 R	CTCATTTGGAGTGATCCTTG GACTGACACCATCATTCTTG
HOMER2	HOMER2 F HOMER2 R	ATATGACCTTCACCAAAACG GTCTTGTCTTTGGCTATCTTG
NCS1	NCS1 F NCS1 R	CCACATTTGTTTTCAACGTC CATCATTGTCCAAGTCGTAG
PBX2	PBX2 F PBX2 R	CAACAAGAGGATTCGCTATAAG AGAAACATGTCTCCAGATCC
PLCE1	PLCE1 F PLCE1 R	AGGATATCGACATCTTCAGC ATTTTCTTCCATCCTTCTGC
POU5F1	POU5F1 F POU5F1 R	GATCACCCTGGGATATACAC GCTTTGCATATCTCCTGAAG
PSMB	PSMB F PSMB R	TTCGAAATAAGGAACGCATC CACAGAACTTCAGACACAG
RNY5	RNY5 F RNY5 R	CGAGTGTTGTGGGTTATTG AAACAGCAAGCTAGTCAAG
SNORD123	SNORD123 F SNORD123 R	AAAATGATGAATTCTGGGGC CAGAATTGAGGTGAATCAGG
SNRPN	SNRPN F SNRPN R	GTCTTCAGAAGCATCAAGTTTTAAC GCCATCTTGCAGGATACATCTC
STYK1	STYK1 F STYK1 R	CTATGAGATGGTGACTCTAGG GGTCTCTTCATGATTTTCCTTC
TEX19	TEX19 F TEX19 R	AGAACTTGTGCCTATTTCAC ACATTTAAAACCAGCTCTCC
lncPOU3F1	lincPOU3F1 F lincPOU3F1 R	TGGTCTTCTCCTTCCTTTGG CCAAGATCTGAAGTTGGCAAG

AC019117.2	AC019117.2 F AC019117.2-1 R AC019117.2-2 R AC019117.2-4 R	TGACTTCTGGTGACTTGGGC ATCATGCCATCCCTCACACC TGAGGCCATTTTTCACACATGC TCACACCACTTAGCATTGCA
lncSKA2	lncSKA2 F lncSKA2 R	CAGAGTCGAGTTCCCTCCTC AGGCGGTTTAGACACCAGAC
lincCOL1A2	lincCOL1A2 F lincCOL1A2-1 R lincCOL1A2-2 R	GGAAGTAATCCAGCGAATCTGG GGAGAGCTGAAATCTCATGTTG GCTGAACTGGACCAGACGATG
lincDISP1	lincDISP1 F lincDISP1 R	ATACCAAGCTGTCAGAAGCAG AGTTGCACTTGTGTAGTCATGG
lncC9orf3	lncC9orf3 F lncC9orf3 R	CCTGCCTGCTCAATGATGTAG GATTGTGCGGTTGGCTTGTTT
lncANXA5	lncANXA5 F lncANXA5 R	GCATTTGTATGCCAGTGCTT CAGCAGTCAAAGAGATCTCCAC
RP11-720L8.1	RP11-720L8.1 F RP11-720L8.1 R	AAGCCCCTTTGTCAAATCAG GACTTGGAAGTCATGCAATGTT
lincCCDC140	lincCCDC140 F lincCCDC140 R	GAGTAGGCCTGGAGGTGGTA GGCAATCTCCTCACAACACTC
lincSLC5A12	lincSLC5A12 F lincSLC5A12 R	GGGTGTCAGTAGCATGATGG GCCACAGAATTGGTGAGTTG
lincMADCAM1	lincMADCAM1 F lincMADCAM1 R	TCAGACTGCTCAAAACCAGTG TCTTCTGTCTTCCAGCTTGC
lincSP4	lincSP4 F lincSP4 R	CTTACATGGGACGCCATTG CCATGTCCATTAGGCCTTACA
lncMETTL16	lncMETTL16 F lncMETTL16 R	ATCGTGCCACTGCACTCC ACACGACATGCATGGTAGCC
lincKCNG2	lincKCNG2 F lincKCNG2 R	CCTGTCTGTGGCCTTCCTT CCACGTCTCTATGGGGGTCA
lincNDUFV3	lincNDUFV3 F lincNDUFV3 R	TTGGCAGTTCACTCACCAAG CGGAAAAAGATCCAGAACCA
lincSPRED2	lincSPRED2 F lincSPRED2 R	ACCATCCTGGCACACTGAG TCTGCTGAGAGAAGCTGTGC
lincROBO1	lincROBO1 F lincROBO1 R	CCAGTGGAATTGTGCCAGTTG ATTGTTCCACTGCATTCAGC
lncARRDC4	lincARRDC4 F lincARRDC4 R	CAGCCTGAAAAACCTTGAGC GTGTCGTCCTGACAGCTTTG
lincGALNTL6	lincGALNTL6 F lincGALNTL6 R	GGATGAACAAGACCAGGAGGA GCAGATTGCTAAGGCAATGTCTTT
lncCKMT1B-1	lncCKMT1B-1 F lncCKMT1B-1 R	CTAGTGACTCAGAACTGGAGAAGG ACATGTGCCTCAGTTTCTGG
lncPTPRQ	lincPTPRQ F lincPTPRQ R	TTCTCCCTGTGTCCACCTTC TGAAGGCAGACCAAGCCAAG
lincOSBPL5	lincOSBPL5 F lincOSBPL5 R	TTCTCCCTGTGTCCACCTTC CGTTGGGCTCCATGTCCTT
lncPPARG	lncPPARG F lncPPARG R1 lncPPARG R2	ACCGAGCTGCGGCTTTTAT GGGAATTAAGCAGAATGCAGA TGGCCTTGTTGTATATTTGTGG
lncAVEN	lncAVEN F lncAVEN R	GAAGACGGAGGAATGCTTGA AATCAACCCATCAGGTGGAG
CTB-78F1.2	CTB-78F1.2 F CTB-78F1.2 R	GCTTAAGCGAACACACATTGA CAGGAGCTGATTGGAGGCTA
RP11-12A2.3	RP11-12A2.3 F RP11-12A2.3 R	TGTGCATATAAGCCCCAACA TCCCTGTCGACATCTGGATT
KCN4-AS1	KCN4-AS1 F KCN4-AS1 R	CTTCTTGTGCCGGATGGAAG ATCATCCAGACAGGCATGGAG
lncEMP2	lncEMP2 F lncEMP2 R	TATAGAAGGCCAGACGCAGTG GCCTCCTTCCCATCTTATCC
lincGNAQ	lincGNAQ F	CTCCCGAGTAGCTGGGACTA

	lincGNAQ R	TTTCATGTTGGATTGCGTTC
lncCC2D1B	lncCC2D1B F lncCC2D1B R	TGCTGAGGGTGGTGTCAG CTGTCAGGGATAAAGGCACA
lincRHOB	lincRHOB F lincRHOB R	GAACACATTTGTCTTCTTCCTGA CAGTGTGTTCTTGTCCTTGGTC
LINC00331	LINC00331 F LINC00331 R	AGAGGTTGACTCTCTCCAGAAAT CCTTTCTGGCTTCACCTCATTC
RP11-393I23.4	RP11-393I23.4 F RP11-393I23.4 R	CAACCAAACATGGAGGTTGCC GCAGGCATGCCCAAAGGTAG
lncCCAT1	lncCCAT1 F lncCCAT1 R	GCCGTGTTAAGCATTGCGAA AGAGTAGTGCCTGGCCTAGA
RP11-180C1.1-1	RP11-180C1.1 F RP11-180C1.1-1 R RP11-180C1.1-2 R	GGAGTGCAGTGGCATGATCT GGCTCAGTTTGTTGGTTGGT AGGACCAGGGACACTTTTCA
lncGFM1-5-6	lncGFM1-5-6 F lncGFM1-5-6 R	TCTGCAAGACAAAGGGAAGAA ACCAACGATGTGTTAAGCCC
RP11-98J23.1	RP11-98J23.1 F RP11-98J23.1 R	CCCAGGCCTCACTAAGAACT TGGGAGCAACAGATGCTAAA
lncSMUG1	lncSMUG1 F lncSMUG1 R	CTACGTGACTCGCTACTGCC TGCTTACTTCCCCAAAGGGC
RP11-809N8.2-1	RP11-809N8.2-1 F RP11-809N8.2-1 R	CCCTTCCCTTTATAGACCTGCT ATGTTGCTCCCCTGAAGGAT
RP11-991C1.1	RP11-991C1.1 F RP11-991C1.1 R	GTTATCCGGTCCTCGCCAAG TTGGCAAGGGTTCCGTCAAT
lncARL15	lncARL15 F lncARL15 R	TTTGATGTATTCAACCTGAGAGTG TCAGTTTTACTGGTTTTCTTTCTTCA
lncADCYAP1R1	lncADCYAP1R1 F lncADCYAP1R1 R	TCTGTGGTGGGTGATCAAAG ACTCATTGCCTCCCATGTCT
RP11-700E23.1	RP11-700E23.1 F RP11-700E23.1 R	GATTATCTGCAGCTTCATCCTG TGCCTCGAGGTTTTCATCTC
lncC1orf148	lncC1orf148 F lncC1orf148 R	ATAAGGACAGGCACCATCCA GGGGTGGATATGTCATAGCAG
RP11-5P4.2	RP11-5P4.2 F RP11-5P4.2 R	CGGTCAGTACAGTATTTCACATTCA CAATGGGTCTCCAGATGGTAA
LOC401242	LOC401242 F LOC401242 R	AAAACAAATGCGAAACCACA TAAGGAGAAAGCCCGAGTCA
Microarray validation - Alternative splicing		
Gene Symbol	**Primer name**	**Primer sequence (5'→3')**
PIK3CD	PIK3CD F1 PÎK3CD R1 PIK3CD F2A PIK3CD F2B PIK3CD R2	AAGATCGGCCACTTCCTTTT TGAGAGCTCAGCTTGACGAA CCGGAGTAGTAGGAGCCACA GCTTTGCTGGTCTTTCTTGG GTTCAGGTAGACCCCTGTGG
NTN1	NTN1 F1 NTN1 R1 NTN1 F2 NTN1 R2A NTN1 R2B	CTGCAAGGAGGGCTACTACC CAGCGGTTGCAGGTGATAC AAAACCTGCAACCAAACCAC AATCTTCAGCTTCCCCTTGG GAAGGAGTGACAACCCCTCA
TMED3	TMED3 F1 TMED2 R1 TMED3 F2 TMED3 R2A TMED3 R2B	CTTCCACGAGGAGGTGGAG TAAACGCCCTTGACTTCAGC TACGACAGCTTCACGTACCG AGAGCCTCATGGATGGTCAC TCACACTGGAACCCTTAGTGG
EPAS1	EPAS1 F1 EPAS1 R1 EPAS1 F2 EPAS1 R2A EPAS1 R2B	TCTGAAAACGAGTCCGAAGC GTCGCAGGGATGAGTGAAGT CAAGGAGACGGAGGTGTTCT GTCCATCTGCTGGTCAGCTT TGTTCTTCCCTGGTCCTGTC

DIAPH2	DIAPG2 F1 DIAPH2 R1 DIAPH2 F2 DIAPH2 R2A DIAPH2 R2B	CACCATGCACAACAACATGA AAGTTTTGCCCTCCTGGTCT AAGACCAGGAGGGCAAAACT ATAGCTCCATTGTGGCGAGA TGCACAGGGATGATTTACCA
GALK1	GALK1 F1 GALK1 R1 GALK1 F2 GALK1 R2A GALK1 R2B	TGTGGCATCATGGACCAGT CGGGCCACTTCTTCACATT GGCACATCCAGGAGCACTAC AGATCGTGTTACCGCACTCC AGCACCCGGATATGGAAGAT
OSBP2	OSBP2 F1 OSBP2 R1 OSBP2 F2 OSBP2 R2A OSBP2 R2B	ACCCTCAACGAGCACGAG CAAACCACAGTGGCGTGTAG GGAGAAGCTGAAGGTGGTGA GCTCAATGGTTTCCTCCAAG AGCTGTTCTGATGGCTTCGT
DDRGK1	DDRGK1 F1 DDRGK1 R1 DDRGK1 F2 DDRGK1 R2A DDRGK1 R2B	AGGAGGAAGGCGTAGGAGAG GGTCTTCCAAGAGCACAACC CCCAGAGCTTCCTGACAGAG GCCAGTTCCTCTGGGGTTAT GGACAAGGTAGACGGTGCAT
MAT2B	MAT2B F1 MAT2B R1 MAT2B F2A MAT2B F2B MAT2B R2	TGCTGTTGGAGCATTTCTCA CACAGCACTTTCTTCGAGCTT GCAAGAGAAGGCAGAGGCTA GCTGGTGGAGGAGGAAGTTA TCTGAAACCACAGCCAACTG
PLAGL1	PLAGL1 F1 PLAGL1 R1 PLAGL1 201 F PLAGL1 203 F PLAGL1 R	CTGCCAGTTATGTGGCAAGA TGGTGAGATTTCTGGGGAGA TCATTCCCTGACGATGTACAAG GGGGGTAACATAATGGAGGAA TATAGCTGGGGCATGTCCTG
Subcellular fractionation		
MALAT1	MALAT1 MALAT1	GAATTGCGTCATTTAAAGCCTAGTT GTTTCATCCTACCACTCCCAATTAAT
NEAT1	NEAT1 F NEAT1 R	TCGGGTATGCTGTTGTGAAA TGACGTAACAGAATTAGTTCTTACCA
DANCR	DANCR F DANCR R	CTCGGAGGTGGATTCTGTTAG CTGCAGAGTATTCAGGGTAAGG
NKILA	NKILA F NKILA R	AACCAAACCTACCCACAACG ACCACTAAGTCAATCCCAGGTG
BACE1-AS	BACE1-AS F BACE1-AS R	TACCATCTCTTTTACCCCCATCCT AAGCTGCAGTCAAATCCATCAA
5`rapid amplification of cDNA ends (5'RACE)		
Gene Symbol	**Primer name**	**Primer sequence (5'→3')**
	Adapt RACE-Qt	CCAGTGAGCAGAGTGACGAGGACTCGAG CTCAAGCTTTTTTTTTTTTTTTT
	RACE Q_0 F	CCAGTGAGCAGAGTGACG
	RACE Q_1 F	GAGGACTCGAGCTCAAGC
MALAT1	MALAT1-RACE R	GAATGATTTAATGGTTTTCTACAC
ACTINß	ACTB-RACE R	CAACTGGTCTCAAGTCAGTGT
AGING MARKERS EXPRESSION IN CCs		
Gene Symbol	**Primer name**	**Primer sequence (5'→3')**
LYZ	LYZ F	CCGCTACTGGTGTAATGATGG

	LYZ R	CATCAGCGATGTTATCTTGCAG
TXNIP	TXNIP F TXNIP R	AGCCAGCCAACTCAAGAGAC AGCAGACACAGGTGCCATTA
CLU	CLU F CLU R	GCAAGACACTGCTCAGCAAC TCAGGCAGGGCTTACACTCT
FABP3	FABP3 F FABP3 R	GGTGGAGTTCGATGAGACAA TCAATTAGCTCCCGCACAAG
ATP5G3	ATP5G3 F ATP5G3 R	ACGTCGCCTGTCACCCAATA TGGTCGAGATAACACTGATGCAGA
NDUFB11	NDUFB11-B F NDUFB11-B R	ACTTGTATGAGAAGAACCCAGA ACGCTCTTGGACACCCTGTGC
C3	C3 F C3 R	GCCAAGACGAAGAGAA GGCACCCAAAGACAAC
IGJ	IGJ F IGJ R	TCCAGGATCATCCGTTCTTC CTCTGATCCCACCTCACCAT
CALB1	CALB1 F CALB1 R	ACAGTGGCTTCATAGAAACTGAG TCCAGGGAATCAAAATGTGTGG
APOD	APOD F APOD R	CTGCATCCAGGCCAACTACTC AGGAGTTGAGAGCTGATGGAAC
TGFBR3	TGFBR3 F TGFBR3 R	TGGAGTCTCCTCTGAATGGCTG CCATTATCACCTGACTCCAGATC

Table 2: List of the antisense oligonucleotides used.

Gene Symbol	**Silencer Select siRNA**	**Primer sequence (5'→3')**
RELT	s39751 F s39751 R	CCCUCCCAUUAGUAGCUUUTT AAAGCUACUAAUGGGAGGGAT
RELT	s39752 F s39752 R	CAAGUUCAAUGGUGUCUGATT UCAGACACCAUUGAACUUGTC
RELT	s39753 F s39753 R	CCUGAGCAGCGGACAAGUUTT AACUUGUCCGCUGCUCAGGAA
RELT	s224977 F s224977 R	CAGCAGGUCUAUAAAGGGATT UCCCUUUAUAGACCUGCUGGA
RELT	s224978 F s224978 R	GGGCCUCAGUGGUUUCUGUTT ACAGAAACCACUGAGGCCCAA
ANXA5	s1392 F s1392 R	GUACAUGACUAUAUCAGGATT UCCUGAUAUAGUCAUGUACTT
ANXA5	s1393 F s1393 R	GACCUGAAAUCAGAACUAATT UUAGUUCUGAUUUCAGGUCAT
ANXA5	s1394 F s1394 R	GGAGUGAGAUUGAUCUGUUTT AACAGAUCAAUCUCACUCCTG
lncANXA5	s535228 F s535228 R	GCUGUAGUACUAAAGUGUATT UACACUUUAGUACUACAGCAG
lncANXA5	s535229 F s535229 R	UAGUGAAGUUCGCAACUAATT UUAGUUGCGAACUUCACUAAT
RP11-809N8.2-1	s535226 F s535226 R	CUUACUUCACAGUCAGAAATT UUUCUGACUGUGAAGUAAGGA
RP11-809N8.2-1	s535227 F s535227 R	GCUAGGGCUCUGUAUCACATT UGUGAUACAGAGCCCUAGCCT

4. RESULTS

4.1. CHAPTER 1: Search for new transcriptomic markers of human oocyte quality

4.1.1. Rationale to conduct this study

The developmental competence of an oocyte is its ability to sustain embryonic development until embryonic genome activation (EGA) and require both cytoplasmic and nuclear maturation (Braude et al., 1988; Eppig, 1996; Vassena et al., 2011). Cytoplasmic maturation entails structural changes in the cytoskeleton and organelles (i.e. mitochondria and cortical granules) that prepare the oocyte for meiosis resumption and fertilization (Watson, 2007; Ajduk et al., 2008; Mao et al., 2014). During nuclear maturation from primordial GV to fully grown GV oocytes, chromatin modifications and gene expression control mechanisms will establish a regulatory state to support early embryo development.

During the last few decades, the average age of first-time mothers has increased world-wide (te Velde and Pearson, 2002) due to educational, social, and economic factors. The negative correlation between age and fertility is well established in the scientific literature (Ubaldi et al., 2019). In addition, a decrease in oocyte quality has been associated with advanced woman age (Miao et al., 2009; Qiao et al., 2014); however, the underlying molecular mechanisms remain poorly understood (Keefe et al., 2015).

It is also well established that as a woman age increases, the ovarian reserve diminishes. It is not clear whether the quantity of follicles left in the ovary is directly related with the quality of the oocytes they contain, on a per-oocyte basis. Currently, it is not possible to distinguish the effect of age versus diminishing ovarian reserve on oocyte developmental competence acquisition (Broekmans, 2009; Eldar-Geva et al., 2005; Younis et al., 2015).

The oocyte developmental competence is determined by the transcripts (coding and non-coding RNAs) accumulated at the GV stage of the oocyte that will regulate the final steps of oocyte maturation as well as the early steps of embryogenesis. The lack of transcription during final oocyte maturation suggests that regulation of the genes involved in this process occurs at the post-transcriptional level (Bachvarova et al., 1985; Do et al., 2018). Among the possible mechanisms, selective degradation of mRNA transcripts is the best understood (Lequarre et al., 2004; Bettegowda et al., 2006; Su et al., 2007). In addition, alternative pre-mRNA splicing (AS) might be also involved in human oocyte transcript regulation (Salisbury et al., 2009; Tang et al., 2011). Studying oocyte gene expression and the spliced mRNA isoforms might provide novel information on the molecular mechanisms driving early development, and might be a source of potential biomarkers of oocyte quality.

The objective of the present study is to identify the transcriptional profiles and the alternative spliced isoforms characterizing different stages of oocyte maturation, and evaluate how these profiles change in oocytes from women of different age and ovarian reserve.

In order to achieve this objective, the project was divided into 2 interrelated phases:

- Phase 1: identification of the transcriptomic profile of MII human oocytes.

    - Identify differentially expressed transcripts in MII oocytes in relation to age and ovarian reserve.

    - Analyze how these transcripts change its expression at different stages of oocyte maturation by studying the differences in gene expression and AS events from GV to MII oocytes.

- Phase 2: analysis of the functional role of the potential biomarkers of oocyte developmental competence identified in Phase 1.

4.1.2. Study population

In this study, a total of 41 MII and 8 GV oocytes from 43 oocyte donors undergoing controlled ovarian stimulation have been collected with the aim to study their transcriptome in order to find markers of oocyte quality. Mean donor age was 26.9 ± 5.3 years old (range 20-35 years), with a mean ovarian reserve, measured by antral follicular count (AFC) of 18.3 ± 10.4 (range 5-43 AFC) (Table 3). The "oldest" women included in this study was 35 years old since it is the maximum age for oocyte donation in Spain.

Table 3: Individualized data from all included donors in the analysis of age and ovarian reserve (AFC) in mature (MII) oocytes. COCs: cumulus-oocyte complexes. AFC; Antral follicle count. BMI; Body mass index. MII; metaphase II oocyte.

Donor #	AFC	Age (years)	BMI (kg/m^2)	COCs	MII	Proven fertility	Analysis group	Array	qPCR
D1	5	32	26.23	6.7	4.5	YES	OL L-MII	1	1
D2	6	34	20.45	4.0	3.0	NO	OL	1	1
D3	6	33	24.34	5.3	1.7	NO	OL	1	1
D4	7	34	21.74	5.5	3.5	YES	OL	1	1
D5	7	34	20.55	7.3	4.3	YES	OL	1	1
D6	7	32	18.29	5.0	4.0	YES	OL L-MII	1	1
D7	7	35	18.97	9.0	4.5	NO	OL	1	1
D8	8	35	22.49	3.0	1.0	YES	OL	1	1
D9	8	35	20.82	6.0	5.5	YES	OL	1	1
D10	5	24	17.78	4.5	3.3	YES	YL	1	
D11	7	24	20.83	4.0	3.0	NO	YL	1	1
D12	8	21	20.57	9.5	7.5	YES	YL L-MII	1	1
D13	8	25	29.27	8.0	3.3	YES	YL L-MII	2	2
D14	10	22	19.33	9.5	6.5	YES	YL	2	2
D15	9	26	17.51	4.0	3.0	NO	YL	2	2
D16	21	20	25.96	12.7	11.3	YES	YH	1	1

D17	21	22	19.71	10.2	8.3	YES	YH H-MII	2	2
D18	21	21	16.61	16.7	12	YES	YH	1	1
D19	22	22	21.63	18.7	17.2	YES	YH H-MII	1	1
D20	22	20	26.99	10.2	9	YES	YH	1	1
D21	24	21	22.68	16.5	10.4	YES	YH	1	1
D22	27	20	23.8	27.7	1.7	YES	YH	1	1
D23	30	21	18.66	8.0	6.7	YES	YH	1	1
D24	20	32	22.68	10.7	10.3	YES	OH O-MII	1	1
D25	24	34	20.7	11.7	8.7	YES	OH O-MII	1	1
D26	28	30	28.93	9.0	5.0	NO	OH H-MII	2	2
D27	30	34	26.49	13.4	7.8	YES	OH O-MII	1	1
D28	41	31	23.83	16.8	14.4	YES	OH	1	1
D29	25	30	22.55	10.7	10.4	YES	OH H-MII	1	1
D30	33	31	25.82	12.7	12.0	YES	OH O-MII	2	2
D31	31	25	21.75	108	84	YES	GV	1	
D32	18	29	20.76	23	20	YES	GV	1	
D33	16	30	21.96	14	8	YES	GV	1	
D34	43	21	19.59	24	14	YES	GV	1	
D35	25	29	27.28	53	28	NO	GV		1
D36	28	28	19.43	12	10	YES	GV		1
D37	24	23	23.66	53	31	YES	GV		1
D38	18	23	22.32	54	33	YES	GV		1
D39	21	21	19.83	17	12	YES	H-MII		1
D40	21	21	25.60	16	10	YES	H-MII		1
D41	30	21	19.72	8	7	YES	H-MII		1
D42	7	24	20.20	4	3	YES	L-MII		1
D43	9	26	20.96	4	3	NO	L-MII		1

To analyze the differentially expressed transcripts in relation to age and/or ovarian reserve a total of 36 in vivo matured (MII) were used. For this analysis, only *in vivo* MII oocytes were collected since is the closest material to an ovulated oocyte in a naturally cycling ovary, giving current ethical and technical restrictions. Mature MII oocytes were divided in 4 experimental groups of 9 oocytes each based on the women's age and AFC: young women with high AFC (YH; age 21 ± 1 years and 24 ± 3 follicles), "old" women with

high AFC (OH; age 32 ± 2 years and 29 ± 7 follicles), young women with low AFC (YL; age 24 ± 2 years and 8 ± 2 follicles), and "old" women with low AFC (OL; age 34 ± 1 years and 7 ± 1 follicles). Six of the donors had two sibling oocytes (D13, D14 and D15 from YL group; D17 from YH; finally, D26 and D30 from OH group) (Table 4).

Table 4: Demographic features of the studied experimental groups in the analysis of age and ovarian reserve (AFC) in MII oocytes. Values are presented as mean ± standard deviation [range] or in percentage when indicated. COCs: cumulus-oocyte complexes

	OL	**YL**	**YH**	**OH**
Donor (n)	9	6	8	7
Oocytes (n)	9	9	9	9
Age (years)	34 ± 1 [32-35]	24 ± 2 [21-26]	21 ± 1 [20-22]	32 ± 2 [30-34]
AFC	7 ± 1 [5-8]	8 ± 2 [5-10]	24 ± 3 [21-30]	29 ± 7 [20-35]
COCs	7 ± 3 [3-10]	6 ± 2 [4-9]	12 ± 15 [3-49]	13 ± 10 [3-35]
MII obtained	4 ± 2 [1-8]	4 ± 3 [1-9]	7 ± 8 [2-25]	11 ± 12 [2-35]

To identify the differentially expressed transcripts and AS events between non-matured (GVs) and MII oocytes, the raw microarray data from 12 MII oocytes was re-analyzed together with the raw data from 4 GV oocytes. Only 12 MII oocytes were selected in order to make 4 groups with the same number of oocytes in each group. The 4 new experimental groups of 4 oocytes each were created according to their maturation stage, and the age and AFC of the women (mean ± SD): GV oocytes from women up to 30 years old with high AFC (GV group; 26±4.1 years old and 27±13 follicles), MII oocytes from women up to 30 years old with high AFC (H-MII group; 26±4.6 years old and 24±3 follicles), MII oocytes from women with low AFC (L-MII group; 27±5.4 years old and 7±1 follicles) and MII oocytes from women above 31 years old with high AFC (O-MII group; 32.8±1.5 years old and 27±6 follicles (Table 5). For the microarray validation by

qPCR of the AS analysis, additional 9 in vivo matured and 4 non-matured oocytes were used

Table 5: Demographic features of the four experimental groups studied: GV, H-MII, L-MII and O-MII in the gene expression and AS analysis during oocyte maturation. Values are presented as mean ± standard deviation [range]. COCs: cumulus-oocyte complexes. $^{\#}p<0.05$ Age compared in O-MII with GV and H-MII groups. $^{\$}p<0.05$ AFC compared in L-MII with GV, H-MII, and O-MII groups.

	GV	**H-MII**	**L-MII**	**O-MII**
Donor (n)	4	4	4	4
Oocytes (n)	4	4	4	4
Age (years)	26.3 ± 4.1 [21-30]	26.0 ± 4.6 [22-30]	27.5 ± 5.4 [21-32]	32.8 ± 1.5 [31-34] $^{\#}$
AFC	27 ± 13 [16-43]	24 ± 3 [21-28]	7 ± 1 [5-8] $^{\$}$	27 ± 6 [20-33]
COCs	42 ± 44 [14-108]	10 ± 6 [3-17]	6 ± 3 [3-9]	8 ± 4 [3-11]
MII obtained	31 ± 35 [8-84]	7 ± 6 [2-15]	3 ± 1 [1-4]	6 ± 4 [3-10]

Analysis of correlation (Spearman R=0.675; p<0.001) between AFC and cumulus- oocyte complexes (COCs) obtained indicate that AFC measurements reflect ovarian response of the woman and, indeed, ovarian reserve (Figure 16).

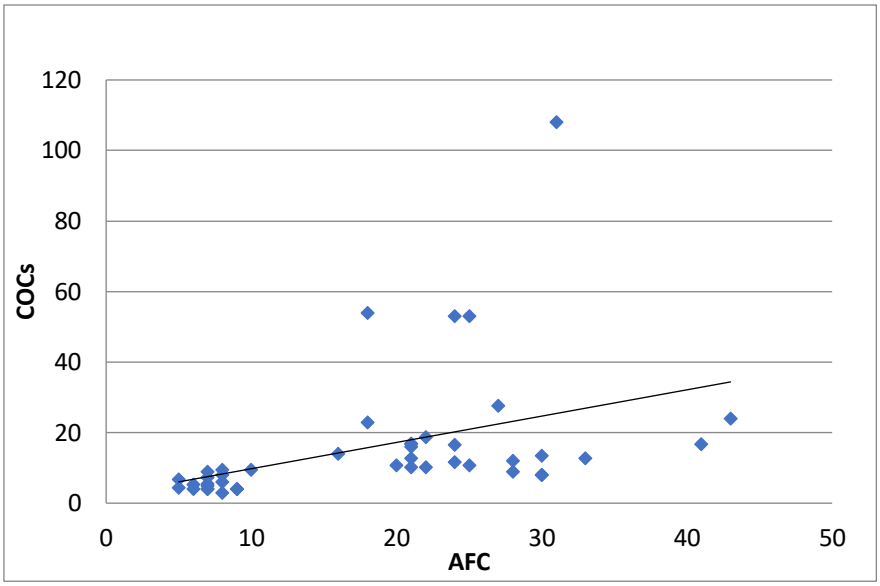

Figure 16: Schematic representation of the correlation between the cumulus-oocyte complexes (COCs) obtained the day of retrieval and the AFC measurements performed at the beginning of the IVF cycle.

4.1.3. Search for new transcriptomic markers of human oocyte quality

4.1.3.1. Phase I: Identification of the oocyte transcriptomic profile

Quality control analysis

We carried out principal component analysis (PCA), using the Transcriptome Analysis Console (TAC, v3.0.0.466) from Affymetrix, to determine the effect of key variables (age-AFC grouping, hybridization batch and RNA extraction batch) over the observations (gene expression measurements), and to simplify the analysis and visualization of multidimensional data sets. Supervised PCA analysis did not reveal any obvious clustering, independently of their biology or the RNA extraction, cDNA amplification or hybridization batches (Figure 17).

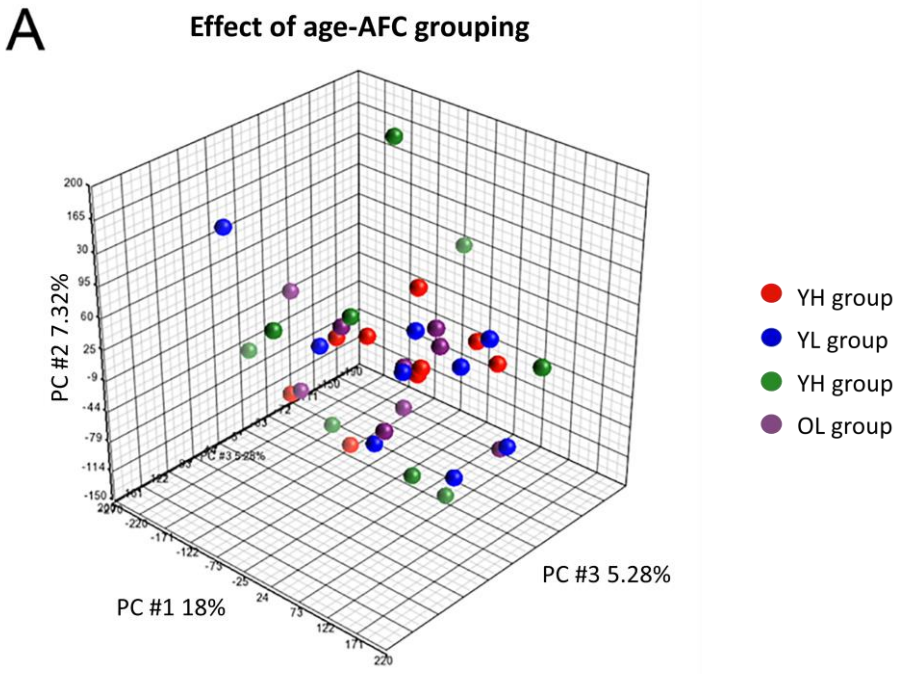
A
Effect of age-AFC grouping
PC #2 7.32%
PC #1 18%
PC #3 5.28%
YH group
YL group
YH group
OL group

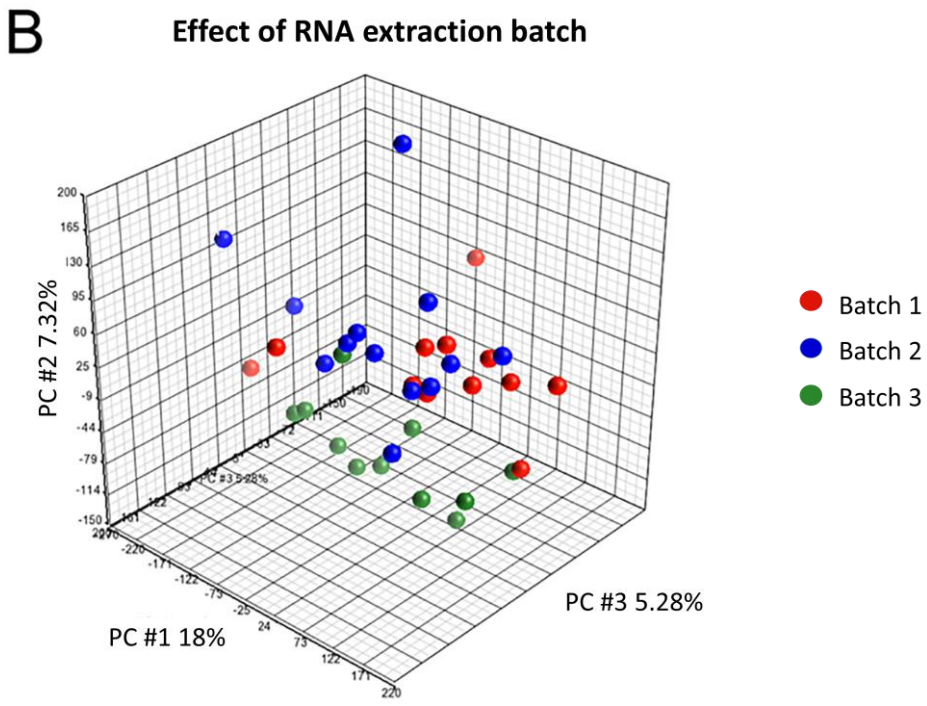
B
Effect of RNA extraction batch
PC #2 7.32%
PC #1 18%
PC #3 5.28%
Batch 1
Batch 2
Batch 3

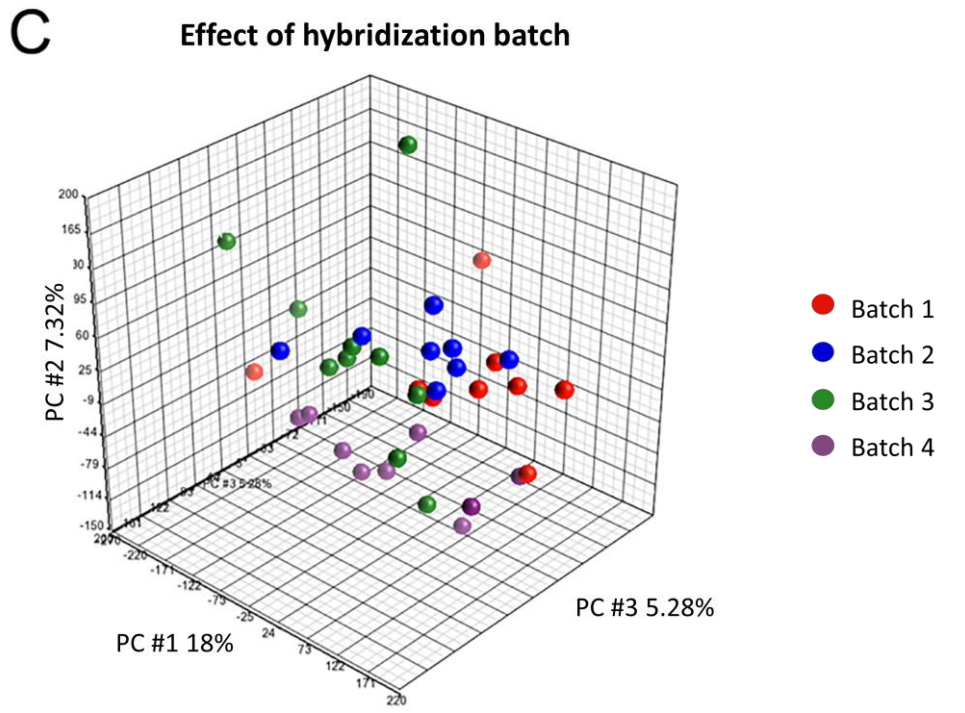

Figure 17: Principal Component Analysis (PCA) plots as quality control assessment for handling batches of the 36 individual human oocytes processed. A) Effect of age-AFC grouping on PCA analysis. (red: YH group; blue: YL group; green: OH group; purple: OL group). B) Effect of RNA extraction batch (red: batch 1; blue: batch 2; green: batch 3;). C) Effect of hybridization batch (red: batch 1; blue: batch 2; green: batch 3; purple: batch 4)

Box-plots representing Relative Log Expression (RLE) values of the 36 MII oocytes were computed for each probe-set by comparing the expression value on each array against the median expression value for that probe-set across all arrays in a dataset (Figure 18) showing similar (but not identical) results, as expected.

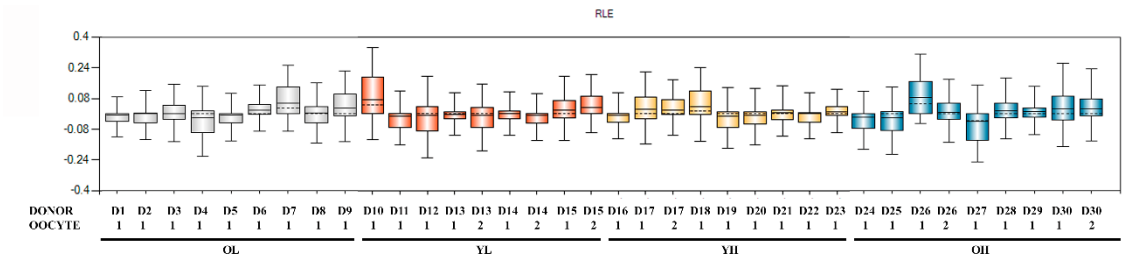

Figure 18: Quality control metrics. Each box-plot corresponds to one array and represents relative log-intensities expression (RLE) for each probe-set before normalization (RMA).

For quality Control (QC), density plots of log-intensity distribution of each array were performed to compare arrays and identify possible outlier arrays. One sample (D10) was found to be an outlier and removed from further analysis.

Differentially expressed transcripts in relation to age and/or ovarian reserve

In order to analyze variability between oocytes from the same donor and donation cycle, we focused on hierarchical clustering of individual oocytes in the age and AFC comparisons, and recorded the distance between siblings in the context of the group. Age comparison revealed that 4 sibling pairs out of 6 (D13, D14, D15, D26) were separated when clustered by differential expressed genes, while only one sibling pair (D30) showed separation when clustered by AFC (Figure 19).

In order to determine the effect of age on the human oocyte transcriptome, we compared oocytes from both young groups (YL+YH) to oocytes from both old groups (OL+OH) independently from the ovarian reserve. We detected 86 differentially expressed transcripts, including 17 mRNA and 69 ncRNAs (6 pre-miRNA, 17 piRNAs-c, 38 lncRNA (including 16 lncRNA and 22 long-intergenic RNA (lincRNA)) and other 8 structural RNA molecules) (Figure 19A, Table 6). A set of 5 miRNA (ENSG00000221162, *hsa-mir-220b*, ENSG00000239174, *hsa-mir-4262* and *hsa-mir-1260a*) were increased in the old group (OL+OH), while piRNAs-c and lncRNAs appeared mostly increased in the young group (YH + YL).

To analyze the effect of the ovarian reserve, we performed comparison of low (YL+OL) vs. high (YH+OH) ovarian reserve independently from age. We detected 22 mRNA and 55 ncRNAs (4 pre-miRNA, 8 piRNAs-c, 27 lncRNA (including 11 lncRNA and 16 lincRNA) and other 16 structural RNA molecules) showing differential expression

(Figure 19B, Table 6). From the differentially regulated transcripts, more than 60% were increased in the high AFC group compared with low AFC group.

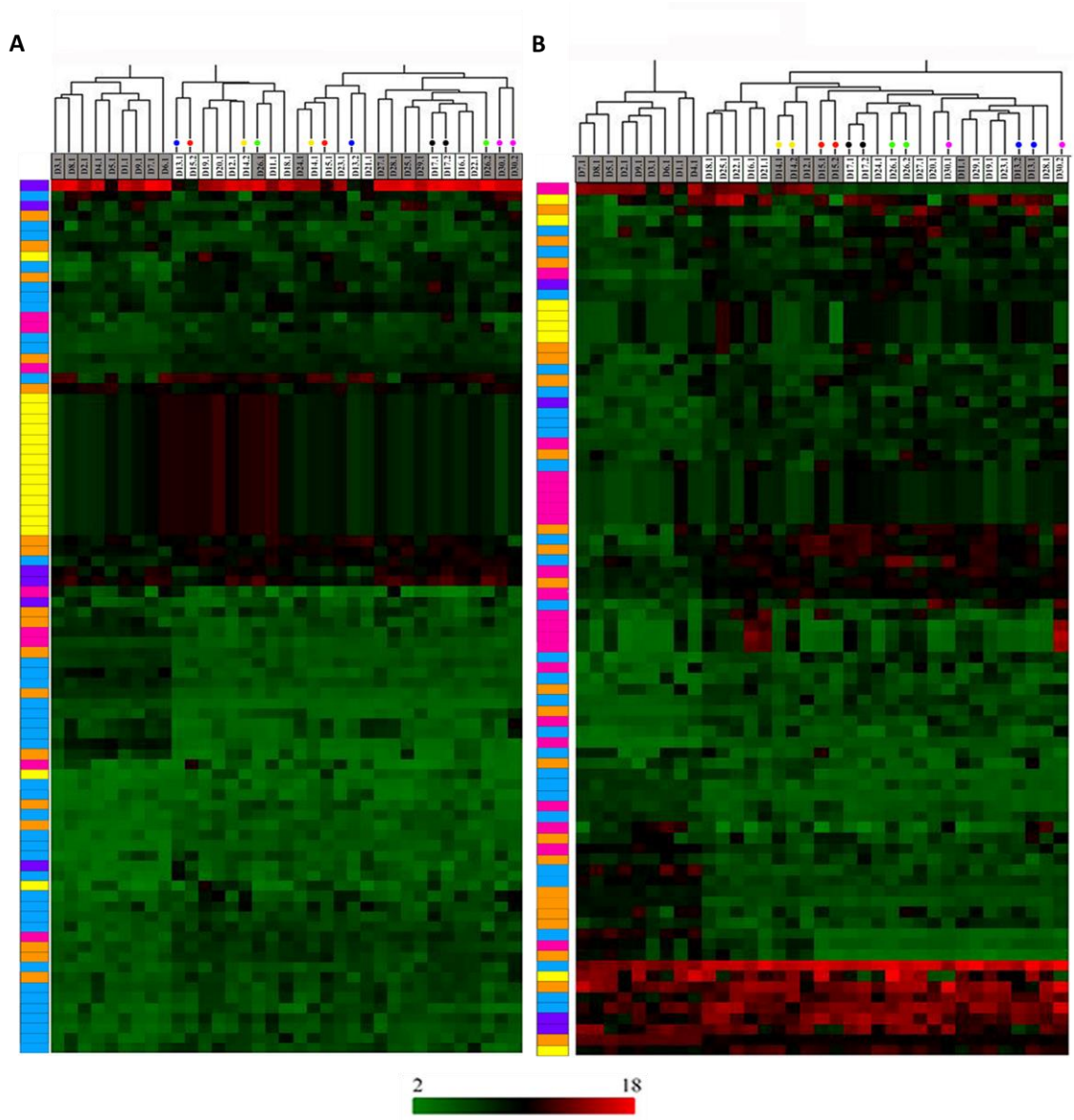

Figure 19: Heat maps for the differentially expressed genes (>|2| fold change; p<0.05) when age (A, white: young; grey: old) or AFC (B; white: high; grey: low) were compared and hierarchical clustering to analyze similarities between individualized samples. The name of the samples is indicated at the bottom of the cluster lines; sibling oocytes are indicated with equal dots of the same color. The color in the heat map (red to green scale) corresponds to relative transcript abundance. Different kinds of transcripts are represented as follow in the left vertical line: orange: messenger RNAs (mRNAs); pink: structural RNA; purple: precursors of microRNAs (pre-miRNAs); yellow: Piwi-interacting RNAs clusters (piRNAs-c); pale blue: long intergenic non-coding RNAs (lincRNAs). and dark blue: long non-coding RNAs (lncRNAs).

While mRNAs and pre-miRNAs represent less than 30% and 10% of differentially expressed transcripts respectively, lncRNAs and other structural RNA molecules represent more than 60% of differentially expressed transcripts. For example, we identified 4 Piwi-interacting RNAs clusters (piRNAs-c) increased in high AFC groups (YH and OH) (*piR-54999, piR-43765, piR-57434, piR-55000*) and 1 increased piRNAs-c in young groups (YH + YL) (*piR-45193*).

When comparing both analysis groups: age (YL+YH vs OL+OH) and ovarian reserve (YH+OH vs YL+OL), 17 transcripts (6 mRNA, 1 pre-miRNA, 7 lncRNA and other 3 structural RNA molecules) were differentially expressed. Five of them (3 mRNA, 1 lncRNA and 1 structural RNA) were increased and 3 (1 mRNA (*ANXA5*) and 2 lncRNA) were decreased in oocytes from older women with low ovarian reserve (including *PRRG1, IGHV3-38* and *IGHV3OR16-9)*. Three were increased in oocytes from younger women with high ovarian reserve (including 1 mRNAs (*DUXAP10*) and 2 lncRNA) and 1 pre-miRNA was decreased in oocytes from older women with high ovarian reserve (*hsa-mir-220b*). In addition, *RNY5*, a member of Y RNA gene family (required for DNA replication), was increased in OL group compared with young groups (YH or YL) regardless of AFC; and in old (OH+OL) and low AFC (YL+OL) groups, regardless of AFC and age respectively.

Table 6. Lists of differentially regulated ncRNA in human oocytes referred to hierarchical clustering shown in figure 19, in the same order of appearance on the figure. Subheading of lists indicate those ncRNA differentially regulated on each group comparison. Accession number is always provided, while gene symbol is provided when available. ↑ increased; ↓ decreased.

Age comparisons (Old vs. Young)				
Transcript type	**Gene Symbol**	**Accession number**	**Fold Change (linear)**	**ANOVA p-value**
Pre-miRNA	AC092143.2	ENSG00000239174	↑ 3,01	0,01892
lincRNA	linc-SLC5A12	ENSG00000254560	↑ 3,72	0,002678
Pre-miRNA	hsa-mir-4262	NR_036226	↑ 3,22	0,033328

mRNA	CLPS	NM_001252597	↓ 2,58	0,044579
lincRNA	linc-ZNF606	NONHSAG026698.2	↑ 3,02	0,004897
lincRNA	linc-KARS-1	XLOC_l2_005554	↑ 2,11	0,011514
mRNA	IGHV3-35	ENSG00000211957	↑ 2,46	0,027332
piRNA-c	piR-54967	DQ587855	↓ 2,56	0,035042
lncRNA	lnc-ANXA5	NONHSAG038790.2	↓ 3,55	0,001444
mRNA	ANXA5	NM_001154	↓ 2,43	0,000877
lincRNA	linc-WDHD1-2	XLOC_011031	↓ 2,08	0,038546
lincRNA	linc-ALX3-1	XLOC_000956	↓ 2,26	0,013946
lncRNA	KCNC4-AS1	ENSG00000224965	↓ 2,46	0,004635
Structural RNA	snoU13	ENSG00000238838	↓ 2,17	0,024947
Structural RNA		JA202350	↓ 2,28	0,027186
lncRNA		NR_024572	↓ 2,02	0,000139
lincRNA	linc-CBWD3-9	XLOC_l2_014835	↓ 2,11	0,000105
mRNA	ZSCAN22	NM_181846	↓ 2,13	0,001093
Structural RNA	NUP88-014	Y08613	↓ 2,08	0,000044
lincRNA	linc-SP4	ENSG00000105866	↓ 3,83	0,007217
mRNA	GEM	NM_181702	↑ 2,74	0,000374
piRNA-c	piR-42870	DQ574758	↓ 2,03	0,041177
piRNA-c	piR-42870	DQ574758	↓ 2,03	0,041177
piRNA-c	piR-42870	DQ574758	↓ 2,03	0,041177
piRNA-c	piR-42870	DQ574758	↓ 2,03	0,041177
piRNA-c	piR-42872	DQ574760	↓ 2,03	0,041177
piRNA-c	piR-49706	DQ581594	↓ 2,03	0,041177
piRNA-c	piR-42872	DQ574760	↓ 2,03	0,041177
piRNA-c	piR-49706	DQ581594	↓ 2,03	0,041177
piRNA-c	piR-49706	DQ581594	↓ 2,03	0,041177
piRNA-c	piR-49706	DQ581594	↓ 2,03	0,041177
piRNA-c	piR-42870	DQ574758	↓ 2,03	0,041177
piRNA-c	piR-49706	DQ581594	↓ 2,03	0,041177
piRNA-c	piR-42870	DQ574758	↓ 2,03	0,041177
piRNA-c	piR-42870	DQ574758	↓ 2,03	0,041177
mRNA	ARL6IP4	EF036485	↓ 2,18	0,004144
mRNA	MAGEE1	NM_020932	↓ 2,1	0,000406
lncRNA	LNC-FAM98A-2	OTTHUMG00000152140	↓ 2,15	0,003938
Pre-miRNA	hsa-mir-220b	ENSG00000215937	↑ 2, 39	0,023932
Pre-miRNA		ENSG00000221162	↑ 2,06	0,019121
Structural RNA	RNY5	NR_001571	↑ 3,54	0,024184
Pre-miRNA	hsa-mir-1260a	NR_031661	↑ 2,87	0,004371

mRNA	STYK1	NM_018423	↑ 2,24	0,042289
mRNA	PRRG1	BC030786	↑ 2,7	0,016353
Structural RNA	Y_RNA	ENSG00000222529	↑ 3,39	0,001988
Structural RNA	RNU6-569P	ENSG00000207188	↑ 2,08	0,003283
mRNA	IGHV3-66	ENSG00000211972	↑ 2,1	0,001827
lincRNA	CTD-3035D6.2	ENSG00000258884	↑ 2,02	0,003701
lincRNA		NONHSAT097326.2	↑ 4,28	0,001906
lncRNA	WDFY3-AS1	ENSG00000251260	↑ 2,36	0,000195
mRNA	SPCS2; SPCS2P4	NR_027268	↑ 2,47	0,001184
lncRNA	AP001476.3	ENSG00000226115	↑ 2,03	0,000208
lncRNA	RP11-180C1.1	ENSG000002500	↑ 3,19	0,000507
lncRNA	LOC284009	NR_028335	↑ 5,96	0,000634
lncRNA	LOC284009	NR_028335	↑ 4,06	0,001199
lncRNA		JN110922	↑ 4,54	0,002843
mRNA	IGHV3-38	ENSG00000211958	↑ 3,87	0,047813
Structural RNA	SNORD77	ENSG00000212279	↓ 2,93	0,022467
piRNA-c	piR-52545	DQ585433	↓ 2,21	0,003684
lncRNA	GRIK1-AS2	NR_033368	↓ 2,08	0,000965
lncRNA	RP11-480I12	BC038775	↓ 2,01	0,00556
mRNA	PFAS	ENSG00000178921	↓ 2,12	0,023414
lncRNA	RP11-327P2.5	ENSG00000231856	↓ 2,01	0,001605
mRNA	SMUG1	NR_045039	↓ 2,19	0,007834
lincRNA	linc-C10orf119-3	ENSG00000227307	↓ 2,13	0,000092
lincRNA	linc-CPEB2-4	XLOC_003463	↓ 2,08	0,000058
lincRNA		n345939	↓ 2,3	0,015557
Pre-miRNA	hsa-mir-548w	NR_036146	↓ 2,3	0,007903
lincRNA	lnc-IKBKG	ENSG00000073009	↓ 2,33	0,008679
piRNA-c	piR-54967	DQ587855	↓ 2,21	0,044568
lincRNA	LINC00363; RP11-632L2.1	ENSG00000232849	↓ 2,55	0,029973
lincRNA	RP11-145M4.1	ENSG00000241042	↓ 2,65	0,01138
lincRNA	linc-NUDCD2-5	XLOC_005075	↓ 2,03	0,025963
lncRNA	RP11-894J14.2	OTTHUMG00000159046	↓ 2,13	0,000947
Structural RNA	SNORD112	ENSG00000251824	↓ 2,4	0,003422
mRNA	PROCR	NM_006404	↓ 2,07	0,002184
mRNA	HIST2H2AC	NM_003517	↓ 2,35	0,001794
lincRNA	linc-ADSS	NONHSAG004855.2	↓ 2,43	0,015954
mRNA	DUXAP10	BC017398	↓ 2,08	0,037174
lincRNA	linc-ROBO1-3	NONHSAG035474.2	↓ 2,54	0,002164

lincRNA	RP11-47P18.1	ENSG00000242828	↓ 2,36	0,024819
lincRNA	TSLC1-AS1	ENSG00000256558	↓ 2,57	0,018523
lincRNA	linc-NGLY1-2	XLOC_003070	↓ 2,36	0,000528
lincRNA	AC099754.1	ENSG00000225386	↓ 2,22	0,000454
lncRNA	LOC100289511	NR_029378	↓ 2,17	0,008514
lncRNA	CTD-2026G22.1	ENSG00000255532	↓ 3,1	0,001067
Ovarian reserve comparisons (Low vs. High)				
Transcript type	**Gene Symbol**	**Accession number**	**Fold Change (linear)**	**ANOVA p-value**
Structural RNA	RP11-170L3.7	ENSG00000197476	↑ 36,82	0,007185
piRNA-c	piR-54999	DQ587887	↓ 6,09	0,049692
mRNA	OR5A1	NM_001004728	↓ 3,42	0,023682
piRNA-c	piR-43765	DQ575653	↓ 3,14	0,020665
lincRNA		NONHSAT071277.2	↓ 3,06	0,015822
mRNA	CRABP1	NM_004378	↓ 2,02	0,022367
lncRNA	FAM215A	NR_026770	↓ 2,05	0,002627
mRNA	INA	NM_032727	↓ 2,05	0,001326
Structural RNA	SNORD112	ENSG00000251824	↓ 3,04	0,000211
Pre-miRNA		ENSG00000221257	↓ 2,09	0,000712
lncRNA		NONHSAT001652.2	↓ 2,08	0,000002
piRNA-c	piR-57434	DQ590322	↓ 2,36	0,012523
piRNA-c	piR-57434	DQ590322	↓ 2,36	0,012523
piRNA-c	piR-55000	DQ587888	↓ 2,36	0,012523
piRNA-c	piR-55000	DQ587888	↓ 2,36	0,012523
mRNA	GPR119	ENSG00000147262	↓ 2,58	0,00645
mRNA	MAP1LC3C	NM_001004343	↓ 2,5	0,028453
lincRNA	linc-ARRDC4	XLOC_011373	↓ 2,62	0,000887
mRNA	DUXAP10	BC017398	↓ 2,25	0,027935
lincRNA	RP11-47P18.1	ENSG00000242828	↓ 2,5	0,009914
Pre-miRNA	hsa-mir-70	ENSG00000221391	↓ 2,08	0,020281
lncRNA		NONHSAT125622.2	↓ 2,21	0,000721
lincRNA	RP11-96C21.1	ENSG00000259473	↓ 2,31	0,001796
lincRNA		NONHSAT087539.2	↓ 2,34	0,000025
Structural RNA	HERV-K	AY395526	↓ 2,16	0,00232
mRNA	NR1D1	M34339	↓ 2,3	0,005877
lncRNA		NONHSAT126113.2	↓ 2,33	0,032292
mRNA	CPLX4	NM_181654	↓ 3,22	0,020349
lncRNA		NONHSAT098146.2	↓ 2,95	0,027468
mRNA	ANXA5	NM_001154	↓ 2,26	0,010995
lincRNA	AC015922.6	ENSG00000237057	↓ 2,32	0,018849

Structural RNA	RP1-96H9.5	ENSG00000256103	↓ 2,07	0,000463
mRNA	SPATC1L	NM_001142854	↓ 2,01	0,000667
Structural RNA	LOC100652999	ENSG00000257550	↓ 2,05	0,004591
lincRNA	LINC00363	ENSG00000232849	↓ 2,18	0,04714
Structural RNA	LINC01422	ENSG00000223704	↓ 3,35	0,029378
Structural RNA	RNU7-144P	ENSG00000238452	↓ 4,36	0,028185
Structural RNA	RNU7-173P	ENSG00000238950	↓ 4,62	0,01722
Structural RNA	RNU7-92P	ENSG00000238785	↓ 4,37	0,010525
lincRNA	RP11-393K12.2	ENSG00000223581	↓ 2,45	0,012923
Structural RNA	SNORA23	NR_002962	↓ 2,37	0,004651
lincRNA	linc-GRM3-3	XLOC_003741	↓ 2,44	0,009196
mRNA	NAT9	NM_015654	↓ 2,24	0,008726
lncRNA		NONHSAT103329.2	↓ 2,13	0,024658
mRNA	MYL6	NM_021019	↓ 2,22	0,000235
Structural RNA	RNA5SP107	ENSG00000223290	↓ 2,02	0,003023
lincRNA	linc-C14orf101-4	XLOC_010840	↓ 2,19	0,044534
Structural RNA	RNU6-787P	ENSG00000206759	↓ 2,1	0,000066
lncRNA	RP11-10J21.4	ENSG00000253307	↑ 2,87	0,021086
mRNA	TEX19	NM_207459	↑ 2,12	0,010305
lincRNA	linc-TP53TG3B-9	XLOC_l2_005462	↑ 2,69	0,024401
lncRNA		NONHSAT113914.2	↑ 2,29	0,000353
lincRNA	linc-DMXL1-4	XLOC_004524	↑ 2,17	0,001496
Structural RNA	RNU6-21P	ENSG00000207441	↑ 2,04	0,012954
lincRNA	linc-C15orf2-10	XLOC_011172	↑ 2,15	0,002206
Structural RNA	RNY5	NR_001571	↑ 4,03	0,045314
mRNA	PLCH1	AK096620	↑ 2,38	0,041759
Structural RNA	Y_RNA	ENSG00000222529	↑ 2,5	0,014439
mRNA	ANXA11	AL357617	↑ 2,36	0,005412
lincRNA		NONHSAT097326.2	↑ 3,78	0,006201
lncRNA	WDFY3-AS1	ENSG00000251260	↑ 2,43	0,000156
mRNA	IGHV3-66	ENSG00000211972	↑ 2,34	0,00018
mRNA	SPCS2; SPCS2P4	NR_027268	↑ 6,2	0,000035
mRNA	PRRG1	BC030786	↑ 2,93	0,030348
mRNA	FIGN	NM_018086	↑ 2,56	0,003292

lncRNA	IGHV	JN110922	↑ 6,79	0,000138
Structural RNA	VG7 IgHCh	GQ233007	↑ 5,07	0,000647
mRNA	IGHV3-38	ENSG00000211958	↑ 5,19	0,00784
lincRNA	RP11-473E2.2	ENSG00000223795	↓ 2,01	0,00344
piRNA-c	piR-51194	DQ584082	↑ 3,65	0,043055
mRNA	CHEK2P2	NR_038836	↓ 2,39	0,006789
lncRNA	AC073218.3	OTTHUMG00000152140	↓ 2,66	0,000882
lincRNA		NONHSAT113858.2	↓ 2,11	0,000067
Pre-miRNA		ENSG00000221576	↓ 2,39	0,006862
Pre-miRNA	hsa-mir-220b	ENSG00000215937	↓ 2,18	0,042736
mRNA	GID4	NM_024052	↑ 2,33	0,000043
piRNA-c	CTD-2647L4.4	ENSG00000259366	↓ 2,29	0,014273

In order to identify specific targets depending of both age and AFC, we compared all groups concomitantly (YL vs YH vs OL vs OH), and we found little overlap of differentially expressed genes across groups. From this comparison, 198 unique genes were differentially expressed among the groups (Fold change 2, ANOVA p-value <0.05; Figure 20, Table 7 and Annex-table 1). The 198 genes were composed by 30 mRNA and 168 ncRNA. In comparison with the rest of the groups, Group YH showed increased differential expression of 2 ncRNAs, *RP11-47P18.1* and *Krtap6-1* (Figure 20A). In Group OH, we detected differential upregulation of the ncRNA *U78793* (Figure 20B). Group YL showed differential downregulation of the ncRNA transcript ENSG0000023917 (Figure 20C). Finally, Group OL presented a set of 5 differentially regulated transcripts (Figure 20D), consisting of 1 less abundant ncRNA (*lncANXA5*), 2 increased mRNAs (*IGHV3-38*, and *IGHV3OR16-9*) and 2 less abundant mRNAs (*ANXA5* and *SPATC1L*).

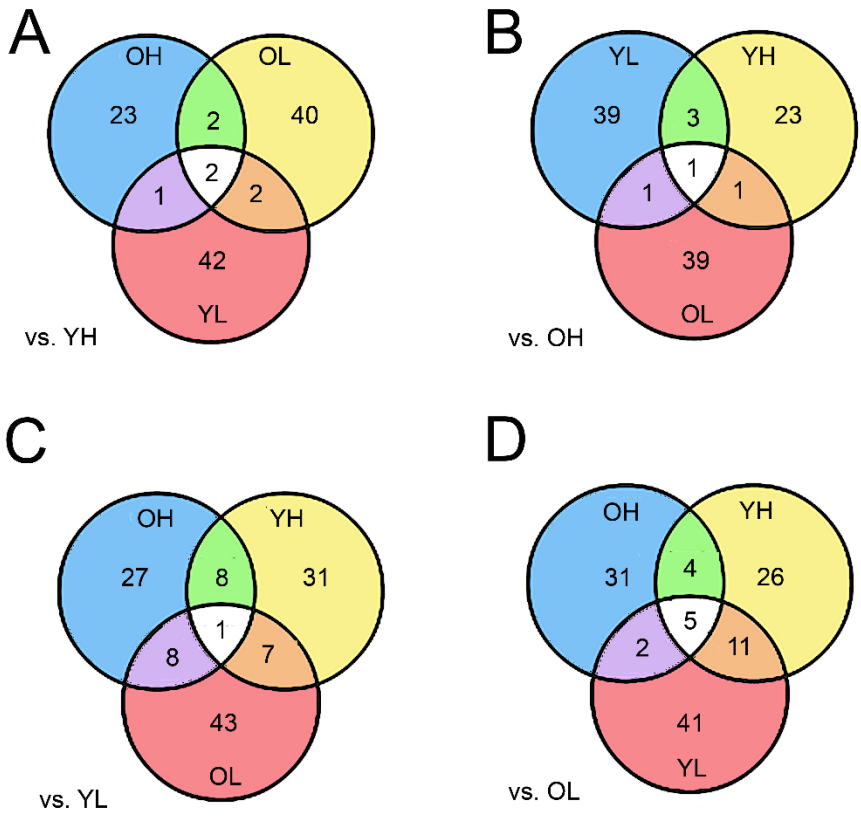

Figure 20: Venn diagrammatic representation of the microarray results comparison derived from individual human oocytes grouped regarding age and AFC. Venn circles indicate the number of transcripts differentially expressed in A) Young with High AFC (YH,; age 21 ± 1 years and 24 ± 3 follicles) group vs. the other three, B) Old with High AFC (OH; age 32 ± 2 years and 29 ± 7 follicles) group vs. the other three, C) Young with Low AFC (YL; age 24 ± 2 years and 8 ± 2 follicles) group vs. the other three, and D) Old with Low AFC (OL; age 34 ± 1 years and 7 ± 1 follicles) group vs. the other three.

Table 7. Number and type of differentially regulated transcripts in human oocytes referred to Venn diagrams shown in figure 20. Subheading of lists indicates those transcripts differentially regulated on each group comparison. #N/A: This identifier is not in the current EnsEMBL database.

YH in comparison with:							
	OH	YL	OL	OH and YL	OH and OL	YL and OL	OH, YL and OL
lincRNA	5	10	10	0	1	1	1
lncRNA	9	11	13	0	0	0	1
piRNA-c	3	6	0	1	0	0	0

Pre-miRNA	2	1	7	0	1	0	0
Structural RNA	2	6	3	0	0	1	0
mRNA	2	8	7	0	0	0	0
OH in comparison with:							
	YH	YL	OL	YH and YL	YH and OL	YL and OL	YH, YL and OL
lincRNA	4	10	3	2	0	0	0
lncRNA	8	13	12	1	1	0	1
piRNA-c	3	1	10	0	0	0	0
Pre-miRNA	3	6	3	0	0	0	0
Structural RNA	2	3	0	0	0	0	0
mRNA	3	6	11	0	0	1	0
YL in comparison with:							
	YH	OH	OL	YH and OH	YH and OL	OH and OL	YH, OH and OL
lincRNA	8	6	8	2	2	4	0
lncRNA	5	10	11	3	3	2	0
piRNA-c	4	0	13	1	2	0	0
Pre-miRNA	0	3	1	0	0	2	1
Structural RNA	7	3	4	0	0	0	0
mRNA	7	5	6	2	0	0	0
OL in comparison with:							
	YH	OH	YL	YH and YL	OH and YL	YH and OH	YH, OH and YL
lincRNA	10	3	14	0	0	0	0
lncRNA	8	10	9	5	1	2	1

piRNA-c	2	10	11	4	0	0	0
Pre-miRNA	2	3	4	0	0	0	0
Structural RNA	1	0	2	2	0	0	0
mRNA	2	5	1	0	1	2	4
#N/A	2	5	1	0	1	2	4

Subsequently, it was intended to investigate how the transcripts identified in this analysis changed compared to their non-matured counterparts. To this end, the transcriptional profile of GV stage oocytes obtained after follicular stimulation (non-matured) was compared with that of *in vivo* matured oocytes (MII).

Identification of differentially expressed transcripts and AS events between non-matured and in vivo matured oocytes.

In order to determine differences in gene expression and AS events between non-matured (GV) and in vivo matured (MII) oocytes three different comparisons were performed: H-MII *vs* GV, L-MII *vs* GV and O-MII *vs* GV. Human exon array CEL files for 4 non-matured oocytes (GV) and 12 in vivo matured MII oocytes were re-analyzed using AltAnalyze software version 2.1.0. This software is an easy-to-use application that allows the study of gene expression and alternative splicing without an advanced knowledge of bioinformatics programs or scripting. With this new software, new PCA analysis was conducted in order to investigate the similarities and differences of each of the four study groups (GV, H-MII, L-MII and O-MII) with respect to the global gene expression. The PCA showed two different groups, with non-matured oocytes (GV) clustered together, while no obvious clustering of mature oocytes (MII) in relation to age or ovarian reserve was observed (Figure 21).

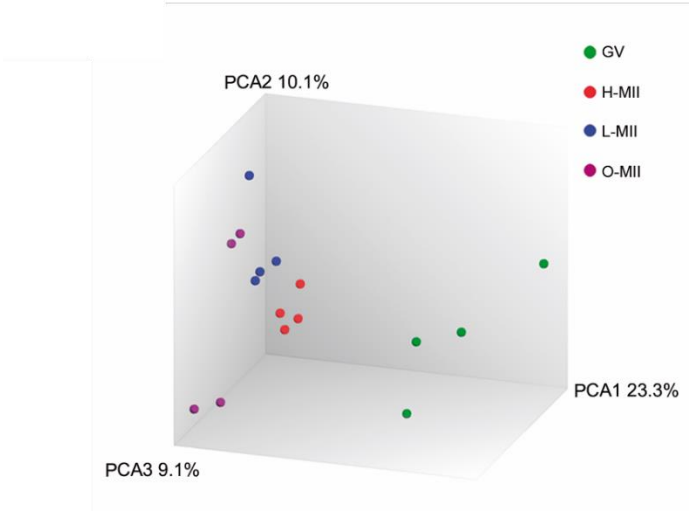

Figure 21: Principal component analysis (PCA) of the 4 studied groups (green: GV; red: H-MII; blue: L-MII and purple: O-MII).

Globally, we found 996 genes differentially expressed between the three comparisons. A majority of genes (702; 70.5%) were decreased in MII oocytes. Hierarchical clustering of these differentially expressed genes showed the expected clustering of the 4 GVs apart from the 12 *in vivo* MIIs. Moreover, sub-clustering of the 4 L-MII samples within the MII cluster was also observed while H-MII and O-MII oocytes did not cluster (Figure 22).

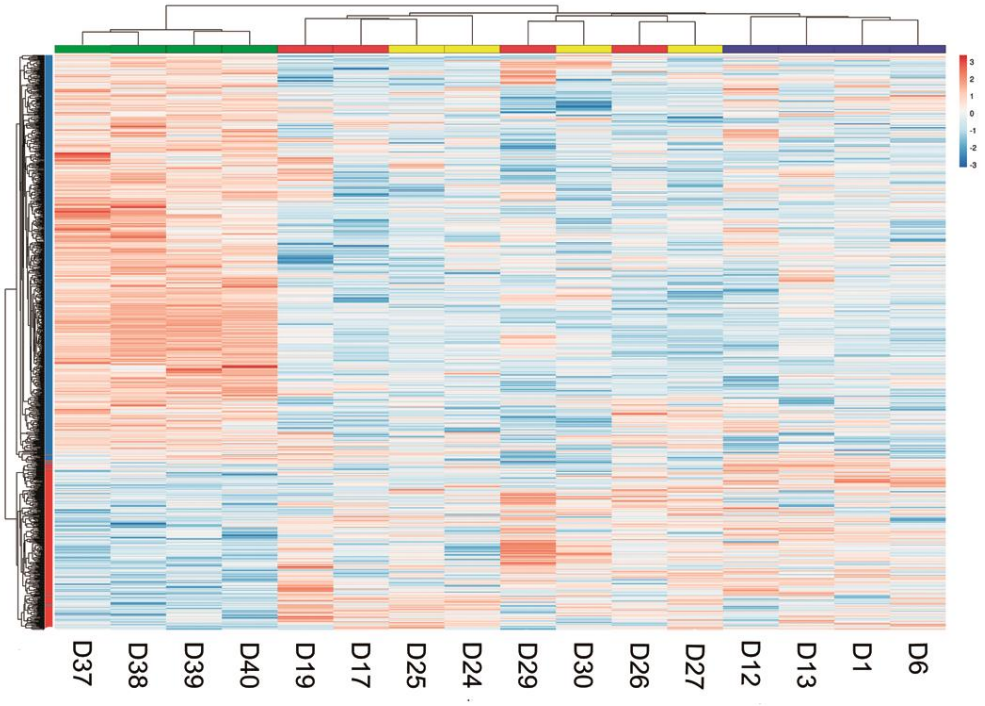

Figure 22: Hierarchical clustering of the differentially expressed genes (fold change > |2| and p-value < 0.05). Top: color map indicates the four groups studied (green: GV; red: H-MII; blue: L-MII and yellow: O-MII). The name of the samples is indicated at the bottom of the cluster lines.

GO biological analysis revealed general and mitochondrial translation processes, oxidative phosphorylation and nucleoside metabolism as the most enriched biological processes (Table 8).

Table 8: GO-analysis for biological processes (PANTHER) of differentially expressed genes between MII and GV oocytes (Fold Change>|2|, p<0.05) applying Fisher test with Bonferroni correction. NA. Non-applicable.

GO biological process complete	**# genes**	**Fold Enrichment**
mitochondrial translational elongation (GO:0070125)	17	5.29
mitochondrial translational termination (GO:0070126)	17	5.23
translational termination (GO:0006415)	17	4.9
cellular protein complex disassembly (GO:0043624)	21	4.18
mitochondrial translation (GO:0032543)	17	4.15
translational elongation (GO:0006414)	18	3.93
mitochondrial gene expression (GO:0140053)	19	3.77
electron transport chain (GO:0022900)	25	3.57
protein-containing complex disassembly (GO:0032984)	26	2.97
generation of precursor metabolites and energy (GO:0006091)	38	2.43
oxidation-reduction process (GO:0055114)	69	1.88
gene expression (GO:0010467)	119	1.54
cellular nitrogen compound metabolic process (GO:0034641)	112	1.37
cellular metabolic process (GO:0044237)	362	1.25
Unclassified (UNCLASSIFIED)	93	0.74
Unmapped non-coding RNAs	26	NA

When analyzing the differences between single MII groups and GV we observed that 489, 468 and 564 genes were differentially expressed in H-MII *vs* GV, L-MII *vs* GV and O-MII *vs* GV, respectively, with around 25% of them representing non-coding genes (Table 9), and 154 (15.5%) of the differentially expressed genes were shared among the 3 comparisons (Figure 23).

Table 9: Differentially expressed genes in the 3 comparisons studied: H-MII vs GV, L-MII vs GV and O-MII vs GV.

	Increased expression	**Decreased expression**	**TOTAL**
H-MII vs GV			
Regulated protein-coding genes	78	291	369
Regulated ncRNA genes	17	103	120
TOTAL	**95**	**394**	**489**
O-MII vs GV			
Regulated protein-coding genes	109	322	431
Regulated ncRNA genes	28	105	133
TOTAL	**137**	**427**	**564**
L-MII vs GV			
Regulated protein-coding genes	84	250	334
Regulated ncRNA genes	36	98	134
TOTAL	**120**	**348**	**468**

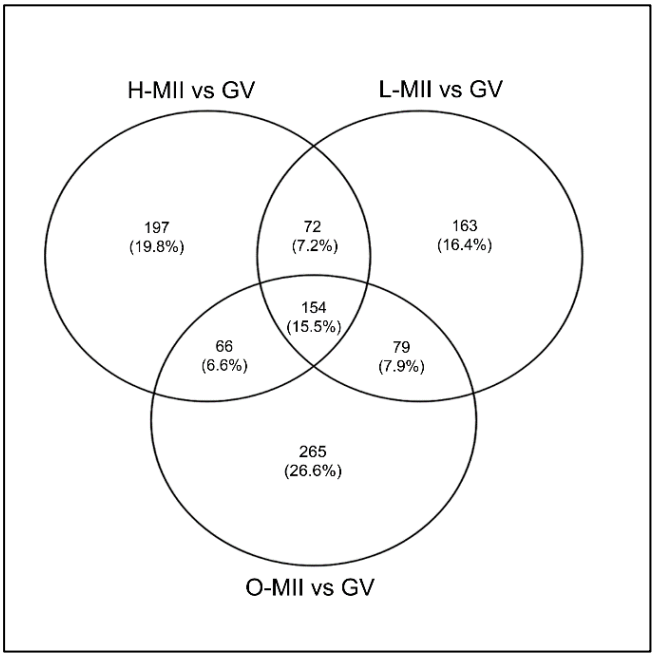

Figure 23: Venn diagrammatic representation of the differentially expressed genes (fold change > |2| and p-value < 0.05) observed, in individual human oocytes, in the 3 comparisons: H-MII *vs* GV, L-MII *vs* GV and O-MII *vs* GV. Venn circles indicate the number of transcripts differentially expressed and, in brackets, their percentages with respect to the total number of genes.

The small number of transcripts differentially expressed detected (996 out of more than 285,000 detectable) revealed that the majority of transcripts maintained stable levels among non-matured and mature oocytes. The repression of the transcription in fully grown oocytes suggests that gamete fertilization and zygote development depend on a very finely tuned regulation of protein expression, driven by mechanisms that are

unrelated to the modulation of transcription rate such as the alternative splicing (AS). In order to determine whether the stably expressed genes underwent regulation by AS, we analyzed the AS profile of *in vivo* matured MII *vs* non-matured GV using the FIRMA algorithm of AltAnalyze. A total of 3,292; 3,153 and 2,720 genes containing differentially expressed exons (AS events) were identified in H-MII, L-MII and O-MII groups respectively, when compared to GVs. Of those AS events, 1,253 were shared among the 3 comparisons (Figure 24). We analyzed the type of AS events across our samples and found cassette exon (38%) as the most represented event followed by alternative C'-terminus (28%) and alternative 3' acceptor site (23%). Alternative N' terminus and alternative 5' donor site accounted for only 8% and 3% of the total splicing events, respectively. GO analysis showed enrichment of biological processes related to mitochondrial translation regulation, nuclear mRNA export, mRNA splicing, positive regulation of translation and regulation of chromosome and organelle organization, among others (Table 10).

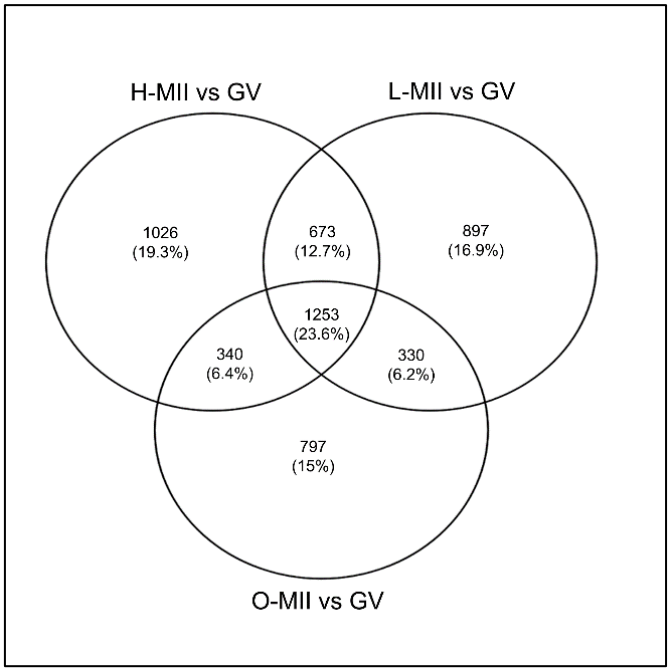

Figure 24: Venn diagrammatic representation of the alternative splicing events observed in the 3 comparisons: H-MII vs GV, L-MII vs GV and O-MII vs GV when analyzed with FIRMA algorithm. Venn circles indicate the number of transcripts affected by AS events and in brackets, their percentages with respect to the total number of transcripts.

Table 10: GO-analysis for significant biological processes (PANTHER; FE ≥ 2) of the 1,253 genes with an alternative spliced (AS) event shared in H-MII vs GV, L-MII *vs* GV and O-MII *vs* GV comparisons (Fold Change>|2|, p<0.05) applying Fisher test with Bonferroni correction.

GO biological process complete	**# genes**	**Fold Enrichment (FE)**
Mitochondrial translation elongation (GO:0070125)	24	4.58
Mitochondrial translation termination (GO:0070126)	23	4.34
mRNA export from nucleus (GO:0006406)	22	3.42
Ribonucleoprotein complex assembly (GO:0022618)	44	3.26
mRNA splicing, via spliceosome (GO:0045292)	54	3.14
rRNA processing (GO:0006365)	32	2.62
Regulation of protein stability (GO:0031647)	38	2.37
Regulation of translation (GO:0006417)	47	2.33
Regulation of chromosome organization (GO:0033044)	47	2.32
DNA repair (GO:0006281)	65	2.24
Mitotic cell cycle regulation (GO:0007346)	71	2.00
Transcription, DNA-templated (GO:0007532)	74	1.85

In order to determine the inclusion or the exclusion of a given exon obtained with the FIRMA algorithm, we subjected these AS events to analysis with the ASPIRE algorithm, which takes into consideration the exon-junction values. Therefore, AS events observed in this new analysis were the result of the exon-junction analysis (ASPIRE) and the single feature (exon or junction) analysis (FIRMA). Globally, the three comparisons yielded a total of 36 high confidence AS events corresponding to 35 genes (Table 11). Only one of these genes presented 2 differentially spliced exons (*ITPA*). Hierarchical clustering of the differentially expressed exons among the four study groups (GV, H-MII, L-MII and O-MII), showed that the 4 GV samples clustered together, and the 12 MII samples were very similar and all clustered in a single group despite their differences in age and ovarian reserve (Figure 25). The majority (24 out of 36; 66%) of the differentially expressed exons were more abundant in GVs (Table 11), indicating that the corresponding AS event was produced to provide the MII oocyte with the correct isoform of the transcript. We found a total of 10 differentially spliced exons (27.7%) from 9 genes to be common in all the comparisons, with 6 of them being decreased (*DIAPH2*, *GALK1*, *PPOX*, *THBS4*,

OSBP2 and *PIK3CD*) and 4 increased in MII (*ITPA, PDXK* and *lincPOLR3G-8*). In addition, 15 exons were found shared when groups were compared in a pair-wise fashion to GVs (8 in H-MII and L-MII; 1 in H-MII and O-MII and 6 in O-MII and L-MII). Finally, 11 AS exons were unique to individual comparisons against GVs (1 in H-MII; 5 in L-MII; and 5 in O-MII) (Table 11).

Table 11: List of genes affected by alternative splicing (AS) events confirmed by FIRMA and ASPIRE algorithms. MII groups compared with GV are shown. ↑ increased exon expression; ↓ decreased exon expression.

Symbol	**Function**	**AS event**	**H-MII**	**L-MII**	**O-MII**
DIAPH2	Development and normal function of the ovaries.	alt-C-term	↓	↓	↓
GALK1	Major enzyme for the metabolism of galactose.	alt-3'	↓	↓	↓
ITPA	Involved in pyrimidine metabolism.	alt-3'	↑	↑	↑
OSBP2	Binds to oxysterols and inhibit their cytotoxicity.	alt-5'	↓	↓	↓
PDXK	Involved in vitamin B6 metabolism.	cassette-exon	↑	↑	↑
PIK3CD	Phosphorylate inositol lipids and is involved in the immune response.	cassette-exon	↓	↓	↓
PPOX	Involved in Porphyrin and chlorophyll metabolism.	cassette-exon	↓	↓	↓
THBS4	Mediates cell-to-cell and cell-to-matrix interactions.	alt-3'	↓	↓	↓
lincPOLR3G-8	Inhibits *TMEM161B*, a gen involved in the nucleic acid binding.	alt-N-term	↑	↑	↑
COX17	Terminal component of the mitochondrial respiratory chain.	alt-3'	↑	↑	
EPAS1	Transcription factor involved in the induction of genes regulated by oxygen.	alt-C-term	↓	↓	
GET4	Intracellular transport of proteins.	alt-N-term	↑	↑	
SLC35E4	Putative transporter.	alt-C-term	↓	↓	
SUMF2	Sulfatase modifying factor involved in the metabolism of proteins.	cassette-exon	↓	↓	
TBC1D7	Regulation of cellular growth and differentiation.	alt-3'	↑	↑	

UFSP2	Regulation of cell proliferation and differentiation.	alt-3'	↓	↓	
XRCC6	Involved in the repair of nonhomologous DNA ends.	alt-C-term	↓	↓	
JMJD7-PLA2G4B	Involved in ovarian steroidogenesis and phospholipase I signaling pathway.	cassette-exon	↓		↓
ARHGEF33	Involved in the Rho guanyl-nucleotide exchange factor activity.	cassette-exon		↓	↓
CCDC126	Involved in the 6-beta-N-acetylglucosaminyltransferase activity.	alt-3'		↑	↑
HNF1A	Transcription factor required for the expression of liver-specific genes.	alt-C-term		↓	↓
NTN1	Involved in axon guidance and cell migration during development.	alt-C-term		↓	↓
PDZD2	Involved in early stages of prostate tumorigenesis.	cassette-exon		↓	↓
TMEM25	Transmembrane protein.	alt-C-term		↓	↓
TMED3	Transmembrane protein involved in the metabolism of proteins.	alt-C-term	↓		
DDRGK1	Ubiquitin-like protein ligase binding.	alt-C-term		↑	
PDPK1	Kinase involved in ERK signaling and gene expression.	cassette-exon		↓	
PLAGL1	Zinc finger that suppresses cell growth.	alt-3'		↑	
TEK	Kinase involved in ERK signaling and Akt signaling.	cassette-exon		↑	
TRIO	GDP to GTP exchange factor. Reorganizes the actin cytoskeleton thereby regulating cell migration and growth.	alt-C-term		↓	
ANO4	Transport of sugars, ions and amine compounds.	cassette-exon			↑
LOXL1-AS1	Inhibits *LOXLI*, a gene involved in the biogenesis of connective tissue.	cassette-exon			↓
MAT2B	Catalyzes the biosynthesis of S-adenosylmethionine from methionine and ATP	cassette-exon			↓
PPIL3	Involved in pre-mRNA splicing.	cassette-exon			↑
SLC29A4	Polyspecific organic cation transporter.	alt-3'			↓

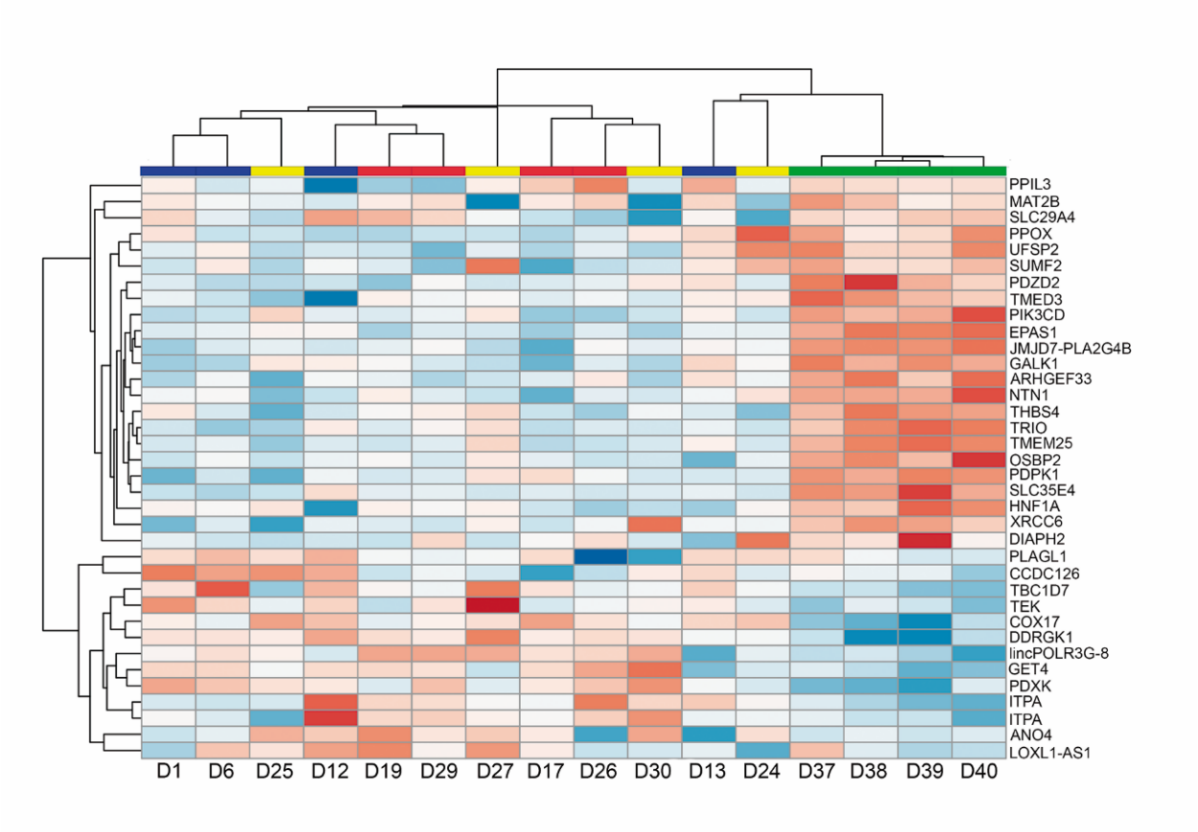

Figure 25: Hierarchical clustering of the alternative splicing events observed in the 3 comparisons: H-MII vs GV, L-MII vs GV and O-MII vs GV. Top: color map indicates the four studied groups (green: GV; red: H-MII; blue: L-MII and yellow: O-MII). The name of the samples is indicated at the bottom of the cluster lines. The gene symbols of the 36 differentially expressed exons are indicated on the right.

Microarray validation by qPCR

A total of 73 transcripts: 15 protein-coding, 48 non-coding and 10 genes showing AS events, were chosen for array validation by qPCR of the differentially gene expression on MII oocytes in relation to age and ovarian reserve (primers used are detailed in Table 1). All the selected primers had efficiencies between (80-110%), a single melting curve peak and amplified the desired nucleotide sequence, analyzed by Sanger sequencing. All the primers that did not match with these criteria were designed again and finally, if they were still not good, were discarded. Overall, we were unable to amplify 22 of these transcripts by qPCR (*PSMB5, RNY5, lincDISP1, lincMADCAM1, lncMETTL16,*

lncCCAT1, lincSPRED2, lincROBO1, lincGALNTL6, lncPPARG, lncEMP2, lincGNAQ, lincRHOB, LINC00331, RP11-393I23.4, RP11-700E23.1, lncC1orf148, RP11-5P4.2, LOC401242, PLAGL1, OSBP2 and *TMED3*). All the non-coding RNAs analyzed were lncRNAs, since were the class of non-coding RNAs more represented as differentially expressed among groups. For each of the 10 selected genes with an AS event, 3 amplicons were analyzed, one targeting the common region of all the isoforms and two targeting the different isoforms produced by the specific AS event observed (Figure 27).

Additionally, 7 housekeeping genes (*ACTß, RPLP0, DNMT1, PGK1, SDHA, UBC,* and *YWHAZ)* and 10 non-coding RNAs (*RP11-473E2.2, RP5-1024G6.2, RP11-260E18.1, RP11-434D9.2, RP11-399K21.11, RP11-284G10.1, RP11-506M13.3, DHPS-002, RP11-129M6.1* and *RP11-314013.1*) that showed stable expression in the array were analyzed for reference gene identification. geNORM algorithm (Vandesompele 2002) was applied to determine the expression stability of the putative reference genes. From these, 3 housekeeping genes (*ACTß, UBC* and *DNMT1*) and 1 stable non-coding RNA (*RP11-314013.1*) presented coefficient of variation (CV) < 0.25 and M value < 0.5, indicating that they could be used as homogeneous reference genes. The expression stability analysis was conducted again for the AS validation since in this analysis GV oocytes were also included. In this new analysis, 3 housekeeping genes appeared as most stable (*UBC, RPLP0* and *ACTß*) and *UBC* and *RPLP0* were used as homogeneous reference genes (CV < 0.25 and M value < 0.5).

Finally, 3 housekeeping genes (*ACTß, UBC* and *DNMT1)* plus 12 coding transcripts plus 2 structural RNAS (*SNORD123* and *SNRPN*) (Figure 26), 31 lncRNAs (Table 12) and 7 genes with an AS event (Figure 27) were used to validate arrays at the non-coding level. Box plot analysis was used to represent the distribution of data from array (RMA) and the data from HRGs-normalized qPCR. Representations showed similar behavior of

selected transcripts and AS events across groups. Overall, we were able to validate the results obtained in the array at the gene expression and AS level by qPCR as representations showed similar behavior in the array and in the qPCR.

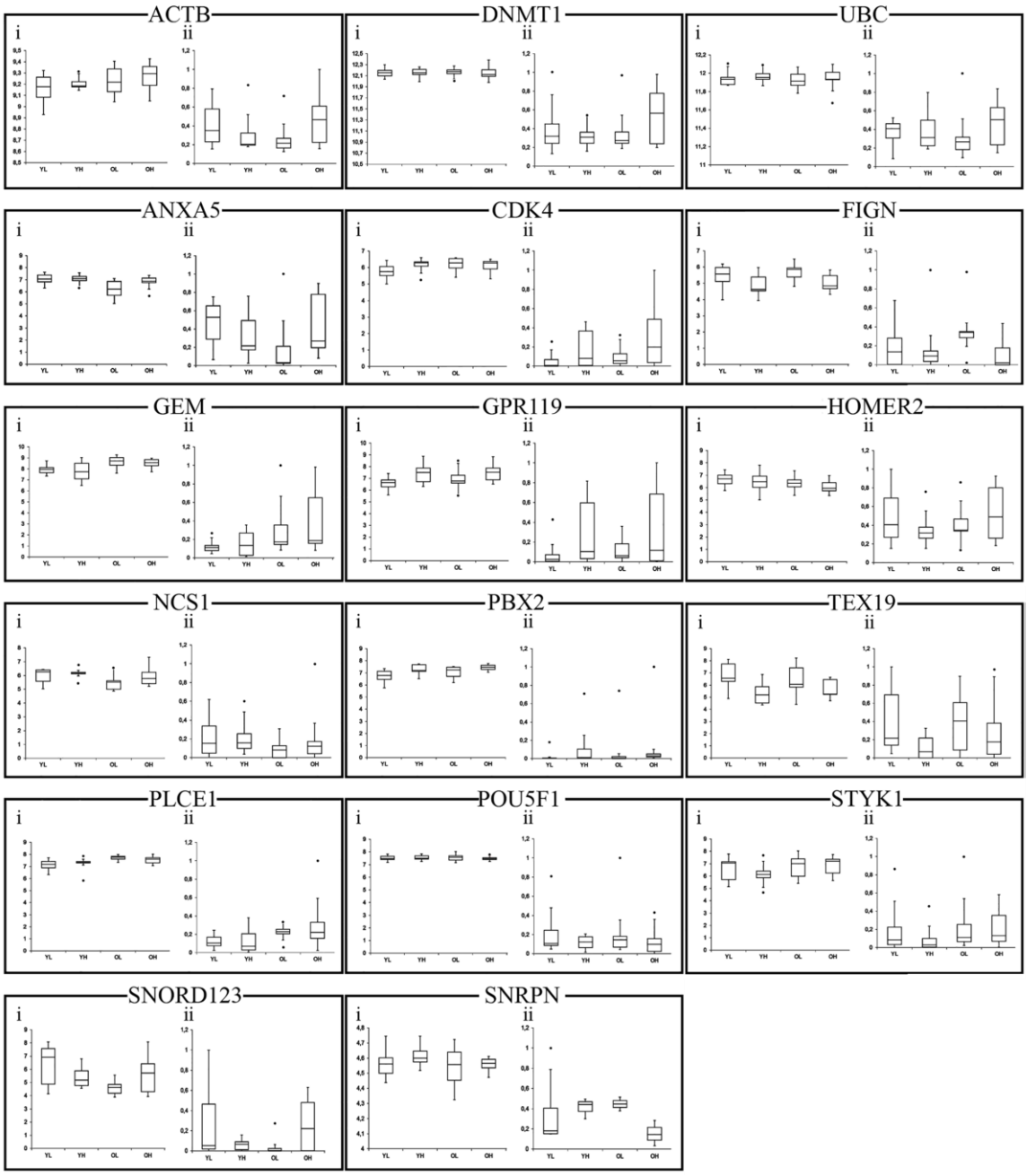

Figure 26: Validation of HTA 2.0 array by qPCR using the same RNA samples. Box-plot analysis of log-intensities expression from the array (i) and gene expression profiles by qPCR (ii) of the selected genes was measured in individualized RNA extraction and amplification from human oocytes. All qPCR data is represented as ΔCq value (delta quantification cycle) ($2^{\wedge-(\text{Cq target-Cq HRGs})}$).

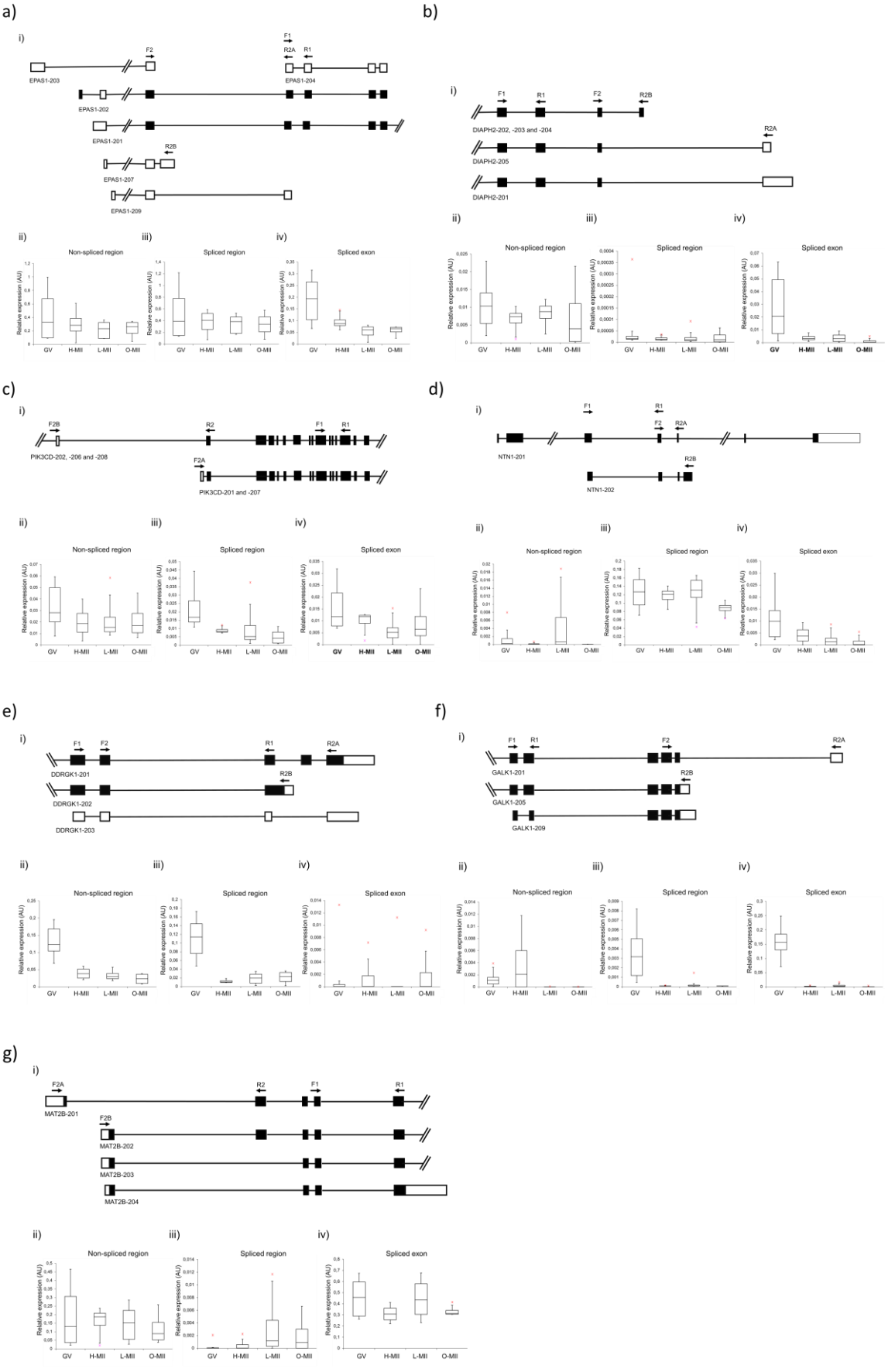
a)
i)
EPAS1-203
EPAS1-202
EPAS1-201
EPAS1-207
EPAS1-209
F2
F1
R2A
R1
R2B
EPAS1-204
ii)
iii)
iv)
Non-spliced region
Spliced region
Spliced exon
Relative expression (AU)
GV
H-MII
L-MII
O-MII
b)
i)
DIAPH2-202, -203 and -204
DIAPH2-205
DIAPH2-201
F1
R1
F2
R2B
R2A
ii)
iii)
iv)
Non-spliced region
Spliced region
Spliced exon
c)
i)
PIK3CD-202, -206 and -208
PIK3CD-201 and -207
F2B
R2
F1
R1
F2A
ii)
iii)
iv)
Non-spliced region
Spliced region
Spliced exon
d)
i)
NTN1-201
NTN1-202
F1
R1
F2
R2A
R2B
ii)
iii)
iv)
Non-spliced region
Spliced region
Spliced exon
e)
i)
DDRGK1-201
DDRGK1-202
DDRGK1-203
F1
F2
R1
R2A
R2B
ii)
iii)
iv)
Non-spliced region
Spliced region
Spliced exon
f)
i)
GALK1-201
GALK1-205
GALK1-209
F1
R1
F2
R2A
R2B
ii)
iii)
iv)
Non-spliced region
Spliced region
Spliced exon
g)
i)
MAT2B-201
MAT2B-202
MAT2B-203
MAT2B-204
F2A
R2
F1
R1
F2B
ii)
iii)
iv)
Non-spliced region
Spliced region
Spliced exon

Figure 27: Array validation by qPCR of AS events confirmed for (a) *EPAS1* (cassette-exon) (b) *DIAPH2* (alternative C-terminus), (c) *PIK3CD* (cassette-exon), (d) *NTNT1* (alt-C-term), (e) *DDRGK1* (alt-C-term), (f) *GALK1* (alt-3') and (g) *MAT2B* (cassette-exon). Relative expression of isoforms was measured in individualized RNA extraction and amplification from human oocytes of the four study groups (GV, H-MII, L-MII and O-MII). i) Schematic diagram of the genomic structure encompassing the corresponding AS event (5'→3'). Boxes represent exons (black: coding and white: non-coding), horizontal lines represent introns and arrows represent the position of the primers used for validation. All isoforms are named according to ENSEMBL version GRCh38.p12. Box plot analysis of the relative expression of transcript isoforms, affected by the confirmed AS event, containing: (ii) Non-spliced region (primers F1 + R1); (iii) Spliced region (primers F2 + R2A); (iv) Spliced exon (primers F2 + R2B). All qPCR data is represented as ΔCq value (delta quantification cycle) ($2^{\wedge-(Cq(target)-Cq\ (HRGs)}$). Black dots represent outliers. AU; arbitrary units.

For the array validation at the lncRNA level, it was decided to focus on the YL group since was the most interesting due to the fact that was composed of young women with low ovarian reserve. In order to assess the influence of age and ovarian reserve in the oocyte quality, the results of the YL vs OL (age) and YL vs YH (ovarian reserve) comparisons were analyzed. The results of this validation are represented in Table 12 and showed similar behavior of the lncRNAs in YL vs YH and YL vs OL comparisons when analyzed by array and qPCR. Overall, from the 31 lncRNAs analyzed, 18 (60%) showed the same trend in the YL vs YH comparison in both techniques, whereas 25 (80%) of the lncRNAs showed same tendencies in the YL vs OL comparison when analyzed by microarray and qPCR (Table 12).

Table 12: Validation of HTA 2.0 array, at the lncRNA level, by qPCR using the same RNA samples. ↑ increased lncRNA expression; ↓ decreased lncRNA expression. All qPCR data is represented as ΔCq value (delta quantification cycle) ($2^{\wedge-(Cq(target)-Cq\ (HRGs)}$).

MII oocytes	**ARRAY**		**qPCR**	
lncRNA	**YL vs YH**	**YL vs OL**	**YL vs YH**	**YL vs OL**
lincPOU3F1-1	↑		↑	
AC019117.2	↑		↑	
lincSKA2	↑			
AC003092.1	↓	↓	↓	↓
lincCOL1A2-2	↓	↓		↓
lncC9orf3	↓	↓	↓	↓
lncANXA5		↑		↑
RP11720L8.1	↑	↑		
lincCCDC140	↓	↓		↓

lincSLC5A12	↓	↓	↓	↓
lincSP4		↑		↑
lincKCNG2	↑		↑	↑
lincNDUFV3-1	↑		↑	
lncCKMT1B-1-1	↓		↓	
lincPTPRQ-7	↓		↓	
lincOSBPL5	↓		↓	↓
lincARRDC4	↓		↓	
lncAVEN-1:1	↑		↑	
CTB-78F1.2	↑	↑		↑
RP11-12A2.3	↑	↑	↑	
KCNC4-AS1		↑	↓	
lincCC2D1B		↓	↓	↓
RP11-180C1.1-001		↓	↓	↓
RP11-180C1.1-002		↓	↓	↓
lncGFM1-5-6		↑	↑	
RP11-98J23.1		↑	↑	↑
lncSMUG1		↑	↓	↑
RP11-991C1.1	↑	↑	↑	↑
lncARL15		↓	↓	↓
lncADCYAP1R1		↓		↓
RP11-809N8.2-001	↑	↑		↑

4.1.3.2. **Phase II: Analysis of the functional role of the potential markers of oocyte developmental competence identified in Phase 1.**

In order to analyze the functional role of the potential markers of oocyte quality, we decided to focus on the lncRNAs since were the class of RNA transcripts most differentially expressed in MII oocytes from women of different age and ovarian reserve. Moreover, lncRNA have been associated with important cellular processes such as proliferation, lineage commitment and development, suggesting a role in early human embryonic development.

Research methods and strategies to study lncRNA are still in its infancy and normally involve 5 strategies: lncRNA new species identification, bioinformatic analysis, subcellular localization, experiments of gain or loss of function and molecular interaction.

As lncRNAs research is complex, human oocytes are scarce and the molecular techniques required to study lncRNA function have not been scaled to single-cell yet, it was decided to use a cellular model (HEK293-T) in order to analyze the function of the lncRNAs. HEK293-T cells are human embryonic cells obtained from the kidney and are widely used in molecular biology to study the function of many gens. Other models more similar to the human oocyte, such as *Xenopus* egg extract, could also be used. However, it was prioritized the use of a model in which many of the techniques to be used were already optimized in order to facilitate the study of the lncRNAs.

LncRNA selection

The 31 lncRNAs differentially expressed in the array and validated by qPCR were pre-selected as candidates, in order to have more certainty of the change in expression experienced by these transcripts. Subsequently the genomic region surrounding each lncRNA was analyzed using several databases: Ensembl, FANTOM, NONCODE, LNCipedia and lncRNAdb. Since most of these lncRNAs were recently discovered (not always reported in all the databases), the use of several databases was useful to compare results between each other. Therefore, similarities between different databases, meant greater confidence regarding the genomic location of a target lncRNA. The lncRNAs overlapping a protein-coding gene were chosen for further analysis, since, being close, the lncRNA is more likely to be acting on the overlapping coding gene (Marchese et al., 2017) (Table 13).

Table 13: LncRNA genomic localization in relation to the closest protein-coding gene at 3'. LncRNAs highlighted in blue are the ones selected for further analysis.

lncRNA	Location with the associated protein-coding gene
lincPOU3F1-1	256 Kb upstream POU3F1
AC019117.2	578 Kb upstream AGR3
lincSKA2	Overlapping SKA2
AC003092.1	372 Kb upstream COL1A2
lincCOL1A2-2	330 Kb upstream COL1A2
lncC9orf3	169 Kb upstream C9orf3
lncANXA5	Overlapping ANXA5
RP11-720L8.1	267 Kb upstream MEIS2
lincCCDC140	2559 Kb upstream CCDC140
lincSLC5A12	465 Kb upstream SLC5A12
lincSP4	258 Kb upstream SP4
lincKCNG2	38 Kb upstream KCNG2
lincNDUFV3-1	Overlapping NDUFV3
lncCKMT1B-1-1	Overlapping MAP1A
lincPTPRQ-7	151 Kb upstream PTPRQ
lincOSBPL5	Overlapping OSBPL5
lincARRDC4	490 Kb upstream ARRDC4
lncAVEN-1:1	7.5 Kb upstream AVEN
CTB-78F1.2	Overlapping TENM2
RP11-12A2.3	100 Kb upstream CITED2
KCNC4-AS1	139 Kb upstream ALX-3
lincCC2D1B	Overlapping CC2D1B
RP11-180C1.1-001	1904 Kb upstream CCKAR
RP11-180C1.1-002	1850 Kb upstream CCKAR
lncGFM1-5-6	Overlapping MFSD1
RP11-98J23.1	529 Kb upstream TAF9
RP11-991C1.1	192 Kb upstream GSC
lncARL15	600 Kb upstream ARL15
lncSMUG1	Overlapping SMUG1
lncADCYAP1R1	Overlapping ADCYAP1R1
RP11-809N8.2-001	Overlapping RELT

Then, the function of the associated coding genes was checked in silico by searching the principal reference webpages such as Gencards and NCBI and also by reviewing relevant literature regarding the gene of interest. The lncRNAs associated with genes whose function could be important for early embryonic development were selected (Table 14).

Table 14: Function of the protein-coding genes overlapping with the selected lncRNAs. LncRNAs highlighted in blue are the ones selected for further analysis.

lncRNA	Associated protein-coding gene	Function
lincSKA2	SKA2	Microtubule binding protein involved in the signalling by GPCR and Rho GTPases.
lncANXA5	ANXA5	Calcium-dependent phospholipid binding protein involved in the regulation of CFTR activity and prostaglandin synthesis and regulation. Diseases associated with ANXA5 include pregnancy loss.
lincNDUFV3-1	NDUFV3	Poly(A) RNA binding protein Involved in metabolism and respiratory electron transport, ATP synthesis by chemiosmotic coupling, and heat production by uncoupling proteins.
lncCKMT1B-1-1	MAP1A	Microtubule associated protein involved in microtubule assembly.
lincOSBPL5	OSBPL5	Cholesterol and oxysterol binding protein involved in the maintenance of cholesterol balance in the body.
CTB-78F1.2	TENM2	Involved in neural development, regulating the establishment of proper connectivity within the nervous system by promoting the formation of filopodia and enlarged growth cone in neuronal cells.
lincCC2D1B	CC2D1B	Transcription factor that binds specifically to the DRE (dual repressor element) and represses HTR1A gene (serotonin receptor) transcription in neuronal cells.
lncGFM1-5-6	MFSD1	Atypical solute carrier identified mostly in neuronal plasma membranes and lysosomes.
lncSMUG1	SMUG1	Uracil-DNA Glycosylase involved in the pyrimidine metabolism and in the DNA double-strand break repair.
lncADCYAP1R1	ADCYAP1R1	Receptor that may regulate the release of adrenocorticotropin, luteinizing hormone, growth hormone, prolactin, epinephrine, and catecholamine.
RP11-809N8.2-001	RELT	TNFalpha receptor that activates the NF-kappaß pathway which regulates proinflammatory genes.

Finally, and because the expression of the lncRNA is very tissue-specific, the expression of the 11 lncRNA selected was analyzed in HEK293-T cells. The two lncRNAs with the

highest expression were *lncANXA5* and *RP11-809N8.2-001*. Nevertheless, the majority of the lncRNAs did not show expression in HEK293-T cells (Figure 28).

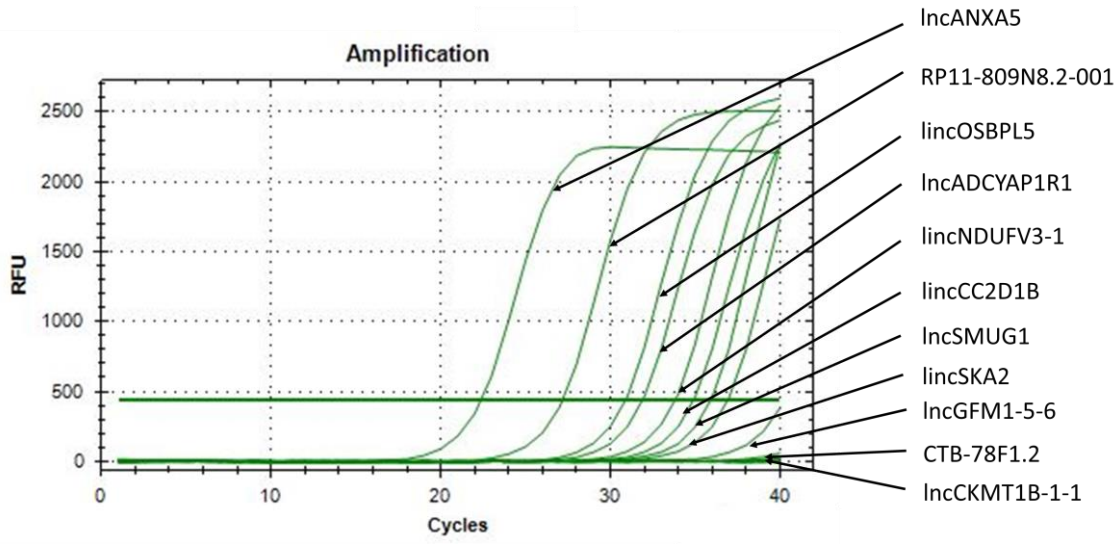

Figure 28: Analysis of the expression of the 11 lncRNAs candidates in HEK-293T. Reported only the lncRNAs that showed expression after the amplification by qPCR.

From the entire pool of lncRNA differentially expressed in MII oocytes in relation to age and ovarian reserve, it was chosen to study the function of *lncANXA5* and *RP11-809N8.2*, since after following the described criteria used for lncRNA selection, were the two most promising.

- *LncANXA5*: This lncRNA had not previously been annotated. The name was given due to the protein-coding gene which is overlapping, since is located in the 3'UTR region (sense strand) of the *ANXA5* gen (Figure 29A). *ANXA5* is a calcium-dependent phospholipid binding protein which has been associated with recurrent pregnancy loss (RPGL) (Hayashi et al., 2013; Demetriou et al., 2015). In the array, both *lncANXA5* and *ANXA5* showed increased expression in the YL group when compared to the OL (Supplementary Table 1 Annex). These results were validated by qPCR (Table 12).

- *RP11-809N8.2:* Is located in the 3'UTR region (antisense strand) of the *RELT* gen (Figure 29B). *RELT* is a member of the TNF-receptor superfamily. *RELT* activates the NF-kappaß pathway which regulates proinflammatory genes that among other functions are involved in inflammation associated with reproductive events e.g. menstruation and implantation (King et al., 2001; McCracken et al 2003). In the array, *RELT* was increased in YL when compared to OL, while *RP11-809N8.2* showed increased expression in YL when compared to YH and OL, independently (Supplementary Table 1 Annex). We were able to validate by qPCR the results of the YL vs OL comparison, but not the ones from the YL vs YH comparison (Table 12).

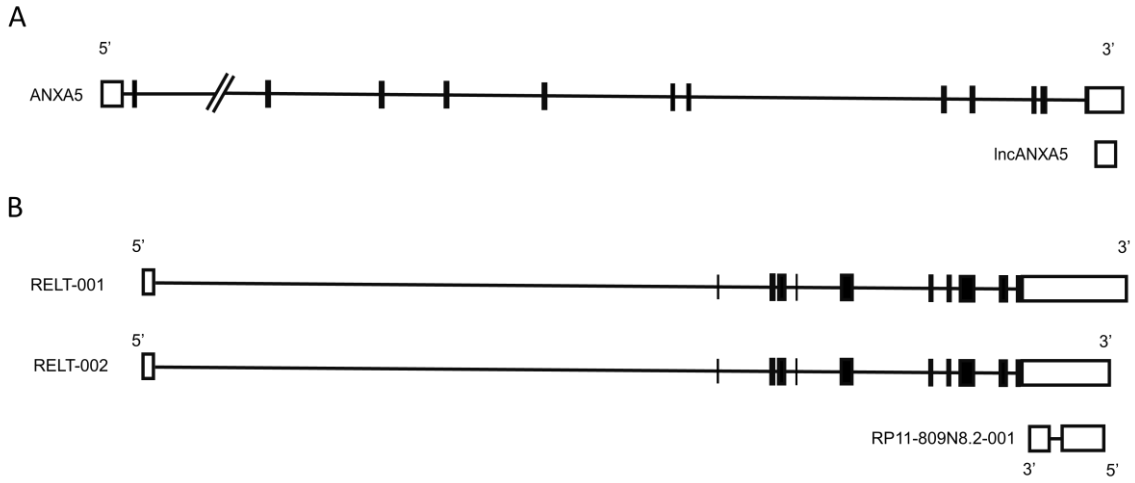

Figure 29: Schematic diagram of the genomic structure encompassing the selected lncRNAs (A) *lncANXA5* and (B) *RP11-809N8.2*. Boxes represent exons (black: coding and white: non-coding) and horizontal lines represent introns. All isoforms are named according to ENSEMBL version GRCh37.p13.

LncRNA subcellular localization

Initially, the subcellular localization of the two selected lncRNAs was determined. It was important to know the location of the lncRNAs at the subcellular level, in order to decide the strategy to knockdown them.

In order to identify the subcellular localization of the selected lncRNA candidates (*lncANXA5* and *RP11-809N8.2-001*) nuclear and cytoplasm fractions were obtained from HEK293-T cells. For that, as explained in materials and methods, several variants of the protocol were tested in order to optimize the technique. The protocol that showed the best results was the one where samples were incubated only with hypotonic buffer (HB), since after the washing, only a small portion of cell membranes was observed next to the nucleus. Moreover, nucleus had similar shape and size to the one observed in untreated HEK293-T cells (Figure 30A). On the other hand, samples incubated with HB and 10% NP-40 (non-ionic detergent) did not have cell membranes or cytoplasmic contamination next to the nucleus, nevertheless the nucleus was bigger when compared to the one observed in untreated HEK293-T cells, due to the pores created in the nuclear membrane by the detergent (Figure 30B).

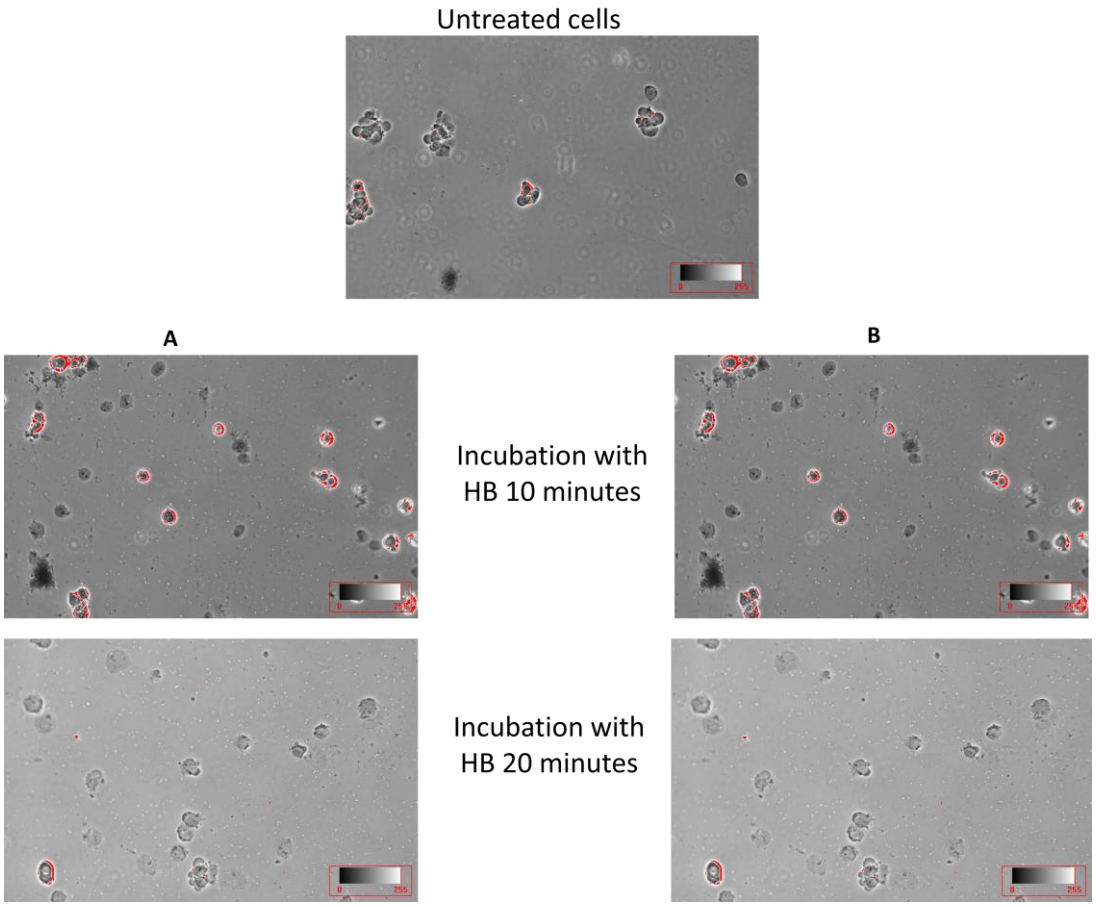

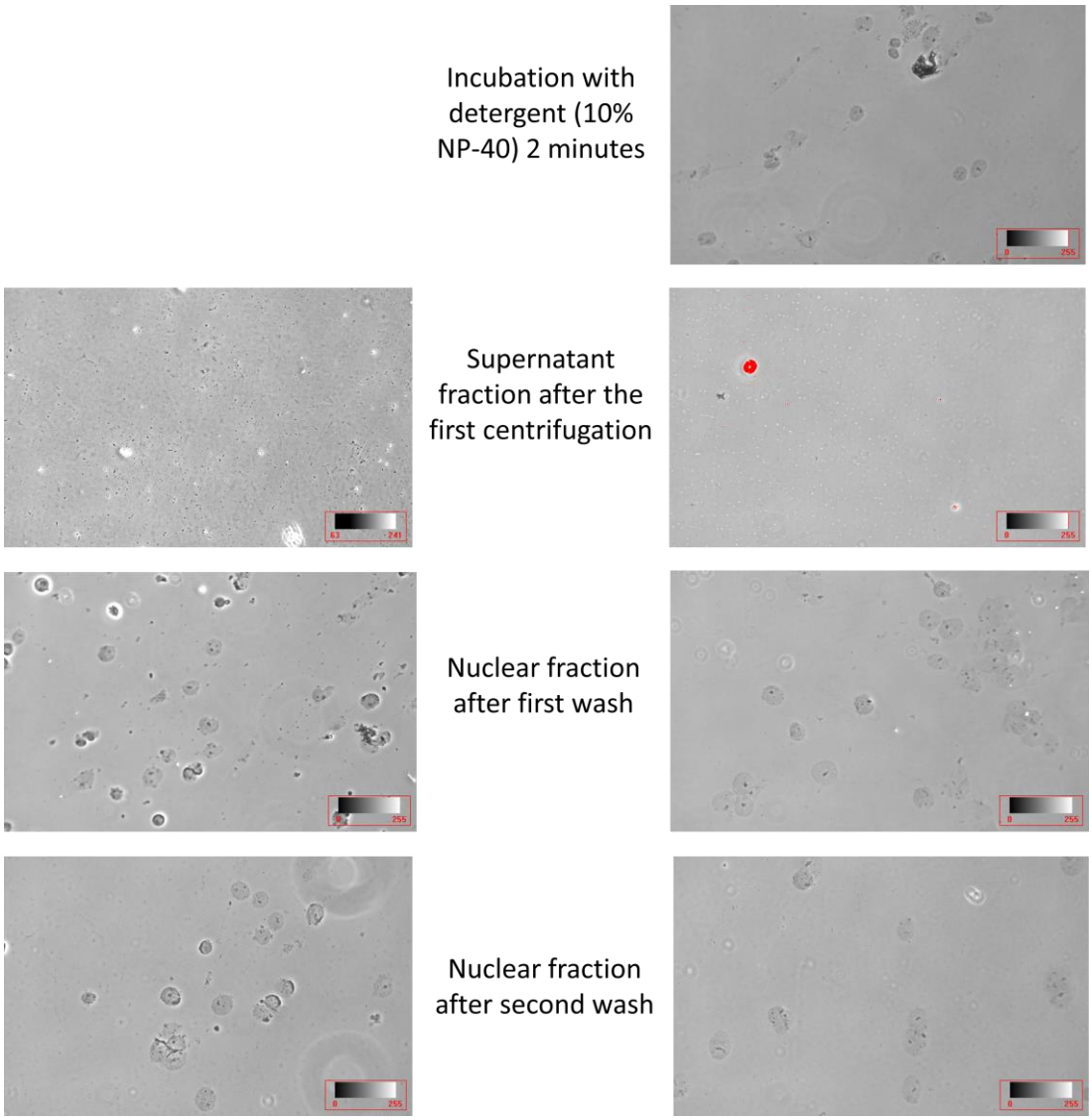

Figure 30: Brightfield microscopic images taken after several time-points of the subcellular fractionation protocol. (A) Samples incubated only with the hypotonic buffer. (B) Samples incubated with the hypotonic buffer and the detergent (NP-40). HB: Hypotonic Buffer. Red color represents image saturation.

The success of the subcellular fractionation was assessed first at the protein level by western blot using an anti-Histone H3 tri methyl K27 antibody (H3K27) as a nuclear marker and α-Tubulin antibody as a cytoplasm marker. After cellular fractionation, the nuclear marker was only detected in the nuclear fraction, whereas the cytoplasm marker was only present at the cytoplasm fraction (Figure 31).

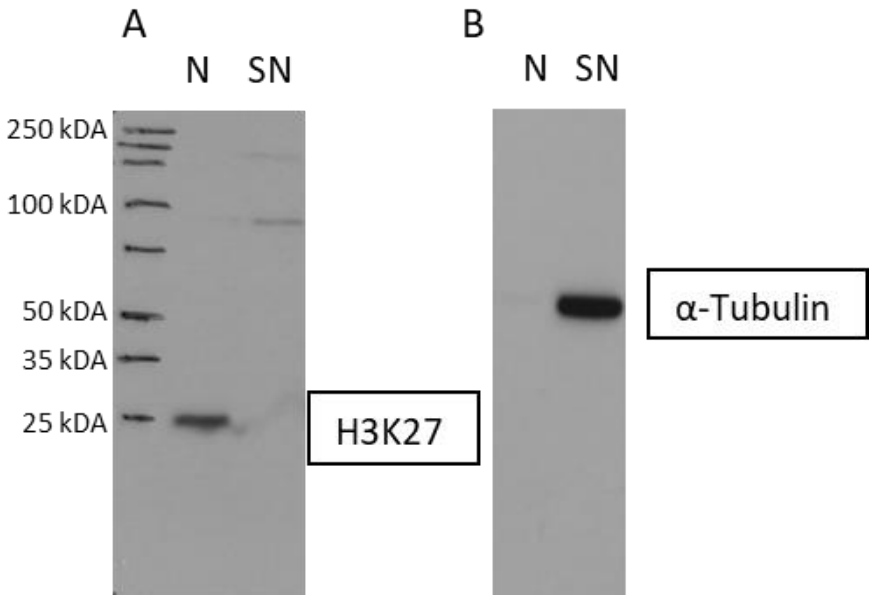

Figure 31: Detection of nuclear and cytoplasmic markers, (A) H3K27 (15kDA) and (B) α-Tubulin (50kDA), respectively, in extracts of HEK293-T cells incubated with the hypotonic buffer solution that separates the cytoplasm and the nuclear fractions. N: Nuclear fraction; SN: Supernatant fraction.

Once the success of the technique was analyzed at the protein level and the best method for subcellular fractionation was selected, the optimization of the subcellular fractionation protocol at the transcript level was conducted in order to determine the efficiency of the fractionation in terms of the distribution of the transcripts among the nucleus and the cytoplasm. Moreover, we wanted to analyze whether this determination could be used to identify the location of the selected lncRNAs in a quantitative way. The efficiency of the subcellular fractionation at the transcript level was assessed by qPCR using the lncRNAs *MALAT1*, *BACE1-AS* and *NEAT1* as nuclear markers and *GAPDH*, *NKILA* and *DANCR* as cytoplasm markers. However, *BACE1-AS* and *NKILA* showed very low expression in HEK293-T (Cq>35), so it was decided to exclude these markers from the analysis.

Subcellular fractionation analysis at the transcript level by qPCR showed the presence of the nuclear and cytoplasm markers in both fractions (nucleus and cytoplasm),

nevertheless, the ratio of expression was different. Nuclear markers showed more difference in expression between the nuclear and cytoplasm fractions, whereas the expression of the cytoplasm markers in each fraction was more similar (Figure 32). A possible explanation for the finding of expression of nucleus markers in the cytoplasm and vice versa, is that what we might be observing is a fraction enrichment and since qPCR is a very sensitive technique, can detect small contaminations from one fraction to another.

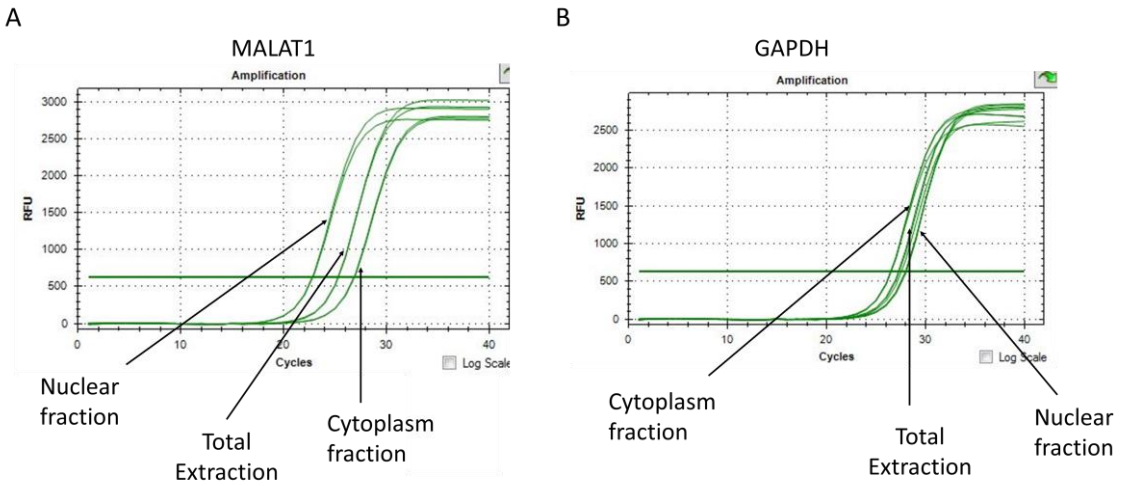

Figure 32: Example of subcellular fractionation analysis by qPCR. Total extraction refers to the RNA extracted from untreated HEK293-T (positive control). (A) nuclear marker and (B) cytoplasm marker.

Although subcellular fractionation was not 100% efficient at the transcript level, it allowed for the differentiation of transcripts located in the nucleus or in the cytoplasm. Thus, subcellular localization of the selected lncRNAs (*lncANXA5* and *RP11-809N8.2-001*) was conducted. Three independent replicates of subcellular fractionation were performed and the expression of the selected lncRNAs was analyzed in each fraction. Untreated HEK293-T was included in each replicate in order to calculate the expression ratio of the lncRNAs in each fraction with respect to the total expression. The results of these experiments showed that the nuclear markers (*MALAT1* and *NEAT1*) were more

present in the nucleus, whereas cytoplasm markers (*GAPDH* and *DANCR*) showed similar expression levels in both fractions. *LncANXA5* seemed to be located in the cytoplasm, since its expression pattern was similar to the cytoplasmic markers. In contrast, *RP11-809N8.2-001* seemed to be more expressed in the nucleus (Table 15).

Table 15: Subcellular fractionation results analyzed by qPCR. Nucleus-cytoplasm ratio = ((logΔCq nucleus/ logΔCq total extraction)/ (logΔCq cytoplasm/ logΔCq total extraction)).

	Experiment 1 Ratio Nucleus : Cytoplasm	**Experiment 2 Ratio Nucleus : Cytoplasm**	**Experiment 3 Ratio Nucleus : Cytoplasm**
Nuclear markers			
MALAT1	48 : 1	125 : 1	145 : 1
NEAT1	39 : 1	76 : 1	139 : 1
Cytoplasm markers			
GAPDH	1 : 2	1 : 2	1 : 1.3
DANCR	1.1 : 1	1 : 1	1 : 2.7
lncRNA candidates			
lncANXA5	1 : 1	1.2 : 1	1.7 : 1
RP11-809N8.2-001	5.4 : 1	6.2 : 1	10.3 : 1

Loss of function experiments (LOF)

Once the subcellular localization analysis was completed, induced depletion assays were carried out. The objective was to deplete the lncRNAs and investigate the resulting changes, focusing first on the expression of the coding genes to which they overlap. As *RP11-809N8.2-001* seemed to be present in the nucleus and some nuclear transcripts can be difficult to target with small interfering RNAs (siRNAs), two types of antisense oligonucleotides were selected to conduct the LOF experiments:

- Silencer® select siRNAs: Double-stranded RNA molecules, 20-25 base pairs (bp) in length, that bind to specific transcripts with complementary nucleotide

sequences and interfere with their expression, causing the degradation of the transcript. Silencer® select are improved siRNAs that incorporate LNA (locked nucleic acids) chemical modifications increasing its thermal stability when hybridized to the complementary RNA.

- Gapmers: Chimeric antisense oligonucleotides that contain a central block of deoxynucleotide monomers sufficiently long to induce RNase H cleavage. RNase H is a ubiquitous enzyme found both in the nucleus and the cytoplasm of all cells, allowing the depletion of nuclear transcripts. RNase H specifically recognizes the A form RNA strand and the B form DNA strand. The enzyme hydrolyzes the RNA of the RNA-DNA heteroduplexes formed after sequence-specific binding of antisense oligonucleotides to their target mRNA or lncRNA.

In vitro transfection conditions for gene knockdown by siRNAs and gapmers were set-up using *GAPDH* silencer select siRNA and *MALAT1* gapmer as positive controls and scrambled RNAs as negative controls. Transfection efficiencies were evaluated by qPCR 48 hours post-transfection. *MALAT1* gapmer at 50 nM inhibit more than 90% of *MALAT1* expression, whereas *GAPDH* silencer select siRNA was able to inhibit more than 80% of *GAPDH* expression when used at 50 nM (Figure 33). Ten putative housekeeping genes (*RPLP0, SDHA, GUSB, PGK1, RPLP1, UBC, YWHAZ, 18S, ACTß* and *DNMT1*) were analyzed by qPCR in triplicate, and their expression stability across different HEK293-T samples was estimated. For that, four different algorithms (geNorm, BestKeeper, NormFinder and the comparative Ct method) were applied to qPCR data and *UBC, RPLP1* and *YWHAZ* were selected as the best normalizer genes in our sample set (CV < 0.25 and M value < 0.5).

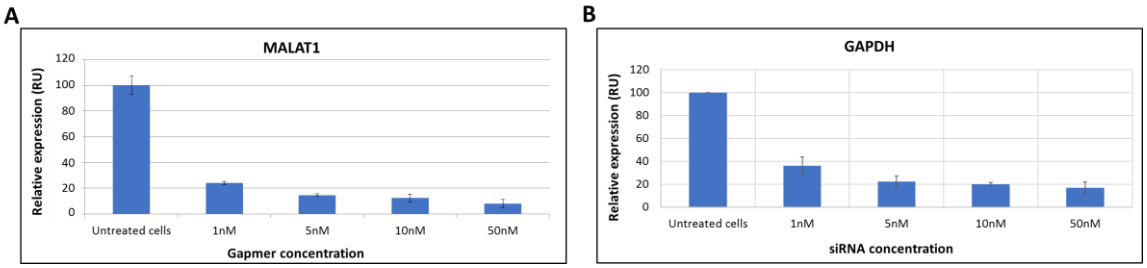

Figure 33: qPCR analysis showing the loss of expression of *MALAT1* (A) and *GAPDH* (B) 48 hours post-transfection.

A total of 7 gapmers (3 for *lncANXA5* and 4 for *RP11-809N8.2-001*) and 12 silencer select siRNAs (5 for *RELT*, 3 for *ANXA5*, 2 for *lncANXA5* and 2 for *RP11-809N8.2-001*) were tested. The antisense oligonucleotides against the protein-coding genes (*ANXA5* and *RELT*) were used in order to compare the change of the expression originated by the inhibition of the lncRNA (in case it affected the expression of the overlapping protein-coding gene), with the inhibition produced by an antisense targeting the same protein-coding gene. The sequence of the silencer select siRNAs are detailed in Table 2, whereas gapmer sequences were not provided by the company.

In order to find the lowest concentration needed for effective knockdown, a dose-curve response was performed at 1, 5, 10 and 50 nM for each gapmer. To find the best silencer select siRNA for each transcript, the inhibition efficiency achieved by each of them at the highest concentration (50 nM) was analyzed. Once the best silencer select siRNA was chosen for each transcript, a dose-curve response at 1, 5, 10, and 50nM was conducted in order to find the optimal concentration.

As shown in figure 34A, gapmer lncANXA5-3 was the one with the highest inhibition effect, inhibiting almost 70% of the *lncANXA5* expression. Then, experiments to increase the percentage of inhibition achieved by this gapmer were performed. For that, the standard protocol was modified lightly and the combined gapmer-Lipofectamine™

RNAiMAX (1:1 ratio) was incubated 5 minutes at RT (in the standard protocol the incubation time was 15 minutes). After three experiments, the transfection efficiency was considered to be completely optimized for this gapmer and around 95% of inhibition efficiency with the 50 nM concentration was obtained (Figure 34B).

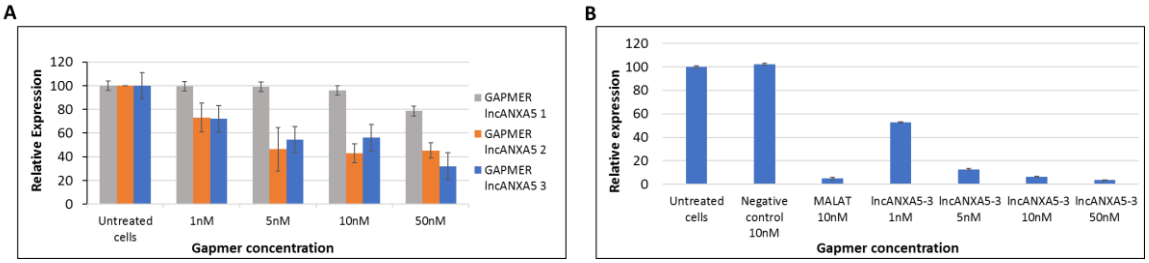

Figure 34: qPCR analysis showing the loss of expression of *lncANXA5* after transfecting and incubating the gapmers for 48h. (A) Three gapmers were used at four different concentrations (1, 5, 10 and 50 nM); blue: gapmer-1, orange: gapmer-2 and grey: gapmer-3. Experiments were repeated in duplicate. (B) Optimization of lncANXA5-3 gapmer transfection.; MALAT 10nM: positive control.

The analysis of the silencer select siRNAs at 50 nM targeting the *ANXA5* protein-coding gene showed very good inhibition efficiencies, with s1394 having the highest inhibition capacity (89%) (Figure 35A). We then performed a dose-curve response (1, 5, 10 and 50 nM) for the silencer select siRNAs s1394 in order to find the optimal concentration and it was found that 10 nM of s1394 already depleted 90% of the *ANXA5* expression (Figure 35B). We did not select any silencer select siRNA for *lncANXA5* since gapmer lncANXA5-3 achieved a better inhibition efficiency than the silencer select siRNAs.

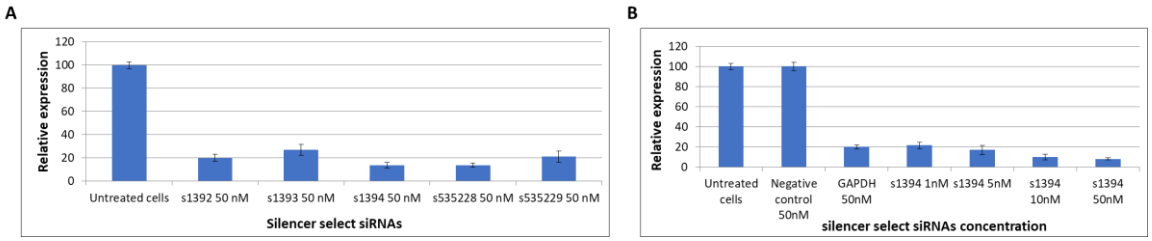

Figure 35: qPCR analysis showing the loss of expression of *ANXA5* and *lncANXA5* after transfecting and incubating the silencer select siRNAs for 48h. (A) Three silencer select were used for *ANXA5* knock-down (s1392, s1393 and s1394) and two for *lncANXA5* (s535228 and s535229). All silencer select siRNAs were first tested at the maximum concentration (50 nM). Experiments were repeated twice. (B) Optimization of s1394 silencer select siRNA transfection. Experiments were repeated twice. GAPDH 50 nM: Positive control.

On the other hand, it was not possible to achieve an inhibition higher than 40% for any of the 3 gapmers used against RP11-809N8.2-001, despite three trials (Figure 36A). Moreover, after requesting a new design from the company, an extra gapmer targeting *RP11-809N8.2-001* was used, achieving only 25% inhibition efficiency (Figure 36B).

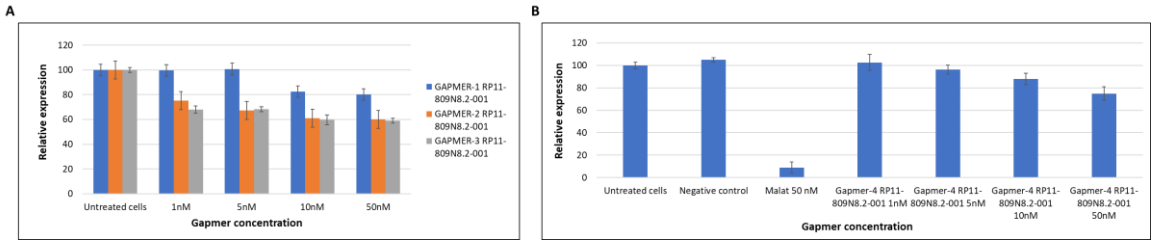

Figure 36: qPCR analysis showing no loss of expression of *RP11-809N8.2-001* lncRNA after transfecting and incubating the gapmers for 48h. (A) Three gapmers were used for *RP11-809N8.2-001* knock-down, blue: gapmer-1, orange: gapmer-2 and grey: gapmer-3. (B) Results of the fourth gapmer targeting *RP11-809N8.2-001*. Malat 50 nM: Positive control. Experiments were repeated twice.

Any of the five silencer select siRNAs against *RELT* showed more than 60% of inhibition efficiency. Moreover, no inhibition was observed for any of the silencer select siRNAs againts *RP11-809N8.2-001* (Figure 37). As the *RP11-809N8.2-001* was the target of our analysis, we did not further investigate this lncRNA and proceeded with the study of the function of *lncANXA5*.

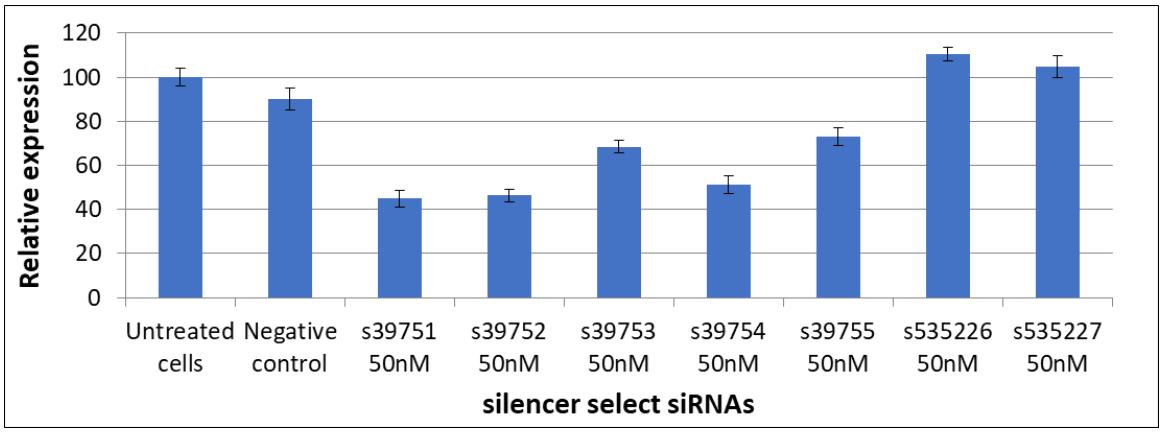

Figure 37: qPCR analysis showing the expression of *RELT* and *RP11-809N8.2-001* after transfecting and incubating the silencer select siRNAs for 48h. Five silencer select siRNAs were used for *RELT* (s39751, s39752, s39753, s39754 and s39755) knock-down and two for *RP11-809N8.2-001* (s535226 and s535227). All silencer select siRNAs were first tested at the maximum concentration (50 nM). Experiments were repeated three times.

Once the most effective oligonucleotides were selected for *lncANXA5* and *ANXA5* transcripts, the effect of *lncANXA5* depletion on *ANXA5* expression was investigated (Figure 38). To detect *ANXA5*, primers complementary to the coding sequence were used, while to detect *lncANXA5*, primers complementary to the 3'UTR region were employed (see Table 1 material and methods). *ANXA5* primers and antisense oligonucleotides only target the protein-coding gene. Nevertheless, since *lncANXA5* is sense-overlapping *ANXA5*, it was no possible to distinguish *lncANXA5* expression from that of the *ANXA5* gene (primers for *lncANXA5* detect also *ANXA5* gene), indicating that when depleting the lncRNA, the antisense oligonucleotide was also affecting the protein-coding gene. Therefore, to proper analyze LOF experiments, a system to visualize the lncRNA independently of the protein-coding gene was needed.

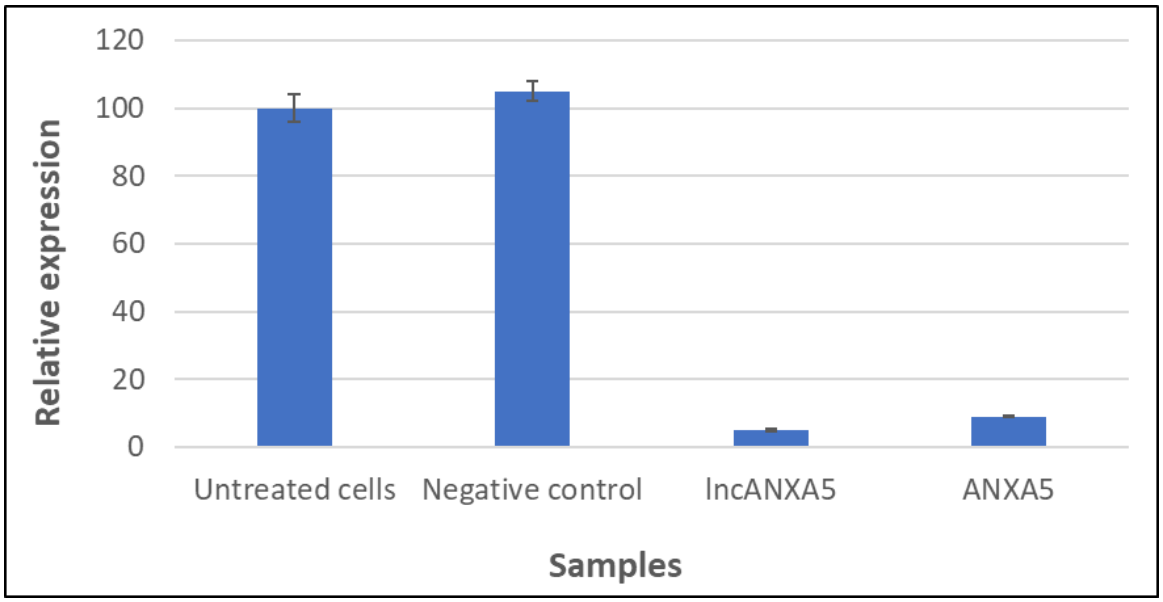

Figure 38: qPCR analysis showing the expression of *lncANXA5* and *ANXA5* after transfecting the HEK293-T cells with 50 nM of lncANXA5-3 gapmer. This experiment was repeated twice.

LncANXA5 detection in HEK293-T

The objective was to check the presence of *lncANXA5* independently of the *ANXA5* gene in HEK293-T cells in order to properly analyze the results in the LOF experiments. As a first approach a northern blot was performed, since this technique allows the detection of transcripts in an RNA sample separating them by size. For that, HEK293-T cells were transfected with 1, 5, 10 and 50 nM of gapmer lncANXA5-3. RNA was extracted after 48 hours of transfection and 1 µg was run in a denaturing agarose gel electrophoresis. Then, RNA samples were transferred by capillary from the gel to a nylon membrane and the DIG-lncANXA5 probe (100 ng/ml) was hybridized. The results of the northern blot showed a clear downregulation of the *ANXA5* gene, observing less amount of the transcript at increasing concentration of the antisense oligonucleotide. As showed in figure 39B, HEK293-T transfected with 1 nM of gapmer lncANXA5-3 showed almost one third of *ANXA5* expression when compared to untreated cells (0 nM lncANXA5-3): 16,622 relative units (RU) and 5,975 RU, respectively whereas no expression of *ANXA5*

was detected when using 5, 10 and 50 nM of gapmer lncANXA5-3. Nevertheless, the presence of the *lncANXA5* lncRNA was not detected in HEK293-T (Figure 39).

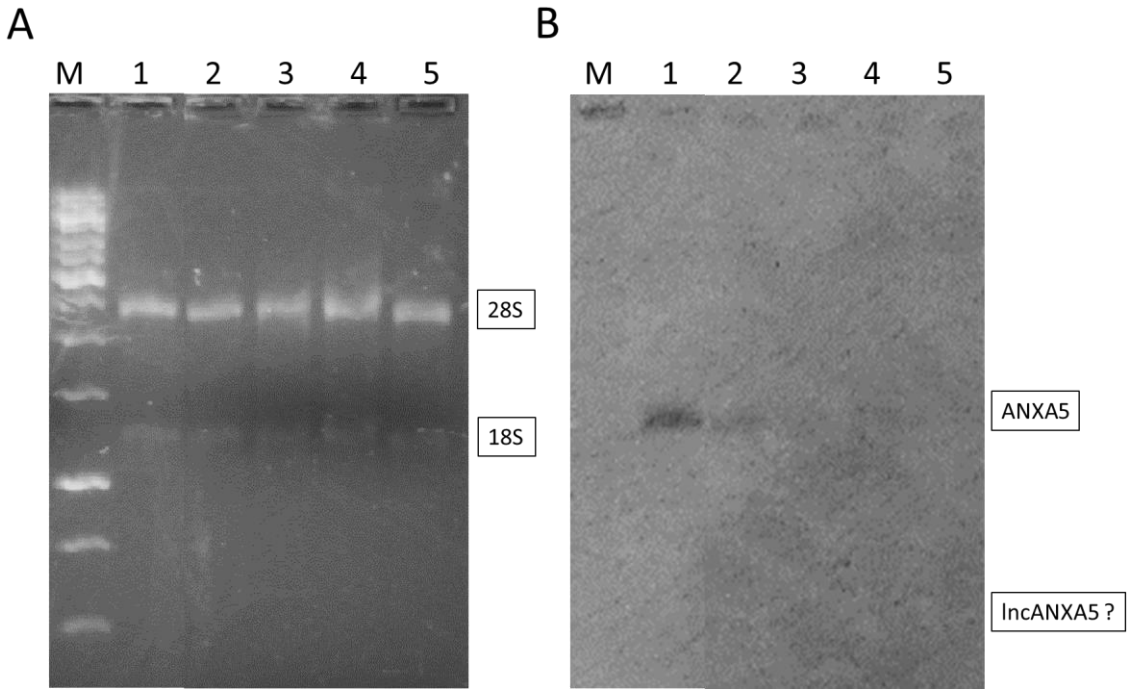

Figure 39: (A) Denaturing agarose gel electrophoresis of 1 µg of total RNA from HEK293-T transfected with increasing concentrations of gapmer lncANXA5-3 against *lncANXA5.* (B) Northern blot detection of *ANXA5* (1,762 pb) and *lncANXA5* (468 pb). M: Thermo Scientific 1 Kb marker; 1: 0 nM; 2: 1 nM; 4: 5 nM; 5: 10 nM and 6: 50 nM.

One of the reasons to explain why *lncANXA5* could not be detected might be that it is scarce in HEK293-T and northern blot could not be sensitive enough to detect it. To overcome this issue, a more sensitive technique, named 5' rapid amplification of cDNA ends (5'RACE) was conducted. 5'RACE is used in molecular biology to obtain the full-length sequence of an RNA transcript which only part of the sequence is known and to identify alternative 5' ends of fully sequenced genes. The method consists to amplify by PCR the regions between the known parts of the RNA sequence and non-specific tags appended to the 5'end of the cDNA. Therefore, with this new approach the 3'UTR region of the *ANXA5* gene could be investigated, and the presence of *lncANXA5* detected.

In order to perform 5'RACE, HEK293-T RNA was reverse transcribed to cDNA using a primer that binds at the end of the 3'UTR of *ANXA5*. Then, a poly(A) tail was appended to the 5'end of the cDNA products. Amplification was achieved using a universal hybrid primer that contains an adaptor sequence and an oligo(dT) that binds to the poly(A) tail, a gene-specific primer complementary to the known region of the 3'UTR of *ANXA5* and two primers that bind to the adaptor sequence of the universal hybrid primer (Figure 13 in materials and methods section). *ACTß* was used for 5'RACE set-up. The results detailed in figure 40, showed a band corresponding to the main isoform of *ACTß* (*ACTß-201*) and smaller bands that might be smaller isoforms of the *ACTß* gene or primer non-specificities. Nevertheless, and after repeating the experiment two times, any clear band was seen in the well corresponding to the *lncANXA5* lncRNA. A smear of bands was observed in the area where most of the described *ANXA5* isoforms should be present according to its size (550-1762 pb), nevertheless, no clear association could be conducted between *ANXA5* isoforms and the smear of bands. However, it seems that there was no band with the same size as the *lncANXA5* lncRNA (468 pb), since the smear of bands was above the 500 bp band of the DNA ladder.

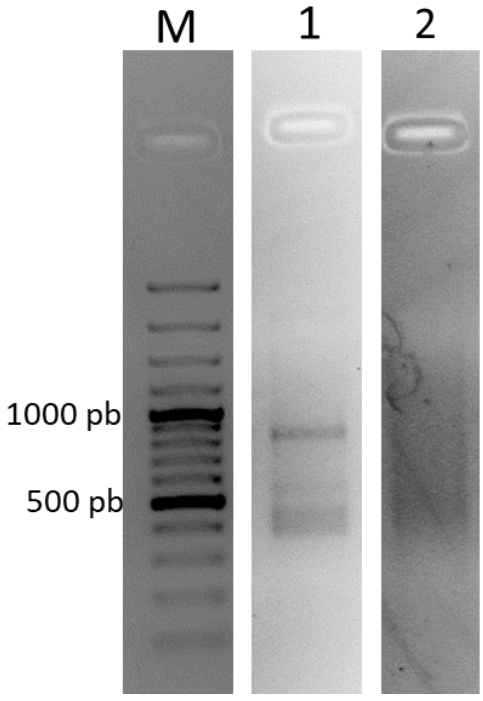

Figure 40: Agarose gel electrophoresis after the second round of amplification of the 5'RACE protocol. M: Thermo Scientific 100 pb marker; 1: Results for *ACTß* gene. Top band is *ACTß-201* (1,921 pb). Bottom bands can be smaller isoforms of the *ACTINß* gene, such as *ACTß-208* (715 pb) or *ACTß-214* (789 pb), among others. 2: Results for *lncANXA5* lncRNA. A smear is observed, no clear band can be identified.

After the analysis of these results, two possible conclusions were reached: a) *lncANXA5* was not present in HEK293-T cells or b) *lncANXA5* was present in HEK293-T, however, it was not detected with the techniques employed. With the aim to visualize the *lncANXA5* in HEK293-T cells, it was cloned into a mammalian green fluorescent protein (GFP) expression vector (pcDNA3.1) and was transfected into HEK293-T cells. pcDNA3.1 vector was selected since it contains the cytomegalovirus (CMV) promoter, a strong viral promoter that allows high levels of expression, which has been extensively used in transient expressions. Around 90% of HEK293-T were GFP positive at 24 hours post-transfection, indicating that these cells had incorporated the vector and GFP was transcribed and translated (Figure 41A). Then, the effects of *lncANXA5* transfection on the expression of the protein-coding gene *ANXA5* was analyzed by northern blot at 24 and 48 hours. The results of the northern blot showed a band that could be linked to the *lncANXA5* in the transfected HEK293-T cells. Nevertheless, this band was not very intense, indicating that the overexpression did not increase significantly the amounts of *lncANXA5*. Moreover, the amounts of the *ANXA5* gene were unaltered after *lncANXA5* transfection. Finally, an intense band was observed at 24 and 48 hours post-transfection. Nonetheless, the size of this band was very big and could not be linked to any *ANXA5* isoform, suggesting that it was probably an artifact product from the vector used for transfection (Figure 41B).

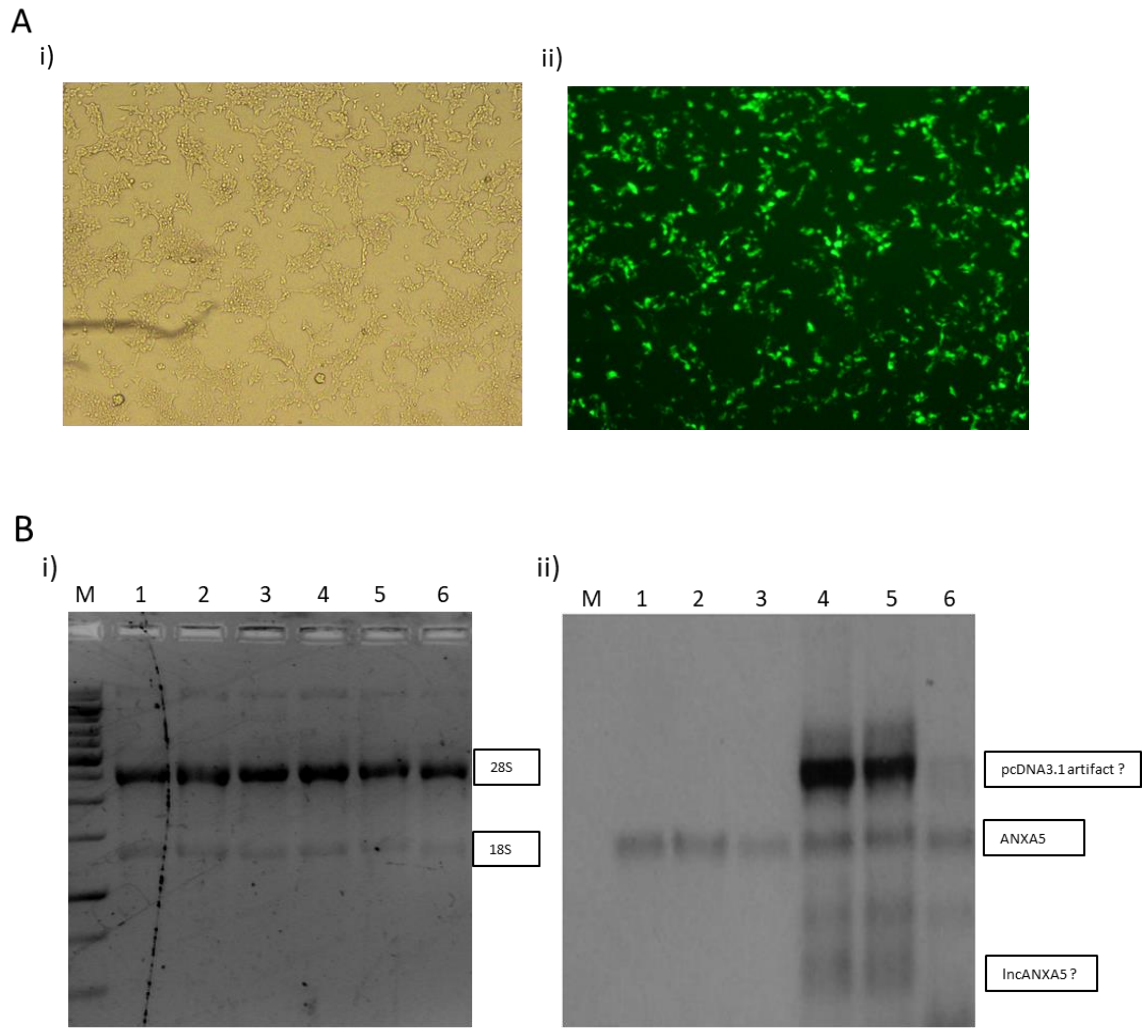

Figure 41: (A) Fluorescence microscope images of HEK293-T cells showing the results of *lncANXA5* transfection after 24 hours post-transfection. i) Untreated HEK293-T cells; ii) HEK293-T transfected with the pcDNA3.1 vector containing the *lncANXA5* sequence and the GFP. B) Northern blot analysis of the *lncANXA5* transfection. i) Denaturing agarose gel electrophoresis of 1 µg of total RNA from transfected HEK293-T. (B) Northern blot detection of ANXA5 (1,762 pb) and lncANXA5 (468 pb). M: Thermo Scientific 1 Kb marker; 2: Untreated HEK293-T cells 0 hours post-transfection; 2: Untreated HEK293-T cells 24 hours post-transfection; 3: Untreated HEK293-T cells 48 hours post-transfection; 4: HEK293-T transfected with lncANXA5, 24 hours post-transfection; 5: HEK293-T transfected with lncANXA5, 48 hours post-transfection and 6: HEK293-T transfected with pcDNA3.1 empty vector, 48 hours post-transfection.

Overall, although the molecular techniques used to study the function of the selected lncRNA seems to have worked properly, they have failed to clarify the questions raised.

Moreover, the *in vitro* system employed (HEK293-T), has been proven to be a good model to study the role of many different transcripts, however, it was not suitable for the study of our lncRNA candidates. One possible explanation might be that the oocyte molecular machinery is very specific and it cannot be extrapolated to the one present in the somatic cells.

4.2. CHAPTER 2: Association of markers of aging with ovarian reserve and oocyte maturation rates in human cumulus cells

4.2.1. Rationale to conduct this study

Aging is a major biological process and a risk factor for many diseases, including infertility. Many studies have been conducted comparing young and old tissues or comparing samples across the lifespan (Ida et al., 2003; Lu et al., 2004; Rodwell et al., 2004; Edwards et al., 2007; Pan et al., 2008; De Magalhães et al., 2009). These studies have identified common signatures of human aging in gene expression (i.e. a set of genes that are consistently overexpressed or downregulated with age). Among these genes, *ANXA5* was of special interest to us, since has already been linked to reproductive disorders, particularly to recurrent implantation failures (Tuttelmann et al., 2013). Moreover, one of our lncRNA candidates (*lncANXA5*) was overlapping the 3'UTR region of *ANXA5*.

Female reproductive aging is associated with a decrease in the ovarian reserve (DOR) and a loss of oocyte developmental competence (Miao et al., 2009; Qiao et al., 2014). Although ovarian reserve declines with age, young women can be affected with DOR as well; nevertheless, it is unknown whether this represents an acceleration of physiologic ovarian aging, or a distinct pathology (Skiadas et al., 2012). To achieve developmental competence, the oocyte maturation process requires of a continuous crosstalk between the oocyte and the somatic follicular cells (cumulus cells, CCs) that surround it in the ovary. Since the crosstalk between CCs and oocytes is mainly established through specialized gap junctions that allow exchange and transport of signaling molecules, CCs have been used in several studies to predict oocyte quality, embryo development and pregnancy outcomes (Fauser et al., 2011; Skiadas et al., 2012; Uyar et al., 2013; Devjak et al., 2016).

As ovarian tissue could behave just like other tissues in the human body, CCs of an aging ovarian tissue could affect oocyte maturation processes and, indeed, alter developmental competence of the oocyte. The analysis of the expression of these genes in CCs and its association with ovarian reserve and oocyte maturation can provide a better understanding of the transcriptional changes related to aging in human ovarian tissues, and could be used as a non-invasive marker for developmental competence of the oocyte quality.

4.2.2. Study population

The CCs used for this study came from 82 women (37 oocyte donors and 45 patients) recruited from March to October 2018. Women included in the study were not previously diagnosed for premature ovarian failure. The mean woman age was 32 years old (SD=8.035, range 18-45), the mean ovarian reserve measured as antral follicle count (AFC) was 18.6 (SD=10.63, range 2-47) and the mean maturation rate, defined as the number of MII oocytes obtained from the number of cumulus-oocyte complexes acquired after oocyte pick-up, was 72.24 (SD=18.19, range 20-100) (Table 16). No woman was included twice in the study.

Table 16: Individualized data for all the included participants. Age is measured in years, ovarian reserve is measured by the antral follicle count (AFC), maturation rates (number MII oocytes / number cumulus-oocyte complexes) is represented as a percentage.

ID	AGE	AFC	Maturation Rate (%)
1	18	33	77.78
2	18	6	75.00
3	19	26	84.78
4	19	19	76.47
5	19	25	93.33
6	19	35	100.00
7	21	23	90.48

8	21	19	84.00
9	22	18	75.00
10	22	35	66.67
11	22	17	100.00
12	22	25	73.91
13	23	20	75.00
14	23	16	66.67
15	23	27	69.23
16	24	47	100.00
17	24	32	77.78
18	24	46	65.63
19	24	22	68.42
20	25	21	77.27
21	25	27	82.86
22	25	22	93.33
23	26	11	57.89
24	26	40	54.17
25	26	36	84.62
26	27	15	88.24
27	27	18	74.19
28	28	16	78.57
29	28	15	60.00
30	28	15	82.76
31	28	13	76.00
32	28	20	76.00
33	29	27	77.42
34	29	15	75.00
35	30	30	89.29
36	31	10	70.00
37	31	14	83.33
38	31	13	75.00
39	32	15	80.00
40	32	21	88.89
41	33	17	76.00
42	33	18	81.48
43	33	26	50.00
44	33	7	72.22
45	34	26	83.33
46	34	30	90.91
47	34	3	33.33
48	34	5	100.00

49	35	10	73.91
50	36	4	50.00
51	36	7	60.00
52	36	10	42.11
53	38	11	80.00
54	38	15	40.00
55	38	33	69.70
56	38	12	80.00
57	38	8	75.00
58	38	31	61.29
59	38	8	75.00
60	38	7	28.57
61	38	24	57.14
62	39	11	20.00
63	39	34	100.00
64	39	6	100.00
65	39	11	83.33
66	40	19	68.42
67	40	10	60.00
68	41	4	50.00
69	41	19	83.33
70	41	12	75.00
71	42	24	92.59
72	42	9	85.71
73	43	20	80.00
74	43	5	50.00
75	44	13	63.64
76	44	2	50.00
77	44	3	80.00
78	44	18	96.15
79	44	36	45.45
80	44	40	45.45
81	45	4	50.00
82	45	9	20.00

Analysis of correlation between age and AFC (Spearman R=-0.422; $p<0.001$) and between age and oocyte maturation rates (Spearman R=-0.292; $p=0.008$) indicated a decrease in the ovarian reserve and oocyte maturation rates with age (Figure 42).

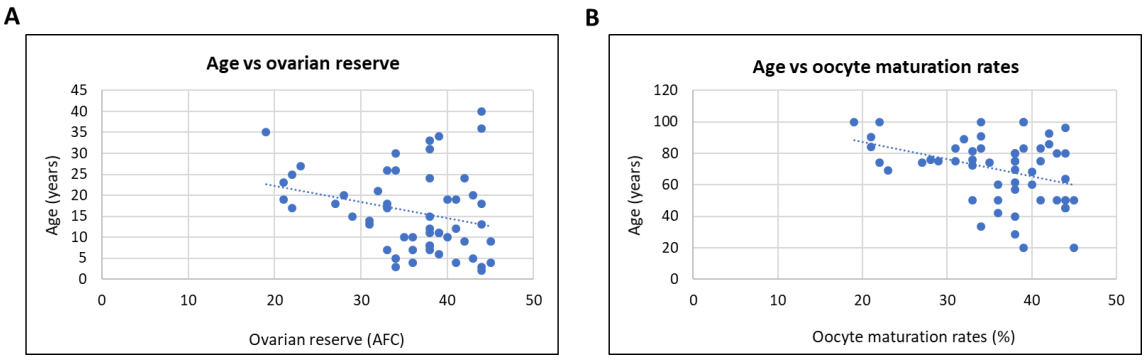

Figure 42: Schematic representation of the correlation between age and ovarian reserve (A) and between age and oocyte maturation rates (B).

4.2.3. Association of markers of aging with ovarian reserve and oocyte maturation rates in human cumulus cells

A bibliographic research was conducted in order to find proper markers of human aging and the ones with the highest difference in expression between young and old human tissues were selected. From these selected markers, the ones that appeared as differentially expressed across various studies were included in the analysis. The idea was to select a reduced list of genes in order to analyze their expression in the cDNA obtained from the CCs. Since the amount of RNA obtained per CC sample was not very high, the list of genes to analyze had to be short. The final list of genes reported to be markers of human tissular aging was: *ANXA*5, *LYZ, TXNIP, CLU, FABP3, TGFBR3, NDUFB11, APOD, IGJ, CALB1* and *C3*. Then, expression levels of the 11 markers of aging were analyzed by qPCR. The expression of six of the 11 genes analyzed (*ANXA5, LYZ, TXNIP, CLU, FABP3* and *TGFBR3*) was found in human CCs (Cq < 36 cycles). Ten putative housekeeping genes (*RPLP0, SDHA, GUSB, PGK1, TBP, UBC, YWHAZ, 18S, ACTß* and *GAPDH*) were analyzed by qPCR in triplicate, and their expression stability across samples was estimated. For that, four different algorithms (geNorm, BestKeeper, NormFinder and the comparative Ct method) were applied to qPCR data and *TBP* was

selected as the best normalizer gene in our sample set (CV < 0.25 and M value < 0.5). The relative expression levels of aging markers were analyzed for each woman and plotted against age, ovarian reserve and oocyte maturation rates (Table 17 and figure 43).

Table 17: Relative expression levels of the 6 aging markers analyzed in each of the participants. qPCR data is represented as ΔCq value (delta quantification cycle) ($2^{\wedge-(Cq(target)-Cq\ (HRGs)}$).

	Relative expression (RU)					
ID	**LYZ**	**TXNIP**	**CLU**	**FABP3**	**ANXA5**	**TGFBR3**
1	0.15	2.44	70.28	10.12	44.71	28.37
2	0.39	1.38	81.95	8.64	28.32	38.06
3	0.33	1.08	33.02	2.99	56.28	18.99
4	0.44	1.24	136.08	1.39	37.21	36.18
5	0.53	1.41	94.84	3.16	59.64	38.92
6	0.78	2.41	57.76	0.87	14.77	6.56
7	0.89	3.91	75.62	4.16	26.75	10.83
8	0.49	2.00	56.04	0.81	28.33	14.63
9	0.11	1.16	82.84	2.09	39.31	42.45
10	0.72	2.12	87.06	3.80	45.55	35.71
11	1.04	0.93	47.07	0.57	30.70	16.88
12	0.51	2.19	37.56	1.40	7.11	11.56
13	0.45	1.93	74.05	1.55	41.17	24.63
14	0.19	1.82	104.77	0.98	51.08	20.87
15	0.14	1.41	53.72	1.27	10.91	6.39
16	0.08	2.60	33.38	3.37	28.71	20.37
17	0.14	2.15	45.88	0.95	26.27	24.08
18	0.37	1.79	84.14	2.60	49.82	48.68
19	0.62	1.69	103.61	2.33	62.40	22.41
20	0.41	2.25	93.33	1.68	37.92	26.34
21	0.40	1.61	75.82	2.51	29.31	26.47
22	0.31	1.44	94.58	2.87	38.96	53.66
23	1.38	2.90	50.13	4.48	44.10	20.77
24	0.95	2.94	42.43	1.07	38.00	24.16
25	0.37	2.39	106.65	5.33	28.82	28.54
26	0.00	0.00	0.00	0.00	0.00	0.00
27	0.54	2.66	66.14	1.24	16.41	6.67
28	0.29	4.46	117.42	1.08	35.82	37.35
29	0.40	1.23	77.95	3.03	64.33	65.22
30	0.62	1.49	159.89	5.56	45.90	35.81
31	0.23	2.07	93.90	1.66	43.87	37.13

32	0.48	1.73	38.41	0.35	14.90	12.46
33	0.22	2.05	114.24	4.23	61.87	37.10
34	0.24	1.19	22.64	1.05	19.00	10.03
35	0.73	1.20	116.57	3.36	60.72	90.09
36	0.26	2.11	197.18	1.47	31.05	16.76
37	0.32	1.85	51.77	0.44	13.38	4.20
38	0.45	1.51	78.80	0.73	19.09	7.65
39	0.26	2.38	66.76	1.01	21.84	14.15
40	1.14	3.01	41.89	0.33	23.69	16.49
41	0.16	2.65	82.33	2.04	55.42	23.23
42	0.20	2.42	143.94	2.05	44.58	50.64
43	1.04	2.08	284.76	1.45	53.68	48.38
44	1.74	2.77	77.70	5.62	46.19	53.22
45	0.52	3.09	72.99	2.28	31.21	25.99
46	0.78	4.94	103.31	1.45	22.34	12.66
47	0.54	0.75	54.04	3.43	78.57	15.81
48	0.20	2.52	81.70	1.85	25.23	16.75
49	0.91	2.67	160.70	4.46	48.93	50.92
50	0.87	1.85	153.43	3.44	49.83	37.63
51	0.90	3.84	42.37	2.76	31.04	8.46
52	0.27	0.28	26.82	1.82	35.41	10.25
53	0.16	3.51	87.12	3.83	37.91	11.76
54	0.39	3.80	134.16	2.09	40.33	12.00
55	0.33	2.06	74.20	0.83	36.24	41.68
56	0.27	2.89	122.06	1.68	32.59	33.19
57	0.53	1.47	88.61	3.81	90.87	55.81
58	2.29	2.49	182.33	2.09	52.76	43.43
59	0.38	2.27	2.25	1.10	30.40	7.28
60	0.21	1.91	38.75	0.93	24.85	7.02
61	0.33	2.20	96.36	0.57	15.61	9.27
62	0.46	3.90	93.38	2.75	38.67	11.07
63	1.27	1.83	124.38	2.33	69.33	26.81
64	0.24	3.48	228.53	2.40	29.49	23.32
65	0.71	3.44	108.46	4.79	35.18	24.98
66	0.44	3.64	72.94	2.65	40.88	24.45
67	0.69	8.93	88.30	2.47	18.44	5.81
68	0.20	2.11	44.70	0.59	38.34	8.58
69	0.73	4.39	79.19	1.68	45.22	50.09
70	0.25	3.47	67.61	1.94	18.61	5.52
71	1.87	2.06	75.80	2.16	74.36	39.16
72	0.60	2.18	78.03	0.80	23.41	8.73

73	0.34	3.39	76.19	2.04	29.72	11.78
74	0.65	2.62	71.11	2.10	38.57	34.19
75	0.27	1.79	87.28	2.94	42.40	15.04
76	0.11	2.43	259.54	2.25	60.31	46.50
77	0.16	2.17	170.15	4.66	71.34	70.75
78	0.45	3.15	200.40	3.14	75.99	35.20
79	0.50	1.95	414.55	0.85	39.87	36.99
80	0.79	1.63	58.56	0.56	9.68	14.34
81	0.27	1.88	113.93	2.16	49.97	20.39
82	0.37	3.68	40.18	2.76	33.70	8.12

We were particularly interested in *ANXA5*, since has been suggested to be involved in recurrent implantation failures. Moreover, in the array performed with *in vivo* mature oocytes, *ANXA5* was found to be differentially expressed with age and also ovarian reserve and had a lncRNA (*lncANXA5*) overlapping its 3'UTR region also differentially expressed with age. However, *ANXA5* was not correlated with age (rs=0.130, p=0.2445), ovarian reserve (rs=-0.057, p=0.6113) or oocyte maturation rates (rs=-0.131, p=0.2442) (Figure 43).

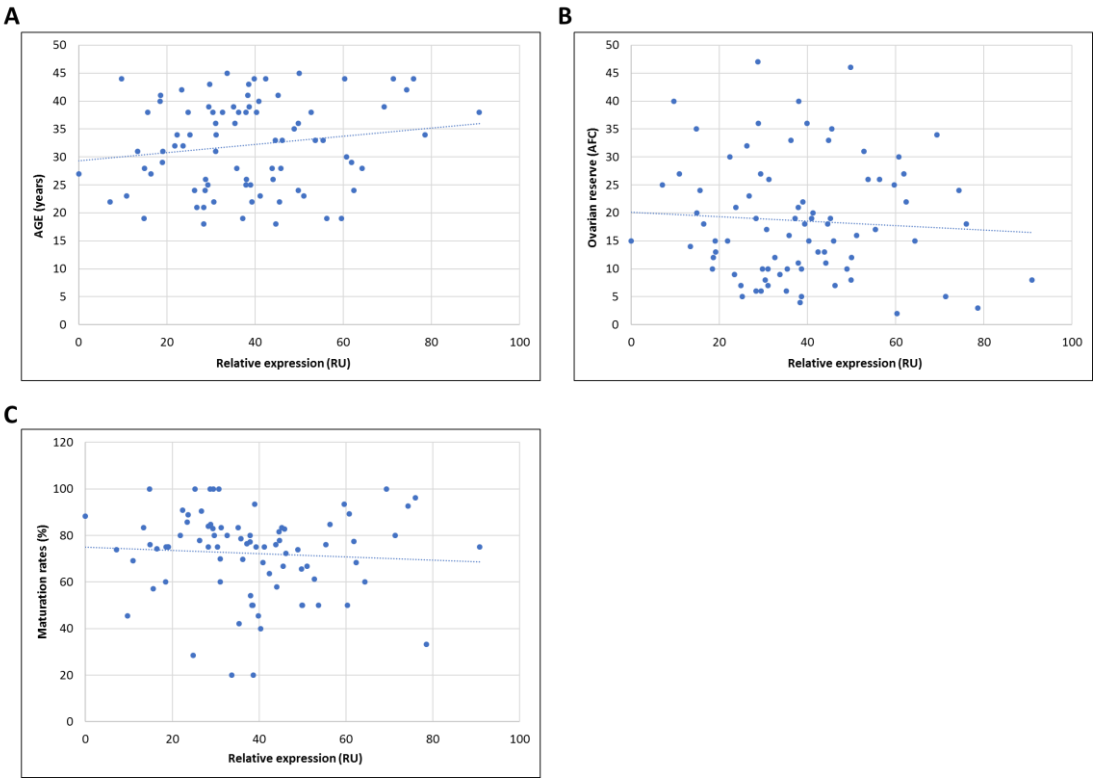

Figure 43: Scatter plot showing no relationship between the relative expression of *ANXA5* and age (A), ovarian reserve (B) and oocyte maturation rates (C). qPCR data is represented as ΔCq value (delta quantification cycle) ($2^{\wedge-(Cq(target)-Cq\ (HRGs))}$).

When plotting the relative expression levels of the remaining aging markers with age, only *TXNIP*, a tumor suppressor involved in redox regulation, (rs=0.367, p=0.0007) and *CLU*, a secreted chaperone involved in cell death and tumor progression, (rs=0.231, p=0.0362) showed a moderate positive correlation with the woman age (Table 18 and Figure 44).

Table 18: Non-parametric analysis (Spearman's rho, r_s) of the relative expression levels of 5 aging markers plotted against age. * means statistically significant. A p-value <0.05 was set as statistically significant.

	AGE (years)
Gene symbol	**r_s**
LYZ	0.031
TXNIP	0.367*
CLU	0.231*
FABP3	-0.006
TGFBR3	-0.054

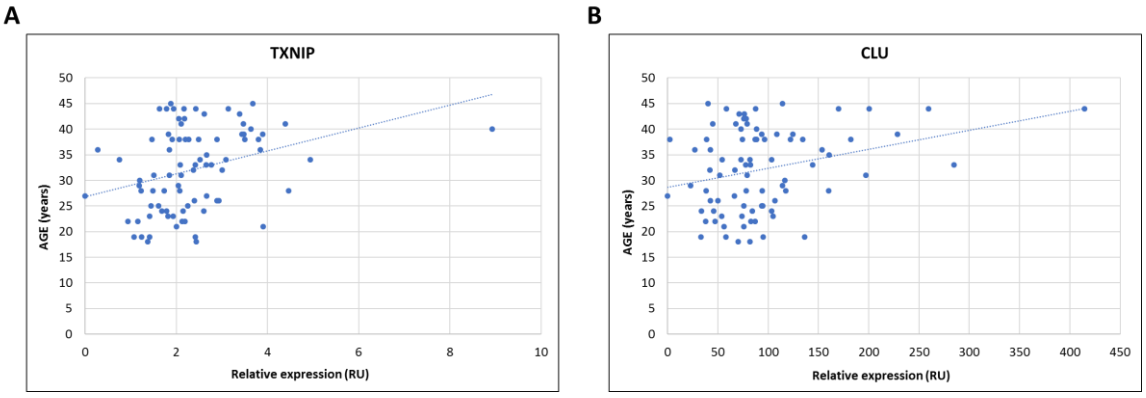

Figure 44: Scatter plot showing the relationship between age and the relative expression of *TXNIP* (A) and *CLU* (B) genes. qPCR data is represented as ΔCq value (delta quantification cycle) ($2^{\wedge-(Cq(target)-Cq\ (HRGs))}$).

In order to find biomarkers associated with oocyte quality, the relative expression levels of the remaining aging markers were plotted against ovarian reserve and oocyte

maturation rates. Nevertheless, none of the aging markers were correlated with ovarian reserve or oocyte maturation rates ($p>0.05$) (Table 19).

Table 19: Non-parametric analysis (Spearman's rho, r_s) of the relative expression levels of 5 aging markers plotted against ovarian reserve and oocyte maturation rates. A p-value <0.05 was set as statistically significant.

	Ovarian reserve (AFC)	**Maturation rate (%)**
Gene symbol	**r_s**	**r_s**
LYZ	0.171	-0.014
TXNIP	-0.087	0.023
CLU	-0.045	0.022
FABP3	-0.135	0.032
TGFBR3	0.147	0.095

4.3. CHAPTER 3: Comparison of reproductive outcomes of IVF cycles with vitrified or fresh donor oocytes coming from the same stimulation cycle

4.3.1. Rationale to conduct this study

All the MII oocytes used in chapter 1 are vitrified oocytes. Therefore, in chapter 3, we intended to analyze whether vitrification affects oocyte developmental competence by comparing the reproductive outcomes of fresh and vitrified donor oocytes from the same stimulation cycle.

Oocyte vitrification has been shown to be a safe and effective procedure to store the reproductive potential of oocytes. It is used to preserve fertility in women undergoing gonadotoxic procedure, affected by certain genetic conditions (e.g. Fragile X and Turner's syndrome) or needing to preserve their reproductive potential in the face of ovarian exhaustion due to age (Layman, 2002; Stoop et al., 2014; Martinez et al., 2016). Importantly, as oocyte vitrification allows for the uncoupling of the ovarian stimulation and oocyte pick-up (OPU) from the use of such oocytes in an ART process, it has brought about the possibility of storing oocytes from donors in oocyte banks, and slowed for provision of third-party reproduction across time and space.

Early randomized controlled trials (RCTs) have shown that this technique has comparable results, in terms of reproductive outcomes, to the use of fresh oocytes (Cobo et al., 2008; Cobo and Diaz, 2011; Rienzi et al., 2010; Parmegiani et al., 2011). These RCTs are carried out by highly trained groups with a significant experience, while vitrification is per se a delicate technique which is prone to errors and inefficiencies, and whose learning curve to be executed appropriately is long (De Munck and Vajta, 2017). Moreover, there are significant operator to operator variations in its efficiency, and the target of >90% survival rate, a signal of good command of the technique, is not achieved in all clinics.

Recently, the analysis of large registries-based cohorts performed in USA has indicated lower reproductive outcomes overall with the use of cryopreserved oocytes (Kushnir et al., 2015; Crawford et al., 2017; Kushnir et al., 2018). Moreover, careful analysis of vitrified/thawed oocytes indicate alterations in their molecular makeup, perhaps leading to lowed ability to develop in a viable embryo (Shirazi et al., 2016; Azari et al., 2017; Amoushahi et al., 2017).

The question then remains: is oocyte vitrification as effective as fresh oocyte use? In other words: is oocyte vitrification harming or affecting the developmental competence of oocytes?

4.3.2. Study population and experimental design

This study includes 37,520 MII sibling oocytes from 1,844 cycles of oocyte donation, each donor providing sibling oocytes for at least one recipient of fresh oocytes (2,561 cycles) and one other of vitrified oocytes (2,471 cycles) from the same oocyte pick-up (OPU). Oocyte donors were between 18 and 35 years old, had normal karyotype, good general health, and a BMI between 18 and 30 kg/m^2. Recipients were women between 23 and 51 years old. Semen samples included donor frozen samples and frozen or fresh partner samples. Cases of testicular biopsy were excluded due to the risk that they were not equally distributed among cycles using fresh or vitrified oocytes.

The main analysis of this study was performed on a total of 5,032 reception cycles, 2,561 (50.9%) with fresh oocytes and 2,471 (49.1%) with vitrified oocytes. All reception cycles were selected from donors' stimulations that resulted in a) enough oocytes collected to treat at least 2 recipients, b) at least 1 recipient being assigned fresh oocytes and at least 1 recipient being assigned vitrified oocytes and c) the recipient being assigned vitrified

oocyte had undergone the reception cycle with reproductive data available. A first sub-analysis (SAME) was conducted selecting the cycles where the same number of paired oocytes, either fresh or vitrified, was available for ICSI (i.e. after the loss of oocytes due to vitrification/warming). The SAME sub-analysis included 1,336 cycles: 668 with fresh and 668 with vitrified oocytes. A second sub-analysis (SAME100) was performed selecting only the cycles that, besides having the same number of paired oocytes available for ICSI, also had 100% survival rate after warming (i.e. optimal technique). The SAME100 sub-analysis included 976 cycles; 488 with fresh and 488 with vitrified oocytes (Figure 45).

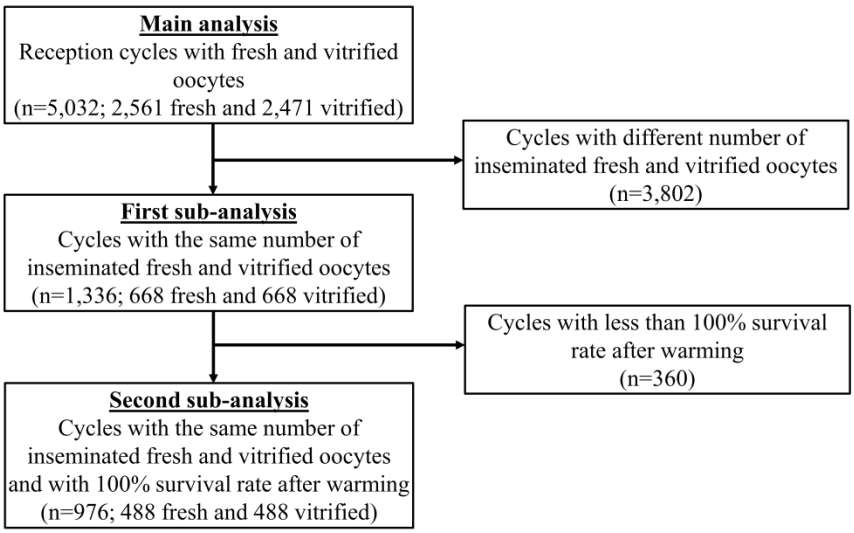

Figure 45: Flow chart of the process followed to design the main analysis and the two sub-analysis.

4.3.3. Comparison of reproductive outcomes of IVF cycles with vitrified or fresh donor oocytes coming from the same stimulation cycle

Baseline and cycle characteristics of study population are shown in Table 20 and were comparable between vitrified and fresh oocytes' cohorts in the main analysis and in the SAME and SAME100 sub-analyses.

Table 20: Descriptive statistics of the studied population in the main analysis.

	Overall n=5,032	Vitrified cycles n=2,471	Fresh cycles n=2,561
Donors' age, Mean (SD)	25.9 (4.6)	25.9 (4.6)	25.9 (4.6)
Donors' BMI, Mean (SD)	22.5 (3.2)	22.6 (3.2)	22.5 (3.2)
Recipients' age, Mean (SD)	41.6 (4.7)	41.6 (4.7)	41.5 (4.6)
Recipients' BMI, Mean (SD)	23.9 (4.4)	23.7 (4.2)	24 (4.6)
Recipient cycle number, Mean (SD)	1.3 (0.6)	1.3 (0.6)	1.3 (0.6)
First reception cycle, n (%)	3,953 (78.6%)	1,897 (76.8%)	2,056 (80.3%)
Sperm used for ICSI, n (%)			
Donor frozen	790 (15.7%)	383 (15.5%)	407 (15.9%)
Partner frozen	3,504 (69.7%)	1,690 (68.4%)	1,814 (70.9%)
Partner fresh	736 (14.6%)	398 (16.1%)	338 (13.2%)
Day of ET			
D2-D3, n (%)	4,671 (92.8%)	2,299 (93%)	2,372 (92.6%)
D5, n (%)	361 (7.2%)	172 (7%)	189 (7.4%)
Number of transferred embryos			
1, n (%)	610 (12.1%)	354 (14.3%)	256 (10%)
2, n (%)	4,396 (87.4%)	2,103 (85.1%)	2,993 (89.5%)
3, n (%)	26 (0.5%)	14 (0.6%)	12 (0.5%)

Laboratory results

Oocyte survival rate after vitrification was above 90% on average. The number of inseminated oocytes per recipient was not statistically different between groups in the main analysis and in the SAME and SAME100 sub-analyses. Nevertheless, vitrified oocytes showed lower fertilization rates when compared to fresh oocytes. The morphological score of the embryo cohort in general and of transferred embryos in particular was also lower in vitrified oocytes than in fresh oocytes. Detailed laboratory results per study cohort are presented in Table 21.

Table 21: Laboratory results of the three analyses performed. Main analysis: Donation cycles with fresh and vitrified oocytes; SAME sub-analysis: Cycles with the same number of inseminated fresh and vitrified oocytes; SAME100 sub-analysis: Cycles with the same number of inseminated fresh and vitrified oocytes and with 100% survival rate after warming. NA; non applicable

Main analysis	Overall n=5,032	Vitrified cycles n=2,471	Fresh cycles n=2,561	p-value
Survival rate of VIT (%)	NA	93%	NA	NA
Inseminated MII, Mean (SD)	6.8 (1.4)	6.7 (1.5)	6.8 (1.2)	0.63
Fertilized MII (2PN), Mean (SD)	4.9 (1.7)	4.7 (1.7)	5 (1.6)	<0.001
Fertilization rate (%)	72%	69.2%	74.6%	<0.001
Number of viable embryos, Mean (SD)	4.2 (1.6)	4 (1.6)	4.4 (1.6)	<0.001
Morphological score of embryo cohort, Mean (SD)	7.1 (1.0)	7.0 (1.0)	7.2 (1.0)	<0.001
Morphological score of transferred embryos, Mean (SD)	7.8 (1.2)	7.6 (1.2)	8.0 (1.1)	<0.001
SAME sub-analysis	Overall n=1,336	Vitrified cycles n=668	Fresh cycles n=668	p-value
Survival rate of VIT (%)	NA	90%	NA	NA
Inseminated MII, Mean (SD)	6.4 (0.9)	6.4 (0.9)	6.4 (0.9)	1.00
Fertilized MII (2PN), Mean (SD)	4.6 (1.5)	4.4 (1.5)	4.7 (1.4)	<0.001
Fertilization rate (%)	71.4%	68.7%	74.2%	<0.001
Number of viable embryos, Mean (SD)	4 (1.5)	3.9 (1.5)	4.2 (1.5)	<0.001
Morphological score of embryo cohort, Mean (SD)	6.9 (1.6)	6.7 (1.6)	7 (1.6)	<0.001
Morphological score of transferred embryos, Mean (SD)	7.8 (1.2)	7.7 (1.2)	8.0 (1.2)	<0.001
SAME100 sub-analysis	Overall n=976	Vitrified cycles n=488	Fresh cycles n=488	p-value
Survival rate of VIT (%)	NA	100%	NA	NA
Inseminated MII, Mean (SD)	6.4 (0.9)	6.4 (0.9)	6.4 (0.9)	1.00
Fertilized MII (2PN), Mean (SD)	4.5 (1.5)	4.3 (1.5)	4.7 (1.5)	<0.001
Fertilization rate (%)	71.3%	68.2%	74.4%	<0.001
Number of viable embryos, Mean (SD)	4 (1.5)	3.9 (1.5)	4.3 (1.5)	<0.001
Morphological score of embryo cohort, Mean (SD)	7.1 (1.0)	7.0 (1.0)	7.2 (1.0)	<0.001
Morphological score of transferred embryos, Mean (SD)	7.8 (1.2)	7.7 (1.2)	8.0 (1.2)	<0.001

Reproductive outcomes

Significantly lower reproductive outcomes were observed for vitrified oocytes compared to fresh sibling oocytes in the main univariable analysis: biochemical pregnancy was 35.7% in vitrified versus 42.6% in fresh oocytes, p<0.001; clinical pregnancy was 35% versus 41.5% oocytes, p<0.001; ongoing pregnancy was 32.4% versus 37.9% oocytes, p<0.001 and live birth was 31% versus 36.2%, p<0.001. The logistic multilevel regression analysis confirmed that using vitrified oocytes had a significant negative effect on all reproductive outcomes, except for live birth (Table 22). The adjusted odd ratio (OR) and 95%CI of vitrified versus fresh sibling oocytes for each reproductive outcome were: 0.83 (95%CI 0.73, 0.94) for biochemical, 0.85 (95%CI 0.75, 0.96) for clinical, 0.87 (95%CI 0.77, 0.99) for ongoing pregnancy, and 0.88 (95%CI 0.77, 1.01) for live birth.

However, in the SAME analysis, when the number of inseminated oocytes was the same for fresh and vitrified oocytes (i.e. when the efficiency of the warming process was taken into account), reproductive outcomes were comparable in the univariable analysis: biochemical pregnancy was 37% in vitrified versus 39.5% in fresh sibling oocytes, p=0.34; clinical pregnancy was 36.4% versus 37.9%, p=0.57; ongoing pregnancy was 33.5% versus 34.1%, p=0.82 and live birth was 32.1% versus 32%, p=0.97. The logistic regression analysis also showed no negative effect of vitrification on pregnancy rates (Table 23). Adjusted ORs of vitrified versus fresh sibling oocytes were: 1.03 (95%CI 0.81, 1.32) for biochemical pregnancy, 1.10 (95%CI 0.86, 1.40) for clinical pregnancy, 1.11 (95%CI 0.87, 1.43) for ongoing pregnancy and 1.15 (95%CI 0.89, 1.48) for live birth.

Finally, when cycles with the same number of inseminated fresh and vitrified sibling oocytes that also had 100% survival rate after warming were selected (SAME100), univariable analysis showed that reproductive results were not different between groups:

biochemical pregnancy was 37.9% in vitrified versus 37.7% in fresh oocytes, p=0.95; clinical pregnancy was 37.5% versus 35.7%, p=0.55; ongoing pregnancy was 34.8% versus 32.6%, p=0.46 and live birth was 32.9% versus 31.2%, p=0.57. The logistic regression analysis confirmed these results (Table 24). Adjusted ORs of vitrified versus fresh sibling oocytes were: 1.18 (95%CI 0.89, 1.57) for biochemical, 1.28 (95%CI 0.96, 1.70) for clinical, and 1.29 (95%CI 0.97, 1.73) for ongoing pregnancy, and 1.26 (95%CI 0.93, 1.69) for live birth.

Table 22: Multivariate analysis of sibling fresh and vitrified oocytes from the same stimulation cycle (main analysis). A p-value <0.05 was set as statistically significant.

			95% CI		
		OR	**Lower**	**Upper**	**p-value**
Biochemical pregnancy	Vitrified vs fresh oocytes	0.826	0.727	0.937	0.003
	Recipients' age	0.983	0.970	0.996	0.013
	Recipients' BMI	0.977	0.964	0.991	0.002
	Partner frozen vs donors'	0.910	0.764	1.083	0.288
	Partner fresh vs donors'	0.866	0.687	1.091	0.222
	1 embryo vs 2	0.471	0.372	0.596	<0.001
	3 embryos vs 2	1.083	0.480	2.443	0.848
	Embryo quality	1.296	1.225	1.370	<0.001
Clinical pregnancy	Vitrified vs fresh oocytes	0.847	0.745	0.962	0.010
	Recipients' age	0.983	0.969	0.996	0.011
	Recipients' BMI	0.978	0.964	0.992	0.002
	Partner frozen vs donors'	0.924	0.775	1.101	0.376
	Partner fresh vs donors'	0.871	0.690	1.099	0.244
	1 embryo vs 2	0.455	0.358	0.579	<0.001
	3 embryos vs 2	0.943	0.411	2.163	0.890
	Embryo quality	1.306	1.234	1.381	<0.001
Ongoing pregnancy	Vitrified vs fresh oocytes	0.869	0.764	0.990	0.034
	Recipients' age	0.982	0.969	0.996	0.010
	Recipients' BMI	0.977	0.963	0.992	0.002
	Partner frozen vs donors'	0.974	0.814	1.165	0.773
	Partner fresh vs donors'	0.963	0.760	1.220	0.755
	1 embryo vs 2	0.475	0.371	0.607	<0.001
	3 embryos vs 2	0.732	0.302	1.774	0.490
	Embryo quality	1.294	1.222	1.370	<0.001
Live birth	Vitrified vs fresh oocytes	0.882	0.773	1.006	0.061
	Recipients' age	0.981	0.968	0.995	0.007
	Recipients' BMI	0.975	0.961	0.990	0.001
	Partner frozen vs donors'	1.013	0.845	1.216	0.886
	Partner fresh vs donors'	0.983	0.773	1.250	0.891
	1 embryo vs 2	0.469	0.365	0.602	<0.001
	3 embryos vs 2	0.771	0.318	1.869	0.565
	Embryo quality	1.302	1.228	1.380	<0.001

Table 23: Multivariate analysis of the SAME sub-analysis: cycles where the same number of paired oocytes, either fresh or vitrified, was available for ICSI. A p-value <0.05 was set as statistically significant.

			95% CI		
		OR	**Lower**	**Upper**	**p-value**
Biochemical pregnancy	Vitrified vs fresh oocytes	1.031	0.808	1.316	0.803
	Recipients' age	0.998	0.971	1.025	0.877
	Recipients' BMI	0.976	0.951	1.002	0.068
	Partner frozen vs donors'	0.644	0.468	0.886	0.007
	Partner fresh vs donors'	0.586	0.370	0.928	0.023
	1 embryo vs 2	0.397	0.249	0.635	<0.001
	3 embryos vs 2	1.725	0.341	8.719	0.510
	Embryo quality	1.291	1.161	1.435	<0.001
Clinical pregnancy	Vitrified vs fresh oocytes	1.097	0.858	1.402	0.460
	Recipients' age	0.998	0.971	1.026	0.898
	Recipients' BMI	0.979	0.954	1.005	0.116
	Partner frozen vs donors'	0.654	0.475	0.901	0.009
	Partner fresh vs donors'	0.580	0.365	0.921	0.021
	1 embryo vs 2	0.416	0.260	0.664	<0.001
	3 embryos vs 2	1.827	0.362	9.232	0.466
	Embryo quality	1.303	1.171	1.450	<0.001
Ongoing pregnancy	Vitrified vs fresh oocytes	1.110	0.865	1.425	0.412
	Recipients' age	0.998	0.970	1.026	0.871
	Recipients' BMI	0.975	0.949	1.001	0.063
	Partner frozen vs donors'	0.705	0.510	0.975	0.035
	Partner fresh vs donors'	0.667	0.418	1.066	0.091
	1 embryo vs 2	0.464	0.289	0.745	0.001
	3 embryos vs 2	1.048	0.188	5.826	0.957
	Embryo quality	1.283	1.151	1.430	<0.001
Live birth	Vitrified vs fresh oocytes	1.150	0.892	1.483	0.282
	Recipients' age	0.993	0.966	1.022	0.644
	Recipients' BMI	0.966	0.940	0.994	0.016
	Partner frozen vs donors'	0.753	0.540	1.049	0.093
	Partner fresh vs donors'	0.688	0.426	1.112	0.127
	1 embryo vs 2	0.408	0.246	0.675	<0.001
	3 embryos vs 2	1.133	0.203	6.317	0.887
	Embryo quality	1.308	1.171	1.462	<0.001

Table 24: Multivariate analysis of the SAME100 sub-analysis: cycles with the same number of inseminated fresh and vitrified oocytes and with a 100% survival rate after warming. A p-value <0.05 was set as statistically significant.

			95% CI		
		OR	**Lower**	**Upper**	**p-value**
Biochemical pregnancy	Vitrified vs fresh oocytes	1.182	0.890	1.571	0.248
	Recipients' age	1.006	0.975	1.038	0.708
	Recipients' BMI	0.979	0.951	1.008	0.152
	Partner frozen vs donors'	0.599	0.410	0.874	0.008
	Partner fresh vs donors'	0.489	0.280	0.851	0.011
	1 embryo vs 2	0.297	0.171	0.514	<0.001
	3 embryos vs 2	1.175	0.192	7.194	0.862
	Embryo quality	1.252	1.107	1.416	<0.001
Clinical pregnancy	Vitrified vs fresh oocytes	1.282	0.963	1.707	0.089
	Recipients' age	1.005	0.973	1.037	0.765
	Recipients' BMI	0.983	0.954	1.012	0.243
	Partner frozen vs donors'	0.623	0.426	0.911	0.015
	Partner fresh vs donors'	0.479	0.273	0.840	0.010
	1 embryo vs 2	0.315	0.182	0.546	<0.001
	3 embryos vs 2	1.223	0.199	7.496	0.828
	Embryo quality	1.251	1.105	1.417	<0.001
Ongoing pregnancy	Vitrified vs fresh oocytes	1.295	0.967	1.733	0.083
	Recipients' age	1.003	0.972	1.036	0.832
	Recipients' BMI	0.975	0.946	1.005	0.102
	Partner frozen vs donors'	0.611	0.417	0.897	0.012
	Partner fresh vs donors'	0.490	0.278	0.867	0.014
	1 embryo vs 2	0.365	0.211	0.633	<0.001
	3 embryos vs 2	1.419	0.231	8.721	0.706
	Embryo quality	1.235	1.088	1.401	0.001
Live birth	Vitrified vs fresh oocytes	1.258	0.935	1.692	0.129
	Recipients' age	1.002	0.970	1.036	0.895
	Recipients' BMI	0.966	0.936	0.996	0.029
	Partner frozen vs donors'	0.656	0.444	0.969	0.034
	Partner fresh vs donors'	0.512	0.285	0.917	0.024
	1 embryo vs 2	0.325	0.181	0.585	<0.001
	3 embryos vs 2	1.513	0.245	9.340	0.655
	Embryo quality	1.244	1.093	1.414	0.001

5. DISCUSSION

In this thesis, we aimed at obtaining a deeper understating of the molecular factors that determine and influence human oocyte quality. To that objective, it is focused on two complementary goals, the first one tackling molecular aspects of oocyte biology and the second related to the analysis of the effect of oocyte vitrification on reproductive results. This allowed us to widen the available knowledge on basic human oocyte biology and their future use in ART, as far as non-invasive techniques are used.

Molecular aspects of oocyte biology

Oocyte maturation is related with dynamic transcriptional events, featuring a high transcriptional activity in growing oocytes and transcriptional silencing in mature oocytes. Understanding the differences in transcript profiles within individual oocytes might provide knowledge about how to predict their competence and potential to produce viable embryos. Classically, transcriptomic analyses of oocytes have focused on mRNA and their role in oocyte maturation and embryo development (Kocabas et al., 2006; Evsikov and Marin de Evsikova, 2009). However, recent reports identified almost 10,000 ncRNAs at different stages of human preimplantation development, indicating that they might represent an important new level of regulation of early development and suggesting they should be present in oocytes as well (Xue et al., 2013; Yan et al., 2013). To date, only a small fraction of these ncRNAs has functional annotations, particularly for human oocytes. Furthermore, the widely accepted idea that transcription is repressed in fully grown oocytes suggests that gamete fertilization and zygote development depend on a very finely tuned regulation of protein expression, driven by mechanisms that are unrelated to the modulation of transcription rate. To this regard, some reports suggested that alternative pre-mRNA splicing might also play a role in the transcriptome regulation

of mature oocytes in vertebrates (Mereau et al., 2007; Salisbury et al., 2009; Tang et al., 2011).

Gene expression analysis of mature MII oocytes of different ages and ovarian reserve

In order to study the differences within the transcriptome of individual oocytes, the first part of this thesis was focused on the analysis of the transcriptional profile of *in vivo* matured MII human oocytes in relation to age and, independently, ovarian reserve, and to evaluate the differences in gene expression and splicing events during the last steps of oocyte maturation (GV and MII stage oocytes). We found small differences in the transcriptomic profiles of oocytes coming from women of different age and ovarian reserve. In addition, we uncovered the transcriptional changes that characterize *in vivo* matured vs non-matured oocytes, and highlighted the fine regulation of specific transcripts in terms of both transcript abundance and alternative splicing regulation.

One important aspect of this study is that the unique dataset obtained from *in vivo* human MII oocytes allow for the generation of transcriptomic data that are as close as possible, to that of ovulated oocytes in a naturally cycling ovary. The GV oocytes were collected after ovulation was triggered, and GVs already started cytoplasmic maturation to some unquantifiable extent; nevertheless, it is very difficult to obtain GVs from unstimulated human ovaries for ethical and clinical reasons alike, making GVs from stimulated ovaries the next to ideal sample of this kind. Further, due to the scarce nature of human oocytes, we acknowledge the use of fresh (GV) and warmed (MII) oocytes in this study. As it is known that vitrification/warming process may alter the gene expression profile of human oocytes (Shirazi et al., 2016; Azari et al., 2017; Amoushahi et al., 2017), this can represent

another source of variability between GV and MII oocytes. This last possibility, was analyzed in the third chapter of this thesis and is discussed in the last section of this dissertation.

The presence of sibling oocytes in our dataset (6 women contributed 2 oocytes each to the study) allowed us to explore the relationship/variability of individual oocytes from the same woman. While sibling oocytes did cluster together in the AFC comparison, they mostly clustered apart in the age comparison. This might indicate that transcripts that vary in their expression with AFC might be more conserved in their expression among sibling oocytes, while those that vary with age might have a less conserved expression pattern among sibling oocytes.

It should also be kept in mind that, although all oocytes were from fertile donors, even in the best cases, no more than 30% of all fertilized oocytes will develop into healthy offsprings, and it is likely that there are significant inter-oocyte variations, as previously reported (Vassena et al., 2011).

Previous reports analyzing global gene expression profiles of mature MII oocytes which did not fertilize after IVF-ICSI from younger (<36 years) and older (>37 years) women identified several hundreds of differentially expressed genes in relation to age and involved in several cellular processes such as cell cycle regulation, cytoskeletal and chromosomal structure, energy pathways, transcription control, and stress response (Steuerwald et al., 2007; Fragouli et al., 2010; Grondahl et al., 2010). Also, it has been reported that the proportion of poor-quality oocytes (te Velde and Pearson, 2002) increases with age, ranging from 50% at 20 years of age to 95% at 35 years of age (Eldar-Geva et al., 2005). Furthermore, a work performed by Qiu and colleagues (Qiu et al., 2016), reported a set of human transcripts containing 464 lncRNAs and 759 mRNAs, that

correlated with the oocyte stage. Nevertheless, none of these 1,223 human transcripts were differentially expressed in our dataset.

In our case, only 17 mRNAs transcripts were differentially expressed in *in vivo* matured MII human oocytes when age groups were compared (*HIST2H2AC, SPCS2, MAGEE-1, ANXA5, CLPS, GEM, PRRG1, STKY1, ARLG1P4, SMUG1, IGHV3-35, IGHV3-36, IGHV3-66, PFAS, ZSCAN22, PROCR,* and *DUXAP10*). The difference between our study and other reports could be explained by the fact that in our study *in vivo* matured MII oocytes from healthy donors (≤35 years) that did not undergo fertilization were used, whereas other reports (Steuerwald et al., 2007; Fragouli et al., 2010; Labrecque and Sirard, 2014) have used oocytes after unsuccessful fertilization. In these cases, the oocytes inevitably underwent in vitro aging since fertilization was checked at least 16 hours post-fertilization and, possibly, there was a paternal RNA cargo from the injected spermatozoon.

Among the 22 differentially expressed mRNAs identified when the effect of AFC was analyzed independently from age, Fidgetin (*FIGN*) was increased in oocytes from women with low AFC, and particularly in the OL group. FIGN has been suggested to be a microtubule-severing enzyme (Sharp and Ross, 2012) and its overexpression in cultured cells results in the destruction of cellular microtubules (Zhang et al., 2007). FIGN could represent a marker of developmental competence in oocytes, as the proportion of oocytes with genetic abnormalities increases with female aging and low AFC (Katz-Jaffe et al 2013; Grande et al., 2014). Other transcripts involved in cytoskeleton regulation such as *MYL6* (myosin light polypeptide) and *MAP1lC3C* (microtubule associated protein) were decreased in oocytes from women with low AFC, suggesting that their presence might be important to prevent genetic abnormalities in the oocyte. Nevertheless, their role in oocytes is not known yet. Moreover, 6 out of the 22 mRNAs differentially expressed in

the ovarian reserve comparison were also differentially expressed with age (*DUXAP-10*, *ANXA5*, *IGHV-38*, *IGHV-66*, *SPCS2* and *PRRG1*). Two of them, *ANXA5* and *DUXAP10*, were more abundant in oocytes from young (<26 y.o.) women with high AFC (>20). ANXA5 is a calcium-dependent phospholipid binding protein that inhibits phospholipase A2 and protein kinase C (PKC) and presents a calcium channel activity (Arispe et al., 1996). PKC has been related to oocyte activation in different animal models (Halet, 2004). In *Xenopus* eggs, a wave of PKC activation accompanies the calcium spikes after fertilization (Larabell et al., 2004), and activators of PKC are able to trigger cortical granule exocytosis (Bement and Capco, 1989). Moreover, ANXA5 has been associated with recurrent pregnancy loss (Hayashi et al., 2013; Demetriou et al 2015) and has been implicated in regulating Cystic fibrosis transmembrane conductance regulator (CFTR) function and intracellular trafficking in *Xenopus* oocytes (Faria et al., 2011; Nader et al., 2016; Perniss et al., 2017). We hypothesize that ANXA5 could have a role in maintaining meiosis arrest before fertilization in human oocytes as well. No function has yet been established for the pseudogene *DUXAP10*, although the DUXA homeobox gene family is expressed in early embryos and have recently been proposed to be involved in the control of gene expression after EGA (Madissoon et al., 2016).

SPCS2, *IGHV-66*, *IGHV-38* and *PRRG1* were more abundant in oocytes from older women with low AFC (<10). SPCS2 is a microsomal signal peptidase of the minor spliceosome, involved in general mRNA processing, whose defects can lead to tissue-specific consequences (Argente et al., 2014). Age alters the activity and the levels of a number of transcription regulators, affecting their role and therefore the basic mechanisms of transcriptional control (reviewed by Roy et al., 2002). We hypothesize that *SPCS2* expression might be dysregulated in aged oocytes, affecting the alternative splicing process and therefore the isoforms produced. PRRG1 is a calcium ion binding

protein. Oocyte fertilization, which is followed by calcium release, resumption of meiosis and mRNA processing until EGA, is lower in aged oocytes (Lanman, 1968; Badenas et al., 1989; Winston et al., 1991; Goud et al., 1999). Alterations in the calcium dynamics in aged oocytes may explain part of their reduced percentage of fertilization and therefore, calcium ion binding proteins such as PRRG1 could be potential regulators of oocyte quality. No function has yet been established for the immunoglobulin heavy variables 38 and 66 (*IGHV-38* and *IGHV-66*).

More than 70% of differential expressed genes in our study were ncRNAs, strongly suggesting a relevant role in human oocyte and early embryo biology. A set of piRNAs-c were differentially expressed in relation to AFC. piRNAs have been described to act at both the epigenetic and post-transcriptional levels in gene silencing of retrotransposons and other genetic elements in both spermatogenesis (Siomi et al., 2011) and oogenesis (Roovers et al., 2015). However, the significance of finding a set of piRNAs-c differentially regulated related to AFC is unknown. Moreover, it is currently believed that piRNAs-c are required primarily for mammalian male spermatogenesis rather than oocyte or ovary development. In fact, several mouse models have demonstrated important roles of piRNAs-c in the male germline (Deng and Lin, 2002; Kuramochi-Miyagawa et al., 2004; Aravin et al., 2007; Carmell et al., 2007), but showed no effect on the female germline development (Kuramochi-Miyagawa et al., 2004). Thus, the presence of piRNAs-c in the oocyte can be adventitious (Pelosi et al., 2015).

miRNAs, another class of ncRNAs which generally act by downregulating specific mRNAs, were also found to be differentially expressed. In particular, the precursor form of *miRNA1260a* and *miR4262* were increased in the older groups (OL+OH). Interestingly, one of the bioinformatically predicted targets of *miR1260a* (among 7,493 annotated in www.microRNA.org) is argonaute (AGO1). Argonaute proteins bind different classes of

small RNA (e.g. miRNA and piRNAs) and mediate mRNA cleavage or translation inhibition. Obviously, deregulation of such a central player could affect oocyte developmental competence in a major way (Wang et al., 2012).

The group of ncRNA most differentially expressed in our study were lncRNAs, since 33 lncRNA out of 68 ncRNA and 27 lncRNA out of 55 ncRNAs were differentially expressed when comparing age and AFC, respectively. Many lncRNAs act as key regulators of transcriptional and translational mechanisms (Cao, 2014). These results suggest a relevant role of lncRNAs in controlling oocyte quality in terms of transcriptional content and, in consequence, their ability to promote correct transcriptional and translational processes during the maternal to zygote transition. For instance, oocytes obtained from young women with low AFC exclusively presented 13 (5 increased and 8 decreased) and 19 (11 increased and 9 decreased) differentially expressed lncRNAs, when compared with oocytes from young women with high AFC and old women with low AFC, respectively.

We observed that lncRNA *lncANXA5* and *RP11-809N8.2-001* were increased when comparing the YL group with the OL group. We noticed that both *lncANXA5* and *RP11-809N8.2-001* are located/annotated at the 3'UTR of *ANXA5* and *RELT* genes, respectively. Given that *ANXA5* was also found increased in oocytes from young women with low AFC (YL) when compared to the OL group, we hypothesized that *ANXA5* and the lncRNA *lncANXA5* could both act as a positive regulator of each other. Furthermore, lncRNA *RP11-809N8.2-001* could also be a positive regulator of *RELT*, as we have observed both transcripts increased in young women with low AFC when compared to old women with low AFC.

Functional characterization of the lncRNA *lncANXA5* and *RP11-809N8.2-001*

For these reasons, it was decided to investigate the functional roles of *lncANXA5* and *RP11-809N8.2-001* and their potential as oocyte developmental competence markers. Since the mechanisms of action of lncRNA are poorly understood in general (and particularly in the human oocyte), its functional characterization is challenging. For that, and considered the scarcity of human oocytes, HEK293-T cells were used as a cellular model, due to its widely usage in molecular biology. Different approaches were performed in order to visualize the *lncANXA5*. The northern blot visualization was not successful, since a band corresponding to *ANXA5* was seen but not the one corresponding the lncRNA *lncANXA5*. One possible explanation can be that, compared to protein-coding genes, lncRNAs are transcribed at low levels (Necsulea et al., 2014). Thus, the northern blot might not be sensitive enough to detect *lncANXA5* expression. Consequently, 5' RACE, a more sensitive technique where the transcripts of interest are amplified using complementary oligonucleotides, was conducted. 5' RACE experiments did not report good results for *lncANXA5*, suggesting that probably this lncRNA was either not expressed in HEK293-T cells or was expressed at very low levels. As these techniques did not have enough sensitivity to detect few amounts of lncRNA, overexpression experiments could help. After transfecting the *lncANXA5* into HEK293-T, a weak band with a similar size to the *lncANXA5* was reported, however more optimization in order to increase the intensity of the *lncANXA5* band and to remove artifact products probably coming from the expression vector would have been necessary. Another technique commonly used to fish out and visualize lncRNA such as fluorescence in situ hybridization (FISH) was not possible to be conducted since *lncANXA5* shared the same nucleotide sequence than the protein-coding gene *ANXA5* and the labelled nucleotide probes would hybridize both transcripts. In summary, it seems that HEK293-T turned out

not to be an adequate *in vitro* model to study the function of these specific lncRNA, since it was not possible to deplete *RP11-809N8.2-001* expression and *lncANXA5* seemed to be not expressed, or at very low levels, in this type of cells. Perhaps, it would have been more appropriate to use a model more similar to the human oocyte, such as *Xenopus* egg extract. Even so, when the cellular model was chosen, we searched for one easy to work with, where the lncRNA candidates were expressed and that had many molecular techniques already optimized in order to facilitate the study of the lncRNA (already difficult in itself). In addition, the expression of lncRNAs is very tissue-specific, which means that their expression in human oocytes does not guarantee their expression in the *Xenopus* egg extract (Taylor et al 2015). Overall, after these unsuccessful results, it was decided to stop lncRNA functional analysis experiments in order to direct our efforts to other projects.

Transcript abundance and alternative splicing profiles differences between non-matured and matured human oocytes

In addition to the analysis of the changes in transcript abundance in mature MII, we also studied which transcripts and AS events were differentially expressed between non-matured GV and *in vivo* matured MII oocytes. The analysis of the gene expression patterns between non-matured and mature human oocytes showed that more than 70% of the differentially expressed genes were decreased in MII oocytes. These results are consistent with the well-known idea that fully-grown GV oocytes are the result of an active transcription during oogenesis, followed by a selective degradation of mRNA transcripts during maturation to MII (Lequarre et al., 2004; Bettegowda et al., 2006; Su et al., 2007; Virant-Klun et al., 2013). GO analysis suggested that the main biological processes involved during meiotic maturation were mitochondrial translation regulation

and electron transport chain. This was mainly caused by the decreased mRNA levels of mitochondrial genes in MII stage oocytes. As it is well-known, mitochondria are responsible for the energy supply (adenosine triphosphate, ATP) required for oocyte maturation, and variations in the correct proportion of ATP in oocytes and embryos affect oocyte quality and embryo development (Slotte et al., 1990; Zhao and Li, 2012). It has been previously described a well-coordinated program of maternal mRNA degradation, that accounts during oocyte maturation, particularly targeting mRNA related to the biogenesis of ribosomes and mitochondria (Paynton et al., 1988, Su et al., 2007; Fair et al., 2007; Salisburi et al., 2009; Jia et al., 2016; Ruebel et al., 2018).

Overall, our data regarding differentially expressed genes between non-matured and *in vivo* matured oocytes are in agreement with the results found in oocyte maturation in mice, cows and rhesus monkeys, which suggests a conserved mechanism for transcriptional regulation during oocyte maturation in mammals (Fair et al., 2007; Ruebel et al., 2018; Su et al., 2007).

One of the most novel parts of this thesis was the characterization of alternative splicing events, both between non-matured and matured oocytes and in relation with age and AFC. Our analysis using the FIRMA algorithm showed a high number of individual exons differentially expressed in human *in vivo* matured MII stage oocytes as compared to non-matured GV oocytes, suggesting that a specific pattern of post-transcriptional regulation in this set of genes is required to ensure acquisition of oocyte developmental competence. Around 70% of the differentially expressed exons were related to cassette-exon and alternative C' termini, suggesting that our results might reflect the physiological control of pre-mRNA processing during oocyte maturation (Kalsotra and Cooper, 2011). Functional enrichment analysis of this set of genes highlighted mitochondrial function, mRNA splicing and regulation of translation, processes that have been associated with

oocyte developmental competence acquisition in different species (Babayev and Seli, 2015; Biase, 2017; Rodriguez and Farin, 2004).

When the AS events detected by the FIRMA algorithm were further filtered by applying the ASPIRE algorithm, a total of 36 differential AS events in 35 genes were identified between MII and GV oocytes. The number of affected genes detected by this analysis was substantially lower due to a significantly higher confidence in the AS event scored by this method, as described by Van Moerbeke and colleagues (Van Moerbeke et al., 2018). Nine of these genes were detected as differentially spliced in all three comparisons, suggesting that they could have a significant role in acquisition of developmental competence. Interestingly, two of these genes, *PIK3CD* and *DIAPH2*, have been previously associated with ovarian dysfunction. The AS event observed in *PIK3CD*, the delta subunit of phosphoinositide 3-kinase, produced the exclusion of a non-coding exon (cassette-exon event). PIK3CD has been linked to ovarian follicle growth regulation as PIK3CD knock out mice are sub-fertile and show reduced follicular growth and a higher proportion of atretic antral follicles in the ovary (Li et al., 2013). Of note, the PI3K protein have also been involved in bovine oocyte developmental competence acquisition. Expression levels of proteins participating in the PI3K-Akt signaling pathway, which regulates cell cycle progression, oxidative response and apoptosis, were higher in the follicular cells surrounding oocytes with higher developmental competence (Andrade et al., 2017). All these studies highlight the importance of *PIK3CD* during follicular development. Since oocytes are in close contact with the CCs of the follicle, this transcript might be also important for oocyte maturation, and therefore the AS event observed from non-matured to matured oocytes can be the result of a regulated machinery to provide the MII oocytes with the correct isoform of the *PIK3CD* gene. DIAPH2 plays a role in the development and normal function of the ovaries and has been associated with premature

ovarian failure in a family presenting the breakpoint of a balanced X;12 translocation affecting the 3'UTR region of the transcript, thus altering translation of the protein (Bione et al., 1998). Interestingly, we observed that the relative levels of the 3'UTR region of the *DIAPH2* transcript decreased from GV to MII. The fact that differential splicing events are detected in non-coding regions of both these genes between non-matured GVs and MII oocytes suggests that both sequences could mediate post-translational regulation mechanisms of their respective transcripts.

The other genes detected as differentially spliced in all three comparisons, have not been previously reported to be directly involved in oocyte biology. For example, *PPOX*, *PDXK*, *GALK1* and *ITPA* are genes involved in metabolism regulation, *THSB4* mediates cell-to-cell and cell-to-matrix interactions, which might be important for maintaining the CCs-oocyte interaction, *OSBP2* binds to oxysterols and inhibits their cytotoxicity, while the function of *lincPOLR3G-8* is not known yet. Additional studies will be required in order to elucidate their involvement in acquisition of developmental competence.

Additionally, we observed that the levels of a non-coding exon of *EPAS1* gene (corresponding to the *EPAS1-207* isoform) decreased from GV to H-MII and L-MII groups, suggesting its exclusion from the transcript pool in MII oocytes from women below 30 years old. This might indicate that the corresponding AS event was produced to provide the MII oocyte with the correct isoform of the transcript and therefore, that *EPAS1-207* might not be needed in matured oocytes. EPAS1 is a transcription factor involved in the induction of oxygen regulated genes and has been suggested as a therapeutic target in the treatment of pregnancy-related diseases such as pre-eclampsia or intrauterine growth restriction (IUGR) (Depoix et al., 2017). Moreover, in a study conducted by Cowden and colleagues with knock-out mice, EPAS1 was found to be required for normal placentation during early pregnancy (Cowden et al., 2005).

Interestingly, Tian and colleagues have determined that EPAS1 null mutation is an embryonic lethal, indicating the importance of this gene in development (Tian et al., 1998).

Evolutionary conservation of the human oocyte transcriptome

Most of the studies discussed so far were performed using oocytes from animal models due to the difficulty of obtaining and using human oocytes. In that sense, efforts are being made in order to compare the transcriptomic profiles of the human oocytes with that of the other animal models. A decade ago, Vallée and colleagues (Vallee et al., 2006) set out to identify evolutionarily conserved genes expressed in oocytes using multi-species cDNA microarray (mouse, bovine and Xenopus); 268 transcripts were identified as both conserved and preferentially expressed in oocytes of all three species. Recently, the same group (Sylvestre et al., 2013) compared the human oocyte transcriptome to an oocyte-enriched subset of mouse, bovine and frog (*Xenopus laevis*) transcripts. Their study revealed that, at the transcriptional level, bovine/human similarity was greater than mouse/human or frog/human similarity. In addition, a high level of conservation, in *Xenopus*, *Mus* and *Bos*, relative to humans, was found in genes involved in early embryonic development. However, none of these transcripts have been detected as differentially expressed in our study.

In 2004, Hamatani and colleagues (Hamatani et al., 2004) described how age could determine alterations of gene expression patterns in mouse oocytes. Mature oocytes were collected from 5- to 6-week-old mice and compared to those collected from 42- to 45-week-old mice, and about 5% of the expressed transcripts showed significant changes in expression. Unfortunately, there is no clear correlation between mice and human aging,

making it difficult to compare side by side these results to our data. Furthermore, the oocytes used in our study were from donors, which means that the oldest women included was 35 years old (maximum age for oocyte donation in Spain), and did not represent women of advanced maternal age. Nevertheless, in Spain, it is extremely difficult to obtain *in vivo* matured MII from women older than 35 years old, since it would involve using patient's oocytes.

Association of markers of aging with ovarian reserve and oocyte maturation rates in human cumulus cells

After analyzing the transcriptomic changes in oocytes of different ages and AFC, we expanded the analysis to the cells supporting oocyte growth, and evaluated the effect of age in the transcriptomic profiles of cumulus cells.

With the aim of studying the effect of aging on oocyte quality, the gene expression levels of selected common signatures of human aging were analyzed in human cumulus cells (CCs). CCs are discarded in ART cycles as by-product biological material, and allowed the use of patient's samples up to 45 years old. It is well established that the crosstalk between CCs and oocytes, which exchange small molecules through specialized gap junctions, sustains the oocyte maturation and allows for the achievement of developmental competence (Fauser et al., 2011; Skiadas et al., 2012; Uyar et al., 2013; Devjak et al., 2016). Therefore, the study of the transcriptomic profiling of CCs (non-invasive technique) may help identify biomarkers of oocyte competence that could be used to improve fertility and pregnancy outcomes in ART cycles.

The selection of the most relevant common aging markers (i.e genes that tend to consistently increase or decrease their expression with age and in different tissues) was

conducted with the aim to limit the number of genes to study. As the RNA obtained from CCs is low, the analysis of large number of genes would imply the need of a pre-amplification step of the cDNA. However, cDNA pre-amplification could introduce bias in the fold change and the dynamic range, affecting the maintenance of the gene expression profiles (Okino et al., 2016).

Overall, our analysis of the somatic aging markers expression (*ANXA5, LYZ, TXNIP, CLU, FABP3* and *TGFBR3*) in 82 samples of human CCs showed a moderate correlation between two of the markers and age: TXNIP, a tumor suppressor involved in redox regulation, and CLU, a secreted chaperone involved in cell death and tumor progression. The rest of the somatic aging markers analyzed (*ANXA5, LYZ, FABP3* and *TGFBR3*) did not show correlation with age. These results contradict the findings observed by Tamadir Al-Eldani and colleagues, who found that *TGFBR3* was differentially expressed in human CCs from patients >37 years, compared to patients <30 years (Tamadir Al-Eldani et al., 2014). Nevertheless, this was a smaller study with only 16 patients included. Another group have also studied determinants of follicular aging in human CCs, revealing that senescence activates genes associated with hypoxia and oxidative stress (E. Molinari et al., 2016). However, *TXNIP* was not among the differentially expressed genes. The general lack of correlation between the signature observed in CCs from women of different ages and that previously found in aged human tissues suggests that these follicle cells were not prematurely aged, but at the end of their reproductive life, as reflected by the decrease in the ovarian reserve and oocyte maturation rates with age observed in our population (Spearman $R=-0.422$; $p<0.001$ and Spearman $R=-0.292$; $p=0.008$, respectively) and also described by other authors (Miao et al., 2009; Stoop et al., 2014; Demond et al., 2016). Therefore, this signature that is valid for somatic tissues does not seem to represent functional ovarian aging in our samples. Nevertheless, our study was

entirely based on transcriptomics analysis of pre-selected markers, so we could not fully evaluate the role played by aging in the biology of cumulus cells.

In addition, there is a need for reliable predictors of oocyte quality that drives discovery of new biomarkers that would allow for the establishment of more objective criteria for selecting competent oocytes. However, previously reported biomarkers associated with successful embryo development and pregnancy outcomes were mainly derived from mural granulosa cells (not CCs) which may imply less correlation with the oocyte, since they are more separated. Furthermore, the biomarkers obtained were not shared among the studies, which as with the aging markers, could be explained by the little consistency in the experimental methodologies applied in the different studies (Huang and Wells, 2010; Parks et al., 2016). In our study, the relative expression levels of aging markers in CCs were plotted against ovarian reserve and oocyte maturation rates. However, no correlation was observed for any of the aging markers. Thus, the somatic aging markers analyzed cannot be used to predict premature ovarian failure or as oocyte quality biomarkers. More studies with larger samples studying previously found biomarkers of oocyte quality need to be conducted in order to obtain a reliable predictor.

Comparison of reproductive outcomes of IVF cycles with vitrified or fresh donor oocytes coming from the same stimulation cycle

The third chapter of this thesis was focused on the study of oocyte quality using clinical correlates. The effect of oocyte vitrification on the oocyte developmental competence was investigated by comparing the reproductive outcomes of fresh and vitrified oocytes from the same stimulation cycle.

To our knowledge, this was the largest study comparing sibling oocytes, vitrified and fresh, reported to date. We observed lower biochemical, clinical and ongoing pregnancies and LBR in vitrified oocytes, despite the high survival rate after warming (93%). These results were in agreement to what Kushnir and colleagues found in their study (Kushnir et al., 2018), but contradicted the findings observed in the early RCTs (Cobo et al., 2008; Cobo and Diaz, 2011; Rienzi et al., 2010; Parmegiani et al., 2011) and also previous reports comparing fresh and vitrified sibling oocytes (Trokoudes et al., 2011). Nevertheless, these last reports were small studies.

In the literature, many large cohort registries studies comparing reproductive outcomes of fresh and vitrified oocytes are based on anonymized aggregate data from publicly available reports uploaded by different clinics (Kushnir et al., 2015; Levi-Setti et al., 2016; Crawford et al., 2017; Kushnir et al., 2018); therefore, information regarding the protocol for cryopreservation used in each clinic is not known. Moreover, different clinics might have different expertise in oocyte vitrification, thus affecting reproductive outcomes in warmed cycles (Levi-Setti et al. 2016). Possible explanations for the conflicting results in the literature include: the physical insult that vitrification causes to the oocyte (effectiveness of the technique), and the loss of oocytes (1 every 10 even in the best laboratories) after warming (efficiency of the technique).

To test the hypothesis that the efficiency of vitrification/warming drives reproductive outcomes in these cycles, we paired fresh cycles with sibling vitrified cycles where the same number of oocytes were available at ICSI, rather than at assignment. We found that reproductive outcomes were similar in those 2 groups, indicating that efficiency plays a significant role in determining reproductive outcomes in these cycles.

Delving further into our analysis, we considered that cycles with vitrified oocytes might be affected two-fold by the technique. One immediate aspect, i.e. the availability of a

certain number of oocytes, affects directly reproductive outcomes, but can be mitigated by increasing the number of assigned oocytes. However, vitrification might also affect the developmental competence of the oocytes that survived the process, as suggested by both the lower fertilization rates and embryo scores in these cycles (see Table 21), and by reports of altered gene expression, reduced mtDNA copy number and increased ROS levels in vitrified mouse and bovine oocytes (Shirazi et al., 2016; Azari et al., 2017; Amoushahi et al., 2017). We reasoned that by analyzing cycles with 100% survival rates, we were selecting those were the biological effect of vitrification should have the lowest impact. In this sense, if efficiency was the source of most variability, we should expect similar reproductive outcome in the SAME and SAME100 analysis. If the biological effect of vitrification (its efficacy), on the other hand, was significantly contributing to the reproductive outcomes, we would expect higher reproductive outcomes in the SAME100 analysis. We further attempted to compare cycles with different survival rates, however the distribution of survival rates in our database was within too small a range to make this last analysis meaningful (not reported). The results of this second sub-analysis analysis overlapped almost perfectly with the first one, indicating that oocyte vitrification *per se* is as clinically effective as using fresh oocytes, when executed appropriately of high-quality oocytes.

We did detect a direct and sizeable effect of vitrification *per se* on fertilization rates and embryo quality, however, this did not translate into relevant clinical differences after the first embryo transfer (ET). We cannot exclude that this finding might affect cumulative LBR; however, as there was a difference of 0.2 points (on a 10 points scale) on the embryo cohort morphological score, and a difference of 0.4 less embryos available for transfer (Table 21), we suspect that the effect of oocyte vitrification on cumulative LBR might not be large.

Overall, our results of the third chapter of this thesis indicated that oocyte vitrification *per se* maintains the developmental potential of human oocytes within a reasonable biological range, clinically comparable to fresh oocytes. Moreover, we reported that the loss of oocytes at warming was likely the main reason for the reported lower clinical results in these cycles. This is important, as measures can be easily put in place to offset oocyte loss (i.e. assigning 10% more vitrified oocytes in high-quality programs). Consequently, clinics and oocyte banks should enforce strict quality controls on their vitrification processes and maximize survival rates to keep treatment effective and efficient.

Throughout the different objectives of this dissertation, we have studied new criteria to identify novel biomarkers of oocyte quality and we have answered a relevant question in the ART community by providing evidences that vitrification *per se* maintains the developmental potential of human oocytes within a reasonable biological range, clinically comparable to fresh oocytes. To the best of our knowledge, this is the first research of the transcriptional profile of several single *in vivo* mature human oocyte from reproductive age, healthy, and fertile women. Moreover, we are also the first to report of the splicing events that define *in vivo* matured human oocytes that have acquired developmental competence during the last steps of oocyte maturation (GV and MII stage oocytes).

Collectively, we believe that these results have contributed to the understanding of the factors influencing human oocyte developmental competence.

6. CONCLUSIONS

- This is the first report of the transcriptional profiles and splicing events characterizing single *in vivo* matured human oocytes from women of reproductive age, healthy and fertile. Our results suggest an important role for ncRNAs and alternative splicing in human oocyte biology.
- Age and ovarian reserve have been shown to independently affect the ncRNAs transcriptome of *in vivo* matured oocytes. These results might provide valuable information for the search of oocyte quality markers, and for the (re)interpretation of existing dataset.
- The differences in the transcribed spliced variants between GV and MII oocytes can provide biomarkers of oocyte quality, since the profile of confirmed AS events could determine the specific transcriptome of the mature oocyte. In particular, *PIK3CD* and *DIAPH2*, which are involved in maintaining a correct ovarian function, should be further investigated with functional studies.
- The expression of common somatic aging markers in human cumulus cells have been analyzed, and results didn't show a clear correlation between the analyzed genes and age, suggesting that CCs of reproductively old women do not present the typical transcriptome of aged tissues. When looking at future clinical applications, these markers have not been found useful for the development of non-invasive markers for oocyte developmental competence.
- This study showed that oocyte vitrification *per se* maintained the developmental potential of human oocytes within a reasonable biological range, clinically comparable to fresh oocytes. As a consequence, we established that the main reason for the reported lower clinical results in vitrified cycles has to be attributed to the loss of oocytes during the warming step. This has important repercussions in the clinical practice, as measures can be easily put in place to offset oocyte loss

(i.e. assigning 10% more vitrified oocytes in high-quality programs). Consequently, clinics and oocyte banks should enforce strict quality controls on their vitrification processes, and maximize survival rates to keep treatment effective and efficient.

7. BIBLIOGRAPHY

Ajduk, A., Małagocki, A., & Maleszewski, M. (2008). Cytoplasmic maturation of mammalian oocytes: Development of a mechanism responsible for sperm-induced Ca2+ oscillations. *Reproductive Biology*, 8(1): 3–22.

Albertini, D. F., Combelles, C. M. H., Benecchi, E., & Carabatsos, M. J. (2001). Cellular basis for paracrine regulation of ovarian follicle development. *Reproduction*, 121(5):647–653.

Alberts et al. (2008). Molecular Biology of the Cell (5th ed.). New York: Garland Science.

Al-Edani, T., Assou, S., Ferrières, A., Bringer Deutsch, S., Gala, A., Lecellier, C.-H., Aït-Ahmed, O., & Hamamah, S. (2014). Female aging alters expression of human cumulus cells genes that are essential for oocyte quality. *BioMed Research International*, 2014: 964614.

Alizadeh, Z., Kageyama, S. I., & Aoki, F. (2005). Degradation of maternal mRNA in mouse embryos: Selective degradation of specific mRNAs after fertilization. *Molecular Reproduction and Development*, 72(3): 281–290.

Ambekar, A. S., Nirujogi, R. S., Srikanth, S. M., Chavan, S., Kelkar, D. S., Hinduja, I., Zaveri, K., Prasad, T. S., Harsha, H. C., Pandey, A., & Mukherjee, S. (2013). Proteomic analysis of human follicular fluid: A new perspective towards understanding folliculogenesis. *Journal of Proteomics*, 87:68–77.

American College of Obstetricians and Gynecologists (2015). Committee Opinion No. 618: Ovarian reserve testing. Obstetrics & Gynecology, 125(1): 268–73.

Amoushahi, M., Salehnia, M., & Mowla, S. J. (2017). Vitrification of mouse MII oocyte decreases the mitochondrial DNA copy number, TFAM gene expression and mitochondrial enzyme activity. *Journal of Reproduction and Infertility*, 18(4): 343–351.

Anderson, R. A., Sciorio, R., Kinnell, H., Bayne, R. A. L., Thong, K. J., de Sousa, P. A., & Pickering, S. (2009). Cumulus gene expression as a predictor of human oocyte fertilisation, embryo development and competence to establish a pregnancy. *Reproduction*, 138(4): 629–637.

Andrade, G. M., Da Silveira, J. C., Perrini, C., Del Collado, M., Gebremedhn, S., Tesfaye, D., Meirelles, F. V., Perecin, F. (2017). The role of the PI3K-Akt signaling pathway in the developmental competence of bovine oocytes. *PLoS ONE*, 12(9).

Aravin, A. A., Sachidanandam, R., Girard, A., Fejes-Toth, K., & Hannon, G. J. (2007). Developmentally regulated piRNA clusters implicate MILI in transposon control. *Science*, *316*(5825): 744–747.

Argente, J., Flores, R., Gutiérrez-Arumí, A., Verma, B., Martos-Moreno, G. Á., Cuscó, I., Oghabian, A., Chowen, J. A., Frilander, M. J., & Pérez-Jurado, L. A. (2014). Defective minor spliceosome mRNA processing results in isolated familial growth hormone deficiency. *EMBO Molecular Medicine*, 6(3): 299–306.

Arispe, N., Rojas, E., Genge, B. R., Wu, L. N. Y., & Wuthier, R. E. (1996). Similarity in calcium channel activity of annexin V and matrix vesicles in planar lipid bilayers. *Biophysical Journal*, 71(4): 1764–1775.

Armstrong, D. T. (2001). Effects of maternal age on oocyte developmental competence. *Theriogenology*, 55(6): 1303–1322.

Ashburner, M., Ball, C. A., Blake, J. A., Botstein, D., Butler, H., Cherry, J. M., Davis, A. P., Dolinski, K., Dwight, S.S., Eppig, J. T., Harris, M. A., Hill, D. P., Issel-Tarver, L., Kasarskis, A., Lewis, S., Matese, J.C., Richardson, J.E., Ringwald, M., Rubin, G. M., & Sherlock, G. (2000). Gene ontology: Tool for the unification of biology. *Nature Genetics*, 25(1): 25–29.

Assou, S., Haouzi, D., Mahmoud, K., Aouacheria, A., Guillemin, Y., Pantesco, V., Rème, T., Dechaud, H., De Vos, J., & Hamamah, S. (2008). A non-invasive test for assessing embryo potential by gene expression profiles of human cumulus cells: A proof of concept study. *Molecular Human Reproduction*, 14(12): 711–719.

Au, H. K., Lin, S. H., Huang, S. Y., Yeh, T. S., Tzeng, C. R., & Hsieh, R. H. (2005). Deleted mitochondrial DNA in human luteinized granulosa cells. *Annals of the New York Academy of Sciences*, 1042: 136–141.

Azari, M., Kafi, M., Ebrahimi, B., Fatehi, R., & Jamalzadeh, M. (2017). Oocyte maturation, embryo development and gene expression following two different methods of bovine cumulus-oocyte complexes vitrification. *Veterinary Research Communications*, 41(1): 49–56.

Babayev, E., & Seli, E. (2015). Oocyte mitochondrial function and reproduction. *Current Opinion in Obstetrics and Gynecology*, 27(3): 175–181.

Bachvarova, R., De Leon, V., Johnson, A., Kaplan, G., & Paynton, B. V. (1985). Changes in total RNA, polyadenylated RNA, and actin mRNA during meiotic maturation of mouse oocytes. *Developmental Biology*, 108(2): 325–331.

Badenas, J., Santaló, J., Calafell, J. M., Estop, A. M., & Egozcue, J. (1989). Effect of the degree of maturation of mouse oocytes at fertilization: A source of chromosome imbalance. *Gamete Research*, 24(2): 205–218.

Baker, M. (2011). Long noncoding RNAs: The search for function. *Nature Methods*, 8(5): 379–383.

Balaban, B., & Urman, B. (2006). Effect of oocyte morphology on embryo development and implantation. *Reproductive BioMedicine Online*, 12(5): 608–615.

Balakier, H., Bouman, D., Sojecki, A., Librach, C., & Squire, J. A. (2002). Morphological and cytogenetic analysis of human giant oocytes and giant embryos. *Human Reproduction*, 17(9): 2394–2401.

Baralle, F. E., & Giudice, J. (2017). Alternative splicing as a regulator of development and tissue identity. *Nature Reviews Molecular Cell Biology*, 18(7): 437–451.

Bartel, D. P. (2009). MicroRNAs: Target recognition and regulatory functions. *Cell*, 136(2):215–233.

Bavister, B. D., & Squirrell, J. M. (2000). Mitochondrial distribution and function in oocytes and early embryos. *Human Reproduction*,15 (Suppl. 2): 189–198.

Bement, W. M., & Capco, D. G. (1989). Activators of protein kinase C trigger cortical granule exocytosis, cortical contraction, and cleavage furrow formation in Xenopus laevis oocytes and eggs. *Journal of Cell Biology*, 108(3): 885–892.

Benjamini, Y., & Hochberg, Y. (1995). Controlling the False Discovery Rate: A Practical and powerful approach to multiple testing. *Journal of the Royal Statistical Society*, 57(1): 289–300.

Bertone, P., Stolc, V., Royce, T. E., Rozowsky, J. S., Urban, A. E., Zhu, X., Rinn, J. L., Tongprasit, W., Samanta, M., Weissman, S., Gerstein, M., & Snyder, M. (2004). Global identification of human transcribed sequences with genome tiling arrays. *Science*, 306(5705): 2242–2246.

Bettegowda, A., Patel, O. V., Ireland, J. J., & Smith, G. W. (2006). Quantitative analysis of messenger RNA abundance for ribosomal protein L-15, cyclophilin-A, phosphoglycerokinase, beta-glucuronidase, glyceraldehyde 3-phosphate dehydrogenase, beta-actin, and histone H2A during bovine oocyte maturation and early embryogenesis in vitro. *Molecular Reproduction and Development*, 73(3): 267–278.

Beyer, E. C. (1993). Gap junctions. *International Review of Cytology*, 137C: 1-37

Biase, F. H. (2017). Oocyte Developmental Competence: Insights from Cross-Species Differential Gene Expression and Human Oocyte-Specific Functional Gene Networks. *OMICS: A Journal of Integrative Biology*, 21(3): 156–168.

Biase, F. H., Everts, R. E., Oliveira, R., Santos-Biase, W. K. F., Fonseca Merighe, G. K., Smith, L. C., Martelli, L., Lewin, H.,& Meirelles, F. V. (2014). Messenger RNAs in metaphase II oocytes correlate with successful embryo development to the blastocyst stage. *Zygote*, 22(1): 69–79.

Bione, S., Sala, C., Manzini, C., Arrigo, G., Zuffardi, O., Banfi, S., Borsani, G., Jonveaux, P., Philippe, C., Zuccotti, M., Ballabio, A.,& Toniolo, D. (2002). A human homologue of the drosophila melanogaster diaphanous gene is disrupted in a patient with premature ovarian failure: Evidence for conserved function in oogenesis and implications for human sterility. *The American Journal of Human Genetics*, 62(3): 533–541.

Bouckenheimer, J., Assou, S., Riquier, S., Hou, C., Philippe, N., Sansac, C., Lavabre-Bertrand, T., Commes, T., Lemaître, J. M., Boureux, A., & De Vos, J. (2016). Long non-coding RNAs in human early embryonic development and their potential in ART. *Human Reproduction Update*, 23(1): 19–40.

Braude, P., Bolton, V., & Moore, S. (1988). Human gene expression first occurs between the four- and eight-cell stages of preimplantation development. *Nature*, 332(6163): 459–461.

Brevini, T. A. L., Vassena, R., Francisci, C., & Gandolfi, F. (2005). Role of adenosine triphosphate, active mitochondria, and microtubules in the acquisition of developmental competence of parthenogenetically activated pig oocytes. *Biology of Reproduction*, 72(5): 1218–1223.

Broekmans, F. J. (2009). Testing for Ovarian Reserve in Assisted Reproduction programs: the current point of view. *Facts, Views & Vision in ObGyn*, 1(2): 79–87.

Broer, S. L., Dólleman, M., Van Disseldorp, J., Broeze, K. A., Opmeer, B. C., Bossuyt, P. M., Eijkemans, M. J., Mol, B. W., & Broekmans, F. J. M. (2013). Prediction of an excessive response in in vitro fertilization from patient characteristics and ovarian reserve tests and comparison in subgroups: An individual patient data meta-analysis. *Fertility and Sterility*, 100(2): 420-429.

Broer, S. L., Mol, B. W. J., Hendriks, D., & Broekmans, F. J. M. (2009). The role of antimullerian hormone in prediction of outcome after IVF: comparison with the antral follicle count. *Fertility and Sterility*, 91(3): 705–714.

Bromfield, J. J., Coticchio, G., Hutt, K., Sciajno, R., Borini, A., & Albertini, D. F. (2009). Meiotic spindle dynamics in human oocytes following slow-cooling cryopreservation. *Human Reproduction*, 24(9): 2114–2123.

Caley, D. P., Pink, R. C., Trujillano, D., & Carter, D. R. F. (2010). Long noncoding RNAs, chromatin, and development. *TheScientificWorldJournal*, 10:90–102.

Cao, J. (2014). The functional role of long non-coding RNAs and epigenetics. *Biological Procedures Online*, 16:11.

Carmell, M. A., Girard, A., van de Kant, H. J. G., Bourc'his, D., Bestor, T. H., de Rooij, D. G., & Hannon, G. J. (2007). MIWI2 Is Essential for Spermatogenesis and Repression of Transposons in the Mouse Male Germline. *Developmental Cell*, 12(4): 503–514.

Carninci, P., Kasukawa, T., Katayama, S., Gough, J., Frith, M. C., Maeda, N., … Hayashizaki, Y. (2005). The transcriptional landscape of the mammalian genome. Science, 309(5740): 1559–1563.

Chaube, S. K. (2001). Role of meiotic maturation regulatory factors in developmental competence of mammalian oocytes. *Health and Population: Perspectives and Issues*, 24(4): 218–231.

Chu, C. Y., & Rana, T. M. (2008). Potent RNAi by short RNA triggers. *RNA*, 14(9): 1714–1719.

Cillo, F., Brevini, T. A. L., Antonini, S., Paffoni, A., Ragni, G., & Gandolfi, F. (2007). Association between human oocyte developmental competence and expression levels of some cumulus genes. *Reproduction*, 134(5): 645–650.

Ciotti, P. M., Notarangelo, L., Morselli-Labate, A. M., Felletti, V., Porcu, E., & Venturoli, S. (2004). First polar body morphology before ICSI is not related to embryo quality or pregnancy rate. *Human Reproduction*, 19(10), 2334–2339.

Cobo, A., & Diaz, C. (2011). Clinical application of oocyte vitrification: A systematic review and meta-analysis of randomized controlled trials. *Fertility and Sterility*, 96(2): 277–285

Cobo, A., Kuwayama, M., Pérez, S., Ruiz, A., Pellicer, A., & Remohí, J. (2008). Comparison of concomitant outcome achieved with fresh and cryopreserved donor oocytes vitrified by the Cryotop method. *Fertility and Sterility*, 89(6), 1657–1664.

Collado-Fernandez, E., Picton, H. M., & Dumollard, R. (2012). Metabolism throughout follicle and oocyte development in mammals. *International Journal of Developmental Biology*, 56(10–12): 799–808.

Combelles, C. M. H., Carabatsos, M. J. O., Kumar, T. R., Matzuk, M. M., & Albertini, D. F. (2004). Hormonal control of somatic cell oocyte interactions during ovarian follicle development. *Molecular Reproduction and Development*, 69(3): 347–355.

Coroleu, B., Barri, P. N., Carreras, O., Belil, I., Buxaderas, R., Veiga, A., & Balasch, J. (2006). Effect of using an echogenic catheter for ultrasound-guided embryo transfer in an IVF programme: A prospective, randomized, controlled study. *Human Reproduction*, *21*(7): 1809–1815.

Coticchio, G., Sereni, E., Serrao, L., Mazzone, S., Iadarola, I., & Borini, A. (2004). What criteria for the definition of oocyte quality? *Annals of the New York Academy of Sciences*, 1034(1): 132–144.

Cowden Dahl, K. D., Fryer, B. H., Mack, F. A., Compernolle, V., Maltepe, E., Adelman, D. M., Carmeliet, P., Simon, M. C. (2005). Hypoxia-inducible factors 1alpha and 2alpha regulate trophoblast differentiation. *Molecular and cellular biology*, 25(23):10479-10491.

Crawford, S., Boulet, S. L., Kawwass, J. F., Jamieson, D. J., & Kissin, D. M. (2017). Cryopreserved oocyte versus fresh oocyte assisted reproductive technology cycles, United States, 2013. *Fertility and Sterility*, 107(1): 110–118.

De La Fuente, R., & Eppig, J. J. (2001). Transcriptional activity of the mouse oocyte genome: Companion granulosa cells modulate transcription and chromatin remodeling. *Developmental Biology*, *229*(1), 224–236.

De Magalhães, J. P., Curado, J., & Church, G. M. (2009). Meta-analysis of age-related gene expression profiles identifies common signatures of aging. *Bioinformatics*, 25(7): 875–881.

De Munck, N., & Vajta, G. (2017). Safety and efficiency of oocyte vitrification. *Cryobiology*, 78: 119–127.

De Santis, L., Cino, I., Rabellotti, E., Calzi, F., Persico, P., Borini, A., & Goticchio, G. (2005). Polar body morphology and spindle imaging as predictors of oocyte quality. *Reproductive BioMedicine Online*, 11(1), 36–42.

De Vos, A., Van De Velde, H., Joris, H., & Van Steirteghem, A. (1999). In-vitro matured metaphase-I oocytes have a lower fertilization rate but similar embryo quality as mature metaphase-II oocytes after intracytoplasmic sperm injection. *Human Reproduction*, 14(7), 1859–1863.

Demetriou, C., Abu-Amero, S., White, S., Peskett, E., Markoff, A., Stanier, P.Moore, G. E., & Regan, L. (2015). Investigation of the Annexin A5 M2 haplotype in 500 white European couples who have experienced recurrent spontaneous abortion. *Reproductive BioMedicine Online*, 31(5): 681–688.

Demond, H., Trapphoff, T., Dankert, D., Heiligentag, M., Grümmer, R., Horsthemke, B., & Eichenlaub-Ritter, U. (2016). Preovulatory aging in vivo and in vitro affects maturation rates, abundance of selected proteins, histone methylation pattern and spindle integrity in murine oocytes. *PLoS ONE*, *11*(9).

Deng, W., & Lin, H. (2002). Miwi, a murine homolog of piwi, encodes a cytoplasmic protein essential for spermatogenesis. *Developmental Cell*, 2(6): 819–830.

Depoix, C. L., de Selliers, I., Hubinont, C., & Debieve, F. (2017). HIF1A and EPAS1 potentiate hypoxia-induced upregulation of inhibin alpha chain expression in human term cytotrophoblasts in vitro. *Molecular Human Reproduction*, 23(3): 199–209.

Desai, N., Ludgin, J., Sharma, R., Anirudh, R. K., & Agarwal, A. (2013). Female and male gametogenesis. T. Falcone and W.W. Hurd (eds.), Clinical Reproductive Medicine and Surgery: A Practical Guide.

Devjak, R., Burnik Papler, T., Verdenik, I., Fon Tacer, K., & Vrtačnik Bokal, E. (2016). Embryo quality predictive models based on cumulus cells gene expression. *Balkan Journal of Medical Genetics*, 19(1): 5–12.

Diaz, F. J., Wigglesworth, K., & Eppig, J. J. (2007). Oocytes determine cumulus cell lineage in mouse ovarian follicles. *Journal of Cell Science*, 120(8): 1330–1340.

Do, D. V., Strauss, B., Cukuroglu, E., Macaulay, I., Wee, K. B., Hu, T. X., Igor, R. L. M., Lee, C., Harrison, A., Butler, R., Dietmann, S., Jernej, U., Marioni, J., Smith, C. W. J., Göke, J., & Surani, M. A. (2018). SRSF3 maintains transcriptome integrity in oocytes by regulation of alternative splicing and transposable elements. *Cell Discovery*, 4:33.

Ebner, T., Moser, M., & Tews, G. (2006). Is oocyte morphology prognostic of embryo developmental potential after ICSI? *Reproductive BioMedicine Online*, 12(4): 507–512.

Ebner, T. (2002). First polar body morphology and blastocyst formation rate in ICSI patients. *Human Reproduction*, 17(9), 2415–2418.

Edson, M. A., Nagaraja, A. K., & Matzuk, M. M. (2009). The mammalian ovary from genesis to revelation. *Endocrine Reviews*, 30(6): 624–712.

Edwards, M. G., Anderson, R. M., Yuan, M., Kendziorski, C. M., Weindruch, R., & Prolla, T. A. (2007). p53-mediated transcriptional program. *BMC Genomics*, 13:1–13.

Eldar-Geva, T., Ben-Chetrit, A., Spitz, I. M., Rabinowitz, R., Markowitz, E., Mimoni, T., Gal, M., Zylber-Haran, E., & Margalioth, E. J. (2005). Dynamic assays of inhibin B, anti-Mullerian hormone and estradiol following FSH stimulation and ovarian ultrasonography as predictors of IVF outcome. *Human Reproduction*, 20(11): 3178–3183.

Emig, D., Salomonis, N., Baumbach, J., Lengauer, T., Conklin, B. R., & Albrecht, M. (2010). AltAnalyze and DomainGraph: Analyzing and visualizing exon expression data. *Nucleic Acids Research*, *38*: W755-W762.

Eppig, J. J. (2001). Oocyte control of ovarian follicular development and function in mammals. *Reproduction*, 122(6): 829–838.

Eppig, J. J. (1996). Coordination of nuclear and cytoplasmic oocyte maturation in eutherian mammals. *Reproduction, Fertility and Development*, 8(4): 485–489.

Eppig, J. J., & Steckman, M. L. (1976). Comparison of exogenous energy sources for in vitro maintenance of follicle cell-free Xenopus laevis oocytes. *In Vitro: Journal of the Tissue Culture Association*, 12(3): 173–179.

Evsikov, A. V., & De Evsikova, C. M. (2009). Gene expression during the oocyte-to-embryo transition in mammals. *Molecular Reproduction and Development*, 76: 805–818.

Evsikov, A. V., Graber, J. H., Brockman, J. M., Hampl, A., Holbrook, A. E., Singh, P., Eppig, J. J., Solter, D.,& Knowles, B. B. (2006). Cracking the egg: Molecular dynamics and evolutionary aspects of the transition from the fully grown oocyte to embryo. *Genes and Development*, 20(19): 2713–2727.

Faddy, M. J., Gosden, R. G., Gougeon, A., Richardson, S. J., & Nelson, J. F. (1992). Accelerated disappearance of ovarian follicles in mid-life: Implications for forecasting menopause. *Human Reproduction*, 7(10): 1342–1346.

Fair, T., Carter, F., Park, S., Evans, A. C. O., & Lonergan, P. (2007). Global gene expression analysis during bovine oocyte in vitro maturation. *Theriogenology*, 68(Suppl. 1): S91-S97

Familiari, G., Heyn, R., Relucenti, M., Nottola, S. A., & Sathananthan, A. H. (2006). Ultrastructural dynamics of human reproduction, from ovulation to fertilization and early embryo development. *International Review of Cytology*, 249: 53–141.

Fang, C., Tang, M., Li, T., Peng, W. L., Zhou, C. Q., Zhuang, G. L., & Leong, M. (2007). Visualization of meiotic spindle and subsequent embryonic development in in vitro and in vivo matured human oocytes. *Journal of Assisted Reproduction and Genetics*, 24(11): 547–551.

Faria, D., Dahiméne, S., Alessio, L., Scott-Ward, T., Schreiber, R., Kunzelmann, K., & Amaral, M. D. (2011). Effect of annexin A5 on CFTR: Regulated traffic or scaffolding? *Molecular Membrane Biology*, 28(1): 14–29.

Fatica, A., & Bozzoni, I. (2014). Long non-coding RNAs: New players in cell differentiation and development. *Nature Reviews Genetics*, 15: 7–21.

Fauser, B. C. J. M., Diedrich, K., Bouchard, P., Matzuk, F. D., Franks, S., Hamamah, S., Simón, C., Devroey, P., Ezcurra, D., & Howles, C. M. (2011). Contemporary genetic technologies and female reproduction. *Human Reproduction Update*, 17(6): 829–847.

Ferreira, E. M., Vireque, A. A., Adona, P. R., Meirelles, F. V., Ferriani, R. A., & Navarro, P. A. A. S. (2009). Cytoplasmic maturation of bovine oocytes: Structural and biochemical modifications and acquisition of developmental competence. *Theriogenology*, 71(5): 836–848.

Figueira, R. D. C. S., De Almeida Ferreira Braga, D. P., Semião-Francisco, L., Madaschi, C., Iaconelli, A., & Borges, E. (2010). Metaphase II human oocyte morphology: Contributing factors and effects on fertilization potential and embryo developmental ability in ICSI cycles. *Fertility and Sterility*, 94(3): 1115–1117.

FitzHarris, G., Marangos, P., & Carroll, J. (2007). Changes in endoplasmic reticulum structure during mouse oocyte maturation are controlled by the cytoskeleton and cytoplasmic dynein. *Developmental Biology*, 305(1): 133–144.

Fragouli, E., Lalioti, M. D., & Wells, D. (2014). The transcriptome of follicular cells: Biological insights and clinical implications for the treatment of infertility. *Human Reproduction Update*, 20(1): 1–11.

Fragouli, E., Bianchi, V., Patrizio, P., Obradors, A., Huang, Z., Borini, A., Delhanty, J.D., & Wells, D. (2010). Transcriptomic profiling of human oocytes: Association of meiotic aneuploidy and altered oocyte gene expression. *Molecular Human Reproduction*, 16(8): 570–582.

Fried, G., Remaeus, K., Harlin, J., Krog, E., Csemiczky, G., Aanesen, A., & Tally, M. (2003). Inhibin B predicts oocyte number and the ratio IGF-I/IGFBP-1 may indicate oocyte quality during ovarian hyperstimulation for in vitro fertilization. Journal of Assisted Reproduction and Genetics, 20(5):167-176.

Gilchrist, R. B., Lane, M., & Thompson, J. G. (2008). Oocyte-secreted factors: Regulators of cumulus cell function and oocyte quality. *Human Reproduction Update*, 14(2): 159–177.

Gilchrist, R. B. (2006). Molecular basis of oocyte-paracrine signalling that promotes granulosa cell proliferation. *Journal of Cell Science*, 119(18): 3811–3821.

Gondos, B., Westergaard, L., & Byskov, A. G. (1986). Initiation of oogenesis in the human fetal ovary: Ultrastructural and squash preparation study. *American Journal of Obstetrics and Gynecology*, 155(1): 189–195.

Gonzalez-Roca, E., Garcia-Albéniz, X., Rodriguez-Mulero, S., Gomis, R. R., Kornacker, K., & Auer, H. (2010). Accurate expression profiling of very small cell populations. *PLoS ONE*, 5(12).

Gosden, R., & Lee, B. (2010). Portrait of an oocyte: Our obscure origin. *Journal of Clinical Investigation*, 120(4): 973–983.

Goto, T., Adjaye, J., Rodeck, C. H., & Monk, M. (1999). Identification of genes expressed in human primordial germ cells at the time of entry of the female germ line into meiosis. *Molecular Human Reproduction*, 5(9): 851–860.

Goud, P. T. (2002). Effect of post-ovulatory age and calcium in the injection medium on the male pronucleus formation and metaphase entry following injection of human spermatozoa into golden hamster oocytes. *Molecular Human Reproduction*, 5(3): 227–233.

Grande, M., Borobio, V., Jimenez, J. M., Bennasar, M., Stergiotou, I., Peñarrubia, J., & Borrell, A. (2014). Antral follicle count as a marker of ovarian biological age to reflect the background risk of fetal aneuploidy. *Human Reproduction*, 29(6): 1337–1343.

Grenfell, A. W., Heald, R., & Strzelecka, M. (2016). Mitotic noncoding RNA processing promotes kinetochore and spindle assembly in Xenopus. *Journal of Cell Biology*, 214(2): 133–141.

Grøndahl, M. L., Yding Andersen, C., Bogstad, J., Nielsen, F. C., Meinertz, H., & Borup, R. (2010). Gene expression profiles of single human mature oocytes in relation to age. *Human Reproduction*, 25(4): 957–968.

Guil, S., & Esteller, M. (2012). Cis-acting noncoding RNAs: Friends and foes. *Nature Structural and Molecular Biology*, 19(11): 1068–1075.

Guraya, S. S. (2008). Cellular and molecular biology of human oogenesis, ovulation and early embryogenesis: Fundamentals, biomedical and clinical implications in relation to infant disorder. New Age International Publishers.

Halet, G. (2004). PKC signaling at fertilization in mammalian eggs. *Biochimica et Biophysica Acta - Molecular Cell Research*, 1742(1–3): 185–189.

Hamatani, T., Falco, G., Carter, M. G., Akutsu, H., Stagg, C. A., Sharov, A. A., Dudekula, D. B., VanBuren, V., & Ko, M. S. (2004). Age-associated alteration of gene

expression patterns in mouse oocytes. *Human Molecular Genetics*, 13(19): 2263–2278.

Hamel, M., Dufort, I., Robert, C., Gravel, C., Leveille, M. C., Leader, A., & Sirard, M. A. (2008). Identification of differentially expressed markers in human follicular cells associated with competent oocytes. *Human Reproduction*, 23(5): 1118–1127.

Hamel, M., Dufort, I., Robert, C., Léveillé, M. C., Leader, A., & Sirard, M. A. (2009). Genomic assessment of follicular marker genes as pregnancy predictors for human IVF. *Molecular Human Reproduction*, 16(2): 87–96.

Hangauer, M. J., Vaughn, I. W., & McManus, M. T. (2013). Pervasive transcription of the human genome produces thousands of previously unidentified long intergenic noncoding RNAs. *PLoS Genetics*, 9(6).

Hassan-Ali, H., Hisham-Saleh, A., El-Gezeiry, D., Baghdady, I., Ismaeil, I., & Mandelbaum, J. (1998). Perivitelline space granularity: A sign of human menopausal gonadotrophin overdose in intracytoplasmic sperm injection. *Human Reproduction*, 13(12): 3425–3430.

Hassold, T., Hall, H., & Hunt, P. (2007). The origin of human aneuploidy: Where we have been, where we are going. *Human Molecular Genetics*, 16: R203-R208.

Hayashi, Y., Sasaki, H., Suzuki, S., Nishiyama, T., Kitaori, T., Mizutani, E., Suzumori, N., & Sugiura-Ogasawara, M. (2013). Genotyping analyses for polymorphisms of ANXA5 gene in patients with recurrent pregnancy loss. *Fertility and Sterility*, 100(4): 1018–1024.

Huang, Z., & Wells, D. (2010). The human oocyte and cumulus cells relationship: New insights from the cumulus cell transcriptome. *Molecular Human Reproduction*, 16(10): 715–725.

Humblot, P., Holm, P., Lonergan, P., Wrenzycki, C., Lequarré, A. S., Joly, C. G., Herrmann, D., Lopes, A., Rizos, D., Niemann, H., & Callesen, H. (2005). Effect of stage of follicular growth during superovulation on developmental competence of bovine oocytes. *Theriogenology*, 63(4): 1149–1166.

Hussein, T. S., Thompson, J. G., & Gilchrist, R. B. (2006). Oocyte-secreted factors enhance oocyte developmental competence. *Developmental Biology*, 296(2): 514–521.

Ida, H., Boylan, S. A., Weigel, A. L., & Hjelmeland, L. M. (2015). Age-related changes in the transcriptional profile of mouse RPE/choroid. *Physiological Genomics*, 15(3): 258–262.

Inoue, A., Nakajima, R., Nagata, M., & Aoki, F. (2008). Contribution of the oocyte nucleus and cytoplasm to the determination of meiotic and developmental competence in mice. *Human Reproduction*, 23(6): 1377–1384.

Ireland, J. J., Smith, G. W., Scheetz, D., Jimenez-Krassel, F., Folger, J. K., Ireland, J. L. H., Mossa, F., Lonergan, P., & Evans, A. C. (2011). Does size matter in females? An overview of the impact of the high variation in the ovarian reserve on ovarian function and fertility, utility of anti-Müllerian hormone as a diagnostic marker for fertility and causes of variation in the ovarian reserve in cattle. *Reproduction, Fertility and Development*, 23(1): 1–14.

Ireland, J. J., Ward, F., Jimenez-Krassel, F., Ireland, J. L. H., Smith, G. W., Lonergan, P., & Evans, A. C. (2007). Follicle numbers are highly repeatable within individual animals but are inversely correlated with FSH concentrations and the proportion of good-quality embryos after ovarian stimulation in cattle. *Human Reproduction*, 22(6): 1687–1695.

Jamnongjit, M., & Hammes, S. R. (2005). Oocyte maturation: The coming of age of a germ cell. *Seminars in Reproductive Medicine*, 23:234–241.

Jia, L., Li, J., He, B., Jia, Y., Niu, Y., Wang, C., & Zhao, R. (2016). Abnormally activated one-carbon metabolic pathway is associated with mtDNA hypermethylation and mitochondrial malfunction in the oocytes of polycystic gilt ovaries. *Scientific Reports*, 6:19436.

Jiao, Z. X., Xu, M., & Woodruff, T. K. (2012). Age-associated alteration of oocyte-specific gene expression in polar bodies: Potential markers of oocyte competence. *Fertility and Sterility*, 98(2): 480–486.

Johnson, M. H., & Everitt, B. J. (2003). Essential Reproduction. U.K.: Blackwell Science.

Jones, G. M., Cram, D. S., Song, B., Magli, M. C., Gianaroli, L., Lacham-Kaplan, O., Findlay, J.K., Jenkin, G., & Trounson, A. O. (2008). Gene expression profiling of human oocytes following in vivo or in vitro maturation. *Human Reproduction*, 23(5): 1138–1144.

Kalsotra, A., & Cooper, T. A. (2011). Functional consequences of developmentally regulated alternative splicing. *Nature Reviews Genetics*, 12(10): 715–729.

Kampa, D., Cheng, J., Kapranov, P., Yamanaka, M., Brubaker, S., Cawley, S., Drenkow, J., Piccolboni, A., Bekiranov, S., Helt, G., Tammana, H., & Gingeras, T. R. (2004). Novel RNAs identified from an in-depth analysis of the transcriptome of human chromosomes 21 and 22. *Genome Research*, 14(3): 331–342.

Kapranov, P., Drenkow, J., Cheng, J., Long, J., Helt, G., Dike, S., & Gingeras, T. R. (2005). Examples of the complex architecture of the human transcriptome revealed by RACE and high-density tiling arrays. *Genome Research*, 15(7): 987–997.

Karaer, A., Tuncay, G., Mumcu, A., & Dogan, B. (2019). Metabolomics analysis of follicular fluid in women with ovarian endometriosis undergoing in vitro fertilization. *Systems Biology in Reproductive Medicine*, 65(1): 39–47.

Katz-Jaffe, M. G., Surrey, E. S., Minjarez, D. A., Gustofson, R. L., Stevens, J. M., & Schoolcraft, W. B. (2013). Association of abnormal ovarian reserve parameters with a higher incidence of aneuploid blastocysts. *Obstetrics & Gynecology*, 121(1):71-77.

Keefe, D., Kumar, M., & Kalmbach, K. (2015). Oocyte competency is the key to embryo potential. *Fertility and Sterility*, 103(2): 317–322.

Kim, V. N., Han, J., & Siomi, M. C. (2009). Biogenesis of small RNAs in animals. *Nature Reviews Molecular Cell Biology*, 10(2):126–139.

King, A. E., Critchley, H. O., & Kelly, R. W. (2001). The NF-kappaB pathway in human endometrium and first trimester decidua. *Molecular Human Reproduction*, 7(2): 175–183.

Kocabas, A. M., Crosby, J., Ross, P. J., Otu, H. H., Beyhan, Z., Can, H., Tam, W. L., Rosa, G. J., Halgren, R. G., Lim, B., Fernandez, E., & Cibelli, J. B. (2006). The transcriptome of human oocytes. *Proceedings of the National Academy of Sciences*, 103(38): 14027–14032.

Krisher, R. L. (2012). In vivo and in vitro environmental effects on mammalian oocyte quality. *Annual Review of Animal Biosciences*, 1(1): 393–417.

Krisher, R. L. (2004). The effect of oocyte quality on development. *Journal of Animal Science*, 82(Suppl. E): E14-E23.

Kues, W. A., Sudheer, S., Herrmann, D., Carnwath, J. W., Havlicek, V., Besenfelder, U., … Niemann, H. (2008). Genome-wide expression profiling reveals distinct clusters of transcriptional regulation during bovine preimplantation

development in vivo. *Proceedings of the National Academy of Sciences*, 105(50): 19768–19773.

Kumar, N. M., & Gilula, N. B. (1996). The gap junction communication channel. *Cell*, 84(3): 381–388.

Kuramochi-Miyagawa, S. (2004). Mili, a mammalian member of piwi family gene, is essential for spermatogenesis. *Development*, 131(4): 839–849.

Kushnir, V. A., Darmon, S. K., Barad, D. H., & Gleicher, N. (2018). New national outcome data on fresh versus cryopreserved donor oocytes. *Journal of Ovarian Research*, 11(1):2.

Kushnir, V. A., Barad, D. H., & Gleicher, N. (2015). Fresh vs cryopreserved donor oocytes--Reply. *Journal of the American Medical Association* 314(23): 2570.

Kuwayama, M., Vajta, G., Kato, O., & Leibo, S. P. (2005). Highly efficient vitrification method for cryopreservation of human oocytes. *Reproductive Biomedicine Online*, 11(3): 300–308.

Labrecque, R., Sirard, M. A. (2014). The study of mammalian oocyte competence by transcriptome analysis: progress and challenges. *Molecular Human Reproduction*, 20(2):103-116.

Lanman, J. T. (2010). Delays during reproduction and their effects on the embryo and fetus. *New England Journal of Medicine*, 278(18): 993–999.

Larabell, C. A., Rowning, B. A., & Moon, R. T. (2004). A PKC wave follows the calcium wave after activation of Xenopus eggs. *Differentiation*, 72(1): 41–47.

Layman, L. C. (2002). Human gene mutations causing infertility. *Journal of Medical Genetics*, 39(3): 153–161.

Lequarre, A. S., Traverso, J. M., Marchandise, J., & Donnay, I. (2004). Poly(A) RNA is reduced by half during bovine oocyte maturation but increases when meiotic arrest is maintained with CDK Inhibitors. *Biology of Reproduction*, 71(2): 425–431.

Levi-Setti, P. E. P. E., Borini, A., Patrizio, P., Bolli, S., Vigiliano, V., De Luca, R., & Scaravelli, G. (2016). ART results with frozen oocytes: data from the Italian ART registry (2005–2013). Journal of Assisted Reproduction and Genetics, 33(1): 123–128.

Li, Q., He, H., Zhang, Y.-L., Li, X.-M., Guo, X., Huo, R., Bi, Y., Li, J., Fan, H. Y.& Sha, J. (2013). Phosphoinositide 3-Kinase p110δ mediates estrogen- and FSH-Stimulated ovarian follicle growth. *Molecular Endocrinology*, 27(9): 1468–1482.

Li, R., Phillips, D. M., & Mather, J. P. (1995). Activin promotes ovarian follicle development in vitro. *Endocrinology*, 136(3): 849–856.

Liu, R. H., Li, Y. H., Jiao, L. H., Wang, X. N., Wang, H., & Wang, W. H. (2002). Extracellular and intracellular factors affecting nuclear and cytoplasmic maturation of porcine oocytes collected from different sizes of follicles. *Zygote*, 10(3): 253–260.

Louro, R., Smirnova, A. S., & Verjovski-Almeida, S. (2009). Long intronic noncoding RNA transcription: Expression noise or expression choice? *Genomics*, 93(4):291–298.

Louro, R., El-Jundi, T., Nakaya, H. I., Reis, E. M., & Verjovski-Almeida, S. (2008). Conserved tissue expression signatures of intronic noncoding RNAs transcribed from human and mouse loci. *Genomics*, 92(1): 18–25.

Lu, T., Pan, Y., Kao, S. Y., Li, C., Kohane, I., Chan, J., & Yankner, B. A. (2004). Gene regulation and DNA damage in the ageing human brain. *Nature*, *429*(6994): 883–891.

Macaulay, A. D., Gilbert, I., Scantland, S., Fournier, E., Ashkar, F., Bastien, A., Saadi H.A., Gagné, D., Sirard, M. A., Khandjian É. W., Richard F. J., Hyttel, P., & Robert, C. (2016). Cumulus Cell Transcripts Transit to the Bovine Oocyte in Preparation for Maturation1. *Biology of Reproduction*, 94(1).

Madissoon, E., Jouhilahti, E. M., Vesterlund, L., Töhönen, V., Krjutškov, K., Petropoulous, S., Einarsdottir, E., Linnarsson, S., Lanner, F., Månsson, R., Hovatt, O., Bürglin, T. R., Katayama, S.& Kere, J. (2016). Characterization and target genes of nine human PRD-like homeobox domain genes expressed exclusively in early embryos. *Scientific Reports*, 6:28995.

Mandelbaum, J. (2000). Embryo and oocyte cryopreservation. Human Reproduction, 15(4): 43–47.

Mann, J. S., Lowther, K. M., & Mehlmann, L. M. (2010). Reorganization of the endoplasmic reticulum and development of Ca2+ release mechanisms during meiotic maturation of human oocytes. *Biology of Reproduction*, 83(4): 578–583.

Mao, L., Lou, H., Lou, Y., Wang, N., & Jin, F. (2014). Behaviour of cytoplasmic organelles and cytoskeleton during oocyte maturation. *Reproductive BioMedicine Online*, 28(3): 284–299.

Marchal, R., Vigneron, C., Perreau, C., Bali-Papp, A., & Mermillod, P. (2002). Effect of follicular size on meiotic and developmental competence of porcine oocytes. *Theriogenology*, 57(5: 1523–1532.

Marchese, F. P., Raimondi, I., & Huarte, M. (2017). The multidimensional mechanisms of long noncoding RNA function. *Genome Biology*, 18(1):206.

Marjani, S. L., Le Bourhis, D., Vignon, X., Heyman, Y., Everts, R. E., Rodriguez-Zas, S. L., Lewin, H. A. , Renard, J. P. , Yang, X., Tian, X. C. (2009). Embryonic gene expression profiling using microarray analysis. *Reproduction, Fertility and Development*, 21(1): 22–30.

Marteil, G., Richard-Parpaillon, L., & Kubiak, J. Z. (2009). Role of oocyte quality in meiotic maturation and embryonic development. *Reproductive Biology*, 9(3): 203–224.

Martínez, M., Obradors, A., Vernaeve, V., Santaló, J., & Vassena, R. (2016). Oocyte vitrification does not affect early developmental timings after intracytoplasmic sperm injection for women younger than 30 years old. *Molecular Reproduction and Development*, 83(7): 624–629.

Martins da Silva, S. J., Bayne, R. A. L., Cambray, N., Hartley, P. S., McNeilly, A. S., & Anderson, R. A. (2004). Expression of activin subunits and receptors in the developing human ovary: Activin A promotes germ cell survival and proliferation before primordial follicle formation. *Developmental Biology*, 266(2): 334–345.

Mascarenhas, M. N., Flaxman, S. R., Boerma, T., Vanderpoel, S., & Stevens, G. A. (2012). National, regional, and global trends in infertility prevalence since 1990: A systematic analysis of 277 health surveys. *PLoS Medicine*, 9(12).

Mattick, J. S., & Rinn, J. L. (2015). Discovery and annotation of long noncoding RNAs. *Nature Structural and Molecular Biology*, 22(1): 5–7.

Mattson, B. A., & Albertini, D. F. (1990). Oogenesis: Chromatin and microtubule dynamics during meiotic prophase. *Molecular Reproduction and Development*, 25(4): 374–383.

McCracken, S. A., Drury, C. L., Lee H. S., & Morris, J. M. (2003). Pregnancy is associated with suppression of the nuclear factor kappaB/IkappaB activation

pathway in peripheral blood mononuclear cells. *Journal of Reproductive Immunology,* 58(1): 27-47.

Medvedev, S., Pan, H., & Schultz, R. M. (2011). Absence of MSY2 in mouse oocytes perturbs oocyte growth and maturation, RNA stability, and the transcriptome. *Biology of Reproduction*, 85(3), 575–583.

Mehlmann, L. M. (2005). Stops and starts in mammalian oocytes: recent advances in understanding the regulation of meiotic arrest and oocyte maturation. *Reproduction, 130*(6): 791–799.

Mercer, T. R., Dinger, M. E., & Mattick, J. S. (2009). Long non-coding RNAs: Insights into functions. *Nature Reviews Genetics*, 10(3): 155–159.

Méreau, A., Sommer, C., Lerivray, H., Lesimple, M., & Hardy, S. (2007). Xenopus as a model to study alternative splicing in vivo. Biology of the Cell, 99(1): 55–65.

Metsalu, T., & Vilo, J. (2015). ClustVis: A web tool for visualizing clustering of multivariate data using Principal Component Analysis and heatmap. *Nucleic Acids Research*, 43(W1): W566–W570.

Mi, H., Huang, X., Muruganujan, A., Tang, H., Mills, C., Kang, D., & Thomas, P. D. (2017). PANTHER version 11: Expanded annotation data from Gene Ontology and Reactome pathways, and data analysis tool enhancements. *Nucleic Acids Research*, 45(D1): D183–D189.

Miao, Y. L., Kikuchi, K., Sun, Q. Y., & Schatten, H. (2009). Oocyte aging: Cellular and molecular changes, developmental potential and reversal possibility. *Human Reproduction Update*, 15(5): 573–585.

Modrek, B., & Lee, C. (2002). A genomic view of alternative splicing. *Nature Genetics*, 30(1):13–19.

Molinari, E., Patrizio, P., Pyle, A. M., & Bar, H. (2016). Transcriptome analysis of human cumulus cells reveals hypoxia as the main determinant of follicular senescence. *Molecular Human Reproduction*, 22(8): 566–576.

Montani, D. A., Braga, D. P. A. F., Borges, E. Jr, Camargo, M., Cordeiro, F.B., Pilau, E. J., Gozzo, F. C., Fraietta, R., & Lo Turco, E. G. (2019). Understanding mechanisms of oocyte development by follicular fluid lipidomics. Journal of Assisted Reproduction and Genetics.

Moon, J. H., Hyun, C. S., Lee, S. W., Son, W. Y., Yoon, S. H., & Lim, J. H. (2003). Visualization of the metaphase II meiotic spindle in living human oocytes using the polscope enables the prediction of embryonic developmental competence after ICSI. *Human Reproduction*, 18(4): 817–820.

Motola, S., Popliker, M., & Tsafriri, A. (2007). Are steroids obligatory mediators of luteinizing hormone/human chorionic gonadotropin-triggered resumption of meiosis in mammals? *Endocrinology*, 148(9): 4458–4465.

Motta, P. M., Nottola, S. A., Makabe, S., Heyn, R., & Jansen, R. (2000). Mitochondrial morphology in human fetal and adult female germ cells. *Human Reproduction*, 15(Suppl. 2): 129–147.

Nader, N., Courjaret, R., Dib, M., Kulkarni, R. P., & Machaca, K. (2016). Release from Xenopus oocyte prophase I meiotic arrest is independent of a decrease in cAMP levels or PKA activity. *Development*, 143(11): 1926–1936.

Navarro, P. A., de Araújo, M. M., de Araújo, C. M., Rocha, M., dos Reis, R., & Martins, W. (2009). Relationship between first polar body morphology before intracytoplasmic sperm injection and fertilization rate, cleavage rate, and embryo quality. *International Journal of Gynecology and Obstetrics*, 104(3): 226–229.

Necsulea, A., Soumillon, M., Warnefors, M., Liechti, A., Daish, T., Zeller, U., Baker, J. C., Grützner, F.,& Kaessmann, H. (2014). The evolution of lncRNA repertoires and expression patterns in tetrapods. *Nature*, 505(7485): 635–640.

Nicholas, B., Alberio, R., Fouladi-Nashta, A. A., & Webb, R. (2004). Relationship between low-molecular-weight insulin-like growth factor-binding proteins, caspase-3 activity, and oocyte quality. *Biology of Reproduction*, 72(4): 796–804.

O'Shea, L. C., Mehta, J., Lonergan, P., Hensey, C., & Fair, T. (2012). Developmental competence in oocytes and cumulus cells: Candidate genes and networks. *Systems Biology in Reproductive Medicine*, 58(2): 88–101.

Okino, S. T., Kong, M., Sarras, H., & Wang, Y. (2016). Evaluation of bias associated with high-multiplex, target-specific pre-amplification. *Biomolecular Detection and Quantification*, 6:13–21.

Oktay, K., Briggs, D., & Gosden, R. G. (1997). Ontogeny of follicle-stimulating hormone receptor gene expression in isolated human ovarian follicles. *Journal of Clinical Endocrinology and Metabolism*, 82(11): 3748–3751.

Oosterhuis, G. J. E., Vermes, I., Lambalk, C. B., Michgelsen, H. W. B., & Schoemaker, J. (1998). Insulin-like growth factor (IGF)-I and IGF binding protein-3 concentrations in fluid from human stimulated follicles. Human Reproduction, 13(2):285-289.

Palermo, R. (2007). Differential actions of FSH and LH during folliculogenesis. *Reproductive BioMedicine Online*, 15(3):326–337.

Pan, H., Ma, P., Zhu, W., & Schultz, R. M. (2008). Age-associated increase in aneuploidy and changes in gene expression in mouse eggs. *Developmental Biology*, 316(2): 397–407.

Parks, J. C., Patton, A. L., McCallie, B. R., Griffin, D. K., Schoolcraft, W. B., & Katz-Jaffe, M. G. (2016). Corona cell RNA sequencing from individual oocytes revealed transcripts and pathways linked to euploid oocyte competence and live birth. *Reproductive BioMedicine Online*, 32(5): 518–526.

Parmegiani, L., Cognigni, G. E., Bernardi, S., Cuomo, S., Ciampaglia, W., Infante, F. E., Tabarelli de Fatisa, C., Arnonea, A., Maccarini, A. M., & Filicori, M. (2011). Efficiency of aseptic open vitrification and hermetical cryostorage of human oocytes. *Reproductive BioMedicine Online*, 23(4): 505–512.

Patel, O. V., Bettegowda, A., Ireland, J. J., Coussens, P. M., Lonergan, P., & Smith, G. W. (2007). Functional genomics studies of oocyte competence: Evidence that reduced transcript abundance for follistatin is associated with poor developmental competence of bovine oocytes. *Reproduction*, 133(1): 95–106.

Paynton, B. V., Rempel, R., & Bachvarova, R. (1988). Changes in state of adenylation and time course of degradation of maternal mRNAs during oocyte maturation and early embryonic development in the mouse. *Developmental Biology*, 129(2): 304–314.

Pelosi, E., Forabosco, A., & Schlessinger, D. (2015). Genetics of the ovarian reserve. *Frontiers in Genetics*, 6:308.

Perniss, A., Preiss, K., Nier, M., & Althaus, M. (2017). Hydrogen sulfide stimulates CFTR in Xenopus oocytes by activation of the cAMP/PKA signalling axis. *Scientific Reports*, *7*(1):3517.

Picton, H., Briggs, D., & Gosden, R. (1998). The molecular basis of oocyte growth and development. *Molecular and Cellular Endocrinology*, 145(1–2): 27–37.

Piñero-Sagredo, E., Nunes, S., De Los Santos, M. J., Celda, B., & Esteve, V. (2010). NMR metabolic profile of human follicular fluid. *NMR in Biomedicine*, 23(5): 485–495.

Qiao, J., Wang, Z. B., Feng, H. L., Miao, Y. L., Wang, Q., Yu, Y., Wei, Y.C., Yan, J., Wang, W. H., Shen, W., Sun, S.C., Schatten, H., & Sun, Q. Y. (2014). The root of reduced fertility in aged women and possible therapentic options: Current status and future perspects. *Molecular Aspects of Medicine*, 38: 54–85.

Qiu, J., Ren, Z., & Yan, J. (2016). Identification and functional analysis of long non-coding RNAs in human and mouse early embryos based on single-cell transcriptome data. *Oncotarget*, *7*(38):61215-61228.

Raju, G. R., Prakash, G., Krishna, K., & Madan, K. (2010). Meiotic spindle and zona pellucida characteristics as predictors of embryonic development: a preliminary study using PolScope imaging. *Reproductive BioMedicine Online*, 14(2): 166–174.

Rienzi, L., Romano, S., Albricci, L., Maggiulli, R., Capalbo, A., Baroni, E., Colamaria, S., Sapienza, F., & Ubaldi, F. (2010). Embryo development of fresh 'versus' vitrified metaphase II oocytes after ICSI: a prospective randomized sibling-oocyte study. *Human Reproduction*, 25(1): 66–73.

Rienzi, L., Ubaldi, F. M., Iacobelli, M., Minasi, M. G., Romano, S., Ferrero, S., Sapienza, F., Baroni, E., Litwicka, K.,& Greco, E. (2008). Significance of metaphase II human oocyte morphology on ICSI outcome. *Fertility and Sterility*, 90(5): 1692–1700.

Rienzi, L., Ubaldi, F., Giulia Minasi, M., Iacobelli, M., Martinez, F., Tesarik, J., & Greco, E. (2003). Blastomere cytoplasmic granularity is unrelated to developmental potential of day 3 human embryos. *Journal of Assisted Reproduction and Genetics*, 20(8): 314–317.

Rinn, J. L., & Chang, H. Y. (2012). Genome regulation by long noncoding RNAs. *Annual Review of Biochemistry*, 81: 145–166.

Rinn, J. L., Euskirchen, G., Bertone, P., Martone, R., Luscombe, N. M., Hartman, S., Harrison, P. M., Nelson, F. K., Miller, P., Gerstein, M., Weissman, S., & Snyder, M. (2003). The transcriptional activity of human chromosome 22. *Genes and Development*, 17(4): 529–540.

Rodriguez, K. F., & Farin, C. E. (2004). Gene transcription and regulation of oocyte maturation. *Reproduction, Fertility and Development*, *16*(1-2): 55-67

Rodwell, G. E. J., Sonu, R., Zahn, J. M., Lund, J., Wilhelmy, J., Wang, L., Xiao, W., Mindrinos, M., Crane, E., Segal, E., Myers B. D., Brooks J. D., Davis, W. R., Higgins, J., Owen, A. B., & Kim, S. K. (2004). A transcriptional profile of aging in the human kidney. *PLoS Biology*, 2(12).

Roovers, E. F., Rosenkranz, D., Mahdipour, M., Han, C. T., He, N., de Sousa Lopes, S. M. C., Van der Westerlaken, L. A., Zischler, H., Butter, F., Roelen ,B. A.,& Ketting, R. F. (2015). Piwi proteins and piRNAs in Mammalian Oocytes and early embryos. *Cell Reports*, 10(12): 2069–2082.

Rosen, M. P., Shen, S., Dobson, A. T., Rinaudo, P. F., McCulloch, C. E., & Cedars, M. I. (2008). A quantitative assessment of follicle size on oocyte developmental competence. *Fertility and Sterility*, 90(3): 684–690.

Rosenbusch, B., Schneider, M., Gläser, B., & Brucker, C. (2002). Cytogenetic analysis of giant oocytes and zygotes to assess their relevance for the development of digynic triploidy. *Human Reproduction*, 17(9): 2388–2393.

Roy, A. K., Oh, T., Rivera, O., Mubiru, J., Song, C. S., & Chatterjee, B. (2002). Impacts of transcriptional regulation on aging and senescence. *Ageing Research Reviews*, 1(3): 367–380.

Ruebel, M. L., Schall, P. Z., Midic, U., Vincent, K. A., Goheen, B., & Vandevoort, C. A. (2018). Transcriptome analysis of rhesus monkey failed-to-mature oocytes: Deficiencies in transcriptional regulation and cytoplasmic maturation of the oocyte mRNA population. *Molecular Human Reproduction*, 24(10): 478–494.

Salisbury, J., Hutchison, K. W., Wigglesworth, K., Eppig, J. J., & Graber, J. H. (2009). Probe-level analysis of expression microarrays characterizes isoform-specific degradation during mouse oocyte maturation. *PLoS ONE*, 4(10).

Sánchez, F., & Smitz, J. (2012). Molecular control of oogenesis. *Biochimica et Biophysica Acta*, 1822(12):1896–1912.

Santonocito, M., Guglielmino, M. R., Vento, M., Ragusa, M., Barbagallo, D., Borzì, P., Casciano, I., Scollo, P., Romani, M., Tatone, C., Purrello, M., & Di Pietro, C. (2013). The apoptotic transcriptome of the human MII oocyte: Characterization and age-related changes. *Apoptosis*, 18(2): 201–211.

Sathananthan, A. H., Selvaraj, K., & Trounson, A. (2000). Fine structure of human oogonia in the foetal ovary. *Molecular and Cellular Endocrinology*, 161(1–2): 3–8.

Sathananthan, A. H. (1994). Ultrastructural changes during meiotic maturation in mammalian oocytes: Unique aspects of the human oocyte. *Microscopy Research and Technique*, 27(2): 145–164.

Sathananthan, H., Pera, M., & Trounson, A. (2002). The fine structure of human embryonic stem cells. *Reproductive Biomedicine Online*, 4(1): 56–61.

Senger, P. L. (2012). Pathways to pregnancy & parturition. In Pathways to pregnancy and parturition.

Sharp, D. J., & Ross, J. L. (2012). Microtubule-severing enzymes at the cutting edge. *Journal of Cell Science*, 125(11): 2561–2569.

Shen, X., Liu, X., Zhu, P., Zhang, Y., Wang, J., Wang, Y., Wang, W., Liu, J., Li, N., Liu, F. (2017). Proteomic analysis of human follicular fluid associated with successful in vitro fertilization. *Reproductive Biology and Endocrinology*, 15(1):58.

Shen, Y., Stalf, T., Mehnert, C., De Santis, L., Tinneberg, H. R., & Eichenlaub-Ritter, U. (2006). Light retardance by human oocyte spindle is positively related to pronuclear score after ICSI. *Reproductive BioMedicine Online*, 12(6): 737–751.

Shiraki, T., Kondo, S., Katayama, S., Waki, K., Kasukawa, T., Kawaji, H., Kodzius, R., Watahiki, A., Nakamura, M., Arakawa, T., Fukuda, S., Sasaki, D., Podhajska, A., Harbers, M., Kawai, J., Carninci, P., & Hayashizaki, Y. (2003). Cap analysis gene expression for high-throughput analysis of transcriptional starting point and identification of promoter usage. *Proceedings of the National Academy of Sciences*, 100(26): 15776–15781.

Shirazi, A., Naderi, M. M., Hassanpour, H., Heidari, M., Borjian, S., Sarvari, A., & Akhondi, M. M. (2016). The effect of ovine oocyte vitrification on expression of subset of genes involved in epigenetic modifications during oocyte maturation and early embryo development. *Theriogenology*, 86(9): 2136–2146.

Siomi, M. C., Sato, K., Pezic, D., & Aravin, A. A. (2011). PIWI-interacting small RNAs: The vanguard of genome defence. *Nature Reviews Molecular Cell Biology*, 12(4): 246–258.

Sirard, M. A., Richard, F., Blondin, P., & Robert, C. (2006). Contribution of the oocyte to embryo quality. *Theriogenology*, 65(1): 126–136.

Skiadas, C. C., Duan, S., Correll, M., Rubio, R., Karaca, N., Ginsburg, E. S., Quackenbush, J., & Racowsky, C. (2012). Ovarian reserve status in young women is associated with altered gene expression in membrana granulosa cells. *Molecular Human Reproduction*, 18(7): 362–371.

Slotte, H., Gustafson, O., Nylund, L., & Pousette, A. (1990). ATP and ADP in human pre-embryos. *Human Reproduction*, 5(3): 319–322.

Sorensen, R. A., & Wassarman, P. M. (1976). Relationship between growth and meiotic maturation of the mouse oocyte. *Developmental Biology*, 50(2): 531–536.

Steuerwald, N. M., Bermúdez, M. G., Wells, D., Munné, S., & Cohen, J. (2007). Maternal age-related differential global expression profiles observed in human oocytes. *Reproductive BioMedicine Online*, 14(6): 700–708.

Stojkovic, M., Machado, S. A., Stojkovic, P., Zakhartchenko, V., Hutzler, P., Gonçalves, P. B., & Wolf, E. (2001). Mitochondrial distribution and adenosine triphosphate content of bovine oocytes before and after in vitro maturation: Correlation with morphological criteria and developmental capacity after in vitro fertilization and culture. *Biology of Reproduction*, 64(3): 904–909.

Stoop, D., Cobo, A., & Silber, S. (2014). Fertility preservation for age-related fertility decline. *The Lancet*, 384(9950):1311–1319.

Su, Y. Q., Sugiura, K., Woo, Y., Wigglesworth, K., Kamdar, S., Affourtit, J., & Eppig, J. J. (2007). Selective degradation of transcripts during meiotic maturation of mouse oocytes. *Developmental Biology*, 302(1), 104–117.

Sugiura, K., Pendola, F. L., & Eppig, J. J. (2005). Oocyte control of metabolic cooperativity between oocytes and companion granulosa cells: Energy metabolism. *Developmental Biology*, 279(1): 20–30.

Sun, Q.-Y., & Schatten, H. (2006). Regulation of dynamic events by microfilaments during oocyte maturation and fertilization. *Reproduction*, 131(2): 193–205.

Sun, Q. Y., Wu, G. M., Lai, L., Park, K. W., Cabot, R., Cheong, H. T., Day, B. N., & Schatten, H. (2001). Translocation of active mitochondria during pig oocyte maturation, fertilization and early embryo development in vitro. *Reproduction*, 122(1): 155–163.

Sylvestre, E. L., Robert, C., Pennetier, S., Labrecque, R., Gilbert, I., Dufort, I., Léveillé, M. C.,& Sirard, M. A. (2013). Evolutionary conservation of the oocyte transcriptome among vertebrates and its implications for understanding human reproductive function. *Molecular Human Reproduction*, 19(6): 369–379.

Tang, F., Barbacioru, C., Nordman, E., Bao, S., Lee, C., Wang, X., Tuch, B. B., Heard, E., Lao, K., & Surani, M. A. (2011). Deterministic and stochastic allele specific gene expression in single mouse blastomeres. *PLoS ONE*, 6(6).

Taylor, D. H., Chu, E. T. J., Spektor, R., & Soloway, P. D. (2015). Long non-coding RNA regulation of reproduction and development. *Molecular Reproduction and Development*, 82(12): 932–956.

Te Velde, E. R., & Pearson, P. L. (2002). The variability of female reproductive ageing. *Human Reproduction Update*, 8(2): 141–154.

Ten, J., Mendiola, J., Vioque, J., de Juan, J., & Bernabeu, R. (2007). Donor oocyte dysmorphisms and their influence on fertilization and embryo quality. *Reproductive BioMedicine Online*, 14(1): 40–48.

Theurkauf, W. E., Smiley, S., Wong, M. L., & Alberts, B. M. (1992). Reorganization of the cytoskeleton during Drosophila oogenesis: implications for axis specification and intercellular transport. *Development*,115(4): 923–936.

Tian, H., Hammer, R. E., Matsumoto, A. M., Russell, D. W., & McKnight, S. L. (1998). The hypoxia-responsive transcription factor EPAS1 is essential for catecholamine homeostasis and protection against heart failure during embryonic development. *Genes and Development*, *12*(21): 3320–3324.

Tremoleda, J. L., Schoevers, E.J., Stout, T.A.E., Colenbrander, B., & Bevers, M.M. (2001). Organisation of the cytoskeleton during in vitro maturation of horse oocytes. *Molecular Reproduction and Development*, 60(2):260-269.

Trokoudes, K. M., Pavlides, C., & Zhang, X. (2011). Comparison outcome of fresh and vitrified donor oocytes in an egg-sharing donation program. *Fertility and Sterility*, 95(6): 1996–2000.

Tüttelmann, F., Ivanov, P., Dietzel, C., Sofroniou, A., Tsvyatkovska, T. M., Komsa-Penkova, R. S., Markoff, A., Wieacker, P., & Bogdanova, N. (2013). Further insights into the role of the annexin A5 M2 haplotype as recurrent pregnancy loss factor, assessing timing of miscarriage and partner risk. *Fertility and Sterility*, 100(5): 1321–1325.

Ubaldi, F. M., Cimadomo, D., Vaiarelli, A., Fabozzi, G., Venturella, R., Maggiulli, R., Mazzilli, R., Ferrero, S., Palagiano, A., & Rienzi, L. (2019). Advanced maternal age in IVF: Still a challenge? The present and the future of its treatment. *Frontiers in Endocrinology*, 10:94.

Uyar, A., Torrealday, S., & Seli, E. (2013). Cumulus and granulosa cell markers of oocyte and embryo quality. *Fertility and Sterility*, *99*(4): 979–997.

Vallée, M., Robert, C., Méthot, S., Palin, M. F., & Sirard, M. A. (2006). Cross-species hybridizations on a multi-species cDNA microarray to identify evolutionarily conserved genes expressed in oocytes. *BMC Genomics*, 7:113.

Van Moerbeke, M., Kasim, A., & Shkedy, Z. (2018). The usage of exon-exon splice junctions for the detection of alternative splicing using the REIDS model. *Scientific Reports*, *8*(1):8331.

Van Montfoort, A. P., Geraedts, J. P., Dumoulin, J. C., Stassen, A. P., Evers, J. L., & Ayoubi, T. A. (2008). Differential gene expression in cumulus cells as a prognostic indicator of embryo viability: A microarray analysis. *Molecular Human Reproduction*, 14(3): 157–168.

Vandesompele, J., De Preter, K., Pattyn, F., Poppe, B., Van Roy, N., De Paepe, A., & Speleman, F. (2002). Accurate normalization of real-time quantitative RT-PCR data by geometric averaging of multiple internal control genes. *Genome Biology*, 3(7).

Vassena, R., Boue, S., Gonzalez-Roca, E., Aran, B., Auer, H., Veiga, A., & Belmonte, J. C. I. (2011). Waves of early transcriptional activation and pluripotency program initiation during human preimplantation development. *Development*, 138(17): 3699–3709.

Vassena, R., Han, Z., Gao, S., Baldwin, D. A., Schultz, R. M., & Latham, K. E. (2007). Tough beginnings: Alterations in the transcriptome of cloned embryos during the first two cell cycles. *Developmental Biology*, 304(1): 75–89.

Verlinsky, Y., Lerner, S., Illkevitch, N., Kuznetsov, V., Kuznetsov, I., Cieslak, J., & Kuliev, A. (2003). Is there any predictive value of first polar body

morphology for embryo genotype or developmental potential? *Reproductive BioMedicine Online*, 7(3): 336–341.

Vigneault, C., Gravel, C., Vallée, M., McGraw, S., & Sirard, M. A. (2009). Unveiling the bovine embryo transcriptome during the maternal-to-embryonic transition. *Reproduction*, 137(2): 245–257.

Virant-Klun, I., Knez, K., Tomazevic, T., & Skutella, T. (2013). Gene expression profiling of human oocytes developed and matured in vivo or in vitro. BioMed Research International, 2013:879489.

Volders, P. J., Verheggen, K., Menschaert, G., Vandepoele, K., Martens, L., Vandesompele, J., & Mestdagh, P. (2015). An update on LNCipedia: A database for annotated human lncRNA sequences. *Nucleic Acids Research*, *43*: D174–D180.

Wallace, W. H. B., & Kelsey, T. W. (2010). Human ovarian reserve from conception to the menopause. *PLoS One*, 5(1).

Wang, D., Zhang, Z., O'Loughlin, E., Lee, T., Houel, S., O'Carroll, D., Tarakhovsky, A., Ahn, N.,& Yi, R. (2012). Quantitative functions of argonaute proteins in mammalian development. *Genes and Development*, 26(7): 693–704.

Wang, E. T., Sandberg, R., Luo, S., Khrebtukova, I., Zhang, L., Mayr, C., Kingsmore, S. F., Burge, C. B. (2008). Alternative isoform regulation in human tissue transcriptomes. *Nature*, 456(7221): 470–476.

Wang, Q., & Sun, Q. Y. (2007). Evaluation of oocyte quality: Morphological, cellular and molecular predictors. *Reproduction, Fertility and Development*, 19(1):1–12.

Wang, W. H., Meng, L., Hackett, R. J., Odenbourg, R., & Keefe, D. L. (2001). The spindle observation and its relationship with fertilization after intracytoplasmic sperm injection in living human oocytes. *Fertility and Sterility*, 75(2): 348–353.

Wang, Z., Gerstein, M., & Snyder, M. (2009). RNA-Seq: A revolutionary tool for transcriptomics. *Nature Reviews. Genetics*, 10(1): 57–63.

Watson, A. J. (2007). Oocyte cytoplasmic maturation: a key mediator of oocyte and embryo developmental competence. *Journal of Animal Science*, 85(Suppl. 13): E1-3.

Winston, N., Johnson, M., Pickering, S., & Braude, P. (1991). Parthenogenetic activation and development of fresh and aged human oocytes. *Fertility and Sterility*, 56(5): 904–912.

Wong, P. C., Balmaceda, J. P., Blanco, J. D., Gibbs, R. S., & Asch, R. H. (1986). Sperm washing and swim-up technique using antibiotics removes microbes from human semen. *Fertility and Sterility*, 45(1): 97–100.

World Health Organization. (2010). WHO laboratory manual for the examination of human semen and sperm-cervical mucus interaction. Published on behalf of the World Health Organization by Cambridge University Press, Cambridge, UK ; New York, NY. x, 128 p. pp

World Medical, A. (2013). World Medical Association Declaration of Helsinki: ethical principles for medical research involving human subjects. JAMA.

Wu, T., & Du, Y. (2017). LncRNAs: From basic research to medical application. *International Journal of Biological Sciences*, 13(3):295–307.

Xia, P. (1997). Intracytoplasmic sperm injection: Correlation of oocyte grade based on polar body, perivitelline space and cytoplasmic inclusions with fertilization rate and embryo quality. *Human Reproduction*, 12(8): 1750–1755.

Xia, P., & Younglai, E. V. (2000). Relationship between steroid concentrations in ovarian follicular fluid and oocyte morphology in patients undergoing intracytoplasmic sperm injection (ICSI) treatment. *Journal of Reproduction and Fertility*, 118(2): 229–233.

Xu, X. F., Li, J., Cao, Y. X., Chen, D. W., Zhang, Z. G., He, X. J., Ji, D. M., & Chen, B. L. (2015). Differential expression of long noncoding RNAs in human cumulus cells related to embryo developmental potential: A microarray analysis. *Reproductive Sciences*, 22(6): 672–678.

Xue, Z., Huang, K., Cai, C., Cai, L., Jiang, C. Y., Feng, Y., Liu, Z., Zeng, Q., Cheng, L., Sun, Y. E., Liu, J. Y., Horvath, S., & Fan, G. (2013). Genetic programs in human and mouse early embryos revealed by single-cell RNA sequencing. *Nature*, 500(7464): 593–597.

Yamoto, M., Shima, K., & Nakano, R. (1992). Gonadotropin receptors in human ovarian follicles and corpora lutea throughout the menstrual cycle. *Hormone Research in Paediatrics*, *37*(Suppl. 1): 5–11.

Yan, L., Yang, M., Guo, H., Yang, L., Wu, J., Li, R., Liu, P., Lian, Y., Zheng, X., Yan, J., Huang, J., Li, M., Wu, X., Wen, L., Lao, K., Li, R., Qiao, J.,& Tang,, F. (2013). Single-cell RNA-Seq profiling of human preimplantation embryos and embryonic stem cells. *Nature Structural and Molecular Biology*, 20(9): 1131–1139.

Yerushalmi, G. M., Salmon-Divon, M., Yung, Y., Maman, E., Kedem, A., Ophir, L., Elemento, O., Coticchio, G., Dal Canto, M., Mignini Renzinu, M., Fadini, R., & Hourvitz, A. (2014). Characterization of the human cumulus cell transcriptome during final follicular maturation and ovulation. *Molecular Human Reproduction*, 20(8): 719–735.

Yeste, M., Jones, C., Amdani, S. N., Patel, S., & Coward, K. (2016). Oocyte activation deficiency: A role for an oocyte contribution? Human Reproduction Update, 22(1): 23–47.

Yoshida, H., Takakura, N., Kataoka, H., Kunisada, T., Okamura, H., & Nishikawa, S. I. (1997). Stepwise requirement of c-kit tyrosine kinase in mouse ovarian follicle development. *Developmental Biology*, 184(1): 122–137.

Younis, J. S., Ben-Ami, M., & Ben-Shlomo, I. (2015). The Bologna criteria for poor ovarian response: A contemporary critical appraisal. *Journal of Ovarian Research*, 8(1):76.

Zamah, A. M., Hassis, M. E., Albertolle, M. E., & Williams, K. E. (2015). Proteomic analysis of human follicular fluid from fertile women. *Clinical Proteomics*, 12(1):5.

Zhang, D., Rogers, G. C., Buster, D. W., & Sharp, D. J. (2007). Three microtubule severing enzymes contribute to the "Pacman- flux" machinery that moves chromosomes. *Journal of Cell Biology*, 177(2): 231–242.

Zhang, M., & Xia, G. (2012). Hormonal control of mammalian oocyte meiosis at diplotene stage. *Cellular and Molecular Life Sciences*, 69(8): 1279–1288.

Zhang, X., Jafari, N., Barnes, R. B., Confino, E., Milad, M., & Kazer, R. R. (2005). Studies of gene expression in human cumulus cells indicate pentraxin 3 as a possible marker for oocyte quality. *Fertility and Sterility*, *83*(Suppl. 4), 1169–1179.

Zhao, J., & Li, Y. (2012). Adenosine triphosphate content in Human unfertilized oocytes, undivided zygotes and embryos unsuitable for transfer or cryopreservation. *Journal of International Medical Research*, *40*(2): 734–739.

8. ANNEX

Annex-table 1: Lists of differentially regulated transcripts in human MII oocytes in relation to age and ovarian reserve and referred to Venn diagrams shown in figure 20. Subheading of lists indicate those transcripts differentially regulated on each group comparison. Accession number is always provided, while gene symbol is provided when available. Empty cells indicate that no differences were found. ↑ increased; ↓ decreased. #N/A: This identifier is not in the current EnsEMBL database.

YH in comparison with:			**OH**		**YL**		**OL**	
Transcript type	**Gene Symbol**	**Accession number**	**Fold Change (linear)**	**ANOVA p-value**	**Fold Change (linear)**	**ANOVA p-value**	**Fold Change (linear)**	**ANOVA p-value**
lincRNA	RP11-47P18.1	ENSG00000242828	↑ 2.52	0.029623	↑ 2.92	0.003432	↑ 3.4	0.004929
lncRNA	KRTAP6-1	ENSG00000184724	↑ 2.42	0.044544	↑ 2.32	0.042389	↑ 2.16	0.031147
piRNA-c	piR-47032	DQ578920	↑ 7.56	0.024394	↑11.12	0.041644		
lincRNA	RP11-123H22.1	ENSG00000234551	↑ 3.02	0.008146			↑ 2.34	0.049945
Pre-miRNA	hsa-mir-1260A	NR_031661	↓ 8.25	0.00238			↓ 3.13	0.042228
Structural RNA	RNA5SP107	ENSG00000223290			↑ 2.56	0.026093	↑ 2.16	0.024196
lincRNA	linc-PTPRQ-7	ENSG00000165899			↑ 2.25	0.026623	↑ 3.12	0.002154
lncRNA	LOC148709	NR_002929	↑ 2.1	0.049343				
lncRNA	RTCA-AS1	ENSG00000224616	↓ 2.49	0.023644				
lincRNA		ENSG00000231420	↑ 2.03	0.005605				
piRNA-c	piR-47548	DQ579436	↓ 7.61	0.048727				
piRNA-c	piR-55001	DQ587889	↓ 2.97	0.036551				
lincRNA	linc-ROBO1-3	TCONS_00003576	↑ 2.07	0.004328				
mRNA	IL9	NM_000590	↑ 2.39	0.024509				
lncRNA	RP11-72L22.1	ENSG00000249061	↑ 2.23	0.042053				
lncRNA		S63356	↑ 3.18	0.013927				
lncRNA		DQ409330	↓ 2.46	0.010566				
lincRNA	linc-SLC25A37	ENSG00000253390	↑2.22	0.008041				
lincRNA	linc-STX17	NONHSAG053035.2	↓ 3.27	0.029352				
piRNA-c		FU270201	↑ 2.4	0.044695				
lncRNA	CTD-2026G22.1	ENSG00000255532	↑ 3.29	0.022979				
lncRNA	lnc-FOLR1	U78793	↓ 2.54	0.034802				
mRNA	STYK1	NM_018423	↓ 2.53	0.046367				
Pre-miRNA	hsa-mir-4311	NR_036196	↓ 2.83	0.040386				
Structural RNA	RNU7-111P	ENSG00000252645	↓ 2.24	0.030336				
Pre-miRNA	hsa-mir-744	NR_030613	↑ 2.21	0.028955				
Structural RNA	SNORD4B	NR_000009	↓ 4.21	0.031762				
lncRNA	CTD-3035K23.7	ENSG00000274565	↓ 3.15	0.023451				

lincRNA	linc-ZNF606	NONHSAG026698.2	↓ 2.58	0.02424				
lncRNA		AY789479	↓ 2.35	0.049014				
lncRNA	lnc-TOR3A-1:1	ENSG00000228449					↑ 2.22	0.039554
lincRNA	RP11-145M4.1	ENSG00000241042					↑ 3.61	0.011048
lncRNA	KCNC4-AS1	ENSG00000224965					↑ 2.74	0.003828
lncRNA	linc-ALX3-1	NONHSAG002370.2					↑ 2.81	0.004033
lincRNA	linc-ADSS	NONHSAG004855.2					↑ 2.07	0.027123
mRNA	FIGN	NM_018086					↓ 2.64	0.009109
lincRNA	linc-ASAP2-1						↑ 2.13	0.009773
lncRNA	RP11-894J14.2	OTTHUMG00000159046					↑ 2.02	0.021582
lincRNA	linc-CLDN16						↓ 2.01	0.0396
mRNA	ANXA5	NM_001154					↑ 2.61	0.007953
lncRNA	lnc-ANXA5	NONHSAG038790.2					↑ 5.2	0.003713
Pre-miRNA	piR-36165	DQ598099					↓ 3.79	0.033283
Structural RNA	SNORD123	NR_003689					↑ 2.27	0.013761
Pre-miRNA	piR-53770	DQ586658					↓ 2.39	0.006177
Pre-miRNA	piR-53770	DQ586658					↓ 2.39	0.006177
Pre-miRNA	piR-53770	DQ586658					↓ 2.39	0.006177
Pre-miRNA	piR-53770	DQ586658					↓ 2.39	0.006177
lncRNA	ADCYAP1R1	AY495951					↓ 2.42	0.01049
mRNA	GEM	NM_181702					↓ 2.21	0.024079
mRNA	NCS1	NM_014286					↑ 2.01	0.003182
lncRNA	PRRG1	BC030786					↓ -2.2	0.027357
lncRNA	lnc-IKBKG	ENSG00000073009					↑ 3.11	0.041305
lincRNA	RP11-95I16.2	ENSG00000227307					↑ 2.05	0.03496
lincRNA	linc-ARHGAP20-3	NONHSAG063627.1					↑ 2.01	0.01288
Structural RNA	RNY5	NR_001571					↓ 7.58	0.000989
lncRNA	ARL6IP4	EF036485					↑ 2.04	0.033876
lncRNA	SMUG1	NR_045039					↑ 2.15	0.009709
lncRNA	USP12-AS2	ENSG00000230641					↓ 2.39	0.007861
lincRNA	LINC00363	ENSG00000232849					↑ 2.7	0.019468
lincRNA	linc-RPL21-1	ENSG00000230641					↓ 2.39	0.009128
mRNA	IGHV3-38	ENSG00000211958					↓ 8.03	0.018696
Pre-miRNA	piR-52545	DQ585433					↑ 2.84	0.025932
lincRNA	linc-C15orf2-10	NONHSAG016287.2					↓ 2.44	0.01897
lincRNA	lnc-ATF7IP2-1:1	ENSG00000256013					↓ 2.18	0.034688

mRNA	IGHV3OR16-9	ENSG00000270472					↓ 3.24	0.046792
Structural RNA		GQ233007					↓ 3.4	0.049199
Pre-miRNA	hsa-mir-548W	NR_036146					↑ 2.66	0.015916
lncRNA		AB010099					↓ 2.24	0.025952
mRNA	SPATC1L	NM_001142854					↑ 2.01	0.000565
lncRNA	DUXAP10	BC017398					↑ 2.18	0.021777
mRNA	MAP1LC3C	NM_001004343			↑ 2.88	0.001811		
lncRNA	RP11-452F19.3	ENSG00000228106			↑ 2.39	0.042063		
lincRNA	linc-POU3F1-1	NONHSAG001091.2			↓ 3.11	0.042026		
lincRNA	lincRNA	NONHSAT071277.2			↑ 3.57	0.031185		
lncRNA	EAF1-AS1	ENSG00000249786			↓ 2.51	0.007154		
lncRNA	lnc-DAZL-1:1	ENSG00000229271			↑ 2.52	0.030868		
lncRNA	5'UTR-PPARG	AB097931			↑ 2.07	0.033168		
lincRNA	linc-GALNTL6-4	NONHSAG087990			↑ 2.41	0.020265		
lincRNA	CTB-78F1.2	ENSG00000253357			↓ 2.53	0.019246		
piRNA-c	piR-45204	DQ577092			↓ 4.18	0.003178		
piRNA-c	piR-34994	DQ596928			↑ 3.06	0.02985		
lincRNA	AC003092.1	ENSG00000236453			↑ 4.89	0.015675		
lincRNA	AC019117.2	ENSG00000236039			↓ 2.9	0.035676		
lincRNA	linc-COL1A2-2				↑ 3.46	0.023963		
mRNA	TSPYL5	NM_033512			↑ 2.53	0.018673		
piRNA-c	piR-51084	DQ583972			↑ 2.03	0.026864		
lncRNA	PCAT7	ENSG00000231806			↑ 7.39	0.033025		
mRNA	APEX2	NM_014481			↑ 2.09	0.009621		
mRNA	GPR119	ENSG00000147262			↑ 2.68	0.028598		
piRNA-c	piR-44914	DQ576802			↓ 2.16	0.021604		
mRNA	ACTN3	NM_001104			↓ 3.26	0.011928		
lncRNA	RP11-809N8.2-001	ENSG00000256928			↓ 2.11	0.001011		
lncRNA		AJ488208			↑ 2.01	0.024789		
lncRNA	lnc-OSBPL5	AF331964			↑ 2.18	0.024858		
Structural RNA	RN7SL796P	ENSG00000277031			↑ 2.27	0.040695		
Structural RNA	RN7SL495P	ENSG00000277515			↑ 2.27	0.040695		
Structural RNA	RN7SL719P	ENSG00000274632			↑ 2.54	0.041823		
Structural RNA	RN7SL673P	ENSG00000273818			↑ 2.58	0.028508		

Structural RNA	RN7SL539P	ENSG00000274076			↑ 2.22	0.048936		
Structural RNA	RN7SL82P	ENSG00000278696			↑ 2.58	0.028508		
lncRNA	lnc-AVEN-1:1	NONHSAG016476.2			↓ 2.81	0.049575		
lncRNA	lnc-MEIS2-4:1	NONHSAG016539.2			↓ 2.54	0.019191		
piRNA-c	piR-58740	DQ591628			↓ 3.98	0.014528		
lincRNA	linc-ARRDC4-3	NONHSAG018046.2			↑ 2.66	0.011166		
Pre-miRNA		ENSG00000239174			↑ 3.82	0.049038		
mRNA	TEX19	ENSG00000182459			↓ 3.58	0.007438		
mRNA	CXCL16	NM_022059			↑ 2.06	0.007226		
mRNA	NAT9	NM_015654			↑ 2.22	0.021793		
lncRNA	lnc-SKA2	FJ648812			↓ 2.47	0.003701		
lincRNA	linc-KCNG2	NONHSAG024254.2			↓ 2.36	0.037521		
piRNA-c	piR-36520	DQ598454			↑ 3.59	0.016361		
lincRNA	linc-NDUFV3-1	XLOC_013957			↓ 2.12	0.000188		
OH in comparison with:			**YH**		**YL**		**OL**	
Transcript type	**Gene Symbol**	**Accession number**	**Fold Change (linear)**	**ANOVA p-value**	**Fold Change (linear)**	**ANOVA p-value**	**Fold Change (linear)**	**ANOVA p-value**
lncRNA		U78793	↑ 2.54	0.034802	↑ 2.95	0.015619	↑ 2.86	0.004673
lincRNA	linc-STX17	NONHSAG053035.2	↑ 3.27	0.029352	↑ 2.33	0.026879		
lncRNA	CTD-2026G22.1	ENSG00000255532	↓ 3.29	0.022979	↓ 3.92	0.006987		
lincRNA	linc-ZNF606	NONHSAG026698.2	↑ 2.58	0.02424	↑ 2.33	0.017991		
lncRNA	CTD-3035K23.7	ENSG00000274565	↑ 3.15	0.023451			↑ 3.44	0.011241
mRNA	CLEC4A	NM_016184			↑ 2.05	0.039821	↑ 2.17	0.002245
lncRNA	lnc-CC2D1B	NONHSAG001475.2			↑ 2.01	0.013376		
lncRNA	RP11-480I12	BC038775			↓ 2.2	0.019611		
lncRNA	EAF1-AS1-008	ENSG00000249786			↓ 2.12	0.041871		
lincRNA	RP11-180C1	ENSG00000250038			↑ 3.4	0.021102		
lincRNA	linc-GALNTL6-4	NONHSAG087990			↑ 2.82	0.01207		
lncRNA		AF049126			↓ 2.08	0.012945		
lincRNA	CTC-480C2.1	ENSG00000250874			↑ 2.18	0.003406		
lncRNA		AF086511			↑ 2.27	0.024715		
lincRNA	linc-FAM169A	XLOC_004889			↓ 2.43	0.020861		
lincRNA	linc-HARS-1	NONHSAG041748.2			↓ 2.02	0.042326		
Pre-miRNA		ENSG00000221162			↑ 3.12	0.007448		
Pre-miRNA		ENSG00000221162			↑ 2.84	0.009967		

Pre-miRNA	hsa-mir-548i-4 3	NR_031690			↓ 3.33	0.029302		
lincRNA		ENSG00000105866			↓ 2.31	0.015133		
lincRNA	linc-GNAQ-1	NONHSAG052630.2			↑ 2.35	0.001928		
Pre-miRNA		ENSG00000238623			↓ 2.02	0.022484		
mRNA	GPR119	ENSG00000147262			↑ 2.8	0.021965		
piRNA-c	piR-44914	DQ576802			↓ 2.05	0.033952		
mRNA	INA	NM_032727			↑ 2.48	0.00938		
Structural RNA	SNORA23	NR_002962			↑ 2.72	0.045342		
lncRNA		AJ488208			↑ 2.43	0.007481		
lincRNA	linc-SLC5A12	ENSG00000254560			↑ 4.05	0.004462		
lncRNA	RP11-227B21	AF403225			↑ 2.15	0.018328		
Structural RNA	SNORD77	ENSG00000212279			↓ 4.26	0.013527		
mRNA	HOMER2	ENSG00000103942			↓ 2.35	0.029144		
lincRNA	linc-HOMER2	NONHSAG017675			↓ 2.61	0.020442		
Pre-miRNA		ENSG0000023917			↑ 4.5	0.006081		
lncRNA	FAM215A	NR_026770			↑ 2.2	0.009863		
mRNA	SMIM6	NM_001162997			↓ 2.01	0.006374		
mRNA	TEX19	ENSG00000182459			↓ 3.22	0.027438		
lncRNA		NR_026770			↑ 2.14	0.024208		
lncRNA		FJ648812			↓ 2.59	0.0041		
lncRNA		AK091108			↓ 2.15	0.029094		
lincRNA	linc-KCNG2	NONHSAG024254.2			↓ 2.07	0.021985		
Pre-miRNA	hsa-mir-220b	ENSG00000215937			↑ 4.16	0.003453		
Structural RNA	snRNA-U13	RF01210			↓ 3.08	0.041117		
mRNA	WFDC10A	NM_080753			↓ 2.05	0.004641		
lncRNA	GriK1-AS2	NR_033368			↓ 2.21	0.016826		
lncRNA	lnc-UMODL1-7	NONHSAG032924.2			↑ 2.94	0.018698		
lncRNA	RP11-480I12.9	NR_002929	↓ 2.1	0.049343				
lncRNA	RTCA-AS1	ENSG00000224616	↑ 2.49	0.023644				
lincRNA		ENSG00000231420	↓ 2.03	0.005605				
piRNA-c	piR-47548	DQ579436	↑ 7.61	0.048727				
piRNA-c	piR-55001	DQ587889	↑ 2.97	0.036551				
lincRNA	RP11-47P18.2	ENSG00000242781	↓ 2.52	0.029623				
lincRNA	linc-ROBO1-3	NONHSAG035474.2	↓ 2.07	0.004328				
mRNA	IL9	NM_000590	↓ 2.39	0.024509				
lncRNA	CTC-242N15.1	ENSG00000233828	↓ 2.23	0.042053				

lncRNA		S63356	↓ 3.18	0.013927				
lncRNA		DQ409329	↑ 2.46	0.010566				
piRNA-c	piR-47032	DQ578920	↓ 7.56	0.024394				
lincRNA	linc-SLC25A37	ENSG00000253390	↓ 2.22	0.008041				
lncRNA	RP11-442H21.2	ENSG00000269926	↓ 2.4	0.044695				
mRNA	STYK1	NM_018423	↑ 2.53	0.046367				
lncRNA	RP11-123H22.1	ENSG00000234551	↓ 3.02	0.008146				
Pre-miRNA	hsa-mir--1260A	ENSG00000221754	↑ 8.25	0.00238				
Pre-miRNA	hsa-mir-4311	NR_036196	↑ 2.83	0.040386				
structural RNA	RNU7-111P	ENSG00000252645	↑ 2.24	0.030336				
lncRNA	lnc-CKMT1B-1-1	NONHSAG016709.2	↓ 2.42	0.044544				
Pre-miRNA	hsa-mir-744	NR_030613	↓ 2.21	0.028955				
structural RNA	SNORD4B	NR_000009	↑ 4.21	0.031762				
mRNA	KCNE1	ENSG00000180509	↑ 2.35	0.049014				
Pre-miRNA	hsa-mir-197	NR_029583					↑ 2.04	0.04415
lncRNA	RP5-994D16.9	ENSG00000228452					↑ 2.21	0.02413
piRNA-c	piR-39821	DQ601755					↑ 2.75	0.015035
piRNA-c	piR-59381	DQ592269					↑ 2.53	0.027541
piRNA-c	piR-42771	DQ574659					↓ 3.48	0.042938
mRNA	FIGN	NM_018086					↓ 2.32	0.005049
piRNA-c	piR-43765	DQ575653					↑ 2.49	0.035991
lncRNA		DQ229109					↓ 2.27	0.006023
lncRNA	lnc-GFM1-5-6	NONHSAG036514.2					↑ 3.24	0.001992
mRNA	ANXA5	NM_001154					↑ 2.45	0.027703
lncRNA	lnc-ANXA5	NONHSAG038790.2					↑ 4.63	0.028005
mRNA	TNFAIP3	ENSG00000118503					↑ 2.53	0.045315
piRNA-c	piR-43854	DQ575742					↓ 5.13	0.04528
mRNA	NACC2-001	ENSG00000148411					↑ 2.04	0.005529
mRNA	MPC1L	NM_001195522					↓ 3.17	0.01703
lincRNA	RP11-393K12.2	ENSG00000223581					↑ 2.01	0.036929
lincRNA	linc-ZMIZ1-2	NONHSAG006319.2					↓ 2.32	0.040508
lncRNA	USP12-AS2	ENSG00000230641					↓ 2.28	0.012537
lncRNA	linc-RPL21-1	NONHSAG013072.2					↓ 2.13	0.010413
mRNA	IGHV3-38	ENSG00000211958					↓ 7.99	0.011293
piRNA-c	piR-43853	DQ575741					↓ 7.92	0.032743
piRNA-c	piR-43853	DQ575741					↓ 7.92	0.032743

piRNA-c	piR-43853	DQ575741					↓ 7.92	0.032743
piRNA-c	piR-43853	DQ575741					↓ 7.92	0.032743
piRNA-c	piR-43853	DQ575741					↓ 7.92	0.032743
Pre-miRNA	hsa-mir-70	ENSG00000221391					↑ 2.01	0.038749
lncRNA	LINC01580	ENSG00000258785					↓ 2.36	0.041974
pseudogene	RP11-170L3.7	ENSG00000197476					↓ 9	0.004481
mRNA	IGHV3OR16-9	ENSG00000270472					↓ 3.05	0.007621
mRNA	IGHV3OR16-8	ENSG00000271130					↓ 3.61	0.01203
lincRNA	lincTP53TG3B	NONHSAG019235.2					↓ 3.09	0.010473
lncRNA	lnc-C17orf46-1-1	NONHSAG021976.2					↓ 2.65	0.003325
lncRNA	linc-C17orf97-2	NONHSAG020407.2					↓ 4.22	0.01341
lncRNA	linc-ADORA2B	NONHSAG072984.1					↑ 2.14	0.036339
Pre-miRNA		ENSG00000222999					↓ 2.13	0.017147
mRNA	CPLX4	NM_181654					↑ 4.17	0.023496
lncRNA	RP11-644A7.2	ENSG00000278971					↑ 6.07	0.016827
mRNA	KRTAP19-8	NM_001099219					↓ 3.26	0.043228
mRNA	SPATC1L	NM_001142854					↑ 2.58	0.001787

YL in comparison with:			**YH**		**OH**		**OL**	
Transcript type	**Gene Symbol**	**Accession number**	**Fold Change (linear)**	**ANOVA p-value**	**Fold Change (linear)**	**ANOVA p-value**	**Fold Change (linear)**	**ANOVA p-value**
Pre-miRNA		ENSG0000023917	↓ 3.82	0.049038	↓ 4.5	0.006081	↓ 4.44	0.023824
lncRNA	EAF1-AS1-008	ENSG00000249786	↑ 2.51	0.007154	↑ 2.12	0.041871		
lincRNA	linc-GALNTL6-4	NONHSAG087990	↓ 2.41	0.020265	↓ 2.82	0.01207		
mRNA	GPR119	ENSG00000147262	↓ 2.68	0.028598	↓ 2.8	0.021965		
piRNA-c	piR-44914	DQ576802	↑ 2.16	0.021604	↑ 2.05	0.033952		
lncRNA		AJ488208	↓ 2.01	0.024789	↓ 2.43	0.007481		
mRNA	TEX19	ENSG00000182459	↑ 3.58	0.007438	↑ 3.22	0.027438		
lncRNA	lnc-SKA2	FJ648812	↑ 2.47	0.003701	↑ 2.59	0.0041		
lincRNA	linc-KCNG2	NONHSAG024254.2	↑ 2.36	0.037521	↑ 2.07	0.021985		
lncRNA	lnc-CC2D1B	NONHSAG001475.2			↓ 2.01	0.013376	↓ 2.24	0.006118
lincRNA	RP11-180C1	ENSG00000250038			↓ 3.4	0.021102	↓ 2.8	0.024695
lncRNA	lnc-ARL15	AF086511			↓ 2.27	0.024715	↓ 2.71	0.03898
lincRNA		ENSG00000105866			↑ 2.31	0.015133	↑ 4.62	0.033411
lincRNA	linc-GNAQ-1	NONHSAG052630.2			↓ 2.35	0.001928	↓ 2.52	0.02048
Pre-miRNA		ENSG00000238623			↑ 2.02	0.022484	↑ 2.1	0.010877
lincRNA	linc-SLC5A12	ENSG00000254560			↓ 4.05	0.004462	↓ 5.8	0.010289

Pre-miRNA	hsa-mir-220b	ENSG00000215937			↓ 4.16	0.003453	↓ 3.47	0.027206
lncRNA	CTB-78F1	ENSG00000253357	↑ 2.53	0.019246			↑ 2.74	0.035811
piRNA-c	piR-45204	DQ577092	↑ 4.18	0.003178			↑ 5.59	0.008551
piRNA-c	piR-34994	DQ596928	↓ 3.06	0.02985			↓ 3.34	0.049517
lincRNA	AC003092.1	ENSG00000236453	↓ 4.89	0.015675			↓ 4.6	0.01598
lincRNA	linc-COL1A2-2	NONHSAG048230.2	↓ 3.46	0.023963			↓ 3.15	0.022611
lncRNA	Lnc-C9orf3		↓ 7.39	0.033025			↓ 5.79	0.024607
lncRNA	RP11-809N8.2-001	ENSG00000256928	↑ 2.11	0.001011			↑ 2.06	0.001539
lncRNA	RP11-480I12	BC038775			↑ 2.2	0.019611		
lncRNA		AF049126			↑ 2.08	0.012945		
lincRNA	CTC-480C2.1	ENSG00000250874			↓ 2.18	0.003406		
lincRNA	linc-FAM169A	XLOC_004889			↑ 2.43	0.020861		
lincRNA	linc-HARS-1	NONHSAG041748.2			↑ 2.02	0.042326		
Pre-miRNA		ENSG00000221162			↓ 3.12	0.007448		
Pre-miRNA		ENSG00000221162			↓ 2.84	0.009967		
Pre-miRNA	hsa-mir-548i-4 3	NR_031690			↑ 3.33	0.029302		
lincRNA	linc-STX17	NONHSAG053035.2			↓ 2.33	0.026879		
mRNA	INA	NM_032727			↓ 2.48	0.00938		
Structural RNA	SNORA23	NR_002962			↓ 2.72	0.045342		
lncRNA	CTD-2026G22.1	ENSG00000255532			↑ 3.92	0.006987		
lncRNA		U78793			↓ 2.95	0.015619		
mRNA	CLEC4A	NM_016184			↓ 2.05	0.039821		
lncRNA	RP11-227B21	AF403225			↓ 2.15	0.018328		
Structural RNA	SNORD77	ENSG00000212279			↑ 4.26	0.013527		
mRNA	HOMER2	ENSG00000103942			↑ 2.35	0.029144		
lincRNA	linc-HOMER2	NONHSAG017675			↑ 2.61	0.020442		
lncRNA	FAM215A	NR_026770			↓ 2.2	0.009863		
mRNA	SMIM6	NM_001162997			↑ 2.01	0.006374		
lncRNA		NR_026770			↓ 2.14	0.024208		
lncRNA		AK091108			↑ 2.15	0.029094		
Structural RNA	snRNA-U13	RF01210			↑ 3.08	0.041117		
lincRNA	linc-ZNF606	NONHSAG026698.2			↓ 2.33	0.017991		
mRNA	WFDC10A	NM_080753			↑ 2.05	0.004641		
lncRNA	GriK1-AS2	NR_033368			↑ 2.21	0.016826		
lncRNA	lnc-UMODL1-7	NONHSAG032924.2			↓ 2.94	0.018698		
piRNA-c	piR-44067	DQ575955					↑ 2.02	0.005207

lncRNA	KCNC4-AS1	ENSG00000224965					↑ 2.21	0.027292
Structural RNA	RNU6-817P	ENSG00000212385					↓ 2.54	0.029438
piRNA-c	piR-54967	DQ587855					↑ 8.69	0.049326
piRNA-c	piR-41282	DQ573170					↑ 2.02	0.005207
lncRNA	linc-ALX3-1	NONHSAG002370.2					↑ 2.14	0.043686
lincRNA	LOC105373456	ENSG00000224626					↓ 2.19	0.007298
lincRNA	linc-RHOB-8	NONHSAG027159.2					↓ 2.12	0.020253
lincRNA	linc-CCDC140-10	NONHSAG078193.1					↓ 7.78	0.00811
lncRNA	lnc-GFM1-5-6	NONHSAG036514.2					↑ 2.15	0.039328
mRNA	ANXA5	NM_001154					↑ 2.67	0.010401
lncRNA	RP11-180C1	ENSG00000250038					↓ 2.12	0.024235
lncRNA	lnc-ANXA5	NONHSAG038790.2					↑ 4.42	0.004754
structural RNA	SNORD123	NR_003689					↑10.45	0.00409
lncRNA	RP11-98J23	ENSG00000251158					↑ 2.06	0.005056
lincRNA	RP11-12A2-3	NR_033919					↑ 3.13	0.048106
lincRNA	GS1-124K5.4	ENSG00000237310					↓ 2.04	0.020423
piRNA-c	piR-53770	DQ586658					↓ 2.13	0.01061
piRNA-c	piR-53770	DQ586658					↓ 2.13	0.01061
piRNA-c	piR-53770	DQ586658					↓ 2.13	0.01061
piRNA-c	piR-53770	DQ586658					↓ 2.13	0.01061
lncRNA		AY495951					↓ 2.15	0.017595
piRNA-c	piR-49706	DQ581594					↑ 2.47	0.044001
piRNA-c	piR-42870	DQ574758					↑ 2.47	0.044001
lncRNA	RP11-443N24.1	ENSG00000255725					↑ 2.52	0.019216
structural RNA	RNY5	NR_001571					↓ 4.59	0.040171
lncRNA	lnc-SMUG1	NR_045039					↑ 2.28	0.002352
lincRNA	RP11-991C1.1	ENSG00000258933					↑ 2.02	0.010434
lncRNA		BC010517					↓ 2.25	0.027451
mRNA	IGHV3-38	ENSG00000211958					↓ 8.68	0.026413
piRNA-c	piR-39345	DQ601279					↑ 3.65	0.035162
piRNA-c	piR-39345	DQ601279					↑ 3.65	0.035162
piRNA-c	piR-39345	DQ601279					↑ 3.65	0.035162
Pre-miRNA		ENSG00000222586					↑ 2.82	0.038187
piRNA-c	piR-39345	DQ601279					↑ 3.65	0.035162
lincRNA	RP11-720L8.1	NONHSAG016528.2					↑ 2.06	0.013365
lncRNA	RP11-27M24.1	ENSG00000256013					↓ 4.04	0.007135

mRNA	IGHV3OR16-9	ENSG00000270472					↓ 3.81	0.045466
mRNA	PFAS	ENSG00000178921					↑ 2.37	0.002447
Structural RNA	LOC284009	NR_028335					↓ 5.09	0.048555
lincRNA	linc-MADCAM1	NONHSAG024282.2					↑ 5.44	0.034914
mRNA	KRTAP19-8	NM_001099219					↓ 3.99	0.025839
mRNA	RELT	ENSG00000054967					↑ 2.07	0.036585
mRNA	MAP1LC3C	NM_001004343	↓ 2.88	0.001811				
lncRNA	RP11-452F19.3	ENSG00000228106	↓ 2.39	0.042063				
lincRNA	linc-POU3F1-1	NONHSAG001091.2	↑ 3.11	0.042026				
structural RNA	RN5S107	ENSG00000223290	↓ 2.56	0.026093				
lincRNA		ENSG00000236605	↓ 3.57	0.031185				
lincRNA		ENSG00000229271	↓ 2.52	0.030868				
lincRNA	RP11-47P18.2	ENSG00000242781	↓ 2.92	0.003432				
mRNA	PPARG	ENSG00000132170	↓ 2.07	0.033168				
piRNA-c	piR-47032	DQ578920	↓ 11.12	0.041644				
lincRNA		ENSG00000236039	↑ 2.9	0.035676				
mRNA	TSPYL5	NM_033512	↓ 2.53	0.018673				
piRNA-c	piR-51084	DQ583972	↓ 2.03	0.026864				
mRNA	APEX2	NM_014481	↓ 2.09	0.009621				
mRNA	ACTN3	ENSG00000248746	↑ 3.26	0.011928				
lncRNA	lnc-OSBPL5	AF331964	↓ 2.18	0.024858				
lincRNA	linc-PTPRQ-7	ENSG00000165899	↓ 2.25	0.026623				
Structural RNA	RN7SL796P	ENSG00000277031	↓ 2.27	0.040695				
Structural RNA	RN7SL495P	ENSG00000277515	↓ 2.27	0.040695				
Structural RNA	RN7SL719P	ENSG00000274632	↓ 2.54	0.041823				
Structural RNA	RN7SL673P	ENSG00000273818	↓ 2.58	0.028508				
Structural RNA	RN7SL539P	ENSG00000274076	↓ 2.22	0.048936				
Structural RNA	RN7SL82P	ENSG00000278696	↓ 2.58	0.028508				
lncRNA	lnc-AVEN-1:1	NONHSAG016476.2	↑ 2.81	0.049575				
lncRNA	lnc-MEIS2-4:1	NONHSAG016539.2	↑ 2.54	0.019191				
piRNA-c	piR-58740	DQ591628	↑ 3.98	0.014528				
lncRNA	lnc-CKMT1B-1-1	NONHSAG016709.2	↓ 2.32	0.042389				
lincRNA	linc-ARRDC4-3	NONHSAG018046.2	↓ 2.66	0.011166				

mRNA	CXCL16	NM_022059	↓ 2.06	0.007226				
mRNA	NAT9	NM_015654	↓ 2.22	0.021793				
piRNA-c	piR-36520	DQ598454	↓ 3.59	0.016361				
lincRNA	linc-NDUFV3-1	XLOC_013957	↑ 2.12	0.000188				

OL in comparison with:			**YH**		**OH**		**YL**	
Transcript type	**Gene Symbol**	**Accession number**	**Fold Change (linear)**	**ANOVA p-value**	**Fold Change (linear)**	**ANOVA p-value**	**Fold Change (linear)**	**ANOVA p-value**
mRNA	ANXA5	NM_001154	↓ 2.61	0.007953	↓ 2.45	0.027703	↓ 2.67	0.010401
lncRNA	lnc-ANXA5	NONHSAG038790.2	↓ 5.2	0.003713	↓ 4.63	0.028005	↓ 4.42	0.004754
mRNA	IGHV3-38	ENSG00000211958	↑ 8.03	0.018696	↑ 7.99	0.011293	↑ 8.68	0.026413
mRNA	IGHV3OR16-9	ENSG00000270472	↑ 3.24	0.046792	↑ 3.05	0.007621	↑ 3.81	0.045466
mRNA	SPATC1L	NM_001142854	↓ 2.01	0.000565	↓ 2.58	0.001787	↓ 2.13	0.006585
lncRNA	KCNC4-AS1	ENSG00000224965	↓ 2.74	0.003828			↓ 2.21	0.027292
lncRNA	linc-ALX3-1	NONHSAG002370.2	↓ 2.81	0.004033			↓ 2.14	0.043686
structural RNA	SNORD123	NR_003689	↓ 2.27	0.013761			↓ 10.45	0.00409
piRNA-c	piR-53770	DQ586658	↑ 2.39	0.006177			↑ 2.13	0.01061
piRNA-c	piR-53770	DQ586658	↑ 2.39	0.006177			↑ 2.13	0.01061
piRNA-c	piR-53770	DQ586658	↑ 2.39	0.006177			↑ 2.13	0.01061
piRNA-c	piR-53770	DQ586658	↑ 2.39	0.006177			↑ 2.13	0.01061
lncRNA		AY495951	↑ 2.42	0.01049			↑ 2.15	0.017595
structural RNA	RNY5	NR_001571	↑ 7.58	0.000989			↑ 4.59	0.040171
lncRNA	lnc-SMUG1	NR_045039	↓ 2.15	0.009709			↓ 2.28	0.002352
lncRNA	RP11-27M24.1	ENSG00000256013	↑ 2.18	0.034688			↑ 4.04	0.007135
lncRNA	lnc-GFM1-5-6	NONHSAG036514.2			↓ 3.24	0.001992	↓ 2.15	0.039328
mRNA	KRTAP19-8	NM_001099219			↑ 3.26	0.043228	↑ 3.99	0.025839
mRNA	FIGN	NM_018086	↑ 2.64	0.009109	↑ 2.32	0.005049		
lncRNA	USP12-AS2	ENSG00000230641	↑ 2.39	0.007861	↑ 2.28	0.012537		
lncRNA	linc-RPL21-1	NONHSAG013072.2	↑ 2.39	0.009128	↑ 2.13	0.010413		
mRNA	IGHV3OR16-8	ENSG00000271130	↑ 3.4	0.049199	↑ 3.61	0.01203		
piRNA-c	piR-44067	DQ575955					↓ 2.02	0.005207
Structural RNA	RNU6-817P	ENSG00000212385					↑ 2.54	0.029438
piRNA-c	piR-54967	DQ587855					↓ 8.69	0.049326
piRNA-c	piR-41282	DQ573170					↓ 2.02	0.005207
lncRNA	lnc-CC2D1B	NONHSAG001475.2					↑ 2.24	0.006118
lincRNA	LOC105373456	ENSG00000224626					↑ 2.19	0.007298

lincRNA	linc-RHOB-8	NONHSAG027159.2					↑ 2.12	0.020253
lincRNA	linc-CCDC140-10	NONHSAG078193.1					↑ 7.78	0.00811
lincRNA	RP11-180C1	ENSG00000250038					↑ 2.8	0.024695
lncRNA	RP11-180C1	ENSG00000250038					↑ 2.12	0.024235
lncRNA	CTB-78F1	ENSG00000253357					↓ 2.74	0.035811
piRNA-c	piR-45204	DQ577092					↓ 5.59	0.008551
lncRNA	lnc-ARL15	AF086511					↑ 2.71	0.03898
lncRNA	RP11-98J23	ENSG00000251158					↓ 2.06	0.005056
lincRNA	RP11-12A2-3	NR_033919					↓ 3.13	0.048106
piRNA-c	piR-34994	DQ596928					↑ 3.34	0.049517
lincRNA	GS1-124K5.4	ENSG00000237310					↑ 2.04	0.020423
lincRNA	AC003092.1	ENSG00000236453					↑ 4.6	0.01598
lincRNA		ENSG00000105866					↓ 4.62	0.033411
lincRNA	linc-COL1A2-2	NONHSAG048230.2					↑ 3.15	0.022611
lncRNA	PCAT7	ENSG00000231806					↑ 5.79	0.024607
lincRNA	linc-GNAQ-1	NONHSAG052630.2					↑ 2.52	0.02048
Pre-miRNA		ENSG00000238623					↓ 2.1	0.010877
piRNA-c	piR-49706	DQ581594					↓ 2.47	0.044001
piRNA-c	piR-42870	DQ574758					↓ 2.47	0.044001
lncRNA	RP11-809N8.2-001	ENSG00000256928					↓ 2.06	0.001539
lincRNA	linc-SLC5A12	ENSG00000254560					↑ 5.8	0.010289
lncRNA	RP11-443N24.1	ENSG00000255725					↓ 2.52	0.019216
lincRNA	RP11-991C1.1	ENSG00000258933					↓ 2.02	0.010434
lncRNA		BC010517					↑ 2.25	0.027451
piRNA-c	piR-39345	DQ601279					↓ 3.65	0.035162
piRNA-c	piR-39345	DQ601279					↓ 3.65	0.035162
piRNA-c	piR-39345	DQ601279					↓ 3.65	0.035162
Pre-miRNA		ENSG00000222586					↓ 2.82	0.038187
piRNA-c	piR-39345	DQ601279					↓ 3.65	0.035162
lincRNA	RP11-720L8.1	NONHSAG016528.2					↓ 2.06	0.013365
Pre-miRNA		ENSG0000023917					↑ 4.44	0.023824
mRNA	PFAS	ENSG00000178921					↓ 2.37	0.002447
Structural RNA	LOC284009	NR_028335					↑ 5.09	0.048555
Pre-miRNA	hsa-mir-220b	ENSG00000215937					↑ 3.47	0.027206
lincRNA	linc-MADCAM1	NONHSAG024282.2					↓ 5.44	0.034914
Pre-miRNA	hsa-mir-197	NR_029583			↓ 2.04	0.04415		
lncRNA	RP5-994D16.9	ENSG00000228452			↓ 2.21	0.02413		

piRNA-c	piR-39821	DQ601755			↓ 2.75	0.015035		
piRNA-c	piR-59381	DQ592269			↓ 2.53	0.027541		
piRNA-c	piR-42771	DQ574659			↑ 3.48	0.042938		
piRNA-c	piR-43765	DQ575653			↓ 2.49	0.035991		
lncRNA		DQ229109			↑ 2.27	0.006023		
mRNA	TNFAIP3	ENSG00000118503			↓ 2.53	0.045315		
piRNA-c	piR-43854	DQ575742			↑ 5.13	0.04528		
mRNA	NACC2-001	ENSG00000148411			↓ 2.04	0.005529		
mRNA	MPC1L	NM_001195522			↑ 3.17	0.01703		
lincRNA	RP11-393K12.2	ENSG00000223581			↓ 2.01	0.036929		
lincRNA	linc-ZMIZ1-2	NONHSAG006319.2			↑ 2.32	0.040508		
lncRNA		U78793			↓ 2.86	0.004673		
mRNA	CLEC4A	NM_016184			↓ 2.17	0.002245		
piRNA-c	piR-43853	DQ575741			↑ 7.92	0.032743		
piRNA-c	piR-43853	DQ575741			↑ 7.92	0.032743		
piRNA-c	piR-43853	DQ575741			↑ 7.92	0.032743		
piRNA-c	piR-43853	DQ575741			↑ 7.92	0.032743		
piRNA-c	piR-43853	DQ575741			↑ 7.92	0.032743		
Pre-miRNA	hsa-mir-70	ENSG00000221391			↓ 2.01	0.038749		
lncRNA	LINC01580	ENSG00000258785			↑ 2.36	0.041974		
lncRNA	RP11-170L3.7	ENSG00000197476			↑ 9	0.004481		
lincRNA	lincTP53TG3B	NONHSAG019235.2			↑ 3.09	0.010473		
lncRNA	lnc-C17orf46-1-1	NONHSAG021976.2			↑ 2.65	0.003325		
lncRNA	linc-C17orf97-2	NONHSAG020407.2			↑ 4.22	0.01341		
lncRNA	linc-ADORA2B	NONHSAG072984.1			↓ 2.14	0.036339		
lncRNA	CTD-3035K23.7	ENSG00000274565			↓ 3.44	0.011241		
Pre-miRNA		ENSG00000222999			↑ 2.13	0.017147		
mRNA	CPLX4	NM_181654			↓ 4.17	0.023496		
lncRNA	RP11-644A7.2	ENSG00000278971			↓ 6.07	0.016827		
#N/A		ENSG00000228449	↓ 2.22	0.039554				
lincRNA	RP11-145M4.1	ENSG00000241042	↓ 3.61	0.011048				
lincRNA	linc-ADSS	NONHSAG004855.2	↓ 2.07	0.027123				
structural RNA	RN5S107	ENSG00000223290	↓ 2.16	0.024196				
lincRNA	linc-ASAP2-1	NONHSAG026953.2	↓ 2.13	0.009773				
lncRNA	RP11-894J14.2	OTTHUMG00000159046	↓ 2.02	0.021582				
lincRNA	RP11-47P18.2	ENSG00000242781	↓ 3.4	0.004929				
lincRNA	linc-CLDN16	NONHSAG036963.2	↑ 2.01	0.0396				

piRNA-c	piR-36165	DQ598099	↑ 3.79	0.033283				
mRNA	GEM	NM_181702	↑ 2.21	0.024079				
mRNA	NCS1	NM_014286	↓ 2.01	0.003182				
lncRNA	PRRG1	BC030786	↑ 2.2	0.027357				
lncRNA	lnc-IKBKG	ENSG00000073009	↓ 3.11	0.041305				
lincRNA	linc-C10orf119-3	ENSG00000227307	↓ 2.05	0.03496				
lincRNA	linc-ARHGAP20-3	NONHSAG063627.1	↓ 2.01	0.01288				
lincRNA	linc-PTPRQ-7	ENSG00000165899	↓ 3.12	0.002154				
lncRNA	ARL6IP4	EF036485	↓ 2.04	0.033876				
lincRNA	LINC00363	ENSG00000232849	↓ 2.7	0.019468				
lncRNA	RP11-123H22.1	ENSG00000234551	↓ 2.34	0.049945				
Pre-miRNA	hsa-mir--1260A	ENSG00000221754	↑ 3.13	0.042228				
piRNA-c	piR-52545	DQ585433	↓ 2.84	0.025932				
lincRNA	linc-C15orf2-10	NONHSAG016287.2	↑ 2.44	0.01897				
lncRNA	lnc-CKMT1B-1-1	NONHSAG016709.2	↓ 2.16	0.031147				
Pre-miRNA	hsa-mir-548w	NR_036146	↓ 2.66	0.015916				
lncRNA		AB010099	↑ 2.24	0.025952				
lncRNA	LL22NC03-N64E9	ENSG00000271127	↓ 2.18	0.021777				